Unsaturated Soil Property Functions for High Volume Change Materials

by

Feixia Zhang

A thesis submitted in partial fulfillment of the requirements for the degree of Doctor of Philosophy

in

Geotechnical Engineering

Department of Civil and Environmental Engineering
University of Alberta

Abstract

Unsaturated soil property functions are necessary for numerical modeling of geotechnical engineering problems including transient seepage or contaminant transport involving unsaturated soils such as tailings or mine wastes. The accuracy of the input of material properties significantly influences the correctness of the numerical modeling results. Therefore, it is important to use appropriate unsaturated soil property functions in the numerical modeling of geotechnical engineering problems. The existing soil property functions proposed in the literature by many researchers are based on an implicit assumption that the soil does not undergo volume change as soil suction changes. These estimation techniques may produce reasonable results for soils that do not undergo volume change as soil suction changes (e.g., sands and silts). However, they are not suitable for the estimation of the unsaturated soil property functions for soils that undergo significant volume change as soil suction changes (e.g., Regina clay and Oil Sands Tailings). Revisions to the conventional methodology are proposed to accommodate the need of estimating the unsaturated soil properties for soils that undergo volume change as soil suction changes.

The research in this thesis is restricted to the study of hydraulic and volume-mass properties related to the water phrase. The primary objective of this thesis is to develop and verify a revised methodology for estimating

the coefficient of permeability function and the water storage function for soils that undergo volume change as soil suction is increased during a drying process. The scope of this thesis is directed at a theoretical study and research program investigating the hydraulic and volume-mass properties of soils that will change volumes as soil suction changes (e.g., Oil Sands Tailings). Laboratory data sets collected from the literature on Regina clay and Oil Sands Tailings have been used to verify the proposed theory. An experimental program has been carried out on Bulyanhulu tailings and Devon silt. Data collected has been used for verifying the proposed theory. A complete set of experimental data for each soil sample includes measured data of the SWCCs, shrinkage curves and the relationship between the saturated permeability versus void ratio.

Preface

This thesis is an original work by Feixia Zhang under the supervision of Dr. Ward Wilson and Dr. Del Fredlund. All the data analysis and math calculations were done by myself. Data in Chapter 5 were collected by myself from by a lab testing program. Data in Chapter 3 and Chapter 4 were collected from literature (Fredlund, 1964; Fredlund et al., 2011).

Chapter 2 of this thesis has been published as Zhang, F., and Fredlund, D. G. (2015). “Examination of the estimation of relative permeability for unsaturated soils”. Canadian Geotechnical Journal. 52 (12): 2077-2087, 10.1139/cgj-2015-0043. I was responsible for the parametric study and analysis as well as the manuscript composition. Dr. Del Fredlund was the supervisory author and was involved with concept formation and manuscript composition.

Chapter 3 of this thesis has been published as Zhang, F., Fredlund, D. G., and Wilson, G. W. (2016). “Water Permeability Function for Soils that Undergo Volume Change as Suction Changes”. Indian Geotechnical Journal. 46 (3): 210-227. doi:10.1007/s40098-016-0187-5. I was responsible for the data collection from literature and analysis as well as the manuscript composition. Dr. Del Fredlund and Dr. Ward Wilson were the supervisory authors and were involved with concept formation and manuscript composition.

Chapter 4 of this thesis has been submitted to Canadian Geotechnical Journal for review as Zhang, F., Wilson, G. W., and Fredlund, D. G. (2016). “Permeability function for oil sands tailings with volume change in a drying process”. I was responsible for the data collection from literature and analysis as well as the manuscript composition. Dr. Ward Wilson and Dr.

Del Fredlund were the supervisory authors and were involved with concept formation and manuscript composition.

Acknowledgements

First of all, I would like to express my sincere gratitude to my dear supervisors, Dr. Ward Wilson and Dr. Del Fredlund. Their strong support, patience guidance and loving encouragement have upheld me and led me through the whole long program.

I want to thank the National Science and Engineering Research Council (NSERC) for financial support. I also want to thank SoilVision Systems Ltd for financial support and offering me an opportunity to have some work experience.

I also want to thank Louis Kabwe, Christine Hereygers and Mr Steve Gamble for assisting me in the laboratory tests. Their technical support is greatly appreciated. I would like to thank Sally Petaske, Vivian Giang and Annette Busenius for helping me register classes, conferences and fill out various kinds of forms. Their warmhearted help, patience and kindness are really appreciated.

My sincere thanks are also for all my friends, student colleagues and all the people I came across throughout my lifetime. Thanks for being part of my life stories. I want to express special gratitude to James and Ann Siebert and my other IFG friends for their constant loving care and encouragement and prayer support. I want to thank McLarin Baptist Church for welcoming me and involving me in interesting studies and praying for me.

I want to thank those who are never to be forgotten by me, my mother and my brother’s family, for their love and support. And I want to dedicate this thesis to my father who has loved and supported me all his life, though his

love was so quiet and silent that I couldn’t even recognize at the beginning and have misunderstood.

Finally and most importantly, I would like to give my thanks to my God and Jesus my Savior. Your name is to be feared and praised. Thanks for many second chances in this life and keeping no records of wrong. Thanks for mending the broken and making it new and alive and complete. Thanks for the life, promises and the hope you’ve offered. To you be all the glory, honor and praises. “Therefore, if anyone is in Christ, he is a new creation. The old has passed away; behold, the new has come.” (2 Corinthians 5:17)

Table of Contents

List of Tables

List of Figures

Chapter 1. Introduction

1.1 Statement of problem

Unsaturated soil mechanics plays an important role in geotechnical engineering practice involving unsaturated soils, such as foundation design for buildings constructed on unsaturated expansive soils, design of a highway built on unsaturated compacted soils, design of cover systems for mine waste and design of paste tailings storage facilities. There are two advancements in research history of unsaturated soil mechanics that make the implementation of unsaturated soil mechanics into geotechnical engineering practice possible. One is the advancement of numerical computing techniques that provides a means to solve the mathematical problems with complexity and high nonlinearity where unsaturated soil mechanics is applied, and the other is the appropriate mathematical description of constitutive relationships to fully characterize the simulated system for the project involving unsaturated soils, such as the volume-mass constitutive relationships, shear strength constitutive relationships and hydraulic conductivity constitutive relationships (Fredlund, 1999).

Proper unsaturated soil property functions are necessarily required for the numerical modeling of geotechnical engineering problems involving unsaturated soils. Many geotechnical engineering problems such as seepage related to tailings and mine waste can be reduced to a series of partial differential equations. Each partial differential equation contains material properties that are either constants or mathematical functions. The material properties must be provided properly in order to obtain reasonable results. Most computer software available in geotechnical engineering practice is partial differential equation based (e.g., SVOFFICE 2009, GEOSTUDIO 2012, etc.). The correctness of the numerical modeling results depends largely on the accuracy of the input of the material properties. It is important to use appropriate soil property functions when modeling geotechnical engineering problems.

Unsaturated soil properties include shear strength properties, heat flow properties, hydraulic properties for the water phase (liquid phase), and fluid flow properties of the air phase. The research in this thesis is restricted to the study of hydraulic and volume-mass properties related to the water phase. Primary emphasis is on the coefficient of permeability function and the water storage function.

The coefficient of permeability function (saturated/unsaturated coefficient of permeability function) and the water storage function constitute two of those necessary unsaturated soil property functions in the numerical modeling simulation of the drying process where the sludge material is deposited and allowed to dry in order to increase its shear strength. Direct measurement of the coefficient of permeability and water storage for an unsaturated soil is expensive, time-consuming and technique demanding. Direct measurement is only adopted for the purpose of research or large costly projects of high risks. Numerous estimation techniques have been proposed as alternative approaches in the literature to empirically predict the coefficient of permeability function and water storage function. These are based on an implicit assumption that there is no volume change as the soil suction is increased (e.g., sands and silts). The van Genuchten-Burdine (1980) equation, van Genuchten-Mualem (1980) equation and Fredlund-Xing-Huang (1994) permeability function are three well-known equations for the estimation of the unsaturated coefficient of permeability function in geotechnical engineering practice. The existing unsaturated coefficient of permeability functions are often estimated from volumetric water content soil-water characteristic curve (θ-SWCC) in conjunction with a measured constant coefficient of permeability. These conventional estimation methods produce reasonable results for soils that do not undergo volume change as soil suction changes (e.g., sands and silts). The assumption of no volume change may be suitable for sands or coarse-grained materials, but it is not acceptable for some fine-grained silts and clays, particularly soils that are deposited as slurry and then left to dry and increase in strength. Oil Sands Tailings constitute one such type of materials where large volume change occurs as soil suction is increased (Fredlund et al., 2011).

1.2 Objectives of research program

Conventional estimation methods may make an inaccurate prediction of the coefficient of permeability function for a soil that undergoes high volume change as soil suction changes when the implicit assumption is violated. The inaccuracy in the estimation of the coefficient of permeability can cause erroneous numerical modeling results and affect subsequent engineering decisions significantly. An accurate coefficient of permeability function with the consideration of both desaturation and volume change is necessary for the correct numerical modeling simulation of the drying process when optimizing deposition strategies of thickened or paste tailings. Revisions to the conventional estimation methodologies are required for the appropriate estimation of the coefficient of permeability function for soils that undergo volume change as soil suction changes (e.g., Regina clay or Oil Sands Tailings).

The objective of this thesis is to develop and verify a revised methodology to estimate the coefficient of permeability function and the water storage function for high volume change materials. Both degree of saturation and void ratio are taken into account when developing the revised technique for the estimation of the coefficient of permeability for soils that undergo volume change as soil suction is increased (e.g., Regina clay and Oil Sands Tailings). The scope of this thesis is limited to a theoretical study and a research program investigating several soils that change volume as soil suction is increased for the verification of the proposed theory.

1.3 Organization of Thesis

The dissertation is presented in the paper-based format and consists of 6 chapters, supplemented by one appendix. The first chapter serves as an introduction, and each subsequent chapter (Chapter 2 to 5) except for the final chapter is an independent article with its own abstract, body of text and bibliography. The final chapter (Chapter 6) presents conclusions and recommendations. Chapters 2 and 3 have previously been published in peer-reviewed journals and are presented here as part of the dissertation. The chapters' text, font type, size and margin sizes are formatted as the dissertation requires, but the content of the chapters is the same as published in the journals. Chapter 4 has been submitted for publication in a peer-reviewed journal and is presented as submitted. Chapter 5 is prepared for submission to a peer-reviewed journal.

Chapter 2 presents a study of the effect of the lower limit of integration on the calculation of the permeability function. Comparisons are made between starting the integration from various values below the AEV and starting the integration from the calculated air-entry value, AEV. A mathematical algorithm is also proposed for the calculation of the AEV for integration purposes.

Chapter 3 modifies the Fredlund-Xing-Huang (1994) estimation procedure and develops a revised methodology for the estimation of a coefficient of permeability function for a soil that changes volume as soil suction is changed. Both void ratio and degree of saturation are considered in the revised estimation technique. A laboratory data set for Regina clay is presented and interpreted using the revised methodology.

Chapter 4 is an extension of the study of the revised methodology for the estimation of a coefficient of permeability function for volume-change soils during a drying process. The revised methodology is applied to thickened oil sands tailings. The measured gravimetric water content soil-water characteristic curve, *w*-SWCC of thickened oil sands tailings exhibits a bimodal feature. As a result, a simplified bimodal *w*-SWCC equation is used to obtain a proper best-fit for the *w*-SWCC. Effect of best-fitting of the degree of saturation soil-water characteristic curve, *S*-SWCC, on the estimation of the permeability function is explained.

Chapter 5 presents test results on Devon silt and Bulyanhulu tailings from an experimental program. The revised methodology is used to estimate the coefficient of permeability functions of Devon silt and Bulyanhulu tailings as a means of verification and illustration. Shrinkage curves, *w*-SWCCs and the relationships of saturated coefficient of permeability versus void ratio for Devon silt and Bulyanhulu tailings were collected from the testing program.

Chapter 6 summarizes the entire study with conclusions and suggests recommendations for future research.

1.4 Publication related to this research

Journal papers and conference papers published from the results of this research work are listed below.

Journal papers:

Zhang, F., and Fredlund, D. G. (2015). “Examination of the estimation of relative permeability for unsaturated soils”. Canadian Geotechnical Journal. 52 (12): 2077-2087, 10.1139/cgj-2015-0043. (Chapter 2: Published)

Zhang, F., Fredlund, D. G., and Wilson, G. W. (2016). “Water Permeability Function for Soils that Undergo Volume Change as Suction Changes”. Indian Geotechnical Journal. 46 (3): 210-227. doi:10.1007/s40098-016-0187-5. (Chapter 3: Published)

Zhang, F., Wilson, G. W., and Fredlund, D. G. (2016). “Permeability function for oil sands tailings with volume change in a drying process”. Canadian Geotechnical Journal (Chapter 4: Manuscript submitted for review).

Zhang, F., Wilson, G. W., and Fredlund, D. G. (2016). “Estimation of the permeability function for Devon silt and Bulyanhulu tailings with a revised methodology”. Canadian Geotechnical Journal (Chapter 5: Written as a report to be submitted for publication).

Conference papers:

Fredlund, D. G., and Zhang, F. (2013). “Combination of shrinkage curve and soil-water characteristic curves for soils that undergo volume change as soil suction is increased”. Proceedings of the 18th International Conference on Soil Mechanics and Geotechnical Engineering, Paris, France, Sept 2-6.

Zhang, F., Fredlund, D. G., Wilson, G. W., and Sedgwick, A. (2014). “Determination of the permeability function for drying oil sands tailings undergoing volume change and desaturation”. Proceedings of the 4th

International Oil Sands Tailings Conference, Lake Louise, Banff, A.B. Dec 7-10, pp. 37-46.

Zhang, F., Fredlund, D. G., Fredlund, M. D, and Wilson, G. W. 2015. “Role of air-entry value and choice of SWCC in the prediction of the unsaturated permeability”. Proceedings of the 68th Canadian Geotechnical Conference and 7th Canadian Permafrost Conference, Quebec City, Sept 20-23.

Zhang, F., Fredlund, D. G., and Wilson, G. W. (2015). “Hydraulic properties for soils that undergo volume change as soil suction is increased”. Proceedings of AP-UNSAT 2015, Guilin, China, Oct 23 –26, pp. 383-392.

Chapter 2. Examination of the estimation of relative permeability for unsaturated soils

2.1 Introduction

The unsaturated coefficient of permeability function is required when modeling saturated-unsaturated soil systems. Direct measurement of the unsaturated permeability function is costly, technically-demanding, and time-consuming. As a result, the measurement of the unsaturated permeability function is reserved for research studies or large projects where substantial risk may be involved. Considerable research has been directed towards the estimation of the unsaturated coefficient of permeability function. There are four categories of models used for the estimation of unsaturated coefficient of permeability functions (Fredlund et al. 2012), namely: (*i*) empirical models, (*ii*) statistical models, (*iii*) correlation models, and (*iv*) regression models. Empirical models and statistical models appear to be most extensively used in geotechnical engineering. The past decades have witnessed a rapid increase in the combined modeling of the saturated–unsaturated portions as a soil continuum (Fredlund et al. 2012). Considerable effort is expended in measuring the saturated coefficient of permeability of each soil layer and then the unsaturated soil permeability functions are generally estimated based on one of the preceding models. Often the numerical modeling is followed by a parametric study or a probabilistic analysis that quantifies the effect of variations in the permeability function on the final outcome of the analysis. In any case, the estimation of the permeability function has become an integral part of assessing the hydraulic soil properties associated with seepage analyses. Empirical models utilize the similar character of the SWCC and the permeability function to estimate the unsaturated coefficient of permeability function. The Brooks and Corey

(1964) equation is one example of an empirical model. Statistical models make use of the fact that the permeability function and the SWCC are mainly controlled by the pore-size distribution of the soil. Consequently, the permeability function was developed based on the interpretation and application of the SWCC. Childs and Collis-George (1950), Burdine (1953), and Mualem (1976) are three commonly used integral formulas of relative permeability based on different physical models.

The van Genuchten (1980) equation and the Fredlund and Xing (1994) equation are two well-known mathematical equations for the SWCC. The van Genuchten SWCC equation was introduced into the Burdine (1953) equation and the Mualem (1976) integral formulas to obtain a permeability function. This gave rise to two closed-form solutions for the unsaturated soil permeability equation. The Fredlund and Xing (1994) SWCC equation was also introduced into the Childs and Collis-George (1950) integral formula, yielding an integral solution for the permeability equation. These combinations have given rise to three unsaturated soil permeability functions commonly used in geotechnical engineering. The three methodologies for the relative permeability function are referred to as (*i*) the van Genuchten–Burdine (van Genuchten 1980) equation, (*ii*) the van Genuchten–Mualem (van Genuchten 1980) equation, and (*iii*) the Fredlund et al. (1994) (hereafter referred to as “Fredlund, Xing, and Huang”) permeability function. In each of the preceding cases, the unsaturated soil permeability function is obtained by combining the saturated coefficient of permeability and the relative coefficient of permeability. The Fredlund, Xing, and Huang permeability function has the advantage that the integral permeability function retains the independence of the SWCC fitting variables when estimating the coefficients of permeability. On the other hand, the van Genuchten permeability functions are closed-form and simpler to use in engineering practice.

The original relative permeability theory published by Fredlund et al. (1994) specified the air-entry value (AEV), ψ_{aev}, as the lower limit of the integration. However, implementations in engineering practice appear to have used other values between zero and ψ_{aev} as the starting point of integration when calculating the relative coefficient of permeability. It does not appear that any study has been undertaken to assess whether the choice for the lower limit of integration influences the calculation of the Fredlund, Xing, and Huang permeability function.

This paper investigates the error caused by using various values for the lower limit of integration. The effect of the lower limit of integration is examined in terms of the effect of each of the SWCC fitting parameters (i.e., a_f, n_f, m_f, ψ_r) on the resulting error. An empirical procedure for the determination of the AEV is also described. The definition of the "permeability error" is described, followed by a study of the impact of the fitting parameters on the magnitude of the error in the permeability function.

2.2 Determination of AEV from degree of saturation SWCC (*S*-SWCC)

The SWCC for a soil is defined as the relationship between the water content and soil suction (Williams 1982), and is commonly used as the basis for the estimation of unsaturated soil properties (e.g., the permeability function for an unsaturated soil). Different designations for the amount of water in the soil generate different forms of SWCC, such as gravimetric water content SWCC, volumetric water content SWCC, instantaneous volumetric water content SWCC, and degree of saturation SWCC. The volumetric water content is the water content with the volume of water referenced to the original total volume of the soil specimen. The instantaneous volumetric water content is the water content with the volume of water referenced to the instantaneous total volume of the soil specimen. Each form of the SWCC provides similar information to the geotechnical engineer if the soil does not undergo volume change as soil suction is increased. When soil undergoes volume change, as is the case for soft clays and slurry soils, the gravimetric water content SWCC, instantaneous volumetric water content SWCC, and degree of saturation SWCC are distinctly different from one another. The volumetric water content SWCC is not of significance when the soil undergoes high volume change. Conventional permeability functions (e.g., the Fredlund, Xing, and Huang equation; van Genuchten–Burdine equation; van Genuchten–Mualem equation) produce reasonable estimations using the volumetric water content SWCC when there is no volume change during drying. The volumetric water content SWCC is no longer appropriate in the estimation of the relative permeability function when soil undergoes volume change. It is important to know that the relative coefficient of permeability function, as well as the AEV, must be estimated from the degree of saturation SWCC (Fredlund et al. 2011). This paper uses the degree of saturation SWCC to calculate the appropriate estimation of the relative permeability function.

Various forms of mathematical equations have been suggested to characterize the SWCC. The equation proposed by Fredlund and Xing (1994) has been shown to have sufficient flexibility to best-fit laboratory data reasonably well over the entire soil suction range from near zero to 10^6 kPa, provided the material behaves in a mono-modal manner. The form of the Fredlund and Xing (1994) equation written in terms of degree of saturation, (i.e., *S*-SWCC) is shown in Eq. [1].

$$S(\psi)=\frac{S_0\left(1-\ln\left(1+\psi/\psi_r\right)/\ln\left(1+10^6/\psi_r\right)\right)}{\left(\ln\left(\exp(1)+\left(\psi/a_f\right)^{n_f}\right)\right)^{m_f}} \qquad [1]$$

where ψ is the soil suction. $S(\psi)$ is the degree of saturation at a soil suction of ψ. S_0 is the initial degree of saturation at zero soil suction, and a_f, n_f, m_f, ψ_r are four best-fitting parameters controlling the shape of the SWCC.

The shape of the SWCC (e.g., described by the air-entry value, slope, residual conditions) are influenced by the four fitting parameters (i.e., a_f, n_f, m_f, and ψ_r) in a combined and complex manner. There is no simple one-on-one connection between the fitting parameters and the features of the curve, although a_f affects the AEV in a significant way, while n_f significantly influences the slope of SWCC. Bharat and Sharma (2012) studied the validity limits of the Fredlund–Xing parameters and found that small values of ψ_r influenced the SWCC near saturation and m_f also influenced the residual portion of the SWCC. In other words, these variables affect the shape of an SWCC in a coupled manner.

The AEV of the soil is the suction at which air begins to enter the largest pores in the soil (Fredlund and Xing 1994). Vanapalli et al. (1998) proposed an empirical, graphical construction technique to estimate the AEV from the SWCC. The AEV must be determined from the degree of saturation SWCC (Fredlund et al. 2011).

A mathematical algorithm is proposed in this paper for the determination of the AEV based on the graphical construction suggested by Vanapalli et al. (1998). The following steps are outlined with respect to the analysis for the AEV.

Step 1—Find the best-fitting SWCC for the degree of saturation SWCC using the Fredlund and Xing (1994) equation (Figure 2-1).

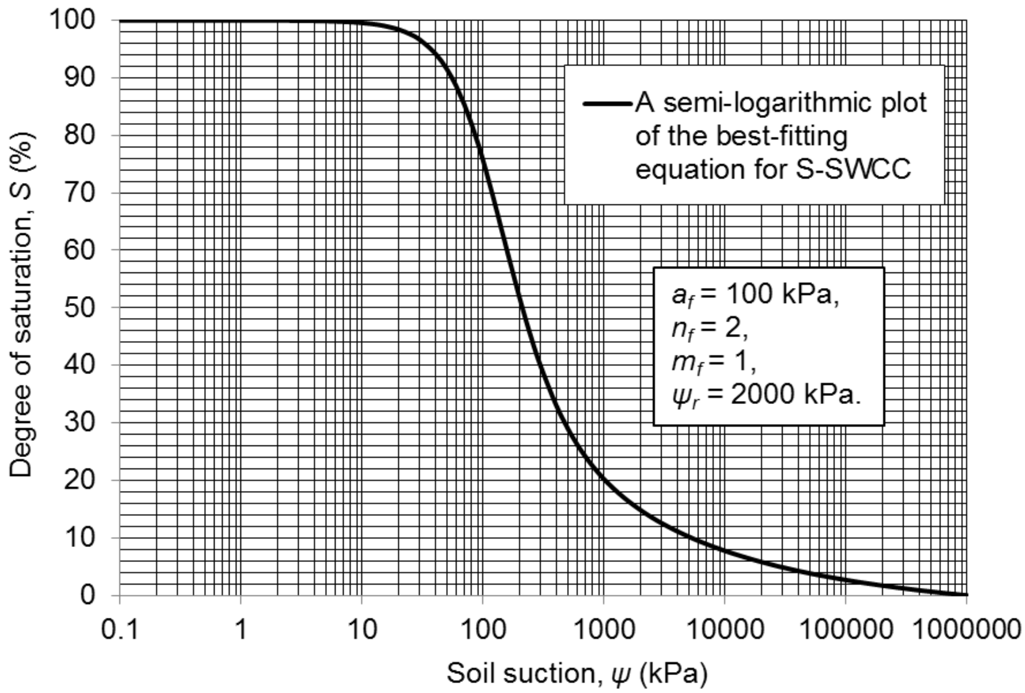

Figure 2-1. *S*-SWCC for a hypothetical soil plotted using semi logarithmic coordinate.

Step 2 — Through use of a variable substitution technique, the Fredlund and Xing (1994) best-fitting equation can be transformed into a substitution equation (i.e., Eq. [2]). The substitution equation describes the relationship between the degree of saturation and the logarithm of soil suction to the base 10 (Figure 2-2). The shape of the curve for the substitution equation plotted using arithmetic coordinates is the same as the shape of the curve for the best-fitting equation plotted using a semi logarithmic coordinate system. The arithmetic plot of the substitution equation has the same inflection point as the semi logarithmic plot of the best-fitting equation.

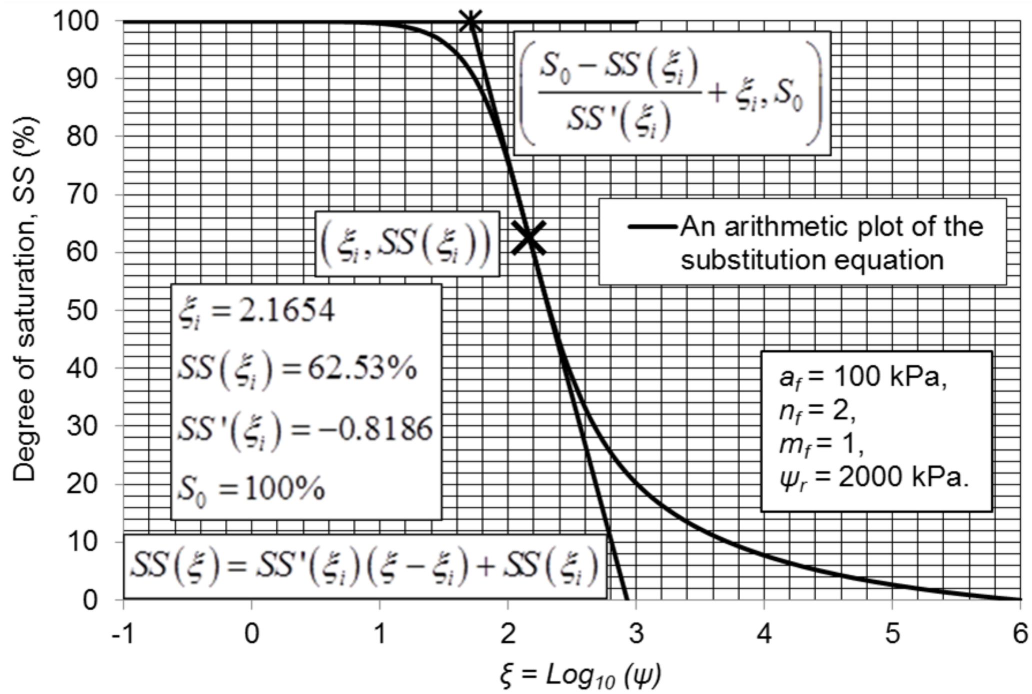

Figure 2-2. Arithmetical plot of substitution equation.

$$SS(\xi) = \frac{S_0\left(1 - \ln\left(1 + 10^{\xi}/\psi_r\right)/\ln\left(1 + 10^6/\psi_r\right)\right)}{\left(\ln\left(\exp(1) + \left(10^{\xi}/a_f\right)^{n_f}\right)\right)^{m_f}} \qquad [2]$$

where, ξ is the $\log_{10}(\psi)$; $SS(\xi)$ is the degree of saturation at a soil suction of ψ; and ψ is soil suction.

Step 3 — Determine the point of maximum slope (or the inflection point) on the arithmetic plot of the substitution equation. The point of maximum slope is also a point of zero curvature. Therefore, the second derivative of Eq. [2] can be set equal to zero as shown in Eq. [3].

$$\frac{\mathrm{d}^2 SS(\xi)}{\mathrm{d}\xi^2} = 0 \qquad [3]$$

Solving Eq. [3] for the ξ value of zero curvature point and substituting the ξ value into Eq. [2] yields the corresponding term, $SS(\xi)$. The determined point of zero curvature has coordinates (ξ_i, $SS(\xi_i)$) (Figure 2-2).

Step 4 — Draw a line tangent to the curve through the point of maximum slope (Figure 2-2). The point of maximum slope is (ξ_i, $SS(\xi_i)$) and the maximum slope is $SS'(\xi_i)$. The equation for the tangent line is as shown in Eq. [4].

$$TL(\xi) = SS'(\xi_i)(\xi - \xi_i) + SS(\xi_i) \qquad [4]$$

where $TL(\xi)$ represents the function of the tangent line.

Step 5 — Draw a horizontal line through the maximum degree of saturation. The intersection of the two lines indicates the AEV (Figure 2-2). The horizontal line is given by Eq. [5].

$$HL(\xi) = S_0 \qquad [5]$$

where $HL(\xi)$ represents the function of the horizontal line. The intersection point can be obtained mathematically by solving Eqs. [4] and [5]. The intersection point is $\left(\dfrac{S_0 - SS(\xi_i)}{SS'(\xi_i)} + \xi_i,\ S_0\right)$ on the arithmetic plot.

Step 6 — Back-calculate the AEV through use of the relationship $\xi = \log_{10}(\psi)$. The AEV for the soil can be written as follows.

$$\psi_{aev} = 10^{\left(S_0 - SS(\xi_i)\right)/SS'(\xi_i) + \xi_i} \qquad [6]$$

2.3 Statement of the integration problem associated with the Fredlund, Xing, and Huang permeability function

Fredlund et al. (1994) suggested a mathematical function for the estimation of the relative coefficient of permeability based on a physical model proposed by Childs and Collis-George (1950) (see Eq. [7]).

$$k_r^S(\psi) = \frac{\int_{\ln(\psi)}^{b} \frac{S(e^y) - S(\psi)}{e^y} S'(e^y)\,dy}{\int_{\ln(\psi_{aev})}^{b} \frac{S(e^y) - S(\psi_{aev})}{e^y} S'(e^y)\,dy} \qquad [7]$$

where $k_r^s(\psi)$ is the relative coefficient of permeability at soil suction of ψ. The superscript S means that the degree of saturation-SWCC is used for the estimation of the relative permeability in Eq. [7]). b is the upper limit of integration (i.e., ln(1 000 000)), y is the dummy variable of integration representing the logarithm of suction, S is the degree of saturation–SWCC equation, S' is the derivative of the degree of saturation–SWCC equation, and e^y is the natural number raised to the dummy variable power.

The denominator of Eq. [7] is an integral, the lower limit of the integration of which is the AEV, ψ_{aev}. Although the original theory (Fredlund et al. 1994) specified the AEV as the lower limit of integration, other values between a value close to zero and ψ_{aev} have been used as the starting point for integration while estimating the relative permeability function. The arbitrarily selected small value for the starting point of integration appears to have been used because no closed-form analytical procedure had been proposed for the calculation of the AEV. Details on how the integration using Fredlund et al. (1994) permeability is to be carried out can be found in the original paper. In addition, the importance of using the degree of saturation SWCC for calculating the permeability function has not been clearly emphasized in the research literature.

If a suction value ψ_i between (near) zero and ψ_{aev} is used as the lower limit of integration, the permeability function of Eq. [7] takes on the form shown in Eq. [8].

$$k_{ri}^{S}(\psi) = \frac{\int_{\ln(\psi)}^{b} \frac{S(e^y) - S(\psi)}{e^y} S'(e^y)\,dy}{\int_{\ln(\psi_i)}^{b} \frac{S(e^y) - S(\psi_i)}{e^y} S'(e^y)\,dy} \qquad [8]$$

where, $k_{ri}^{s}(\psi)$ is the relative coefficient of permeability at soil suction of ψ, when a suction value ψ_i is used as the lower limit of integration for the integral in the denominator of the Eq. [8].

Childs and Collis-George (1950) proposed the use of a statistical model. There are three common assumptions for a methodology characterizing the statistical models:

The porous medium may be regarded as a set of interconnected pores randomly distributed in the sample. The pores are characterized by their length scale called “the pore radius”.

The Hagen–Poiseuille equation is assumed valid at the level of the single pore and thus used to estimate the hydraulic conductivity of the elementary pore unit. The total hydraulic conductivity has to be determined by integration over the contributions of the filled pores.

The SWCC is considered analogous to the pore radius distribution function. The capillary law is used to uniquely relate the pore radius to the capillary head (Mualem and Klute 1986). The AEV of the soil corresponds to the largest pore radius. The change of the lower limit integration implies a change in the largest pore radius of the soil and thus a change in the pore radius distribution function.

The relative coefficient of permeability obtained using Eq. [7] is theoretically correct and is used as the reference value in the present study. An error in the estimation of the relative permeability is introduced when using Eq. [8], along with a variety of the lower limits of integration in the denominator. The slope in the SWCC, prior to the AEV (as defined by the degree of saturation SWCC), contributes to the error in the computed permeability function.

The Fredlund, Xing, and Huang permeability function was developed based on the interpretation of the SWCC. Figure 2-3 illustrates a situation where the effect of the starting point for integration is small. Starting integration at any point from 0.1 kPa to the AEV results in the computation of essentially the same relative permeability function. Figure 2-4, on the other hand, shows how the starting point for integration can have a significant effect on the computed permeability function. The difference between the results shown in Figures 2-3 and 2-4 appears to be mainly due to a change in the n_f (or steepness of the SWCC) variable.

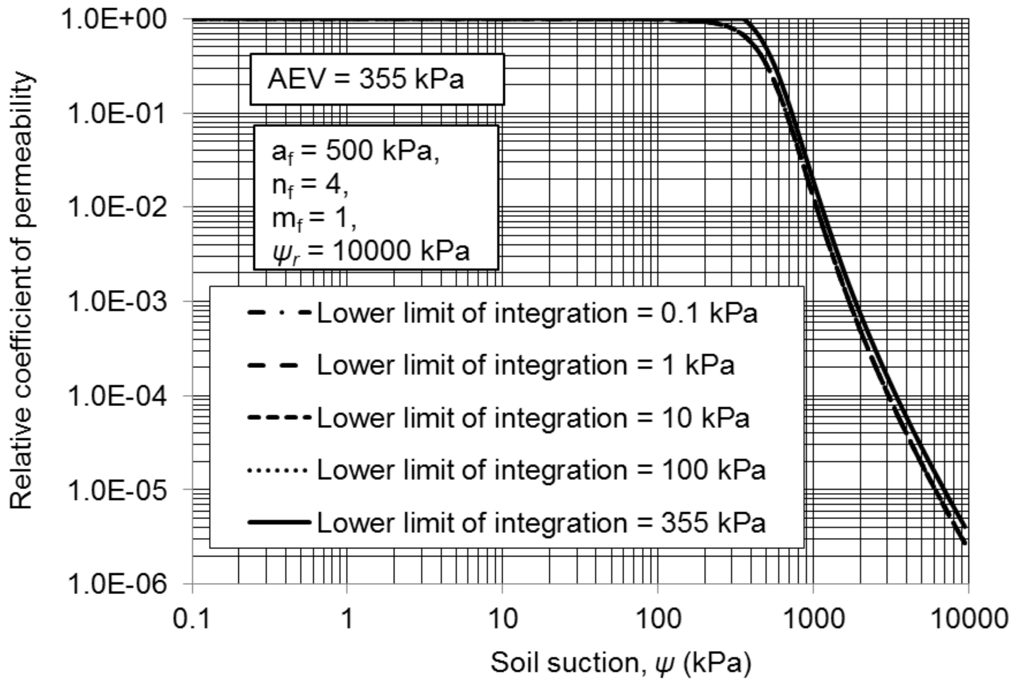

Figure 2-3. Relative coefficient of permeability obtained using Eq. [8] with different lower limits of integration for a soil with a_f = 500 kPa, n_f = 4, m_f = 1, ψ_r = 10000 kPa for SWCC.

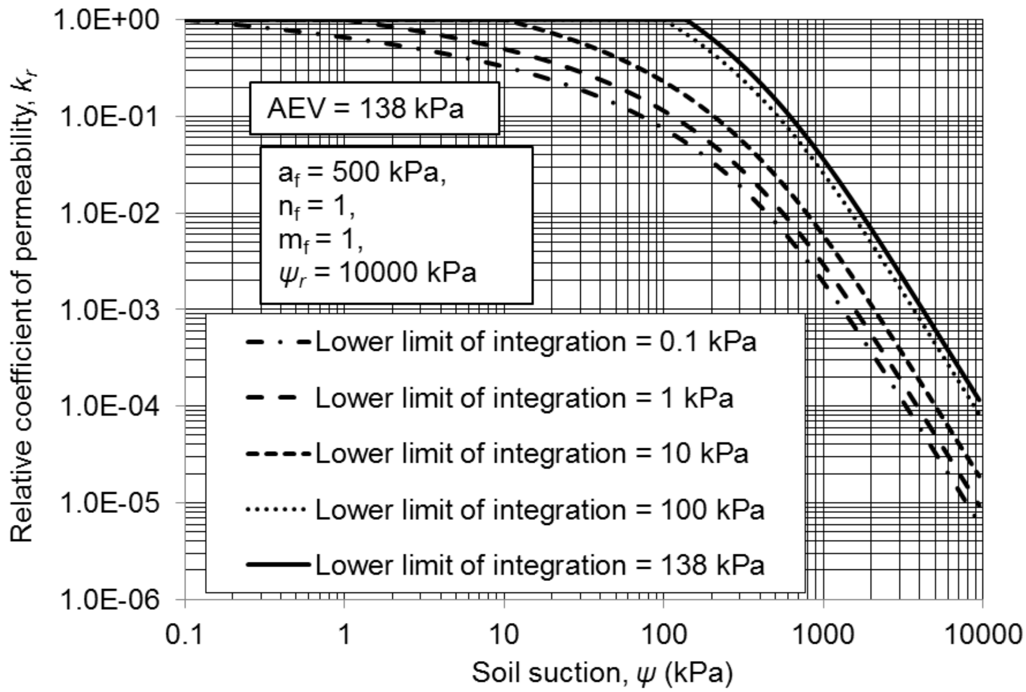

Figure 2-4. Relative coefficient of permeability obtained using Eq. [8] with different lower limits of integration for a soil with a_f = 500 kPa, n_f = 1, m_f = 1, ψ_r = 10000 kPa for SWCC.

The shape of the SWCC greatly influences the errors that could be caused in the estimation results for the permeability function. Therefore, it is important to study the effect of each of the four fitting parameters, a_f, n_f, m_f, and ψ_r, on the errors in the permeability function that is introduced by using a small value as the lower limit of integration. The objective of this paper is to examine the effect of each of the fitting variables, a_f, n_f, m_f, and ψ_r, on errors in the relative permeability function that is caused by using various small values for the lower limit of integration.

2.3.1 Definition of the error introduced by using an inappropriate lower limit of integration

ERR(ψ, ψ_i) is the mathematical function used to quantify the error introduced as a result of selecting various values for the lower limit of integration. More specifically, it is the change in permeability introduced by using Eq. [8] with a lower limit of integration other than the AEV in the denominator. The comparison is made to the permeability obtained when using Eq. [7] with the AEV as the lower limit of integration in the integral in the denominator. The mathematical form of the error ERR(ψ, ψ_i) is given by Eq. [9].

$$ERR\left(\psi,\psi_i\right)=\begin{cases} 0 & ,\ 0<\psi<\psi_i<\psi_{aev} \\ \mathrm{Log}_{10}\left(\dfrac{\displaystyle\int_{\ln(\psi_i)}^{b}\frac{S\left(e^y\right)-S\left(\psi_i\right)}{e^y}S'\left(e^y\right)dy}{\displaystyle\int_{\ln(\psi)}^{b}\frac{S\left(e^y\right)-S\left(\psi\right)}{e^y}S'\left(e^y\right)dy}\right) & ,\ 0<\psi_i\le\psi\le\psi_{aev} \\ \mathrm{Log}_{10}\left(\dfrac{\displaystyle\int_{\ln(\psi_i)}^{b}\frac{S\left(e^y\right)-S\left(\psi_i\right)}{e^y}S'\left(e^y\right)dy}{\displaystyle\int_{\ln(\psi_{aev})}^{b}\frac{S\left(e^y\right)-S\left(\psi_{aev}\right)}{e^y}S'\left(e^y\right)dy}\right) & ,\ 0<\psi_i<\psi_{aev}<\psi \end{cases} \qquad [9]$$

The error is defined in terms of orders of magnitude. ERR(ψ, ψ_i) in Eq. [9] is the common logarithm of the ratio of the permeability at any soil suction, ψ, estimated by Eq. [7], to the permeability estimated by Eq. [8] with ψ_i set at various lower limits of integration in the denominator. The lower limit of integration ψ_i in Eq. [8] is a suction value between the AEV and a lower suction. The definition of ERR(ψ, ψ_i) implies that the closer the value ERR(ψ, ψ_i) is to 0, the smaller the error. The error ERR(ψ, ψ_i) remains at a constant value equal to ERR(AEV, ψ_i) for soil suctions greater than the AEV. ERR(AEV, ψ_i) is the upper bound of the error ERR(ψ, ψ_i) and it represents the largest error across the entire soil suction range when using various ψ_i values as the lower limit of integration rather than the AEV in Eq. [8] when calculating the relative permeability.

The error at the AEV, ERR(AEV, ψ_i) rather than the error, ERR(ψ, ψ_i), across the entire suction range is studied in a parametric manner. Figure 2-5 illustrates the meaning of the error at the AEV, ERR(AEV, ψ_i) in terms of orders of magnitude caused by using ψ_i as the lower limit of integration in Eq. [8].

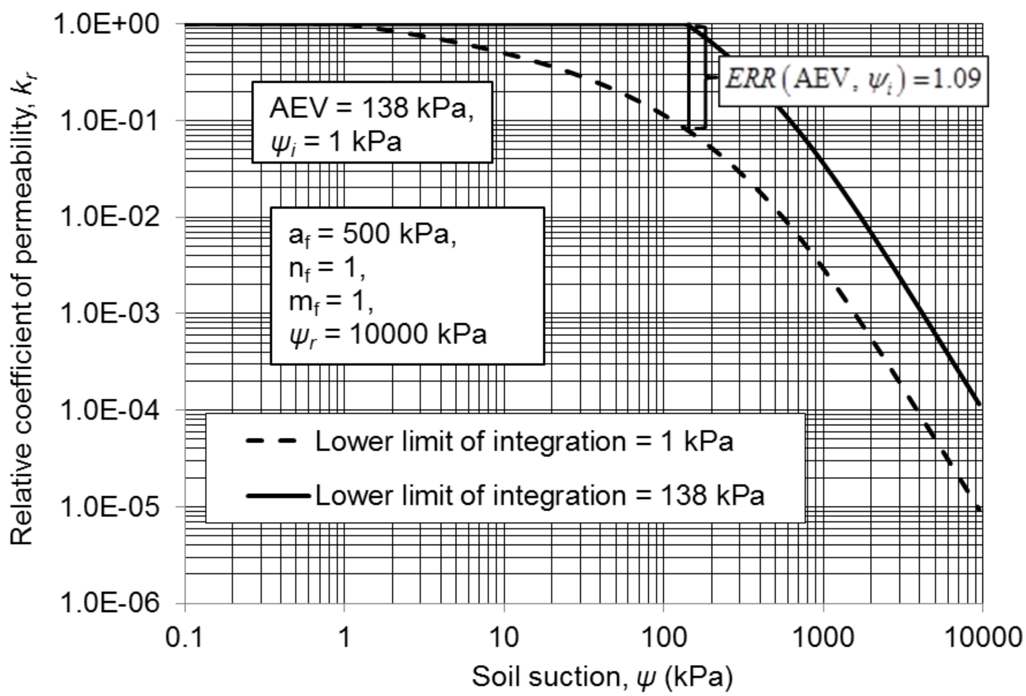

Figure 2-5. Error at AEV in terms of orders of magnitude caused by using ψ_i equal to 1 kPa as the lower limit of integration in Eq. [8].

2.4 The sensitivity of ERR (AEV, ψ_i) to changes in the best-fitting parameters a_f, n_f, m_f, and ψ_r for the SWCC

A parametric study was undertaken to investigate the empirical relationships between the best-fitting parameters a_f, n_f, m_f, and ψ_r of the SWCC and the error of ERR(ψ, ψ_i), associated with the Fredlund, Xing, and Huang permeability function. The error at the AEV, ERR(AEV, ψ_i), rather than the error, ERR(ψ, ψ_i), across the entire suction range is studied for simplification. Table 2-1 summarizes the parametric study in matrix form.

Table 2-1. Matrix of fitting parameters used in the parametric study.

Figure No.	Designated values				
	n_f	m_f	a_f (kPa)	ψ_r (kPa)	Lower limit of integration (in terms of Log_{10} cycles less than the AEV)
Figure 2-6	1	1	10	2000	various
Figure 2-7	1	1	100	2000	various
Figure 2-8	0.5 - 12	1	10	2000	various
Figure 2-9	0.5 - 12	1	100	2000	various
Figure 2-10	0.5 - 12	1	various	2000	4
Figure 2-11	2	0.5 - 4	10	2000	various
Figure 2-12	2	0.5 - 4	100	2000	various
Figure 2-13	2	0.5 - 4	various	2000	4

2.4.1 Influence of n_f value on ERR (AEV, ψ_i)

The sensitivity of the error in the permeability function at the AEV to the change of the n_f value on the SWCC is studied for permeability functions obtained using Eq. [8]. Seven different lower limits of integration ψ_i were selected for the integral in the denominator. These seven different lower limits of integration are 10, 4, 2, 1, 0.5, 0.2, and 0.1 $\log_{10}$ cycles less than the empirical AEV. Figures 2-6 and 2-7 show the errors in the estimation of the relative coefficient of permeability caused by using various lower limits of integration when a_f = 10 kPa and a_f = 100 kPa, respectively (Note: n_f = 1; m_f = 1; ψ_r = 2000 kPa).

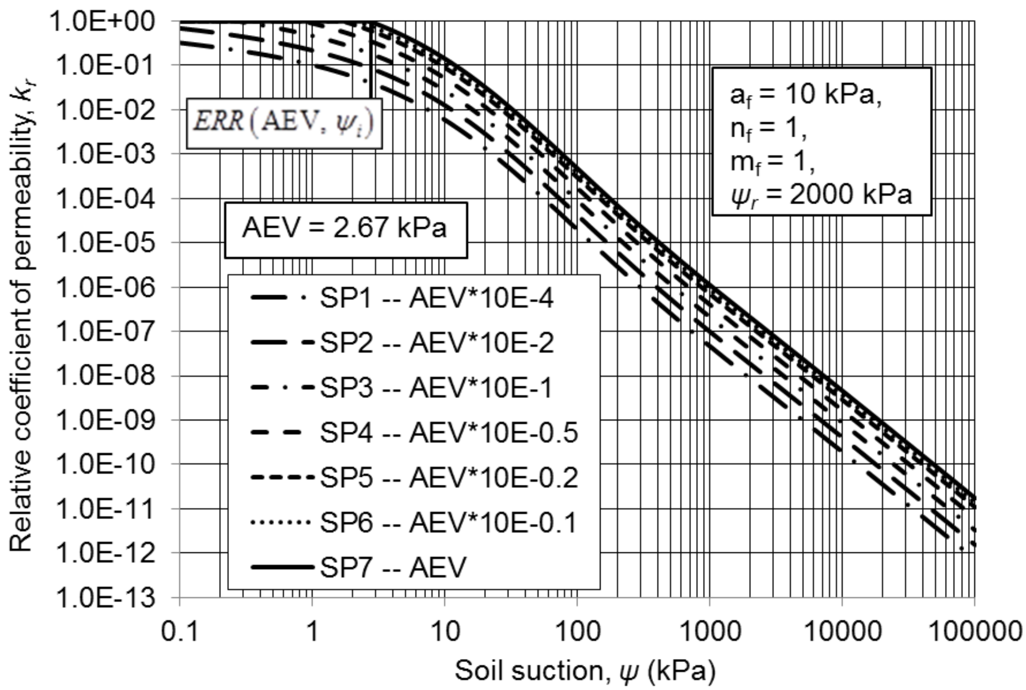

Figure 2-6. Error in estimation of relative coefficient of permeability caused by various lower limits of integration (a_f = 10 kPa; n_f = 1; m_f = 1; ψ_r = 2000 kPa).

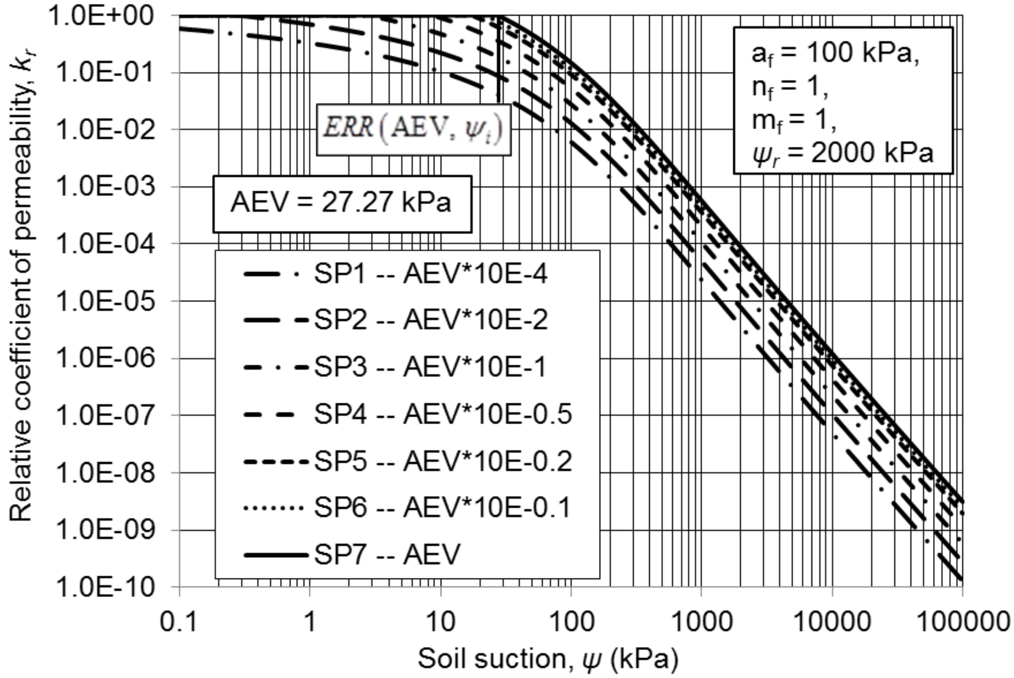

Figure 2-7. Error in estimation of relative coefficient of permeability caused by various lower limits of integration (a_f = 100 kPa; n_f = 1; m_f = 1; ψ_r = 2000 kPa).

The empirical relationships between ERR(AEV, ψ_i) and the corresponding n_f value for various ψ_i are plotted in Figures 2-8 and 2-9. A value of 1 on the vertical coordinate refers to one order of magnitude change in the coefficient of permeability at the AEV, and a value of 4 would mean four orders of magnitude. Figure 2-8 reveals the influence of n_f on the errors when a_f = 10 kPa; m_f = 1; ψ_r = 2000 kPa. Figure 2-9 shows the influence of n_f on the errors when a_f = 100 kPa; m_f = 1; ψ_r = 2000 kPa. In Figures 2-6 to 2-9, the curve denoted by SP1 in the legend is related to the error caused by using a value four $\log_{10}$ cycles less than the empirical AEV as the lower limit of integration. The curve denoted by SP2 in the legend is for the error caused by using a lower limit of integration that is two $\log_{10}$ cycles less than the empirical AEV. The other notations (e.g., SP3, SP4, SP5, and SP6) can be interpreted in the same way as interpreted for SP1 and SP2.

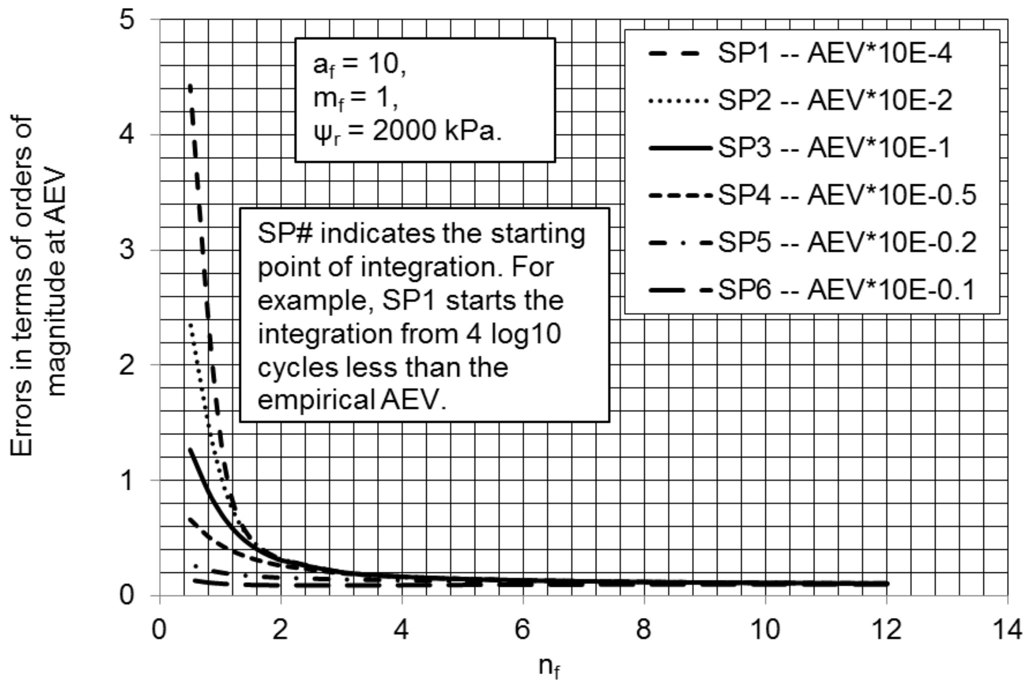

Figure 2-8. Influence of n_f on errors caused by using various lower limits of integration (a_f = 10 kPa; n_f = 1; m_f = 1; ψ_r = 2000 kPa).

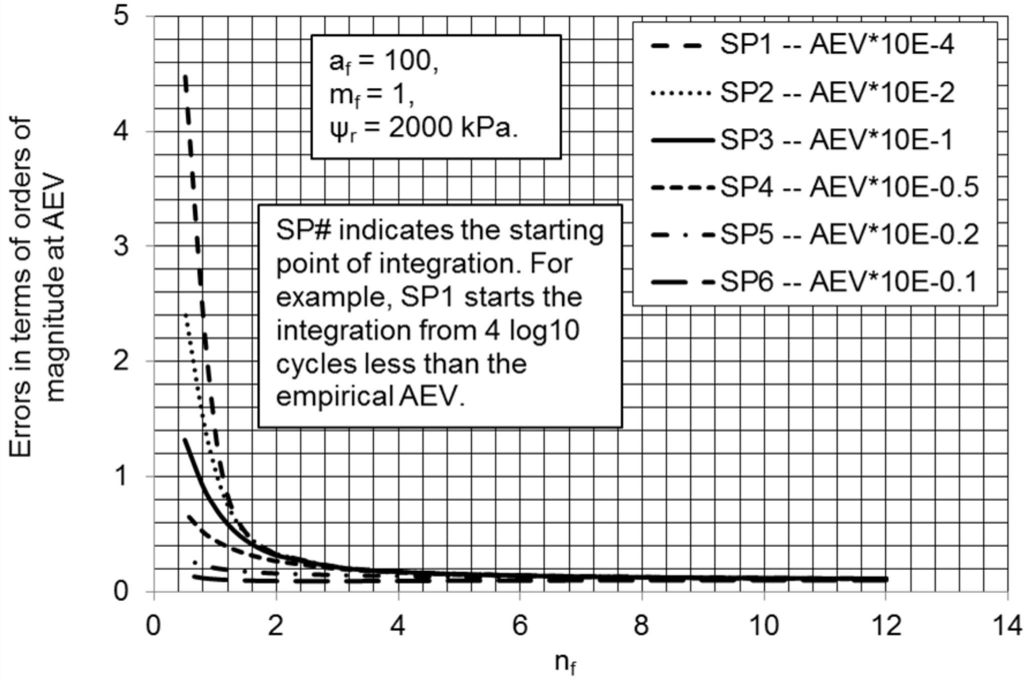

Figure 2-9. Influence of n_f on errors caused by using various lower limits of integration (a_f = 100 kPa; n_f = 1; m_f = 1; ψ_r = 2000 kPa).

Figures 2-7 and 2-8 show a similar pattern when different a_f values are selected. The results show the errors in the estimation of the relative permeability at the AEV when using Eq. [8] with different lower limits of integration ψ_i instead of using Eq. [7] with the AEV as the starting integration point. The results in Figures 2-7 and 2-8 reveal that the error decreases with an increase in the n_f value, particularly when the n_f value is smaller than 2. The slope of the change of the error versus the n_f value becomes much steeper at small n_f values. This is particularly true for errors caused by using a lower limit of integration that is beyond two $\log_{10}$ cycles less than the AEV. The results also show that using a value of more $\log_{10}$ cycles separated from the AEV as the lower limit of integration produces a greater error in the estimated permeability function for a particular SWCC. This phenomenon is more apparent when the n_f value is smaller than 2. In this case, the estimated relative permeability is significantly influenced by the selected lower limit of integration for a particular SWCC. It is important to use the correct lower limit of integration (i.e., the computed AEV), in the estimation of the permeability function.

Figure 2-10 presents errors caused by using a lower limit of integration of four $\log_{10}$ cycles less than the AEV for permeability functions obtained from SWCCs with various a_f values. The purpose of arranging the results in this manner is to show how the a_f value affects the error in the estimation of the permeability function when an inappropriate lower limit of integration is used. The starting point for integration is denoted in terms of the $\log_{10}$ cycles less than the AEV. It was found that the a_f value does not have much influence on the error caused by using the inappropriate lower limit of integration. However, the error is more sensitive to the a_f value when it is combined with small n_f values. Table 2-2 presents the range of the magnitude of the error in the estimation of permeability when the n_f value changes from 0.5 to 12, with m_f = 1 and ψ_r = 2000 kPa. The table shows that if a_f is equal to 1 kPa and the integration starts from a value of 10 $\log_{10}$ cycles less than the AEV, the error would range from 0.1 to 10 orders of magnitude when the n_f value changes from 0.5 to 12, respectively.

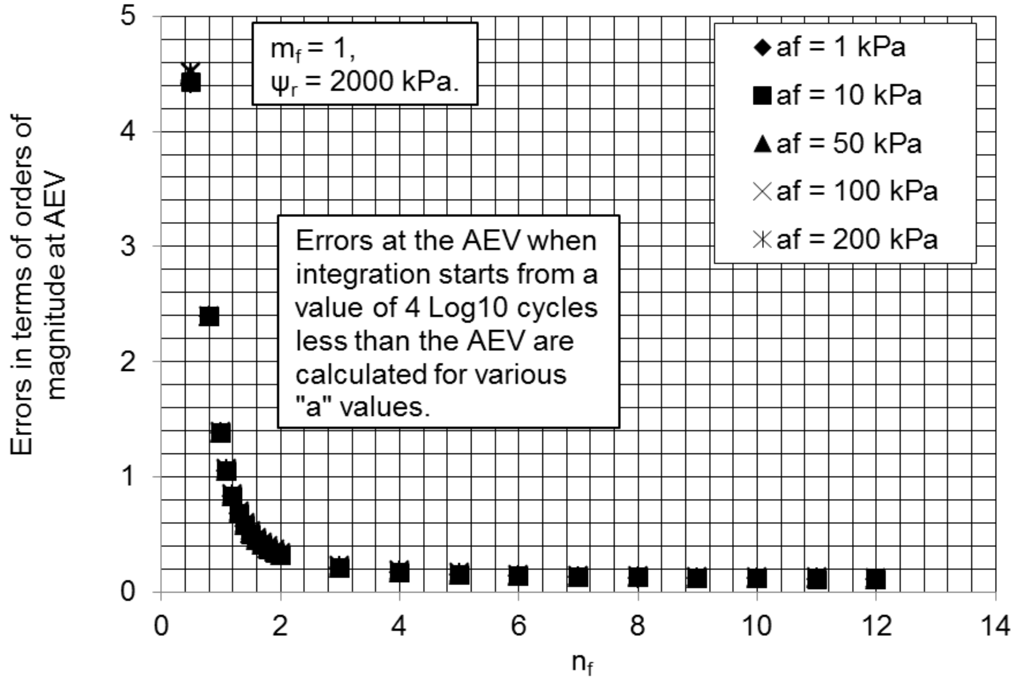

Figure 2-10. Influence of n_f on errors caused by using a lower limit of integration of four $\log_{10}$ cycles less than the AEV in cases of various a_f values.

Table 2-2. Range of the magnitude of the error in estimation of permeability when n_f value changes from 0.5 to 12. (m_f = 1; ψ_r = 2000 kPa)

Integration starts at this number of Log_{10} cycles less than the AEV	Error when a_f is a designated value				
	a_f = 1 kPa	a_f = 10 kPa	a_f = 50 kPa	a_f = 100 kPa	a_f = 200 kPa
10	0.107~10.424	0.107~10.434	0.110~10.495	0.113~10.527	0.124~10.521
4	0.107~4.418	0.107~4.427	0.109~4.487	0.112~4.519	0.119~4.512
2	0.107~2.367	0.107~2.375	0.109~2.425	0.111~2.451	0.117~2.443
1	0.107~1.262	0.107~1.267	0.109~1.301	0.110~1.316	0.114~1.309
0.5	0.107~0.659	0.107~0.662	0.108~0.681	0.108~0.689	0.110~0.683
0.2	0.106~0.272	0.106~0.273	0.106~0.281	0.105~0.284	0.104~0.281
0.1	0.091~0.137	0.091~0.138	0.090~0.142	0.090~0.143	0.089~0.142

2.4.2 Influence of m_f value on ERR (AEV, ψ_i)

The sensitivity of the error in the permeability function (at the AEV) to changes in the m_f value is studied for permeability functions obtained using Eq. [8] with various lower limits of integration. The results are shown in Figures 2-11 to 2-13. Figures 2-11 and 2-12 are for different a_f values and show the errors in the estimation of permeability at AEV caused by using Eq. [8] with different lower limits of integration ψ_i instead of the AEV. Figure 2-13 presents the errors in a different manner to show the effect of the a_f value on the error in the estimation of the permeability function when an inappropriate lower limit of integration is used. The errors in the comparison at particular m_f value are for permeability functions obtained from SWCCs with varying a_f values.

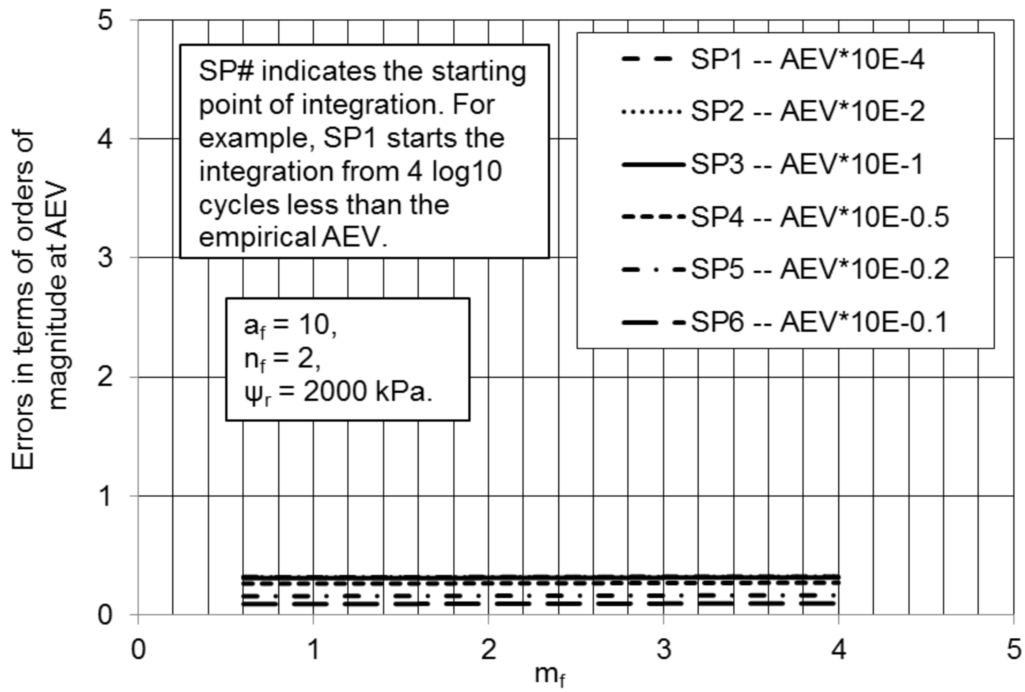

Figure 2-11. Influence of m_f on errors caused by using various lower limits of integration (a_f = 10 kPa; n_f = 2; ψ_r = 2000 kpa).

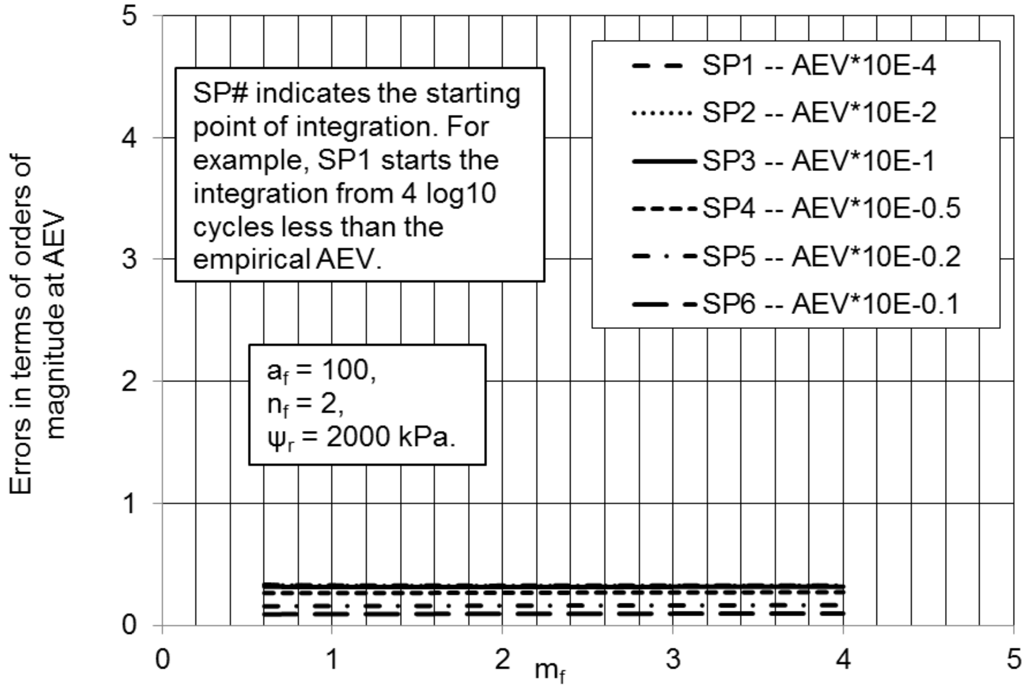

Figure 2-12. Influence of m_f on errors caused by using various lower limits of integration (a_f = 100 kPa; n_f = 2; ψ_r = 2000 kpa).

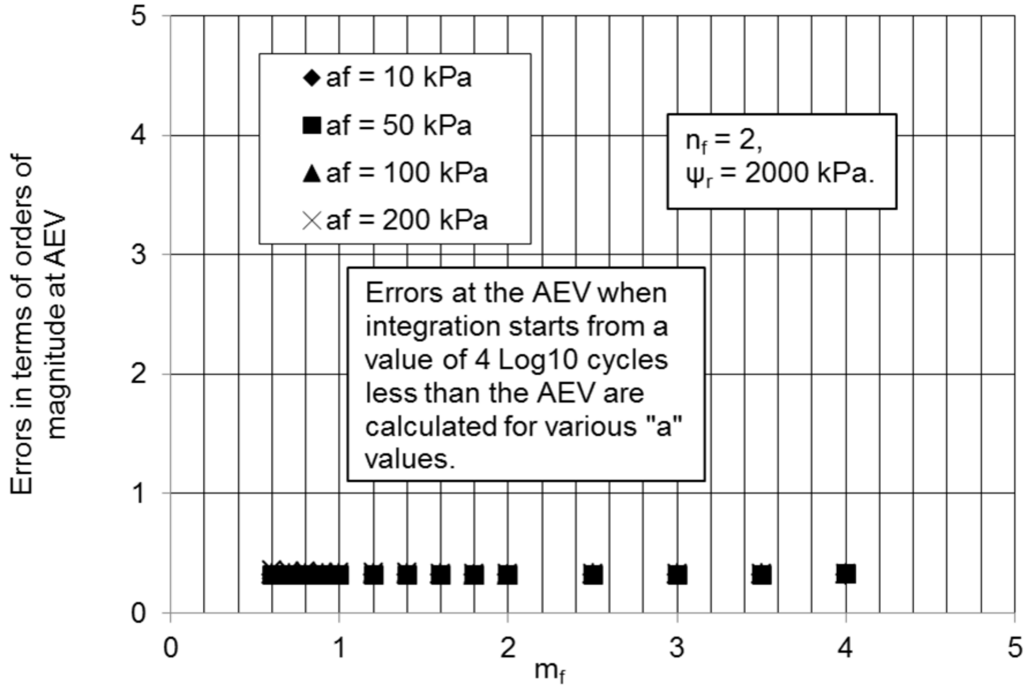

Figure 2-13. Influence of m_f on errors caused by using a lower limit of integration of four $\log_{10}$ cycles less than the AEV in cases of various a_f values.

The results show that the error caused by a lower limit of integration of several $\log_{10}$ cycles less than the AEV does not change much with changing m_f values for the SWCCs. In other words, the m_f value of the SWCC has limited influence on the errors in the estimation of the permeability function that may be caused by a low starting point of integration. The greater difference the lower limit of integration has from the AEV, the larger the error for the permeability function for a particular SWCC. Figure 3-12 also shows that the influence of the a_f value of the SWCC having on the error is small when n_f, m_f, and ψ_r are fixed. The smaller the a_f value, the less the error caused by using a lower limit of integration below the AEV. The influence of the a_f value on the error is relatively apparent at small m_f values. Table 2-3 shows the range of the magnitude of the error in the estimation of permeability when the m_f value changes from 0.5 to 4 with n_f = 2 and ψ_r = 2000 kPa.

Table 2-3. Range of magnitude of the error in estimation of permeability when m_f value changes from 0.5 to 4. (n_f = 2; ψ_r = 2000 kPa)

Integration starts at this number of Log_{10} cycles less than the AEV	Error when a_f is a designated value			
	a_f = 10 kPa	a_f = 50 kPa	a_f = 100 kPa	a_f = 200 kPa
10	0.317~0.323	0.321~0.326	0.325~0.339	0.333~0.374
4	0.317~0.323	0.320~0.324	0.324~0.333	0.331~0.353
2	0.317~0.322	0.320~0.324	0.323~0.330	0.329~0.344
1	0.309~0.315	0.311~0.316	0.313~0.317	0.317~0.324
0.5	0.262~0.270	0.263~0.270	0.264~0.271	0.266~0.271
0.2	0.156~0.164	0.156~0.164	0.156~0.164	0.156~0.164
0.1	0.090~0.096	0.090~0.096	0.090~0.096	0.089~0.096

2.4.3 Influence of ψ_r/a_f value on ERR (AEV, ψ_i)

The influence of the ψ_r/a_f value on the error in the permeability function at the AEV was also studied using Eq. [8] with different lower limits of integration. The results show that the magnitude of the error caused by a small value for the lower limit of integration (i.e., $\log_{10}$ cycles less than the AEV) does not significantly change with the ψ_r/a_f value except when the ψ_r/a_f value is smaller than 10. Also, the influence of the a_f value on the error is negligible.

2.4.4 Comparison of influences of n_f, m_f, and ψ_r/a_f values on magnitude of error

The error in terms of orders of magnitude caused by using an inappropriate lower limit of integration that is 10 $\log_{10}$ cycles less than the AEV can vary from 0.1 to 10 when the n_f value changes from 12 to 0.5 with m_f = 1 and ψ_r = 2000 kPa. The change in the magnitude of error is within 0.05 orders of magnitude when the m_f value changes between 0.5 to 4 with n_f = 2 and ψ_r = 2000 kPa. There is a change of about 0.5 orders of magnitude in the error when the ψ_r/a_f value changes from 1 to 1000 kPa with n_f = 2 and m_f = 1 kPa.

The analysis reveals that the influence of the n_f on the error caused by using too low a lower limit of integration is much greater than the influence of the m_f and ψ_r/a_f values. The a_f has limited influence on the error. The lower the starting point of integration below the AEV is, the greater the calculation error.

2.5 Conclusions

Following is a summary of the conclusions that can be drawn from the study related to the starting point of integration for the Frendlund, Xing, and Huang (Fredlund et al. 1994) permeability function.

1. If a lower limit of integration used in the integral of Fredlund et al. (1994) is smaller than the AEV, the computed results will underestimate the relative coefficient of permeability. The smaller the value used for the starting point of integration compared to the AEV, the greater will be the difference between the computed results and the relative permeability.

2. The error caused by using a small value for the lower limit of integration is influenced by the fitting parameters of the Fredlund and Xing (1994) SWCC equation, namely a_f, n_f, m_f, and ψ_r. The analysis reveals that the influence of the n_f value is much greater than the influence of the a_f, m_f, and ψ_r/a_f values.

3. The difference caused by a particular lower limit of integration, defined in terms of a particular number of $\log_{10}$ cycles less than the AEV, decreases with an increase in the n_f value when the values of a_f, m_f, and ψ_r are fixed. This is particularly true when the n_f value is smaller than 2.

4. The m_f value for the SWCC has limited influence on the difference in the estimation of the permeability function that may be caused by a low starting point of integration.

5. The difference in the estimation of the relative coefficient of permeability caused by using a particular low starting point of integration usually does not change much with the change in the a_f value. However, the difference becomes more sensitive to the a_f value when it is combined with small n_f and m_f values.

6. It is recommended that the AEV always be used as the lower limit of integration when estimating the relative permeability function with the Fredlund et al. (1994) estimation procedure.

7. Further studies regarding the importance of the AEV in the estimation of the relative permeability function are recommended to be undertaken where other physical models are used along with other SWCCs.

References

Bharat, T.V., and Sharma, J. 2012. Validity limits of Fredlund–Xing–Kunze model for the estimation of hydraulic properties of unsaturated soils. In Proceedings of the Canadian Geotechnical Conference, Winnipeg, Man., 30 September – 3 October. Paper No. 263.

Brooks, R.H., and Corey, A.T. 1964. Hydraulic properties of porous media. Colorado State University, (March) Hydraulic Paper No. 3.

Burdine, N. 1953. Relative permeability calculations from pore size distribution data. Transactions of the AIME, 198: 71–77.

Childs, E.C., and Collis-George, N. 1950. The permeability of porous materials. Proceedings of the Royal Society of London, Series A: Mathematical and Physical Sciences, 201(1066): 392–405.

Fredlund, D.G., and Xing, A. 1994. Equations for the soil-water characteristic curve. Canadian Geotechnical Journal, 31(4): 521–532.

Fredlund, D.G., Xing, A., and Huang, S. 1994. Predicting the permeability function for unsaturated soils using the soil-water characteristic curve. Canadian Geotechnical Journal, 31(4): 533–546.

Fredlund, D.G., Stone, J., Stianson, J., and Sedgwick, A. 2011. Determination of water storage and permeability functions for oil sands tailings. In Proceedings of the Tailings and Mine Waste Conference, Vancouver, B.C.

Fredlund, D.G., Rahardjo, H., and Fredlund, M.D. 2012. Unsaturated soil mechanics in engineering practice. John Wiley & Sons, New York.

Mualem, Y. 1976. A new model for predicting the hydraulic conductivity of unsaturated porous media. Water Resources Research, 12(3): 513–522.

Mualem, Y., and Klute, A. 1986. Hydraulic conductivity of unsaturated soils: prediction and formulas. In Methods of soils analysis. Part 1. Physical and mineralogical methods. pp. 799–823.

van Genuchten, M.T. 1980. A closed-form equation for predicting the hydraulic conductivity of unsaturated soils. Soil Science Society America Journal, 44(5): 892–898.

Vanapalli, S.K., Sillers, W.S., and Fredlund, M.D. 1998. The meaning and relevance of residual state to unsaturated soils. In Proceedings of the Fifty-First Canadian Geotechnical Conference, Edmonton, Alta., 4–7 October. pp. 1–8.

Williams, P.J. 1982. The surface of the Earth, an introduction to geotechnical science. Longman Inc., New York.

Chapter 3. Water permeability function for soils that undergo volume change as suction changes

3.1 Introduction

Geotechnical engineering problems involving transient seepage and contaminant transport can be reduced to the solution of a partial differential equation. Most computer software packages available in geotechnical engineering practice are partial differential equation based (e.g., SVOffice 2009, GeoStudio 2012). Each partial differential equation contains material properties that are either constants or mathematical functions. The correctness of the numerical modeling results depends largely on the accuracy of the input of the material properties. In other words, the material properties must be accurate in order to obtain reasonable output results from the computer software. The permeability function (i.e., saturated/unsaturated coefficient of permeability function) constitutes one of the soil property functions necessary for numerical modeling simulations.

Direct measurement of the coefficient of permeability for an unsaturated soil is time-consuming and expensive. Numerous estimation techniques have been proposed in the literature to obtain the unsaturated permeability function. These estimation procedures have been based on the implicit assumption that the soil undergoes negligible overall volume change as soil suction is increased. Leong et al. (1997) examined permeability functions for unsaturated soils with no volume change. The existing unsaturated coefficient of permeability functions have been most often estimated from the volumetric water content soil-water characteristic curve (θ-SWCC) in conjunction with a measured constant saturated coefficient of permeability. The van Genuchten-Burdine (1980) equation, van Genuchten-Mualem (1980) equation and Fredlund-Xing-Huang (1994) permeability function are three well-known equations used for the estimation of the unsaturated permeability function. The assumption of zero overall volume change with suction increase may be suitable for sands or coarse-grained materials, but it is not acceptable for some fine-grained soils and initially slurry clays. Many of the studies have noticed the influence of both the degree of saturation and the void ratio on the coefficient of permeability function for a deformable soil. Huang et al. (1998) developed a coefficient of permeability for a deformable unsaturated porous medium considering only the volume change before desaturation. Huang et al. (1998) proposed to account for the effect of void ratio on the saturated coefficient of permeability, but the relative permeability was obtained from the volumetric water content SWCC, which is not appropriate for a volume-change soil. Parent et al. (2007) conducted SWCC test on deinking by-products (DBP), a highly compressible industrial by-product which have been successfully used as a cover material in both landfills and mining applications as well as a soil structural enhancement material in agricultural applications.

The presently existing methods are not adequate for estimating the permeability function for a soil that undergoes high volume change as soil suction changes. Inaccuracies in the estimation of the unsaturated permeability function can cause erroneous numerical modeling results and consequently affect engineering decisions. The estimation procedure for the permeability function should take into consideration both desaturation and volume change when estimating the permeability function. Only then is it possible to undertake a reliable numerical modeling simulation of high volume change soils.

This paper presents a revised estimation method for the prediction of the saturated/unsaturated coefficient of permeability function for soils that undergo volume change as soil suction changes. The proposed methodology is based on the Fredlund-Xing-Huang (1994) permeability function. Both void ratio and degree of saturation are taken into account as factors that affect the estimated unsaturated permeability function. Experimental data for initially slurry Regina clay (Fredlund 1964) are presented and interpreted for the illustration of the revised estimation methodology. Regina clay initially in a slurry form undergoes significant volume change when the soil is saturated before reaching the air-entry value (AEV) during a drying process. The proposed methodology can also be applied to soils such as DBP that continue to undergo considerable amount of volume changes when the applied suction exceeds the air-entry value.

3.2 Literature review

The shrinkage curve and the soil-water characteristic curve are two soil property curves pivotal to the estimation of the coefficient of permeability function for high volume change materials. Numerous research studies have been undertaken related to the shrinkage curve, the soil-water characteristic curve and the unsaturated coefficient of permeability function. A brief summary of findings follows.

The shrinkage of a soil involves the process of drying a soil under increasing soil suction. Researchers in the early 1900s undertook studies to investigate the character of shrinkage (Tempany 1917). Efforts were made to define the shrinkage process of soils (Bronswijk 1991, Haines 1923, Keen 1931, Stirk 1954). Structural shrinkage, normal shrinkage, residual shrinkage and zero shrinkage are four shrinkage phases that were identified. A detailed interpretation of the shrinkage curve was presented by Haines (1923). The study focused on normal shrinkage and residual shrinkage. Terzaghi (1925) studied shrinkage behavior and compared shrinkage to the compression of a soil. Sridharan and Rao (1971) discussed the physical mechanism involved in the process of shrinkage in a clay soil. The shrinkage behavior was explained through use of a modified effective stress concept. Marinho (1994) carried out a comprehensive study of shrinkage curve functions. Fredlund (2000) presented a mathematical equation describing the shrinkage curve and also provided a theoretical method for estimating the shrinkage curve. The shrinkage curve equation proposed by Fredlund (2000) is later used in the development of a revised theory for the estimation of the coefficient of permeability function for high volume change soils.

The soil-water characteristic curve (SWCC) is an unsaturated soil property that shows the relationship between the amount of water in a soil and various applied soil suction values (Fredlund and Rahardjo 1993). SWCC has been commonly used for the estimation of other unsaturated soil property functions such as the unsaturated coefficient of permeability function, the water storage function, and the shear strength function. It is important that the SWCC be accurately represented by the proposed mathematical equation. Numerous equations have been proposed in the literature by various researchers (Assouline et al. 1998, Assouline et al. 2000, Brooks and Corey 1964, Brutsaert 1967, Bumb et al. 1992, Campbell 1974, Farrell and Larson 1972, Fredlund and Xing 1994, Gardner 1958, Groenevelt and Grant 2004, Kosugi 1994, Laliberte 1968, McKee and Bumb 1984, McKee and Bumb 1987, Pachepsky et al. 1995, Parent et al 2007, Pereira and Fredlund 2000, Pham and Fredlund 2008, Russo 1988, van Genuchten 1980). Each equation has been developed in response to the desire to provide a representation of a soil-water characteristic curve that better represents the characteristics observed in natural soils.

The Brooks and Corey (1964) equation, the Gardner (1974) equation, three forms of van Genuchten (1980) equation and the Fredlund-Xing (1994) equation appear to be the six most commonly used SWCC equations in geotechnical engineering. The Brooks and Corey (1964) equation takes the form of a power-law relationship starting at the air-entry value for the soil. Although the Brooks and Corey (1964) equation has the advantage of simplicity in form, it has the primary drawback that it is discontinuous at the air-entry value where desaturation starts. The Gardner (1974) equation is a continuous function originally proposed to best-fit laboratory unsaturated soil permeability data to form a coefficient of permeability function. (The Gardner permeability function was later used to define the SWCC). Van Genuchten (1980) originally developed a three-parameter SWCC equation with the flexibility to fit a wide range of soils. Simplification of the van Genuchten (1980) equation was made by prescribing a fixed relationship between the *m* and *n* fitting variables. The proposed simplifications made it possible to obtain a closed-form permeability function for an unsaturated soil when substituting the SWCC equation into the Burdine (1953) and the Mualem (1976) integral formula for the unsaturated permeability function. The two-parameter van Genuchten (1980) equations have less mathematical flexibility than the original three-parameter van Genuchten (1980) equation when best-fitting the experimental SWCC data. The van Genuchten (1980) equation provides a reasonable fit for laboratory test data at high and medium water contents but does not apply to suctions higher than the residual conditions (Zhang 2010). The Fredlund-Xing (1994) equation is a four-parameter equation which has increased flexibility in fitting a wide range of soils. The equation is capable of fitting experimental data over essentially the entire range of soil suctions. The Fredlund-Xing (1994) SWCC equation is later used in this paper to develop a revised estimation procedure for the permeability function. The development of the revised method for the permeability function focuses on the drying (or desorption) curve; however, in general, the proposed methodology also applies for the wetting (or adsorption) curve.

Research directed towards the estimation of the unsaturated coefficient of permeability function has been extensive. There are four categories of models that have been proposed for the estimation of unsaturated permeability function; namely, empirical models, statistical models, correlation models and regression models (Fredlund et al. 2012). Empirical models and statistical models are the most commonly used models. Empirical models utilize the relationship between the character of the SWCC and the unsaturated permeability function to empirically estimate the unsaturated permeability function from the SWCC. The Brooks and Corey (1964) equation is one of the empirical estimation equations. Statistical models are based on the assumption that both the permeability function and the SWCC are primarily determined by the pore-size distribution of the soil under consideration.

Childs and Collis-George (1950), Burdine (1953) and Mualem (1976) are three commonly used integral formulas that have been used for the further development of various statistical models. Three well-known statistical models have been obtained in the form of the relative coefficient of permeability equations. These are referred to as the van Genuchten-Burdine (1980) equation, the van Genuchten-Mualem (1980) equation and the Fredlund-Xing-Huang (1994) permeability function. These permeability equations were developed by introducing, i.) the van Genuchten (1980) SWCC equation into the Burdine (1953) formula, ii.) the van Genuchten (1980) SWCC equation into the Mualem (1976) formula, and iii.) the Fredlund-Xing (1994) SWCC equation into the Childs and Collis-George (1950) formula. Table 3-1 presents these three well-known statistical equations. A constant saturated coefficient of permeability is generally combined with the relative coefficient of permeability functions to generate the continuous unsaturated coefficient of permeability function.

Table 3-1. Three well-known statistical equations for the relative permeability.

#	Equations
van Genuchten-Burdine equation (1980)	$k_r(\psi) = \frac{k_w(\psi)}{k_s} = \frac{1-(a_{vb}\psi)^{n_{vb}-2}\left[1+(a_{vb}\psi)^{n_{vb}}\right]^{-m_{vb}}}{\left[1+(a_{vb}\psi)^{n_{vb}}\right]^{2m_{vb}}}$
van Genuchten-Mualem equation (1980)	$k_r(\psi) = \frac{\left\{1-(a_{vm}\psi)^{n_{vm}-1}\left[1+(a_{vm}\psi)^{n_{vm}}\right]^{-m_{vm}}\right\}^2}{\left[1+(a_{vm}\psi)^{n_{vm}}\right]^{0.5m_{vm}}}$
Fredlund-Xing-Huang (1994) permeability function	$k_r(\psi) = \int_{\ln(\psi)}^{b} \frac{\theta(e^y)-\theta(\psi)}{e^y}\theta'(e^y)\mathrm{d}y \Big/ \int_{\ln(\psi_{aev})}^{b} \frac{\theta(e^y)-\theta_s}{e^y}\theta'(e^y)\mathrm{d}y$
Notes: $m_{vb} = 1-2/n_{vb}$; $m_{vm} = 1-1/n_{vm}$	

The estimation methods for the prediction of the coefficient of permeability function for an unsaturated soil have been based on the assumption that soil does not undergo volume change as soil suction is increased. The Fredlund-Xing-Huang (1994) permeability function is revised (in this paper) for the development of a coefficient of permeability function that can be used for materials that undergo volume change as suction is changed.

3.3 Theory

The theory section deals with the relationship between the soil-water characteristic curve and the shrinkage curve for a soil, as well as the consistency that must be maintained with respect to the designations of volume change and water content change.

3.3.1 Designations of water content and basic volume-mass relationships

Water content can be designated in terms of either mass or volume as a ratio that quantifies the amount of water contained in a soil. There are four designations of water content that are used to define the amount of water in a soil:

1.) Gravimetric water content, w; $w = \frac{m_w}{m_s} \times 100\%$, where m_w is the mass of water and m_s is the mass of solids.

2.) Volumetric water content, θ; $\theta = \frac{V_w}{V_{to}} \times 100\%$, where V_w is the volume of water and V_{to} is the original total volume of the soil specimen.

3.) Instantaneous volumetric water content, θ_i; $\theta_i = \frac{V_w}{V_{ti}} \times 100\%$, where the volume of water, V_w is referenced to the instantaneous total volume of the soil specimen, V_{ti};

4.) Degree of saturation, S; $S = \frac{V_w}{V_v} \times 100\%$, where the volume of water, V_w is referenced to the instantaneous volume of voids in the soil specimen, V_v.

The most commonly used designation of water content in geotechnical engineering practice is gravimetric water content w. The degree of saturation S is another variable commonly used to indicate the percentage of the voids filled with water. Volumetric water content, θ, has been most commonly used in soil science and agriculture-related disciplines. Volumetric water content, θ, has little meaning in unsaturated soil mechanics except under conditions where there is no overall volume change during a process. In this case the volumetric water content, θ, becomes equal to the instantaneous volumetric water content, θ_i.

The four different quantitative measures of water content are connected by three basic volume-mass relationships as shown below:

$$S = \frac{wG_s}{e} \qquad [10]$$

$$\theta = \frac{Se}{1+e_0} = \frac{wG_s}{1+e_0} \qquad [11]$$

$$\theta_i = \frac{Se}{1+e} = \frac{wG_s}{1+e} \qquad [12]$$

where:
G_s = specific gravity of the solids,
e = void ratio referring to an instantaneous state of a soil specimen, and
e_0 = original void ratio referring to the original state of a soil specimen.

Gravimetric water content is usually measured in most laboratory tests due to the convenience of the mass measurements. Other designations of water contents are usually obtained indirectly using basic volume-mass relationships based on the measurement of the gravimetric water content and the shrinkage curve.

Water content in a dimensionless form can be obtained by dividing each of the defined water contents by the value at its original wetted (or zero suction) state. Four types of water content in a dimensionless form are presented as the following equations.

$$w_d = \frac{w}{w_0} = \frac{S\,e}{G_s} \bigg/ \frac{S_0\,e_0}{G_s} = \frac{e}{e_0}\frac{S}{S_0} \quad [13]$$

$$\theta_d = \frac{\theta}{\theta_0} = \frac{S\,e}{1+e_0} \bigg/ \frac{S_0\,e_0}{1+e_0} = \frac{e}{e_0}\frac{S}{S_0} \quad [14]$$

$$\theta_{id} = \frac{\theta_i}{\theta_{i0}} = \frac{S\,e}{1+e} \bigg/ \frac{S_0\,e_0}{1+e_0} = \frac{e\left(1+e_0\right)}{e_0\left(1+e\right)}\frac{S}{S_0} \quad [15]$$

$$S_d = \frac{S}{S_0} \quad [16]$$

where,

d = subscript of d means dimensionless,

0 = subscript of 0 refers to the original state,

w_d = dimensionless gravimetric water content,

θ_d = dimensionless volumetric water content referenced to the original total volume of the soil specimen, V_{to}

θ_{id} = dimensionless instantaneous volumetric water content referenced to the instantaneous total volume of the soil specimen, $V_{ti.}$.

S_d = dimensionless degree of saturation,

w_0 = gravimetric water content at the original state, usually referring to the saturated gravimetric water content corresponding to the initial state of a specimen,

θ_0 = volumetric water content at the original state, usually referring to the saturated volumetric water content at the initial state of a specimen,
θ_{i0} = instantaneous volumetric water content at the original state, which is equal to θ_0.
S_0 = degree of saturation at the original state, usually referring to a value of 1 (or 100%) representing the saturation of a specimen.

If a soil specimen does not change volume during a testing process, it means the void ratio of the specimen remains constant.

$$e=e_0 \qquad [17]$$

Substituting Eq. [17] into Eqs. [13] to [15] and comparing the results to Eq. [16] leads to the following equality for a soil with no volume change.

$$w_d=\theta_d=\theta_{id}=S_d \qquad [18]$$

Eq. [18] reveals that the four types of water content are the same when presented in their dimensionless forms for a soil that does not change overall volume during a process.

If a soil changes overall volume during a testing process (such as the drying of the soil) when measuring the SWCC, the void ratio is changing as well and it is concluded that,

$$e\neq e_0 \qquad [19]$$

Combining Eqs. [13] to [16] and Eq. [19] can produce the following results for a soil that undergoes volume change during a process.

$$w_d \neq \theta_{id} \neq S_d \quad [20]$$

$$w_d = \theta_d \quad [21]$$

Eq. [20] indicates that w_d, θ_{id}, S_d are different from one another when there is volume change. Eq. [21] indicates that w_d is still equal to θ_d when a soil undergoes volume change. However, volumetric water content, θ (or θ_d) does not have any meaningful value when a soil undergoes volume change.

3.3.2 Shrinkage curves

Shrinkage tests are usually conducted in the laboratory in order to record how the void ratio of a soil changes with changes in gravimetric water content during a drying process. A shrinkage curve establishes the relationship between void ratio and gravimetric water content.

Fredlund (2000) proposed the use of a hyperbolic equation to define the shrinkage curve. The equation is as follows.

$$e(w) = a_{sh}\left[\left(\frac{w}{b_{sh}}\right)^{c_{sh}} + 1\right]^{\frac{1}{c_{sh}}} \quad [22]$$

where:
a_{sh} = minimum void ratio, e_{min},
a_{sh}/b_{sh} = slope of the line of tangency,
c_{sh} = curvature of the shrinkage curve, and
w = gravimetric water content.

The Fredlund (2000) equation has the following relationship between the fitting parameters and the volume-mass properties.

$$\frac{a_{sh}}{b_{sh}} = \frac{G_s}{S_0} \tag{23}$$

where: S_0 = initial degree of saturation.

The Fredlund (2000) shrinkage equation describes the shrinkage behavior quite accurately for most soils. The equation is a one-piece smooth curve with $e(w) = \frac{a_{sh}}{b_{sh}} w$ as its asymptotic line. The shrinkage curve moves closer and closer to a straight asymptotic line as the gravimetric water content increases.

Defining the shrinkage curve becomes particularly important when solving geotechnical engineering problems that involve high volume change materials where the total volume changes at various soil suctions must be known.

3.3.3 Soil-water characteristic curves

Soil-water characteristic curves, SWCCs, describe the relationship between the amount of water in a soil and various applied soil suction. The SWCC forms the basis for the estimation of unsaturated soil property functions such as unsaturated permeability function and water storage function. The amount of water in a soil can be defined using four different designations as discussed above. As a result, the SWCC can accordingly take four different forms; namely, gravimetric water content-SWCC (*w*-SWCC), volumetric water content-SWCC (θ-SWCC), instantaneous volumetric water content-SWCC (θ_i -SWCC), and degree of saturation-SWCC (*S*-SWCC).

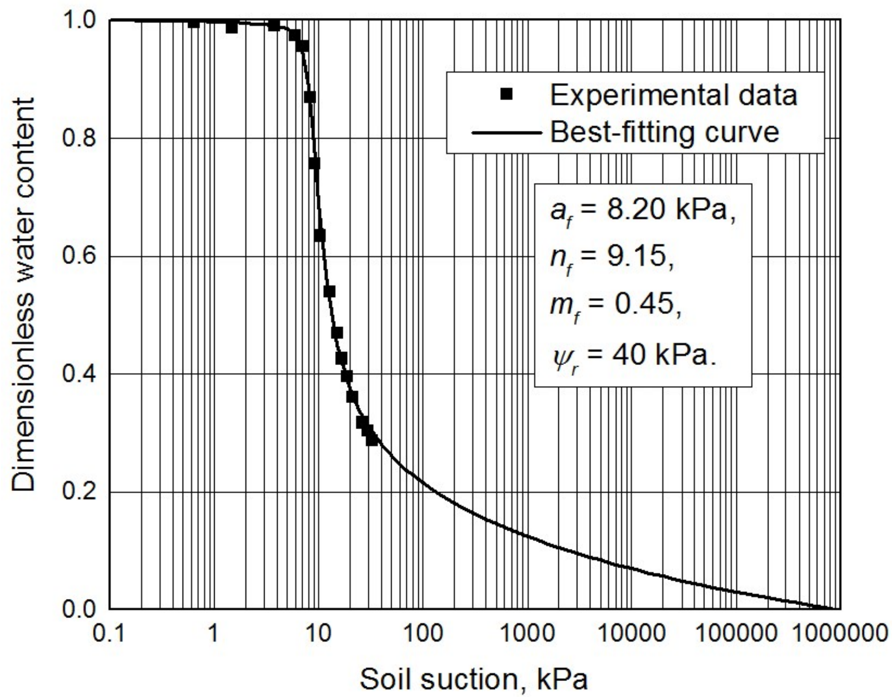

Figure 3-1. Fredlund-Xing (1994) SWCC fit to experimental data for GE3 (Data from Brooks and Corey (1964))

For soils that do not undergo volume change as soil suction changes, all four SWCCs provide the same information to the geotechnical engineer when estimating other unsaturated soil property functions (Figure 3-1). However, for a soil that undergoes volume change as soil suction changes during a drying process, *w*-SWCC, θ_i-SWCC and *S*-SWCC are different from one another. The *w*-SWCC and θ-SWCC provide similar information for a soil that undergoes volume change, but it should be noted that θ-SWCC has no meaningful value in the case where soils undergo high volume changes as soil suction is changed. Regina clay is one such typical example (Figure 3-2).

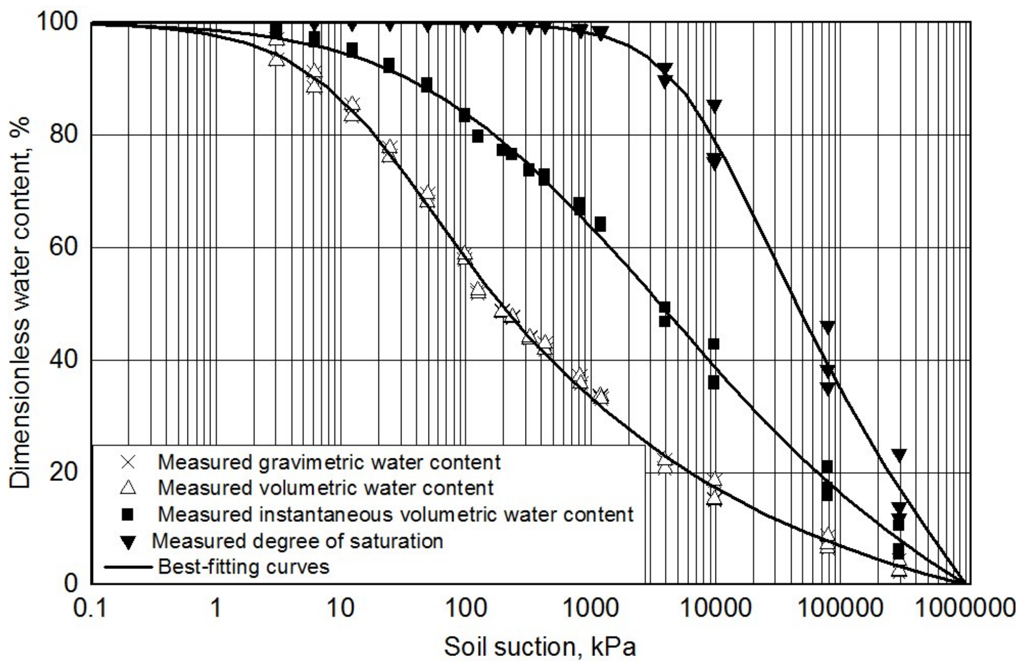

Figure 3-2. Gravimetric water content, volumetric water content (based on both instantaneous and initial total volumes) and degree of saturation versus soil suction for Regina clay. (Data from Fredlund (1964))

Numerous forms of mathematical equations have been suggested to characterize the soil-water characteristic curve. The Fredlund-Xing (1994) equation can be used to provide a reasonable fit of laboratory data over the entire soil suction range. The Fredlund-Xing (1994) SWCC equation is used to best-fit the measured data of the *w*-SWCC in this paper. The equation can be written as follows.

$$w(\psi)=\frac{w_s\left(1-\ln\left(1+\psi/\psi_r\right)/\ln\left(1+10^6/\psi_r\right)\right)}{\left(\ln\left(\exp(1)+\left(\psi/a_f\right)^{n_f}\right)\right)^{m_f}} \qquad [24]$$

where:

ψ = soil suction,

a_f, n_f, m_f, and ψ_r = mathematical fitting parameters,

w_s = initial saturated gravimetric water content, and

$w(\psi)$ = gravimetric water content at a soil suction of ψ.

The best-fitted *w*-SWCC using the Fredlund-Xing (1994) equation can be combined with the shrinkage curve best-fitted equation by Fredlund (2000) equation to calculate the best-fitted curves for the remaining SWCCs.

By substituting Eq. [24] into Eq. [22], a relationship of void ratio versus soil suction can be obtained.

$$e(\psi)=a_{sh}\left[\left(\frac{w_s\left(1-\ln\left(1+\psi/\psi_r\right)/\ln\left(1+10^6/\psi_r\right)\right)}{b_{sh}\left(\ln\left(\exp(1)+\left(\psi/a_f\right)^{n_f}\right)\right)^{m_f}}\right)^{c_{sh}}+1\right]^{\frac{1}{c_{sh}}} \qquad [25]$$

Substituting Eq. [24] and Eq. [25] into the basic volume-mass relationships, (i.e., Eqs. [10] to [12]), leads to the best-fit equations for *S*-SWCC, θ-SWCC and θ_i -SWCC, as shown in Eqs. [26] to [28], respectively.

$$S(\psi)=\frac{G_s w_s\left(1-\ln\left(1+\psi/\psi_r\right)/\ln\left(1+10^6/\psi_r\right)\right)}{a_{sh}\left(\ln\left(\exp(1)+\left(\psi/a_f\right)^{n_f}\right)\right)^{m_f}\left[\left(\dfrac{w_s\left(1-\ln\left(1+\psi/\psi_r\right)/\ln\left(1+10^6/\psi_r\right)\right)}{b_{sh}\left(\ln\left(\exp(1)+\left(\psi/a_f\right)^{n_f}\right)\right)^{m_f}}\right)^{c_{sh}}+1\right]^{\frac{1}{c_{sh}}}}$$

[26]

$$\theta(\psi)=\frac{G_s w_s\left(1-\ln\left(1+\psi/\psi_r\right)/\ln\left(1+10^6/\psi_r\right)\right)}{\left(1+e_0\right)\left(\ln\left(\exp(1)+\left(\psi/a_f\right)^{n_f}\right)\right)^{m_f}} \quad [27]$$

$$\theta_i(\psi)=\frac{G_s w_s\left(1-\ln\left(1+\psi/\psi_r\right)/\ln\left(1+10^6/\psi_r\right)\right)}{\left(\ln\left(\exp(1)+\left(\psi/a_f\right)^{n_f}\right)\right)^{m_f}\left(1+a_{sh}\left[\left(\dfrac{w_s\left(1-\ln\left(1+\psi/\psi_r\right)/\ln\left(1+10^6/\psi_r\right)\right)}{b_{sh}\left(\ln\left(\exp(1)+\left(\psi/a_f\right)^{n_f}\right)\right)^{m_f}}\right)^{c_{sh}}+1\right]^{\frac{1}{c_{sh}}}\right)}$$

[28]

It should be noted that the best-fitting soil parameters that appear in Eqs. [26] to [28] are inherited from the use of Eqs. [22] and [24]. The parameters, a_f, n_f, m_f, and ψ_r are obtained when best-fitting the *w*-SWCC using the Fredlund-Xing (1994) equation (i.e., Eq. [24]). The parameters, a_{sh}, b_{sh}, and c_{sh} are obtained from the fitting by the Fredlund (2000) shrinkage curve equation (i.e., Eq. [22]).

Four SWCCs mentioned above essentially provide the same information to the geotechnical engineer when the soil involved has no volume change in a drying process. When dealing with high volume change soils such as Regina clay, *w*-SWCC, θ_i -SWCC and *S*-SWCC are considerably different from one another, with the θ -SWCC having no meaningful value. It is important to use the appropriate type of SWCC when estimating unsaturated soil property functions for a soil that undergoes volume change as soil suction changes. *S*-SWCC is the proper SWCC to use when determining the true AEV and estimating the relative coefficient of permeability function associated with the desaturation of the soil (Fredlund and Zhang 2013, Zhang et al. 2014). The θ_i -SWCC should always be used to predict the water storage function. Misuse of SWCC in the estimation of unsaturated soil property functions can produce erroneous results.

3.3.4 Estimation of coefficient of permeability function

In order to accommodate numerical modeling needs for seepage through soils that undergo volume change during a drying process, a revised methodology must be used for the estimation of the coefficient of permeability function. The changes required to existing theories for the unsaturated permeability function are presented in the following sections. The degree of saturation and void ratio are two controlling factors that influence the coefficient of permeability for a particular soil. Both the degree of saturation and void ratio will be taken into account in the revised methodology.

The relative coefficient of permeability of a particular phase within a multiphase flow system is a dimensionless measure of the coefficient of permeability corresponding to that phase. The relative coefficient of permeability is the ratio of the coefficient of permeability of a particular phase in multiphase flow system to the coefficient of permeability of that phase when the porous medium is subjected to single-phase flow. In water-air flow in soil, the relative coefficient of permeability of the water phase is the ratio of the coefficient of permeability of the water phase to the coefficient of permeability of the soil saturated with water.

Water-air flow in soil is the two-phase flow system that is of interest to geotechnical engineers when solving problems related to seepage. In water-air flow through a soil, the flow of water phase is emphasized because of its greater significance. The relative coefficient of permeability commonly studied in research refers to the relative coefficient of permeability of the water phase.

The coefficient of permeability at a particular soil suction during a drying process is the product of the relative coefficient of permeability and the corresponding saturated coefficient of permeability of the soil when it is the single-phase of water flow, (see Eq. [29]).

$$k(\psi) = k_r(\psi) \times k_{rs}(\psi) \tag{29}$$

where:

$k(\psi)$ = coefficient of permeability at a particular soil suction, ψ,

$k_r(\psi)$ = relative coefficient of permeability at the soil suction, ψ, and

$k_{rs}(\psi)$ = reference saturated coefficient of permeability at a soil suction of ψ. The reference permeability is the corresponding saturated coefficient of permeability when the soil at a suction of ψ is in single-phase water flow.

The relative coefficient of permeability must be between zero and 1.0. When soil suction, ψ, is less than the AEV (air-entry value), and corresponds to a particular void ratio, the soil is assumed to be saturated. The relative coefficient of permeability $k_r(\psi)$ for the saturated soil is 1.0. The coefficient of permeability, $k(\psi)$, of the saturated soil is equal to the reference saturated coefficient of permeability $k_{rs}(\psi)$. When the soil suction, ψ, exceeds the AEV, desaturation starts and the relative coefficient of permeability decreases from 1.0, as the soil continues to dry. The coefficient of permeability $k(\psi)$ for the unsaturated soil is smaller than the reference saturated coefficient of permeability $k_{rs}(\psi)$ due to the desaturation of the soil.

Both the degree of saturation and void ratio influence the coefficient of permeability for a particular soil. However, the void ratio controls the permeability function when the soil is saturated before the AEV is reached. The degree of saturation begins to influence the permeability together with the void ratio when desaturation starts. The degree of saturation gradually becomes the dominant factor while the influence of the void ratio diminishes as desaturation continues during a drying process. Eq. [29] reveals that degree of saturation influences the relative coefficient of permeability $k_r(\psi)$ while the void ratio affects the reference saturated coefficient of permeability $k_{rs}(\psi)$. The change in degree of saturation changes the tortuosity of the flow path within the porous media. The tortuosity, in turn, controls the relative coefficient of permeability. In other words, the degree of saturation exerts its influence upon the relative coefficient of permeability mainly by impacting the tortuosity of the flow path within the porous media. The saturated coefficient of permeability of a soil depends mainly on the pore sizes and the pore size distribution (Chapuis 2012). A change in void ratio changes the pore sizes, thereby influencing the reference saturated coefficient of permeability of the soil. The degree of saturation and void ratio together control the coefficient of permeability $k(\psi)$ for a soil that undergoes volume change as soil suction changes during a drying process.

Numerous researchers have undertaken studies on the effect of void ratio changes on the saturated permeability of a soil that undergoes overall volume change (Chapuis 2012). Eq. [30] (Taylor 1948) and Eq. [31] (Somogyi 1980) mathematically describe the relationship of the saturated coefficient of permeability, k_{sat}, to void ratio, e. Each of these equations (i.e., Eqs. [30] and [31]) can be used in conjunction with a relative coefficient of permeability function to generate a coefficient of permeability function for a soil that undergoes overall volume change.

$$k_{sat}(e) = \frac{10^{-11} C e^{x}}{1+e} \qquad [30]$$

$$k_{sat}(e) = 10^{-11} A e^{B} \qquad [31]$$

where:

k_{sat} = saturated coefficient of permeability,

e = void ratio,

C, x = fitting parameters for Eq. [30], and

A, B = fitting parameters for Eq. [31],

During the drying process of a soil that undergoes volume change, the void ratio also changes with soil suction. The relationship of void ratio versus soil suction can be mathematically established using Eq. [25]. By substituting Eq. [25] into Eq. [30] or Eq. [31], a mathematical function for the reference saturated coefficient of permeability, $k_{rs}(\psi)$, in Eq. [29] can be obtained, as shown in Eq. [32] and Eq. [33] respectively.

$$k_{rs}(\psi) = \frac{10^{-11} C \left\{ a_{sh} \left[\left(\dfrac{w_s \left(1 - \ln\left(1+\psi/\psi_r\right) / \ln\left(1+10^6/\psi_r\right)\right)}{b_{sh} \left(\ln\left(\exp(1) + \left(\psi/a_f\right)^{n_f} \right) \right)^{m_f}} \right)^{c_{sh}} + 1 \right]^{\frac{1}{c_{sh}}} \right\}^{x}}{1 + a_{sh} \left[\left(\dfrac{w_s \left(1 - \ln\left(1+\psi/\psi_r\right) / \ln\left(1+10^6/\psi_r\right)\right)}{b_{sh} \left(\ln\left(\exp(1) + \left(\psi/a_f\right)^{n_f} \right) \right)^{m_f}} \right)^{c_{sh}} + 1 \right]^{\frac{1}{c_{sh}}}} \qquad [32]$$

$$k_{rs}(\psi)=10^{-11}A\left\{a_{sh}\left[\left(\frac{w_s\left(1-\ln\left(1+\psi/\psi_r\right)/\ln\left(1+10^6/\psi_r\right)\right)}{b_{sh}\left(\ln\left(\exp(1)+\left(\psi/a_f\right)^{n_f}\right)\right)^{m_f}}\right)^{c_{sh}}+1\right]^{\frac{1}{c_{sh}}}\right\}^{B} \qquad [33]$$

The relative coefficient of permeability function, $k_r(\psi)$, forms an important component composing the coefficient of permeability function, $k(\psi)$, for a soil that undergoes volume change as soil suction changes. The relative coefficient of permeability of a soil is a function that reflects the influence of degree of saturation on the coefficient of permeability of the soil. Considerable research has already been undertaken on estimating the relative coefficient of permeability in unsaturated soil mechanics (Burdine 1953, Childs and Collis-George 1950, Fredlund et al. 1994, Mualem 1976, van Genuchten 1980). The relationship of the relative coefficient of permeability to soil suction is primarily determined by the pore-size distribution of the soil and its prediction is usually based on the soil-water characteristic curve.

The Fredlund-Xing-Huang (1994) permeability function is used in this study to estimate the relative coefficient of permeability. The Fredlund-Xing-Huang (1994) permeability function is obtained by substituting the Fredlund-Xing (1994) SWCC equation into the integral formula proposed by Childs and Collis-George (1950). The permeability function takes the form of:

$$k_r(\psi)=\frac{\displaystyle\int_{\ln(\psi)}^{b}\frac{\theta\left(e^y\right)-\theta(\psi)}{e^y}\theta'\left(e^y\right)dy}{\displaystyle\int_{\ln(\psi_{aev})}^{b}\frac{\theta\left(e^y\right)-\theta\left(\psi_{aev}\right)}{e^y}\theta'\left(e^y\right)dy} \qquad [34]$$

where:

b = ln(1000000), and

y = a dummy variable of integration representing the logarithm of soil suction.

The soil-water characteristic curve used in the originally proposed Fredlund-Xing-Huang (1994) function is θ-SWCC. However, a different relative coefficient of permeability function is obtained when using different SWCCs as the basis for the relative permeability estimation. Three estimation functions for the relative coefficient of permeability can be obtained by modifying the Fredlund-Xing-Huang (1994) permeability function (Eq. [34]) using different SWCCs. Table 3-2 shows four estimation functions for the relative coefficient of permeability based on different SWCCs.

Table 3-2. Estimation of the relative coefficient of permeability from different SWCCs.

Type of SWCC	Estimation functions of $k_r(\psi)$
w-SWCC	$k_r^w(\psi)=\dfrac{\int_{\ln(\psi)}^{b}\frac{w(e^y)-w(\psi)}{e^y}w'(e^y)dy}{\int_{\ln(\psi_{aev})}^{b}\frac{w(e^y)-w(\psi_{aev})}{e^y}w'(e^y)dy}$
S-SWCC	$k_r^S(\psi)=\dfrac{\int_{\ln(\psi)}^{b}\frac{S(e^y)-S(\psi)}{e^y}S'(e^y)dy}{\int_{\ln(\psi_{aev})}^{b}\frac{S(e^y)-S(\psi_{aev})}{e^y}S'(e^y)dy}$
θθ_i-SWCC	$k_r^{\theta_i}(\psi)=\dfrac{\int_{\ln(\psi)}^{b}\frac{\theta_i(e^y)-\theta_i(\psi)}{e^y}\theta_i'(e^y)dy}{\int_{\ln(\psi_{aev})}^{b}\frac{\theta_i(e^y)-\theta_i(\psi_{aev})}{e^y}\theta_i'(e^y)dy}$
θ-SWCC	$k_r^\theta(\psi)=\dfrac{\int_{\ln(\psi)}^{b}\frac{\theta(e^y)-\theta(\psi)}{e^y}\theta'(e^y)dy}{\int_{\ln(\psi_{aev})}^{b}\frac{\theta(e^y)-\theta(\psi_{aev})}{e^y}\theta'(e^y)dy}$

Notes:

$k_r^\theta(\psi)$ is the original form of Fredlund-Xing-Huang (1994) permeability function. $k_r^w(\psi)$, $k_r^S(\psi)$ and $k_r^{\theta_i}(\psi)$ are three estimation functions modified from the Fredlund-Xing-Huang (1994) permeability function.

For soils that do not undergo volume change as soil suction changes, the four functions ($k_r^w(\psi)$, $k_r^S(\psi)$ and $k_r^{\theta_i}(\psi)$and $k_r^\theta(\psi)$) produce the same results when estimating the relative coefficient of permeability. For a soil that undergoes volume change, the $k_r^w(\psi)$, $k_r^S(\psi)$ and $k_r^{\theta_i}(\psi)$ generate different estimation results for the relative coefficient of permeability, while $k_r^w(\psi)$ and $k_r^{\theta}(\psi)$ remain the same results. It is important to note that *S*-SWCC is the SWCC that should be used for the estimation of the relative coefficient of permeability (Fredlund and Zhang 2013, Zhang et al. 2014). Only the estimation results given by the $k_r^S(\psi)$ function are acceptable when a soil changes volume with soil suction changes.

The overall coefficient of permeability function for a high-volume-change material can now be determined by multiplying the reference saturated coefficient of permeability function by the relative coefficient of permeability function. By substituting $k_r^S(\psi)$ and either Eqs. [32] or [33] into Eq. [29], a function can be obtained for the estimation of the coefficient of permeability for a soil that undergoes volume change as soil suction changes during a drying process, (see Eq. [35] and Eq. [36]).

The fitting parameters in Eqs. [35] and [36] are obtained from the shrinkage curve, (i.e., Eq. [22]), the *w*-SWCC, (i.e., Eq. [24]) and the best-fitting curve for the saturated coefficient of permeability versus the void ratio, (i.e., Eqs. [30] and [31]).

$$k(\psi)=\frac{10^{-11}C\left\{a_{sh}\left[\left(\frac{w_s\left(1-\ln\left(1+\psi/\psi_r\right)/\ln\left(1+10^6/\psi_r\right)\right)}{b_{sh}\left(\ln\left(\exp(1)+\left(\psi/a_f\right)^{n_f}\right)\right)^{m_f}}\right)^{c_{sh}}+1\right]^{\frac{1}{c_{sh}}}\right\}^x\displaystyle\int_{\ln(\psi)}^{b}\frac{S(e^y)-S(\psi)}{e^y}S'(e^y)\,dy}{\left\{1+a_{sh}\left[\left(\frac{w_s\left(1-\ln\left(1+\psi/\psi_r\right)/\ln\left(1+10^6/\psi_r\right)\right)}{b_{sh}\left(\ln\left(\exp(1)+\left(\psi/a_f\right)^{n_f}\right)\right)^{m_f}}\right)^{c_{sh}}+1\right]^{\frac{1}{c_{sh}}}\right\}\displaystyle\int_{\ln(\psi_{aev})}^{b}\frac{S(e^y)-S(\psi_{aev})}{e^y}S'(e^y)\,dy}$$

[35]

$$k(\psi)=10^{-11}A\left\{a_{sh}\left[\left(\frac{w_s\left(1-\ln\left(1+\psi/\psi_r\right)/\ln\left(1+10^6/\psi_r\right)\right)}{b_{sh}\left(\ln\left(\exp(1)+\left(\psi/a_f\right)^{n_f}\right)\right)^{m_f}}\right)^{c_{sh}}+1\right]^{\frac{1}{c_{sh}}}\right\}^B\frac{\int_{\ln(\psi)}^{b}\frac{S\left(e^y\right)-S(\psi)}{e^y}S'\left(e^y\right)dy}{\int_{\ln(\psi_{aev})}^{b}\frac{S\left(e^y\right)-S\left(\psi_{aev}\right)}{e^y}S'\left(e^y\right)dy}$$

[36]

3.4 Presentation of the experimental data

The following sections illustrate the procedure whereby the revised theory is applied to Regina clay test results. The results are an example of a coefficient of permeability function for a soil that undergoes volume change during a drying process. The laboratory test results were obtained by Fredlund (1964) and are presented herein to illustrate the revised theory.

Regina clay had a liquid limit of 75%, a plastic limit of 25% and contained 50% clay size particles (Fredlund 1964). The material was prepared as slurry at gravimetric water content slightly above the liquid limit and then subjected to various consolidation pressures under one-dimensional, K_o loading. After the applied load was removed, the soil specimens were subjected to various applied matric suction values. High suction values, (i.e., in excess of 1500 kPa) were applied through equalization in a constant relative humidity environment.

Shrinkage curves and soil-water characteristic curves were measured on Regina clay. The shrinkage curve for Regina clay is presented in Figure 3-3. The void ratio of Regina clay decreased as water evaporated from the soil. The best-fitting parameters for the shrinkage curve are a_{sh} = 0.487, b_{sh} = 0.159, and c_{sh} = 4.422. The specific gravity of the soil was 2.835.

Figure 3-4 shows the gravimetric water content, w, plotted versus soil suction for Regina clay that was initially preloaded at 6.125 kPa. The gravimetric water content soil-water characteristic curve, w-SWCC was best-fitted with the Fredlund-Xing (1994) equation, (i.e., Eq. [24]). The best-fitting parameters for the w-SWCC are a_f = 17.2 kPa, n_f = 0.871, m_f = 0.770, and ψ_r = 922 kPa. The initial gravimetric water content was 86.1%. The w-SWCC was used in conjunction with the shrinkage curve to calculate other forms of the SWCC. The volume-mass properties versus soil suction were interpreted to obtain other unsaturated soil properties. The "true" air-entry value, AEV was determined (Vanapalli et al. 1998) and the relative permeability function was computed using the modified Fredlund-Xing-Huang (1994) permeability function.

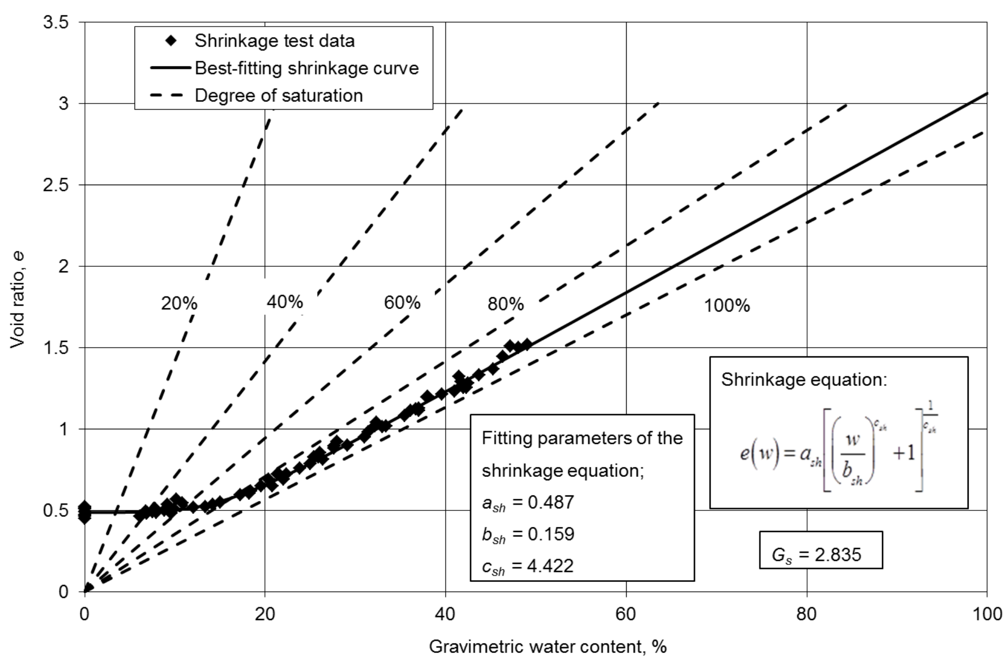

Figure 3-3. Shrinkage curve for Regina clay (Fredlund, 1964).

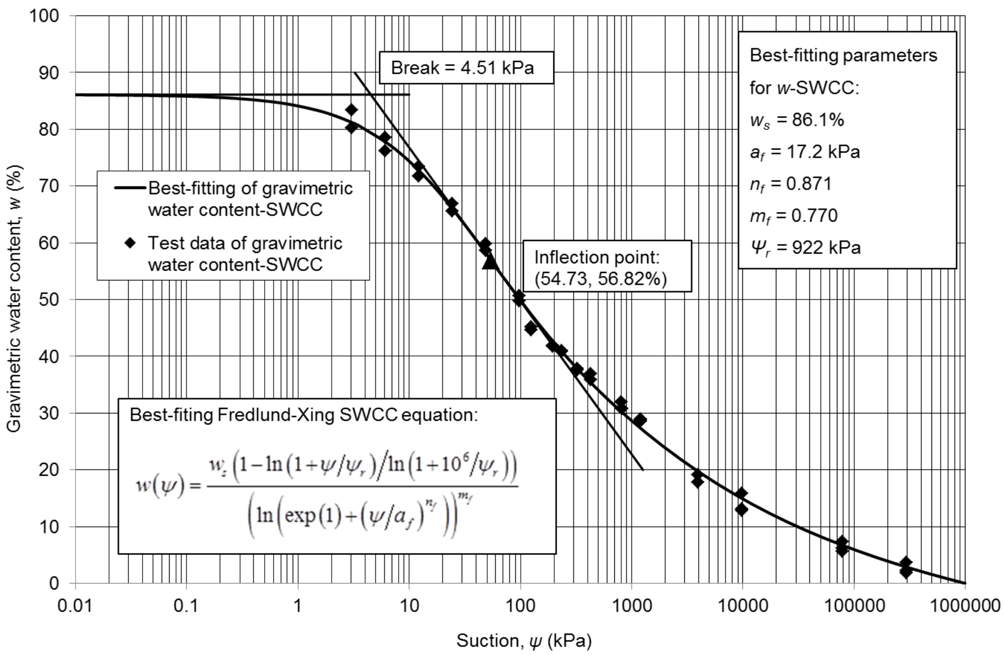

Figure 3-4. Measured *w*-SWCC best-fitted by Fredlund-Xing (1994) equation (data from Fredlund, 1964).

The data for the saturated coefficient of permeability versus void ratio relationship were also measured for Regina clay. The experimental data were best-fitted using Eq. [30] and Eq. [31]. Figure 3-5 shows the measured results and the best-fitting curves. Both equations produce reasonable fitting curves for the saturated coefficient of permeability versus void ratio relationship for Regina clay. The fitting parameters for Eq. [30] are C = 2.005 and x = 5.311, while the fitting parameters for Eq. [31] are A = 1.02 and B = 4.68.

These three curves were obtained from the laboratory test; namely the shrinkage curve, the *w*-SWCC and the curve of saturated coefficient of permeability versus void ratio, and are used to estimate the appropriate coefficient of permeability function for Regina clay.

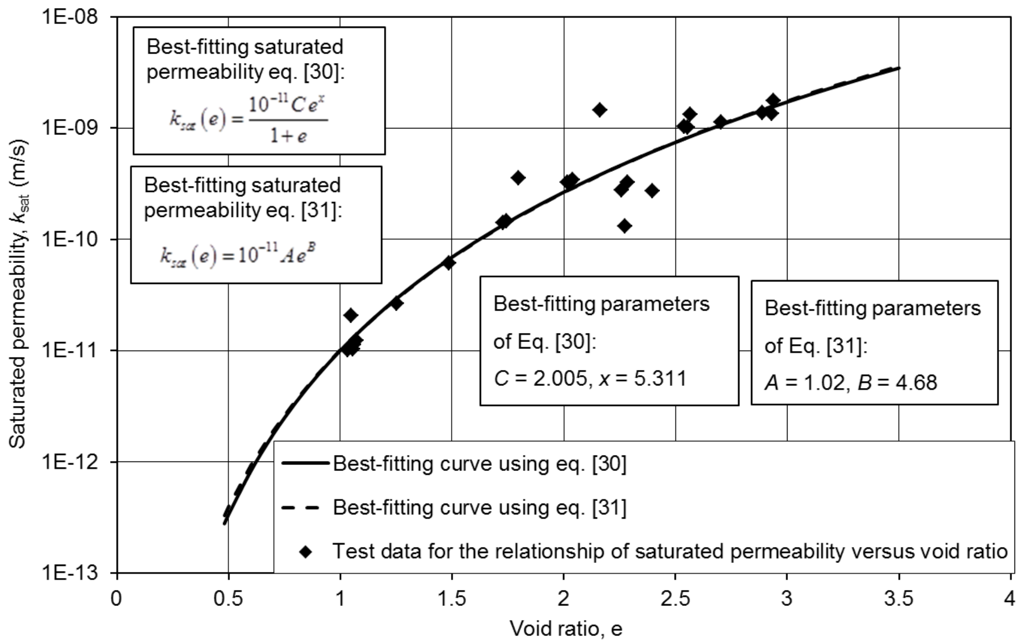

Figure 3-5. Saturated permeability versus void ratio best-fitted using Eq. [30] and Eq. [31] (data from Fredlund, 1964).

3.5 Interpretation and discussion of the experimental data

The gravimetric water content-SWCC, *w*-SWCC is combined with the shrinkage curve to obtain other forms of the SWCC. The resulting plot of degree of saturation, *S*, versus soil suction is shown in Figure 3-6. The plot of instantaneous volumetric water content, θ_i, versus soil suction is shown in Figure 3-7. The breaking points on different SWCCs appear at different soil suctions (Table 3-3). The breaking point on the *w*-SWCC is at a soil suction of 4.51 kPa. The breaking point on the *S*-SWCC is at a soil suction of 4853 kPa. The breaking point on the θ_i -SWCC is at a soil suction of 46.05 kPa. The air-entry value, AEV, of the soil must be estimated from the S-SWCC. The degree of saturation versus soil suction plot indicates that the AEV is 4853 kPa. The corresponding gravimetric water content and instantaneous volumetric water content at the point of AEV are 18.57% and 32.43% respectively.

Table 3-3. Comparison of the breaking points on different SWCCs.

# Form of SWCC	w-SWCC	S-SWCC	θ_i-SWCC
Suction at the breaking of the curve	4.51 kPa	4853 kPa	46.05 kPa

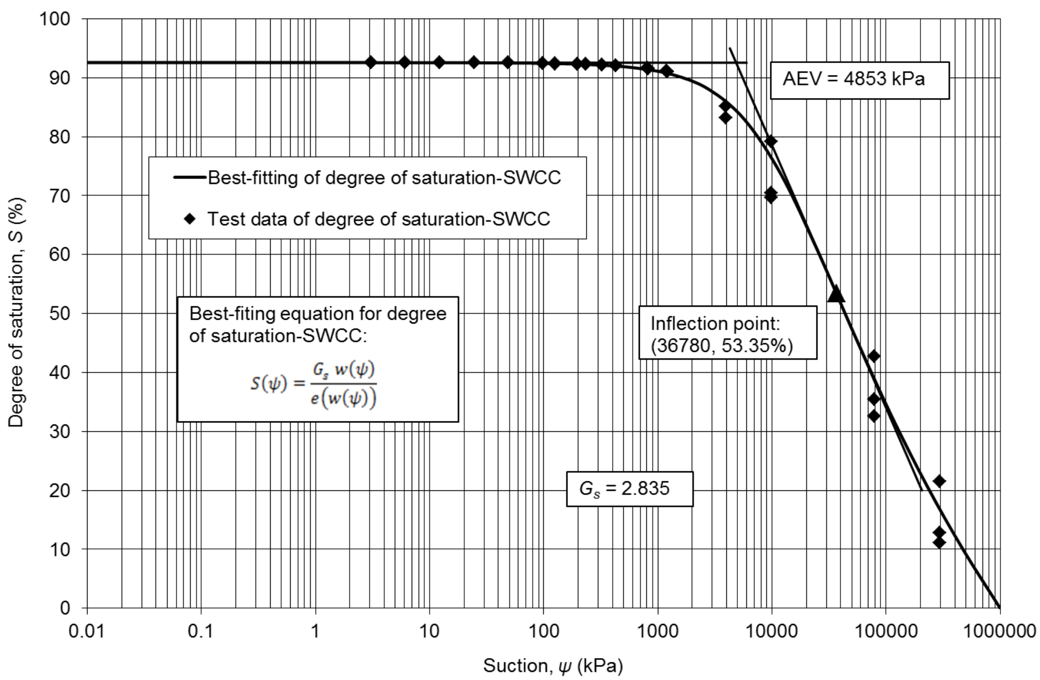

Figure 3-6. Degree of saturation versus soil suction (data from Fredlund, 1964).

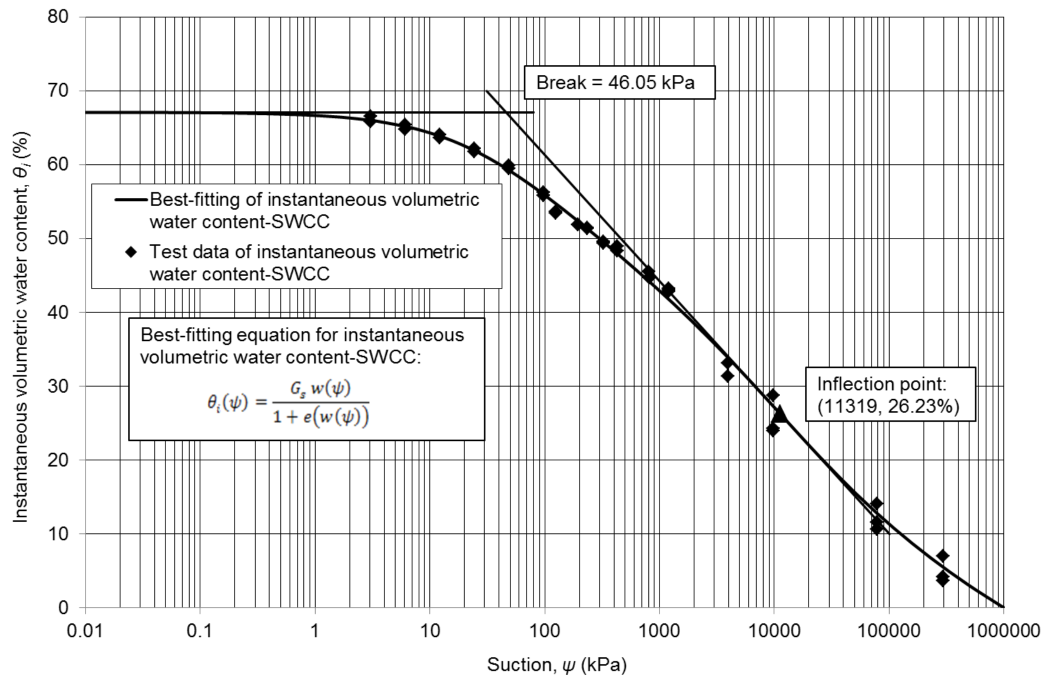

Figure 3-7. Instantaneous volumetric water content versus soil suction (data from Fredlund, 1964).

The relative coefficient of permeability function is one important component constituting the coefficient of permeability function for a soil that undergoes volume change as soil suction changes. Different relative permeability functions are obtained when using different forms of SWCC for the estimation (Table 3-2). Three curves of the relative permeability function obtained respectively from *w*-SWCC, θ_i-SWCC, and *S*-SWCC are shown in Figure 3-8. These three curves are obtained using equations listed in Table 3-2, namely, $k_r^w(\psi)$, $k_r^S(\psi)$ and $k_r^{\theta_i}(\psi)$. Soil suction at the breaking point on each SWCC was used as the lower limit of integration for the denominator of each estimation equation. The correct relative coefficient of permeability function is the one obtained from the *S*-SWCC.

Misinterpretation of the SWCC can lead to erroneous results (e.g., using the wrong SWCC or the wrong starting point for integration). Figure 3-8 shows that the result obtained from the *w*-SWCC under-estimated the relative permeability by 6.46 orders of magnitude, while the results obtained from the θ_i-SWCC under-estimated the relative permeability by 3.7 orders of magnitude.

Figure 3-9 shows three curves estimated from different types of SWCCs with the AEV from the *S*-SWCC as the lower limit of integration. Two curves obtained from *w*-SWCC and θ_i-SWCC are much closer to the permeability curve obtained from the *S*-SWCC when using the AEV as the lower limit of integration. The results illustrate the important role that the AEV has on the estimation of the relative permeability function. The difference is substantial. It is important to use the *S*-SWCC for the estimation of the relative permeability function for soils that undergo volume change as soil suction changes.

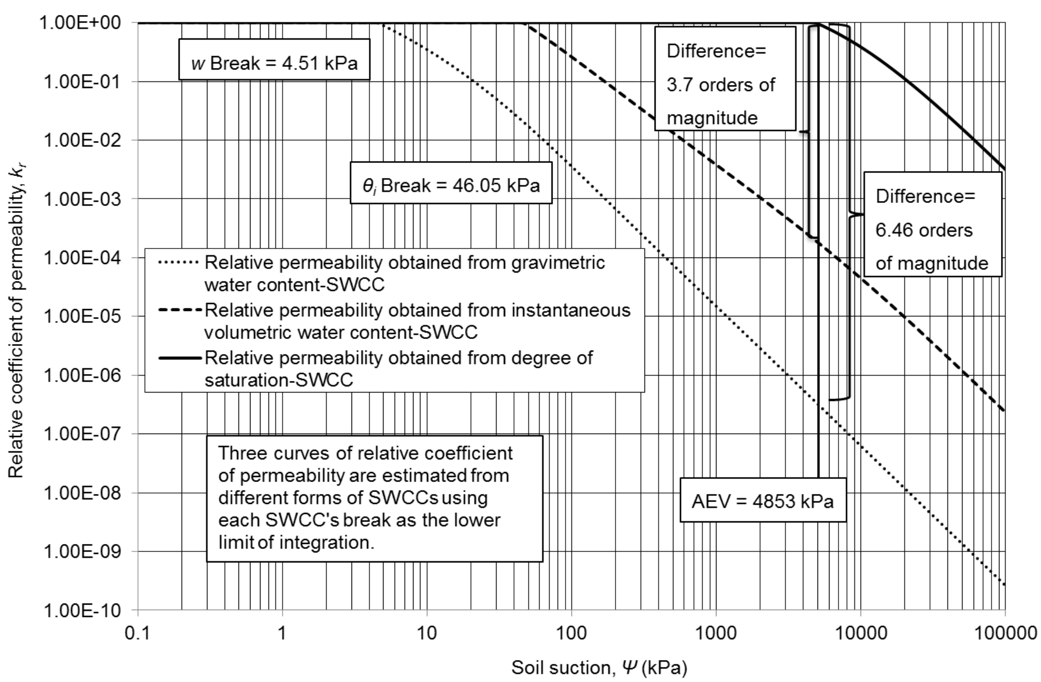

Figure 3-8. Relative coefficient of permeability versus soil suction.

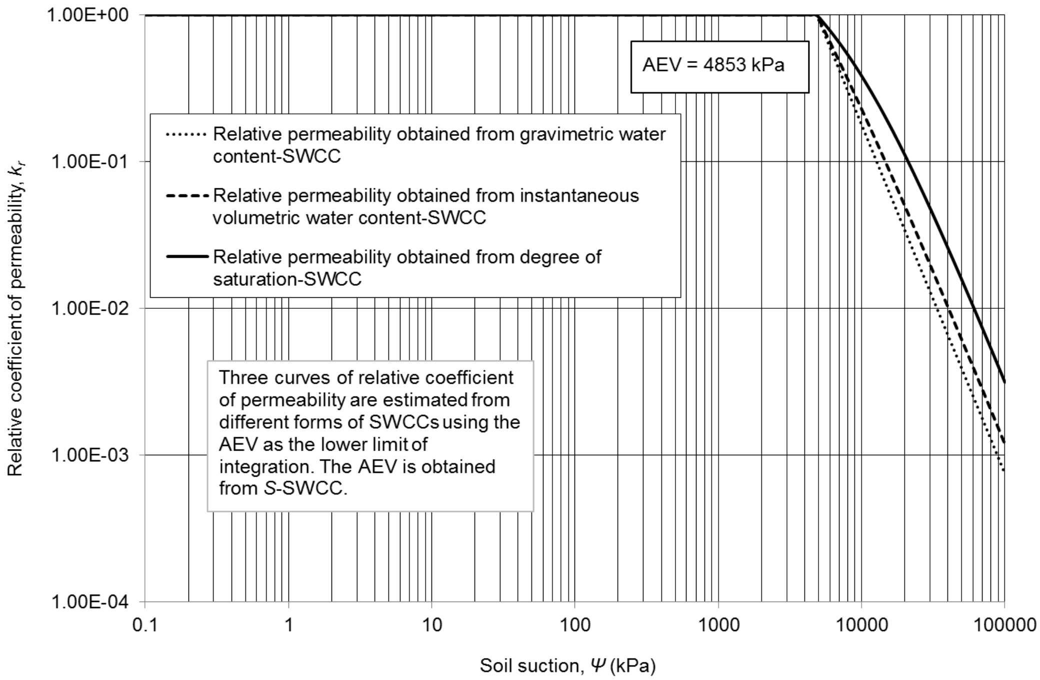

Figure 3-9. Comparison of the relative coefficient of permeability functions obtained from different SWCCs using the AEV as the lower limit of integration.

Figure 3-10 illustrates the importance of determining the correct AEV for the estimation of the relative permeability function. The results show that the relative coefficient of permeability versus soil suction obtained from *S*-SWCC differs when different values are used for the lower limit of integration. The original equation for $k_r^S(\psi)$ listed in Table 2 specifies that the AEV should be used as the lower limit of integration for the integral in the denominator of the equation. It is suggested that the most reasonable curve to use for the relative coefficient of permeability versus soil suction is the one obtained when using the AEV as the lower limit of integration.

Table 3-4 presents the difference that could result when using a smaller value as the lower limit of integration. When the value used as the lower limit of integration is 0.5 Log_{10} cycles less than the AEV, the results are under-estimated by 0.394 orders of magnitude. When the value used as the lower limit of integration is 4 Log_{10} cycles less than the AEV, the resulting relative coefficient of permeability would be under-estimated by 0.971 orders of magnitude. The difference in the resulting estimation for the relative coefficient of permeability caused by using a lower limit of integration different than the AEV is significant. Zhang and Fredlund (2015) studied in detail the effect of the lower limit of integration on the calculation of the relative permeability function. The AEV should be used as the lower limit of integration when estimating the relative coefficient of permeability function using the equation of $k_r^s(\psi)$.

Table 3-4. Difference in the estimated relative permeability in terms of orders of magnitude between using the correct starting integration value (i.e., AEV) and using a different lower limit of integration.

Lower limit of integration (Number of Log_{10} cycles less than the AEV)	0.5	1	2	3	4
Difference in terms of orders of magnitude	0.394	0.597	0.801	0.898	0.971

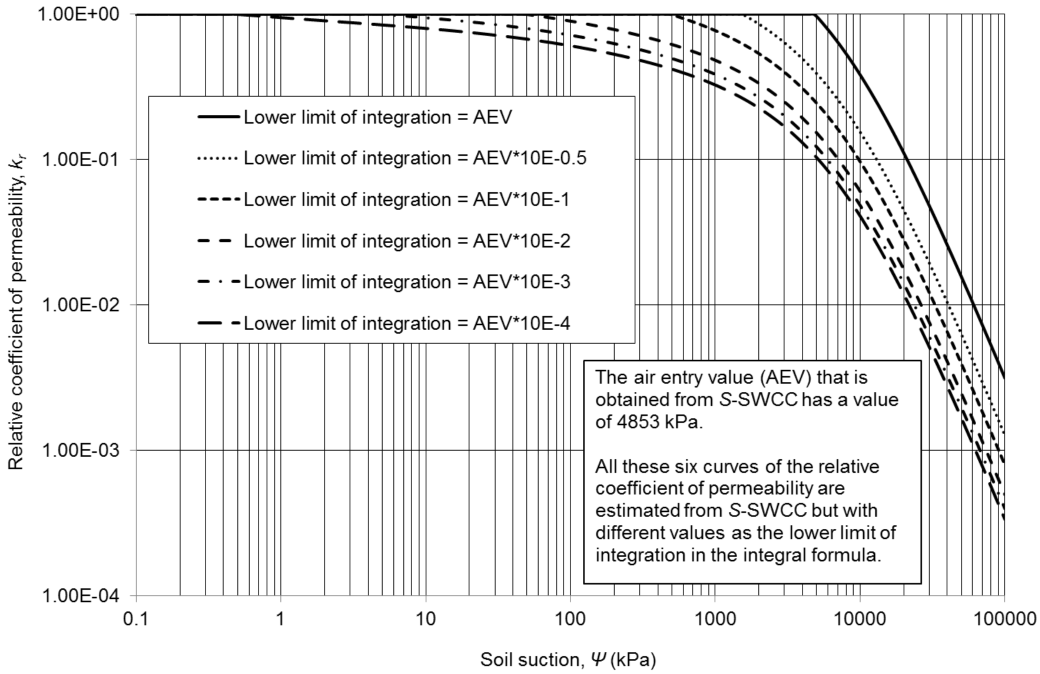

Figure 3-10. Relative coefficient of permeability versus soil suction obtained from *S*-SWCC using different lower limits of integration.

Figure 3-11 shows the curve of the relative coefficient of permeability versus soil suction obtained from *S*-SWCC with the AEV as the lower limit of integration.

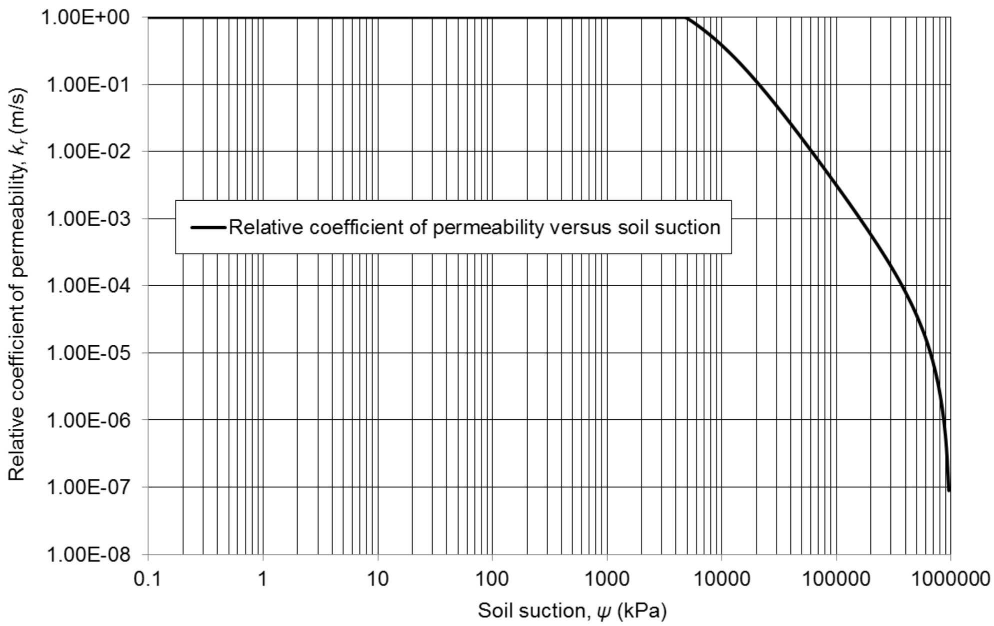

Figure 3-11. Relative coefficient of permeability versus soil suction.

The relationship between void ratio and soil suction can be obtained by combining the *w*-SWCC and the shrinkage curve. The plot of void ratio versus soil suction is shown in Figure 3-12. The void ratio decreases from 2.637 down to 0.624 when the soil suction increases from 0 to its AEV. The void ratio at the AEV of 4853 kPa is 0.624. The soil specimen experiences a large volume change while it remains saturated during its drying process before the soil suction reaches the AEV. After the soil suction exceeds its AEV, the desaturation occurs while volume change continues with a limited amount of volume change (i.e., the void ratio changes from 0.624 to 0.487).

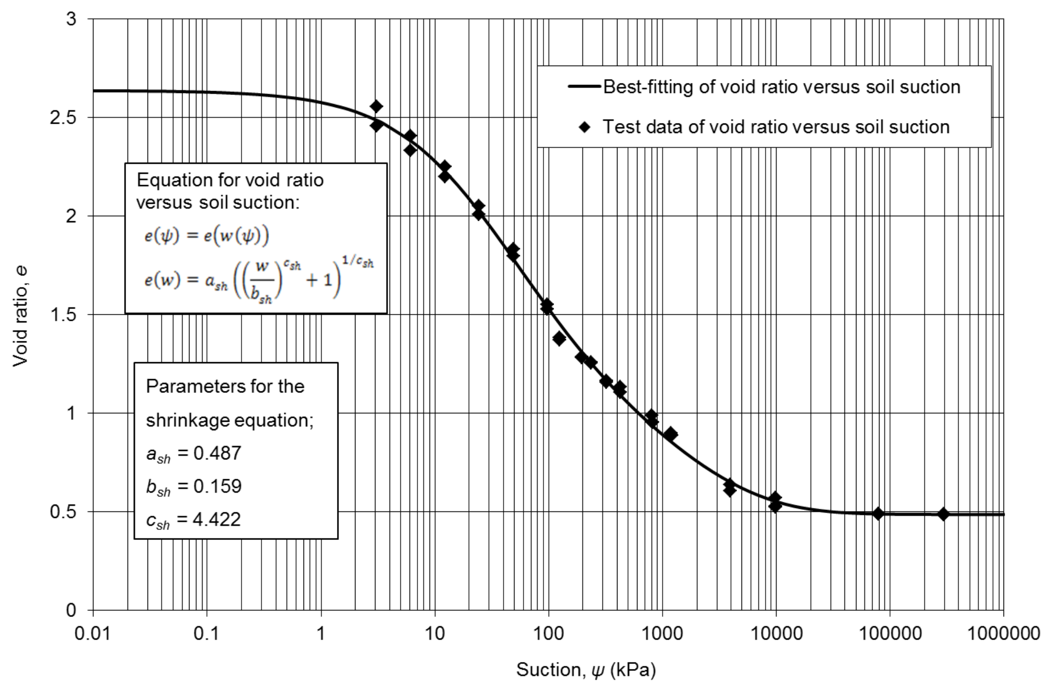

Figure 3-12. Void ratio versus soil suction (data from Fredlund, 1964).

The saturated coefficient of permeability is a function of void ratio as shown in Figure 3-5. Both Eq. [30] and Eq. [31] can be used to mathematically describe the relationship of saturated coefficient of permeability to void ratio. The void ratio is a function of soil suction as Regina clay dries from its initial saturated state to a completely dry condition (as shown in Figure 3-12). The saturated coefficient of permeability changes with void ratio, while void ratio changes with soil suction during the drying process. As a result, the saturated coefficient of permeability can be related to soil suction. When the saturated coefficient of permeability in this study is related to soil suction, it is termed as the reference saturated coefficient of permeability to make a distinction because both saturated and unsaturated conditions are involved in the entire drying process. The reference saturated coefficient of permeability versus soil suction is shown in Figure 3-13. Two curves showing the reference saturated coefficient of permeability versus soil suction are given by Eq. [32] and Eq. [33] respectively. The two curves overlap at soil suctions below a value of 200 kPa and deviate slightly in the higher suction range.

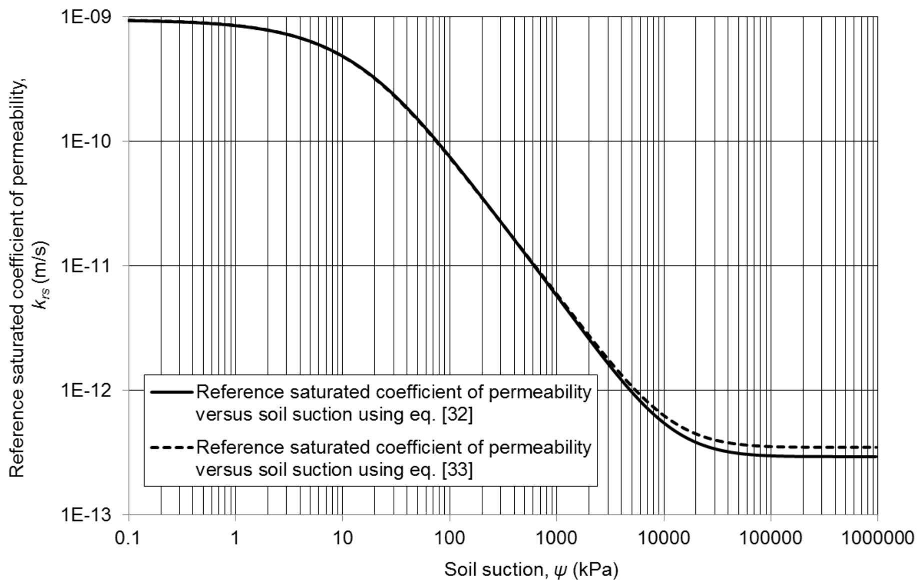

Figure 3-13. Reference saturated coefficient of permeability versus soil suction.

After obtaining the relative coefficient of permeability function shown in Figure 3-11 and the reference saturated coefficient of permeability function shown in Figure 3-13, the coefficient of permeability function can be obtained by combining the relative coefficient of permeability function and the reference saturated coefficient of permeability function according to Eq. [29]. The relationship of the coefficient of permeability versus soil suction for Regina clay preconsolidated to 6.125 kPa is shown in Figure 3-14.

For the Regina clay investigated in this study, the analyses show that the permeability function is dominated by saturated flow until the AEV, during which most of the soil volume change occurs as shown in Figure 3-12. The AEV for the investigated Regina clay is 4853 kPa. Beyond the AEV, the void ratio changes relatively little from 0.624 to 0.487 for the Regina clay. The reference saturated permeability changes relatively little from a value of around 10^{-12} m/s to a value of around 3×10^{-13} m/s for changes in void ratio beyond the AEV. Though both changes in void ratio and degree of saturation are important for the estimation of the permeability function, it appears the void ratio change is dominant up to the AEV while the degree of saturation dominates after the AEV. For simplicity in the case of Regina clay, it is possible to estimate the permeability function from saturated test results using Eq. [30] or Eq. [31] up to the AEV. After the AEV, a relative permeability function obtained from the degree of saturation SWCC together with a proper constant reference saturated permeability can be used to produce a reasonable estimation of the permeability function for the unsaturated soil portion.

It may not be the case that all soils show relatively little volume changes beyond the AEV. “Deinking by-products”, (DBP) is an industrial by-product that has been successfully used as a cover material in both landfills and mining applications as well as soil structural enhancement material in agricultural applications (Parent et al. 2007). DBP is a highly compressible soil that continues to undergo considerable volume change when the applied suction exceeds the air-entry value. The proposed methodology is useful when giving consideration to soils such as DBP that undergo significant volume changes both below and above the AEV.

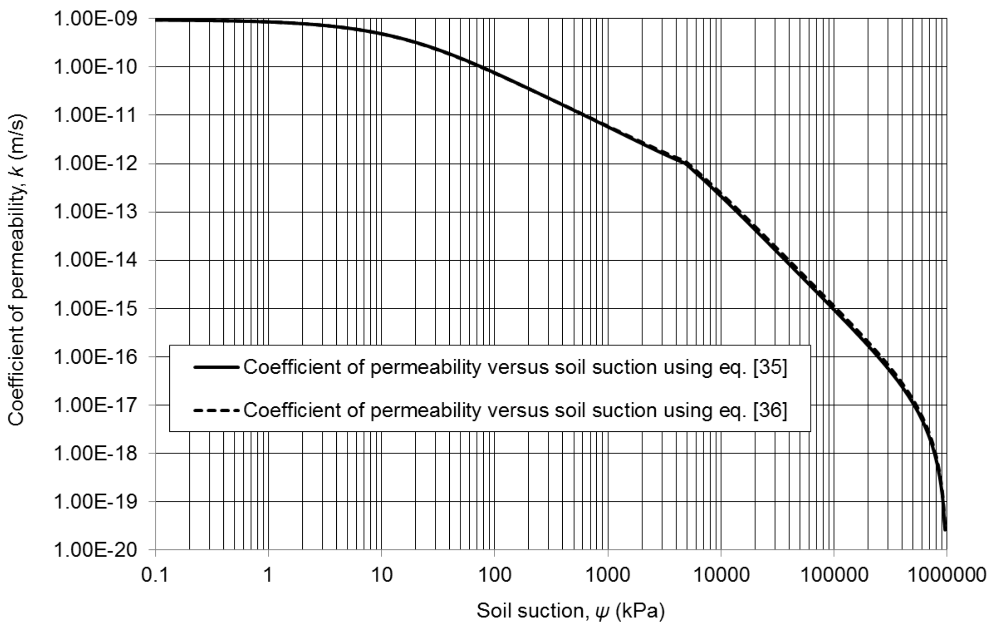

Figure 3-14. Coefficient of permeability versus soil suction

Three curves must be measured in order to estimate the appropriate permeability function using the methodology proposed in this study for a soil that undergoes significant volume change. These curves are: i.) the shrinkage curve, ii.) the *w*-SWCC and iii.) the curve of saturated coefficient of permeability versus void ratio. The change in void ratio associated with the proposed modified permeability function is associated with unrestrained shrinkage of an initially saturated, but not a structured soil, under zero net normal stress and increasing suction. In geotechnical engineering practice, soils are subjected to various stress conditions and complex stress histories. For example, soils at-depth will experience an overburden pressure and possibly other externally applied stresses. Shrinkage is generally not unrestrained and desiccation cracks may result. Compacted soils and natural soils under investigation typically do not exist in a saturated state at the starting point for an engineering analysis. Soil structure and stress history are important factors that influence the estimation of unsaturated soil properties including the permeability function. To apply the proposed permeability function to real or "structured" soils under various stress conditions and complex stress histories, the shrinkage curve, the *w*-SWCC and the curve of saturated coefficient of permeability versus void ratio for the corresponding situations have to be obtained. Detailed discussion on the influence of soil structures, desiccation cracks and stress path histories on the permeability function is beyond the scope of this paper. However, these are important topics for further study.

3.6 Conclusions

Changes in the volume of a soil specimen occur as soil suction is increased. These changes can significantly affect the interpretation of the SWCC and the estimation of the coefficient of permeability function. Both volume change and desaturation should be independently taken into account when estimating the coefficient of permeability function for high volume change soils (e.g., Regina clay). This paper presents a revised theory for the prediction of the saturated/unsaturated coefficient of permeability function for soils that undergo volume change. The revised theory is based on the Fredlund-Xing-Huang (1994) permeability function. The coefficient of permeability function proposed in this paper consists of two main components, namely, the reference saturated coefficient of permeability function and the relative coefficient of permeability function. The reference saturated coefficient of permeability function is controlled by the void ratio as soil suction changes and reflects the influence of volume change on the coefficient of permeability. The relative coefficient of permeability function must be estimated from *S*-SWCC using the AEV as the lower limit of integration. Using other forms of the SWCC or other values as the lower limit of integration can lead to large estimation errors. The influence of desaturation on the coefficient of permeability is reflected in the relative coefficient of permeability function. The overall coefficient of permeability function is the result of the multiplication of the reference coefficient of permeability function by the relative coefficient of permeability function. The detailed procedure for the estimation of the coefficient of permeability function using the proposed theory in this paper is explained and illustrated using the laboratory data sets for Regina clay. The shrinkage curve, the gravimetric water content versus soil suction and the saturated coefficient of permeability versus void ratio are three basic experimental measurements required for the estimation of the coefficient of permeability function for soils that undergo volume change as soil suction is increased.

References

Assouline, S., D. Tessier, and A. Bruand (1998) A conceptual model of the soil water retention curve. Water Resources Research, 34(2): 223-231.

Assouline, S., D. Tessier, and A. Bruand (2000) Correction to “A conceptual model of the soil water retention curve” by S. Assouline, D. Tessier, and A. Braund. Water Resource Research, 36(12): 3769.

Bronswijk, J. J. B. (1991) Relation between vertical soil movements and water-content changes in cracking clays. Soil Science Society of America Journal, 55(5): 1220-1226.

Brooks, R. H. and A. T. Corey (1964) Hydraulic properties of porous media. Hydrol. Pap. 3, Civ. Eng. Dep., Colo. State Univ., Fort Collins, Colorado.

Brutsaert, W. (1967) Some methods of calculating unsaturated permeability. Trans. ASAE, 10(3): 400-404.

Bumb, A. C., Murphy, C. L., and Everett, L. G. (1992) A comparison of three functional forms for representing soil moisture characteristics. Groundwater, 30(2): 177-185

Burdine, N. (1953) Relative permeability calculations from pore size distribution data. Journal of Petroleum Technology, 5 (03): 71–78.

Campbell, G. S. (1974) A simple method for determining unsaturated conductivity from moisture retention data. Soil science, 117(6): 311-314.

Chapuis, R. P. (2012) Predicting the saturated hydraulic conductivity of soils: a review. Bulletin of Engineering Geology and the Environment, 71(3): 401-434.

Childs, E. C., and Collis-George, N. (1950) The permeability of porous materials. In Proceedings of the Royal Society of London A: Mathematical, Physical and Engineering Sciences. The Royal Society, Vol. 201, No. 1066, pp. 392-405.

Farrell, D. A., and W. E. Larson (1972) Modeling the pore structure of porous media, Water Resources Research, 8(3): 699-706.

Fredlund, D. G. (1964) Comparison of soil suction and one-dimensional consolidation characteristics of a highly plastic clay. Dissertation, University of Alberta.

Fredlund, D. G., and Rahardjo, H. (1993) Soil mechanics for unsaturated soils. John Wiley & Sons.

Fredlund, D. G., and Xing, A. (1994) Equations for the soil-water characteristic curve. Canadian geotechnical journal, 31(4): 521-532.

Fredlund, D. G., Xing, A. and Huang, S. (1994) Predicting the permeability function for unsaturated soils using the soil-water characteristic curve. Canadian Geotechnical Journal, 31(4): 533-546.

Fredlund, D. G., Rahardjo, H., and Fredlund, M. D. (2012) Unsaturated soil mechanics in engineering practice. John Wiley & Sons, New York.

Fredlund, D. G., and Zhang, F. (2013) Combination of shrinkage curve and soil-water characteristic curves for soils that undergo volume change as soil suction is increased. Proceedings of the 18th International Conference on Soil Mechanics and Geotechnical Engineering, Paris 2013.

Fredlund, M. D. (2000) The role of unsaturated soil property functions in the practice of unsaturated soil mechanics. Dissertation, University of Saskatchewan.

Gardner, W. R. (1958) Some steady-state solutions of the unsaturated moisture flow equation with application to evaporation from a water table. Soil science, 85(4): 228-232.

Gardner, W. R. (1974) The permeability problem. Soil Science, 117(5): 243-249.

Groenevelt, P. H., and Grant, C. D. (2004) A new model for the soil-water retention curve that solves the problem of residual water contents. European Journal of Soil Science, 55(3): 479-485.

Haines, W. B. (1923) The volume-changes associated with variations of water content in soil. The Journal of agricultural science, 13(03): 296-310.

Huang, S., Barbour, S. L., and Fredlund, D. G. (1998) Development and verification of a coefficient of permeability function for a deformable unsaturated soil. Canadian Geotechnical Journal, 35(3): 411-425.

Keen, B. A. (1931) The physical properties of the soil. Longmans, Green.

Kosugi, K. I. (1994) Three-parameter lognormal distribution model for soil water retention. Water Resources Research, 30(4): 891-901.

Laliberte, G. E. (1969) A mathematical function for describing capillary pressure-desaturation data. Hydrological Sciences Journal, 14(2): 131-149.

Leong, E. C., and Rahardjo, H. (1997) Permeability functions for unsaturated soils. Journal of Geotechnical and Geoenvironmental Engineering, 123(12): 1118-1126.

Marinho, F. A. M. (1994). Shrinkage behaviour of some plastic soils. Doctoral dissertation, University of London, UK.

McKee, C. R., Bumb, A. C. (1984) The importance of unsaturated flow parameters in designing a hazardous waste site. In Hazardous Waste and Environmental Emergencies, Hazardous Materials Control Research Institute National Conference, Houston, Texas, pp. 12-14.

McKee, C. R., and Bumb, A. C. (1987) Flow-testing coalbed methane production wells in the presence of water and gas. SPE formation Evaluation, 2(04): 599-608.

Mualem, Y. (1976) A new model for predicting the hydraulic conductivity of unsaturated porous media. Water Resources Research, 12(3): 513-522.

Pachepsky, Y. A., Shcherbakov, R. A. and Korsunskaya, L. P. (1995) Scaling of soil water retention using a fractal model. Soil Science, 159(2): 99-104.

Parent, S. E., Cabral, A., and Zornberg, J. G. (2007). Water retention curve and hydraulic conductivity function of highly compressible materials. Canadian Geotechnical Journal, 44(10): 1200-1214

Pereira, J. H., and Fredlund, D. G. (2000) Volume change behavior of collapsible compacted gneiss soil. Journal of geotechnical and geo-environmental engineering, 126(10): 907-916.

Pham, H. Q., and Fredlund, D. G. (2008) Equations for the entire soil-water characteristic curve of a volume change soil. Canadian geotechnical journal,45(4): 443-453.

Russo, D. (1988) Determining soil hydraulic properties by parameter estimation: On the selection of a model for the hydraulic properties, Water Resources Research, 24(3): 453-459.

Somogyi, F. (1980) Large-strain consolidation of fine-grained slurries. Proceedings of the Canadian Society for Civil Engineering 1980 Annual Conference, Winnipeg, Manitoba, Canada.

Sridharan, A., and Rao, G. V. (1971) Effective stress theory of shrinkage phenomena. Canadian Geotechnical Journal, 8(4): 503-513.

Stirk, G. B. (1954) Some aspects of soil shrinkage and the effect of cracking upon water entry into the soil. Crop and Pasture Science, 5(2): 279-296.

Taylor, D. W. (1948) Fundamentals of soil mechanics. J. Wiley & Sons; London: Chapman & Hall.

Tempany, H. A. (1917) The shrinkage of soils. The Journal of Agricultural Science, 8(03): 312-330.

Terzaghi, K. (1925) Principles of soil mechanics, IV -- Settlement and consolidation of clay. Engineering News-Record, 95(3): 874-878.

Van Genuchten, M. T. (1980) A closed-form equation for predicting the hydraulic conductivity of unsaturated soils. Soil science society of America journal, 44(5): 892-898.

Vanapalli, S.K., Sillers, W.S., and Fredlund, M.D. (1998) The meaning and relevance of residual state to unsaturated soils. Proceedings of the 51st Canadian Geotechnical Conference, Edmonton, AB, October 4-7, pp.1-8.

Zhang, F. (2010) Soil water retention and relative permeability for full range of saturation (No. PNNL-19800). Pacific Northwest National Laboratory (PNNL), Richard, WA (US).

Zhang, F., Fredlund, D. G., Wilson, G. W., and Sedgwick, A. (2014) Determination of the permeability function for drying oil sands tailings undergoing volume change and desaturation. Proceedings of the 4th International Oil Sands Tailings Conference, Banff, A.B. 2014.

Zhang, F. and Fredlund, D. G. (2015) Examination of the estimation of relative permeability for unsaturated soils. Canadian Geotechnical Journal, Published on the web 3 June 2015, 10. 1139/cgj-2015-0043.

Chapter 4. Permeability function for oil sands tailings undergoing volume change during drying

4.1 Introduction

The oil sands bitumen extraction process in northern Alberta produces large volumes of high water content tailings composed of sand, silt, clay, and a small amount of unrecovered bitumen. Significant portions of the fines remain in suspension after deposition resulting in a tailings management challenge for the industry. Various processes and technologies have been suggested to improve the water release characteristics of the tailings. One of the disposal methodologies advanced to improve the dewatering behavior of the tailings is thin lift deposition of thickened oil sands tailings (TT). The design of tailings disposal often involves numerical modeling of TT at various sand-to-fines ratios, (SFRs). Numerical modeling of the dewatering process requires the use of an appropriate permeability function and water storage function.

Research has shown that changes in the void ratio and changes in the degree of saturation are factors that influence the permeability function of a soil (Zhang et al. 2014). The effect of changing void ratio on changes in the saturated coefficient of permeability has previously been given consideration (Chapuis 2012; Taylor 1948). Methodologies for the estimation of the permeability function for an unsaturated soil are based on the assumption that no volume change occurs as soil suction is changed. In other words, changes in the permeability of an unsaturated soil are assumed to occur as a result of changes in degree of saturation. Reasonable permeability functions can be obtained for unsaturated soils that do not undergo volume change as soil suction is changed. Oil sands tailings have been found to undergo significant volume change as soil suction is increased during drying (Fredlund et al. 2011). Commonly used unsaturated permeability estimation methodologies cannot adequately represent the permeability function for oil sands tailings subjected to drying.

This paper proposes a methodology for the estimation of the permeability function for soils that undergo volume change as soil suction is increased. Changes in void ratio and degree of saturation are taken into account as two independent factors of significance. Laboratory test results are used to illustrate the application of the proposed methodology for oil sands tailings. The extreme nonlinearity in the gravimetric water content versus soil suction relationship (i.e., *w*-SWCC) can make it difficult to accurately best-fit a laboratory dataset with any of the commonly used equations for the SWCC (Fredlund et al. 2011). One means of circumventing this problem is to use a bimodal form of the Fredlund-Xing (1994) SWCC equation. The soil-water characteristic curve, SWCC, forms the basis for the estimation of various unsaturated soil property functions. Research has shown that the soil-water characteristic curve, SWCC, strongly influences the estimation of the permeability function for an unsaturated soil (Rahimi et al. 2015).

4.2 Literature review on the role of the SWCC

The soil-water characteristic curve, SWCC, describes the relationship between the amount of water in the soil and its corresponding soil suction, and the drying relationship differs from the wetting relationship. One of several variables can be used to designate the amount of water in the soil (e.g., gravimetric water content, volumetric water content and degree of saturation. The SWCC has become pivotal to the estimation of unsaturated soil property functions such as the permeability function and the water storage function (Fredlund et al. 2012). The SWCC can be represented by a mathematical function and then used to determine the unsaturated soil property functions. A number of equations have been proposed in the literature by various researchers.

The Brooks and Corey (1964) equation, the Gardner (1974) equation, various forms of the van Genuchten (1980) equation and the Fredlund-Xing (1994) equation appear to be the most commonly used SWCC equations in geotechnical engineering. The original van Genuchten (1980) is a 3-parameter equation that has the ability to best-fit data from a wide range of soils. The van Genuchten (1980) equation has been simplified by prescribing a fixed relationship between the m and n fitting parameters. The proposed simplification made it possible to obtain a closed-form permeability function for an unsaturated soil when substituting a simplified van Genuchten (1980) SWCC equation into the Burdine (1953) equation or the Mualem (1976) integral equation for the unsaturated permeability function. The simplified van Genuchten (1980) equations resulted in less mathematical flexibility than the original van Genuchten (1980) equation when best-fitting the experimental SWCC data. The Fredlund-Xing (1994) equation is a four-parameter equation that provides increased flexibility in fitting SWCC data over the complete range of soil suction values (i.e., up to 1,000,000 kPa). Leong and Rahardjo (1997) evaluated various proposed sigmoidal SWCC equations and identified the Fredlund-Xing (1994) equation as performing best for fitting all soil types.

Aforementioned sigmoidal SWCC equations are intended for unimodal SWCCs for soils that are well-graded with one dominant series of pore sizes. When two or more pore series exist, the corresponding SWCC tends to be bimodal or multimodal (Zhang and Chen 2005). A modification to the fitting equation is required to properly represent the bimodal or multimodal SWCC for a gap-graded soil, where there is more than one pore series. Burger and Shackelford (2001a; 2001b) presented piecewise-continuous forms of the Brooks-Corey (1964), van Genuchten (1980), and Fredlund-Xing (1994) SWCC functions to account for the bimodal patterns of experimental SWCCs. The piecewise-continuous forms for the SWCC were tested on pelletized diatomaceous earth and sand-diatomaceous earth mixtures with dual porosity. Zhang and Chen (2005) proposed a method to predict bimodal or multimodal SWCCs for bimodal or multimodal soils using the unimodal SWCCs for the characteristic components corresponding to respective pore series.

4.3 Literature review on the shrinkage curve

The shrinkage curve establishes a relationship between the instantaneous void ratio and gravimetric water content. The shrinkage curve can play an important role in estimating unsaturated soil property functions for soils that exhibit significant volume change as soil suction is changed. Researchers have investigated the character of the shrinkage of soils since the early 1900s (Tempany 1917). An interpretation of the shrinkage curve was presented by Haines (1923) that included the concept of normal shrinkage and residual shrinkage. Terzaghi (1925) noted that the shrinkage behavior could be compared to the isotropic compression of a soil. Sridharan (1971) discussed the physical mechanism involved in the process of shrinkage using a modified effective stress concept. Kim et al. (1992) studied shrinkage processes and the geometry of volume shrinkage with respect to the physical ripening naturally occurring in a marine clay soil. Marinho (1994) carried out a comprehensive study of shrinkage curve functions. Fredlund (2000) presented a mathematical equation for the shrinkage curve as well as a theoretical procedure for estimating the shrinkage curve. Cornelis et al. (2006) proposed a simplified parametric model and assessed the magnitude and geometry of soil shrinkage. The Fredlund (2000) shrinkage equation accurately represents the shrinkage behavior for the drying of soils from a near-saturated state. The shrinkage curve equation proposed by Fredlund (2000) is used in this study as the basis for separating the effects of volume change and degree of saturation effects when estimating the permeability function for high volume change soils.

4.4 Literature review related to the permeability function

Direct measurement of the permeability function of an unsaturated soil in the laboratory is time-consuming, expensive and technically demanding. Measurements of the SWCC and the subsequent estimation of permeability functions have become the more common approach in geotechnical engineering for determining an acceptable permeability function.

There are four main categories of models that have been proposed for the estimation of unsaturated permeability function; namely, empirical models, statistical models, correlation models and regression models (Leong and Rahardjo 1997; Fredlund et at. 2012). Empirical models and statistical models are most common. Empirical models estimate the unsaturated permeability function from the SWCC by utilizing the similarities between the SWCC and the unsaturated permeability function. The Brooks and Corey (1964) equation is one of the empirical estimation equations. Statistical models are based on the assumption that both the permeability function and the SWCC are primarily influenced by the pore-size distribution of the soil.

Childs and Collis-George (1950), Burdine (1953) and Mualem (1976) respectively proposed an integral formula for the estimation of the unsaturated permeability function based on different physical models. Various statistical models have been further developed from one of three integral formulas. The three well-known statistical models can be presented in the form of relative permeability equations and can be referred to as the van Genuchten-Burdine (1980) equation, the van Genuchten-Mualem (1980) equation and the Fredlund-Xing-Huang (1994) permeability function. These permeability equations were developed by introducing, i.) the van Genuchten SWCC (1980) equation into the Burdine (1953) formula, ii.) the van Genuchten SWCC (1980) equation into the Mualem (1976) formula, and iii.) the Fredlund-Xing SWCC equation (1994) into the Childs and Collis-George (1950) formula. A constant saturated coefficient of permeability is generally combined with the relative permeability functions to generate a continuous unsaturated soil permeability function. Historically, the estimation methods for these permeability functions have been based on the assumption that the soil does not undergo volume change as soil suction is increased.

Studies on deformable soils have been conducted for various purposes. Croney and Coleman (1954) measured soil suction and volume change for several compressible soils. Mbonimpa et al., (2006) proposed a model for the soil-water characteristic curve of deformable clayey soils by introducing the volumetric shrinkage curve in the formulation of the modified Kovacs (MK) model. Parent et al. (2007) conducted SWCC tests on “deinking by-product” (DBP), a highly compressible industrial by-product which has been used as a cover material for landfills and mining applications as well as a soil structural enhancement material in agricultural applications. Tripathy et al. (2014) studied in detail the SWCCs of three deformable clays in terms of the water content and the degree of saturation. Huang et al. (1998) develop a coefficient of permeability model for a deformable unsaturated porous medium considering volume change prior to desaturation. Huang et al. (1998) suggested accounting for the effect of void ratio change on the saturated permeability, while the relative permeability was obtained using the volumetric water content SWCC (θ-SWCC). More recently, studies have been undertaken to observe the influence of both desaturation and volume change on the permeability function for deformable soils (Fredlund and Zhang 2013).

Existing methods are not adequate for estimating the permeability function for soils that undergo significant volume change both before and after the applied suction exceeds the air-entry value. It is necessary to develop a permeability function for a volume change soil that considers both the influence of volume change and desaturation during drying from saturation to oven-dry conditions.

A revised methodology for estimating the permeability function for a soil that undergoes volume change during a drying process is presented in this paper.

4.5 General information on the permeability function theory

The permeability theory is limited to using the soil-water characteristic curve in the case where significant volume changes occur as suction is increased. The SWCC has been used in a general sense to describe the amount of water in a soil as a function of soil suction. The designation for the amount of water in the soil defines the character of the SWCC. There are four different designations that have been used for defining the amount of water in a soil; namely, gravimetric water content w, volumetric water content (referenced to the initial total volume) θ, instantaneous volumetric water content (referenced to the instantaneous total volume) θ_i and degree of saturation S. However, volumetric water content referenced to the initial volume of soil has no value when considering the case of volume change with respect to suction change. Only the instantaneous volumetric water content is discussed in this paper and used for comparison with gravimetric water content and degree of saturation.

The SWCC can accordingly take on three different forms; namely, gravimetric water content-SWCC (*w*-SWCC), instantaneous volumetric water content-SWCC (θ_i -SWCC), and degree of saturation-SWCC (*S*-SWCC). For soils that undergo insignificant volume change as soil suction is increased (e.g., sands and dense silts), all three SWCC designations provide the same information to geotechnical engineers for estimating unsaturated soil property functions. Figure 4-1 shows that the three SWCCs (i.e., *w*-SWCC, θ_i-SWCC and *S*-SWCC) produce the same curve when plotted in terms of dimensionless water content versus soil suction. However, for a soil that undergoes volume change as soil suction is increased during a drying process, the three SWCCs are different from one another. Figure 4-2 presents the results of SWCC tests performed on oil sands tailings and show that there is a difference amongst the *w*-SWCC, θ_i-SWCC and *S*-SWCC. Oil sands tailings represent a material that undergoes significant volume change as soil suction is increased during drying.

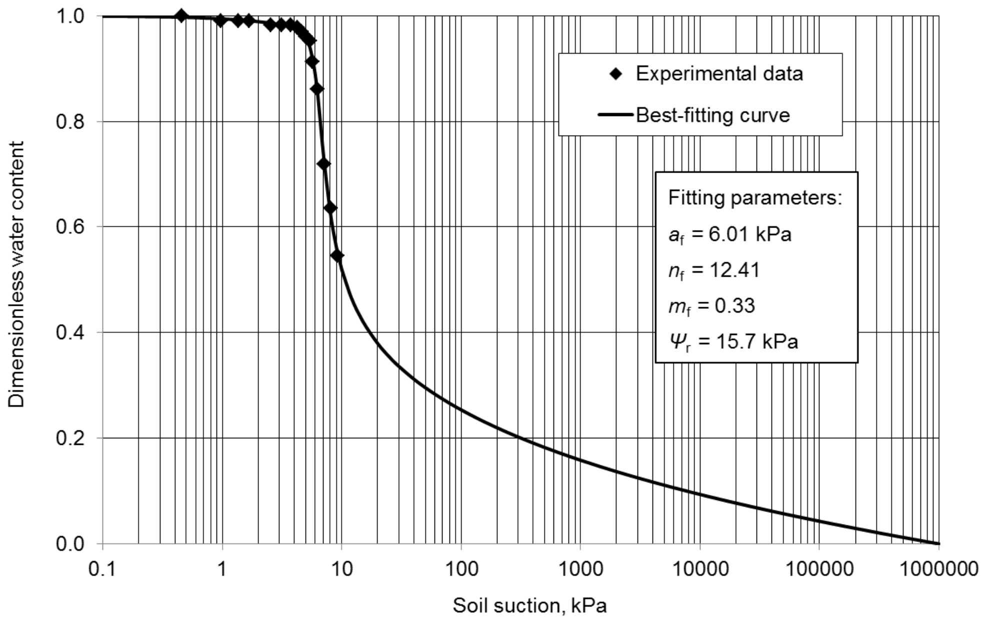

Figure 4-1. Fredlund-Xing (1994) SWCC fit to experimental data for Columbia sandy silt (Data from Brooks and Corey (1964)).

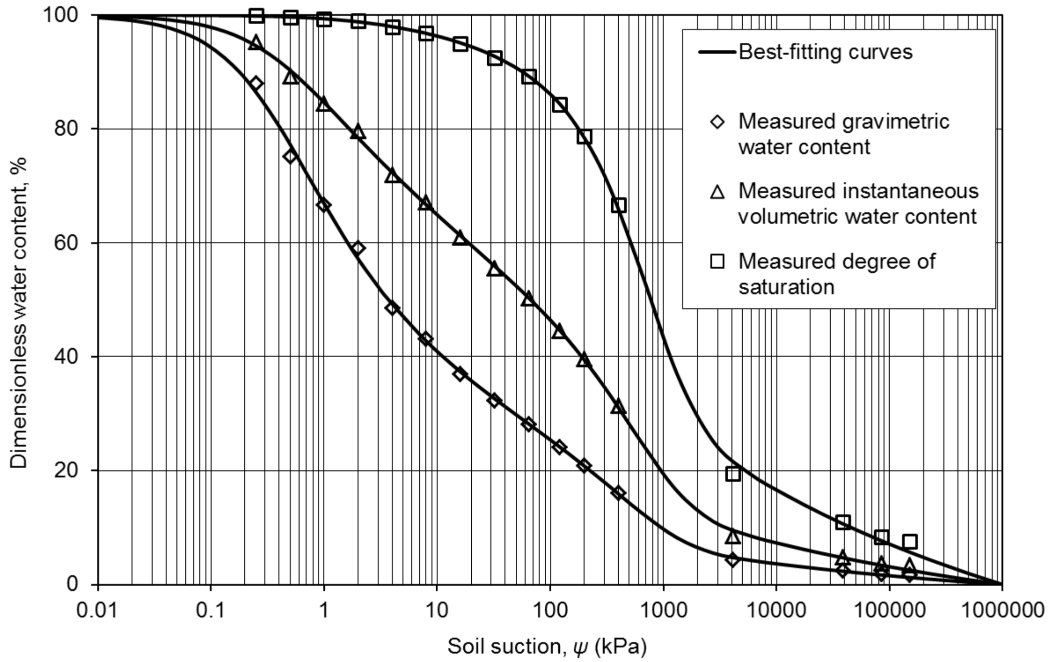

Figure 4-2. Gravimetric water content, the instantaneous volumetric water content and degree of saturation versus soil suction for thickened oil sands tailings tested

4.6 Relationship between volume-mass variables

Gravimetric water content constitutes the standard measurement used in the laboratory when performing a SWCC test. The degree of saturation and the instantaneous volumetric water content are indirectly calculated from the gravimetric water content measurements along with a shrinkage curve for the soil. The basic volume-mass relationships that relate the three designations of the amount of water in a soil are as below:

$$S = \frac{wG_s}{e} \qquad [37]$$

$$\theta_{\mathrm{i}} = \frac{Se}{1+e} = \frac{wG_{\mathrm{s}}}{1+e} \quad [38]$$

where:

S = degree of saturation,

w = gravimetric water content,

G_s = specific gravity of the solids,

e = void ratio,

θ_i = instantaneous volumetric water content where the volume of water is referenced to the instantaneous total volume of the tested soil.

The shrinkage curve test involves the measurement of volume and mass of water in the soil as drying occurs. This allows to describe the relationship between void ratio and gravimetric water content. The following hyperbolic equation proposed by Fredlund (2000) can be used to represent the shrinkage curve.

$$e(w) = a_{\mathrm{sh}} \left(\left(\frac{w}{b_{\mathrm{sh}}} \right)^{c_{\mathrm{sh}}} + 1 \right)^{\frac{1}{c_{\mathrm{sh}}}} \quad [39]$$

where:

a_{sh} = minimum void ratio, e_{min},

a_{sh}/b_{sh} = slope of the line of tangency,

c_{sh} = curvature of the shrinkage curve, and

w = gravimetric water content.

The Fredlund (2000) equation has the following relationship between the fitting parameters and the volume-mass properties.

$$\frac{a_{\mathrm{sh}}}{b_{\mathrm{sh}}} = \frac{G_{\mathrm{s}}}{S_0} \quad [40]$$

where:
S_0 = initial degree of saturation.

The equation forms a continuous function with $e(w) = \frac{a_{sh}}{b_{sh}} w$ as its asymptotic line. The shrinkage curve moves closer and closer to a straight asymptotic line of constant degree of saturation as gravimetric water content increases.

The shrinkage curve becomes an important mathematical relationship when solving geotechnical engineering problems where drying produces significant volume change. Eq. [39] is used as the basis for the development of a revised methodology for estimating the permeability function for high volume change materials.

4.7 various forms of SWCC

The Fredlund-Xing (1994) equation has been used to provide a reasonable fit of SWCC laboratory data over the entire suction range. The SWCC equation, written in terms of gravimetric water content versus soil suction, is as follows.

$$w(\psi) = \frac{w_s \left(1 - \ln\left(1 + \psi/\psi_r\right) / \ln\left(1 + 10^6/\psi_r\right)\right)}{\left(\ln\left(\exp(1) + \left(\psi/a_f\right)^{n_f}\right)\right)^{m_f}} \qquad [41]$$

where:
ψ = soil suction,
a_f, n_f, m_f, and ψ_r = mathematical fitting parameters,
w_s = initial saturated gravimetric water content, and

$w(\psi)$ = gravimetric water content at a soil suction of ψ.

Equation [41] is a sigmoidal equation that can be used to best-fit unimodal soil-water characteristics data. The large deformations associated with the oil sands tailings give the appearance of bimodal behavior and consequently it is also possible to more closely fit the data using a bimodal form for *w*-SWCC. Zhang and Chen (2005) presented a method for the determination of soil-water characteristic curves for soils with bimodal or multimodal pore-size distributions. The theoretical bimodal SWCC function developed by Zhang and Chen (2005) made use of the Fredlund and Xing (1994) function in the following manner:

$$\theta(\psi) = p_l n_{pl}\left(1-\frac{\ln\left(1+\frac{\psi}{\psi_{rl}}\right)}{\ln\left(1+\frac{10^6}{\psi_{rl}}\right)}\right)\left(\frac{1}{\ln\left(\exp(1)+\left(\frac{\psi}{a_l}\right)^{n_l}\right)}\right)^{m_l} + p_s n_{ps}\left(1-\frac{\ln\left(1+\frac{\psi}{\psi_{rs}}\right)}{\ln\left(1+\frac{10^6}{\psi_{rs}}\right)}\right)\left(\frac{1}{\ln\left(\exp(1)+\left(\frac{\psi}{a_s}\right)^{n_s}\right)}\right)^{m_s} \qquad [42]$$

where,

θ = volumetric water content;

p_l and p_s =, respectively, volumetric percentages of the components with the large-pore series and the small-pore series in the soil mass that can be calculated easily based on the density values and the percentages by dry weight of the soil components;

n_{pl} and n_{ps} = porosities of the components with the large-pore series and the small-pore series when they are considered individually.

a_l, n_l, m_l, ψ_{rl}, and as, n_s, m_s, ψ_{rs} = parameters of the SWCC function for the components with the large-pore series and the small-pore series.

The bimodal function is quite complex and contains many fitting parameters. Fitting the model to data can also result in variances in the estimated parameters for the same soil. There will consequently be a greater dependency of the estimated model parameters on their initial estimates. It is also possible that the computer algorithm may become trapped within a local minimum. Although the bimodal model has a sound theoretical base, it is preferable to keep the SWCC expression as simple as possible. It should be noted that it is the mathematical form of analytical expressions that determines the accuracy of the estimated permeability function rather than the physical meaning of the fitting parameters as was demonstrated by Cornelis et al. (2005). On the other hand, empirical models have limitations when compared to the deterministic models that they do not allow for better understanding of the real process. The original theoretical bimodal equation by Zhang and Chen (2005) (Eq. [42]) has two correction functions. The role of the correction function is to bring the calculated water content to zero at the limiting point where ψ is equal to 10^6 kPa. Therefore, it is possible to use one correction function rather than two correction functions. In the original theoretical bimodal, there is a correlation between the fitting parameters as shown below:

$$\theta_s = p_l n_{pl} + p_s n_{ps} \qquad [43]$$

Where:

θ_s is saturated volumetric water content,

$p_l n_{pl}$ and $p_s n_{ps}$ are the saturated volumetric water content of each pore series, $p_l n_{pl}$ and $p_s n_{ps}$ denotes the proportions of two pore series.

A weighting factor p between 0 and 1.0 can be used to represent the proportion of the large pore series, and 1-p the small pore series. The saturated volumetric water content of the large pore series is θ_{sp}, which is represented by $p_l n_{pl}$. The saturated volumetric water content of the small pore series is θ_s(1-p), which is represented by $p_s n_{ps}$. It is possible to use a simplified bimodal equation to that proposed by Zhang and Chen (2005).

The simplified bimodal equation written in terms of gravimetric water content versus soil suction is.

$$w(\psi) = w_s \left(1 - \frac{\ln\left(1 + \frac{\psi}{\psi_{rb}}\right)}{\ln\left(1 + \frac{10^6}{\psi_{rb}}\right)} \right) \left(\frac{p}{\left(\ln\left(\exp(1) + \left(\frac{\psi}{a_{f1}}\right)^{n_{f1}}\right)\right)^{m_{f1}}} + \frac{1-p}{\left(\ln\left(\exp(1) + \left(\frac{\psi}{a_{f2}}\right)^{n_{f2}}\right)\right)^{m_{f2}}} \right) \quad [44]$$

where:

ψ = soil suction,

a_{f1}, n_{f1}, m_{f1}, a_{f2}, n_{f2}, m_{f2}, and ψ_{rb} = mathematical fitting parameters,

p = a weighting factor between 0 to 1.0 used to divide the bimodal behavior,

w_s = initial saturated gravimetric water content, and

$w(\psi)$ = gravimetric water content at a soil suction of ψ.

The simplified bimodal model (Eq. [44]) is used to best-fit the bimodal measured *w*-SWCC data, while the Fredlund-Xing (1994) equation, (i.e., Eq. [41]) is recommended to best-fit the unimodal measured *w*-SWCC data. The θ_l-SWCC and *S*-SWCC functions can be obtained by combining the best-fit *w*-SWCC with the Fredlund (2000) shrinkage curve equation. The simplified bimodal equation (Eq. [44]) is used for handling the bimodal behavior and to develop the revised methodology for estimating the permeability function. The revised procedure for estimating the permeability function of a high-volume-change soil with a unimodal *w*-SWCC is outlined in Appendix A.

A relationship of void ratio versus soil suction can be obtained by substituting Eq. [44] into Eq. [39].

$$e(\psi)=a_{\mathrm{sh}}\left(\left(\frac{w_{\mathrm{s}}}{b_{\mathrm{sh}}}\left(1-\frac{\ln\left(1+\dfrac{\psi}{\psi_{\mathrm{rb}}}\right)}{\ln\left(1+\dfrac{10^{6}}{\psi_{\mathrm{rb}}}\right)}\right)\left(\frac{p}{\left(\ln\left(\exp(1)+\left(\dfrac{\psi}{a_{\mathrm{f1}}}\right)^{n_{\mathrm{f1}}}\right)\right)^{m_{\mathrm{f1}}}}+\frac{1-p}{\left(\ln\left(\exp(1)+\left(\dfrac{\psi}{a_{\mathrm{f2}}}\right)^{n_{\mathrm{f2}}}\right)\right)^{m_{\mathrm{f2}}}}\right)\right)^{c_{\mathrm{sh}}}+1\right)^{\frac{1}{c_{\mathrm{sh}}}}$$

[45]

Substituting Eq. [44] and Eq. [45] into the basic volume-mass relationships, (i.e., Eqs. [37] and [38]), leads to the best-fitting equations for *S*-SWCC and θ_l-SWCC, as shown in Eqs. [46] and [47], respectively.

$$S(\psi)=\frac{G_{\mathrm{s}}\,w_{\mathrm{s}}\left(1-\dfrac{\ln\left(1+\dfrac{\psi}{\psi_{\mathrm{rb}}}\right)}{\ln\left(1+\dfrac{10^{6}}{\psi_{\mathrm{rb}}}\right)}\right)\left(\dfrac{p}{\left(\ln\left(\exp(1)+\left(\dfrac{\psi}{a_{\mathrm{f1}}}\right)^{n_{\mathrm{f1}}}\right)\right)^{m_{\mathrm{f1}}}}+\dfrac{1-p}{\left(\ln\left(\exp(1)+\left(\dfrac{\psi}{a_{\mathrm{f2}}}\right)^{n_{\mathrm{f2}}}\right)\right)^{m_{\mathrm{f2}}}}\right)}{a_{\mathrm{sh}}\left(\left(\dfrac{w_{\mathrm{s}}}{b_{\mathrm{sh}}}\left(1-\dfrac{\ln\left(1+\dfrac{\psi}{\psi_{\mathrm{rb}}}\right)}{\ln\left(1+\dfrac{10^{6}}{\psi_{\mathrm{rb}}}\right)}\right)\left(\dfrac{p}{\left(\ln\left(\exp(1)+\left(\dfrac{\psi}{a_{\mathrm{f1}}}\right)^{n_{\mathrm{f1}}}\right)\right)^{m_{\mathrm{f1}}}}+\dfrac{1-p}{\left(\ln\left(\exp(1)+\left(\dfrac{\psi}{a_{\mathrm{f2}}}\right)^{n_{\mathrm{f2}}}\right)\right)^{m_{\mathrm{f2}}}}\right)\right)^{c_{\mathrm{sh}}}+1\right)^{\frac{1}{c_{\mathrm{sh}}}}}$$

[46]

$$\theta_{\mathrm{i}}(\psi)=\frac{G_{\mathrm{s}}\,w_{\mathrm{s}}\left(1-\frac{\ln\left(1+\frac{\psi}{\psi_{\mathrm{rb}}}\right)}{\ln\left(1+\frac{10^6}{\psi_{\mathrm{rb}}}\right)}\right)\left(\frac{p}{\left(\ln\left(\exp(1)+\left(\frac{\psi}{a_{\mathrm{f1}}}\right)^{n_{\mathrm{f1}}}\right)\right)^{m_{\mathrm{f1}}}}+\frac{1-p}{\left(\ln\left(\exp(1)+\left(\frac{\psi}{a_{\mathrm{f2}}}\right)^{n_{\mathrm{f2}}}\right)\right)^{m_{\mathrm{f2}}}}\right)}{1+a_{\mathrm{sh}}\left(\left(\frac{w_{\mathrm{s}}}{b_{\mathrm{sh}}}\left(1-\frac{\ln\left(1+\frac{\psi}{\psi_{\mathrm{rb}}}\right)}{\ln\left(1+\frac{10^6}{\psi_{\mathrm{rb}}}\right)}\right)\left(\frac{p}{\left(\ln\left(\exp(1)+\left(\frac{\psi}{a_{\mathrm{f1}}}\right)^{n_{\mathrm{f1}}}\right)\right)^{m_{\mathrm{f1}}}}+\frac{1-p}{\left(\ln\left(\exp(1)+\left(\frac{\psi}{a_{\mathrm{f2}}}\right)^{n_{\mathrm{f2}}}\right)\right)^{m_{\mathrm{f2}}}}\right)\right)^{c_{\mathrm{sh}}}+1\right)^{\frac{1}{c_{\mathrm{sh}}}}} \tag{47}$$

Equations [45] to [47] are changed in response to the best-fit equations used for the *w*-SWCC and the shrinkage curve. Improved fitting of the *w*-SWCC results in improved fitting of the *S*-SWCC and the θ_i-SWCC. Laboratory oil sands tailings measurements are used for illustration and verification purposes.

It is important to use the appropriate form of the SWCC when estimating unsaturated soil property functions for a soil that undergoes volume change with respect to suction changes. The degree of saturation SWCC (*S*-SWCC), should be used to determine the correct air-entry value, AEV, which forms the starting point for integration for the relative permeability function (Zhang and Fredlund 2015; Fredlund and Zhang 2013). Likewise, the θ_i–SWCC should be use for the calculation of the water storage function. Misuse of SWCCs when estimating unsaturated soil property functions can result in significant errors.

4.8 Revised methodology for estimating the permeability function

The proposed methodology for the estimation of the permeability function for soils undergoing large volume changes is presented in the following section. The degree of saturation and the void ratio are two controlling factors that influence the computed permeability function. The permeability at a particular suction during a drying process is the product of the relative permeability and the corresponding saturated permeability of the soil as shown in Eq. [48].

$$k(\psi) = k_{\mathrm{r}}(\psi) \times k_{\mathrm{rs}}(\psi) \qquad [48]$$

where:

$k(\psi)$ = permeability at a particular soil suction, ψ,

$k_r(\psi)$ = relative permeability at the soil suction, ψ, and

$k_{rs}(\psi)$ = reference saturated permeability at the soil suction of ψ.

The reference saturated permeability corresponds to the saturated permeability when the soil at a particular suction is in single-phase water flow.

The effect of degree of saturation is considered in the relative permeability function, $k_r(\psi)$ while the influence of the void ratio is included in the reference saturated permeability function, $k_{rs}(\psi)$. Changes in the degree of saturation change the tortuosity of the flow path within the porous media. The tortuosity, in turn, changes the relative permeability. In other words, the degree of saturation influences the relative permeability because of its impact on the tortuosity of the flow path. The saturated permeability of a soil depends mainly on the pore sizes and the pore size distribution (Chapuis 2012). A change in void ratio changes the pore sizes, thereby influencing the reference saturated permeability of the soil.

The two components in Eq. [48], $k_r(\psi)$ and $k_{rs}(\psi)$ can be separately calculated. The relative permeability function, $k_r(\psi)$ is estimated from the *S*-SWCC. The reference saturated permeability function, $k_{rs}(\psi)$ is calculated based on two relationships, the relationship of void ratio versus soil suction and the relationship of saturated permeability versus void ratio. Studies on the relationship between the void ratio and the saturated permeability of a soil have been undertaken by numerous researchers (Chapuis 2012). Equation [49] (Taylor 1948) and Eq. [50] (Somogyi 1980) are two mathematical equations that describe the relationship of the saturated coefficient of permeability, k_{sat}, to void ratio, *e*.

$$k_{\mathrm{sat}}(e) = \frac{C e^x}{1+e} \qquad [49]$$

$$k_{\mathrm{sat}}(e) = A e^B \qquad [50]$$

where:

k_{sat} = saturated permeability,

e = void ratio,

C, x = fitting parameters for Eq. [49], and

A, B = fitting parameters for Eq. [50].

Each of these equations (i.e., Eqs. [49] and [50]) can be used in conjunction with the relationship between void ratio and soil suction (Eq. [45]) to generate the reference saturated permeability function, $k_{rs}(\psi)$. Equation [50] is used in this paper to illustrate how to obtain the reference saturated permeability function, $k_{rs}(\psi)$. By substituting Eq. [45] into Eq. [50], the term of the reference saturated permeability function, $k_{rs}(\psi)$ in Eq. [48] can be obtained, as shown by Eq. [51].

$$k_{\mathrm{rs}}(\psi) = \left(A \left(a_{\mathrm{sh}} \left(\left(\frac{w_{\mathrm{s}}}{b_{\mathrm{sh}}} \left(1 - \frac{\ln\left(1+\frac{\psi}{\psi_{\mathrm{rb}}}\right)}{\ln\left(1+\frac{10^6}{\psi_{\mathrm{rb}}}\right)} \right) \left(\frac{p}{\left(\ln\left(\exp(1) + \left(\frac{\psi}{a_{\mathrm{f1}}}\right)^{n_{\mathrm{f1}}} \right) \right)^{m_{\mathrm{f1}}}} + \frac{1-p}{\left(\ln\left(\exp(1) + \left(\frac{\psi}{a_{\mathrm{f2}}}\right)^{n_{\mathrm{f2}}} \right) \right)^{m_{\mathrm{f2}}}} \right) \right)^{c_{\mathrm{sh}}} + 1 \right)^{\frac{1}{c_{\mathrm{sh}}}} \right) \right)^{B}$$

[51]

Considerable research has also been undertaken on the estimation of the relative permeability function. Its prediction is usually based on the volumetric water content SWCC, *θ*-SWCC under the assumption of no volume change during a drying process. The original Fredlund-Xing-Huang (1994) permeability function takes the following form:

$$k_{\mathrm{r}}(\psi) = \frac{\int_{\ln(\psi)}^{\mathrm{b}} \frac{\theta(e^y) - \theta(\psi)}{e^y} \theta'(e^y)\,dy}{\int_{\ln(\psi_{\mathrm{aev}})}^{b} \frac{\theta(e^y) - \theta(\psi_{\mathrm{aev}})}{e^y} \theta'(e^y)\,dy} \qquad [52]$$

where:

b = ln(1000000), and

y = a dummy variable of integration representing the logarithm of soil suction.

The original Fredlund-Xing-Huang (1994) permeability function produces appropriate relative permeability estimations for no volume change materials such as sands or silts because the *θ*-SWCC provides essentially the same information as the *S*-SWCC when there is no volume change. When a soil undergoes volume change, the degree of saturation SWCC, (*S*-SWCC) should be used to estimate the relative permeability function since it is the degree of saturation that influences the relative permeability of a soil and the *S*-SWCC is very different from the *θ*-SWCC. Therefore, the Fredlund-Xing-Huang (1994) permeability function should be modified and using the *S*-SWCC for estimation purposes:

$$k_{\mathrm{r}}^{s}(\psi)=\frac{\int_{\ln(\psi)}^{\mathrm{b}}\frac{S(e^{y})-S(\psi)}{e^{y}}S'(e^{y})dy}{\int_{\ln(\psi_{\mathrm{aev}})}^{b}\frac{S(e^{y})-S(\psi_{\mathrm{aev}})}{e^{y}}S'(e^{y})dy} \quad [53]$$

where:

$k_{\mathrm{r}}^{\mathrm{s}}$ = the relative coefficient of permeability and the superscript “s” denotes that the *S*-SWCC is used as the basis for the permeability estimation.

A different relative permeability function is obtained when using different forms of SWCC as the basis for calculating the permeability functions. The following two equations (i.e., Eqs [54] and [55]) are based on the *w*-SWCC and the θ_{i}-SWCC and are used in the following section to illustrate the errors that can occur when the wrong SWCC designations are used. The correct equation to use is Eq. [53] when estimating the unsaturated permeability function.

$$k_{\mathrm{r}}^{w}(\psi)=\frac{\int_{\ln(\psi)}^{\mathrm{b}}\frac{w(e^{y})-w(\psi)}{e^{y}}w'(e^{y})dy}{\int_{\ln(\psi_{\mathrm{aev}})}^{b}\frac{w(e^{y})-w(\psi_{\mathrm{aev}})}{e^{y}}w'(e^{y})dy} \quad [54]$$

where:

k_r^w = the relative coefficient of permeability with the superscript "*w*" denoting that the *w*-SWCC is used as the basis for calculating the permeability function.

$$k_r^{\theta_i}(\psi)=\frac{\int_{\ln(\psi)}^{b}\frac{\theta_i(e^y)-\theta_i(\psi)}{e^y}\theta_i'(e^y)dy}{\int_{\ln(\psi_{aev})}^{b}\frac{\theta_i(e^y)-\theta_i(\psi_{aev})}{e^y}\theta_i'(e^y)dy} \qquad [55]$$

where:

$k_r^{\theta_i}$ = the relative coefficient of permeability with the superscript θ_i denoting that the θ_i-SWCC is used as the basis for the permeability function.

For a soil that undergoes volume change, different estimation results of the relative permeability function can be obtained when using $k_r^s(\psi)$, $k_r^w(\psi)$, $k_r^{\theta_i}(\psi)$. Only the results given by the $k_r^s(\psi)$ function are acceptable when a soil changes volume as soil suction changes. It should also be noted that the AEV should be used as the lower limit of integration for the integral in the denominator (Zhang and Fredlund 2015).

S-SWCC best-fitted by Eq. [46] is suggested to be used in the $k_r^s(\psi)$ function for the estimation of the relative permeability function of a high-volume-change soil with bimodal *w*-SWCC such as oil sands tailings. For a high-volume-change soil with unimodal *w*-SWCC such as Regina clay, *S*-SWCC best-fitted by Eq. [61] in the Appendix A can be used in the $k_r^S(\psi)$ function for the estimation of the relative permeability function.

The overall permeability function for a high-volume-change material can be determined by multiplying the reference saturated permeability function by the relative permeability function as shown in Eq. [48]. By substituting the $k_r^S(\psi)$ function (Eq. [53]) and Eq. [51] into Eq. [48], a function can be obtained for the estimation of the permeability function for a soil that undergoes volume change as soil suction changes during a drying process. The simplified form of the computed permeability function is shown as Eq. [20].

$$k(\psi)=\frac{A(e(\psi))^B \int_{\ln(\psi)}^{b} \frac{S(e^y)-S(\psi)}{e^y} S'(e^y)\,dy}{\int_{\ln(\psi_{aev})}^{b} \frac{S(e^y)-S(\psi_{aev})}{e^y} S'(e^y)\,dy} \qquad [56]$$

The fitting parameters in Eq. [56] are obtained from the shrinkage curve, (i.e., Eq. [39]), the *w*-SWCC, (i.e., Eq. [44]) and the best-fitting curve for the relationship of the saturated permeability versus the void ratio, (i.e., Eq. [50]). Equation [56] changes when the best-fitting equation for the *w*-SWCC changes. An appropriate best-fitting curve for *w*-SWCC is important for obtaining a desirable permeability function using Eq. [56]. Equation [41] is recommended for best-fitting unimodal measured *w*-

SWCC data while Eq. [44] is suggested to best-fit bimodal measured *w*-SWCC data. Both Equations [41] and [44] are used to best-fit *w*-SWCC and estimate the relative permeability function for oil sands tailings for comparison. The steps for estimating the permeability function of a soil exhibiting unimodal *w*-SWCC that changes volume as soil suction increases are presented with the corresponding equations in Appendix A.

4.9 Experimental data for oil sands tailings

The experimental data used for analysis purposes were previously published by Fredlund et al. (2011). The data was part of a research study undertaken for the oil company, TOTAL. An experimental procedure was developed to measure the entire shrinkage curve for a soil. Each soil specimen was prepared at high water contents in a slurry state and placed into shrinkage rings and allowed to slowly dry by exposure to air. Rings (brass rings) with no bottom were used to contain each soil specimen. The rings with the soil were placed onto wax paper and drying was commenced. The dimensions of the soil specimens were selected such that cracking of the soil was unlikely to occur during the drying process. The ring dimensions selected for the shrinkage curve specimens had a diameter of 3.7 cm and a thickness of 1.2 cm.

The mass and volume of each soil specimen were measured on a daily basis. A digital micrometer was used to measure the volume of the specimen at various stages of drying. Four to six measurements of the diameter and thickness of the specimen were made at different locations on the specimens. Figure 4-3 shows typical measurements of water content and void ratio as the soil dried. It was observed that as the specimen diameter began to decrease, with the specimen pulling away from the brass ring, the rate of evaporation increased significantly. The increase in the evaporation rate was related to the increased surface area from which evaporation was occurring. Consequently, it is recommended that the measurements of mass and volume should be increased to once every two to three hours once the soil shows signs of pulling away from the sides of the ring.

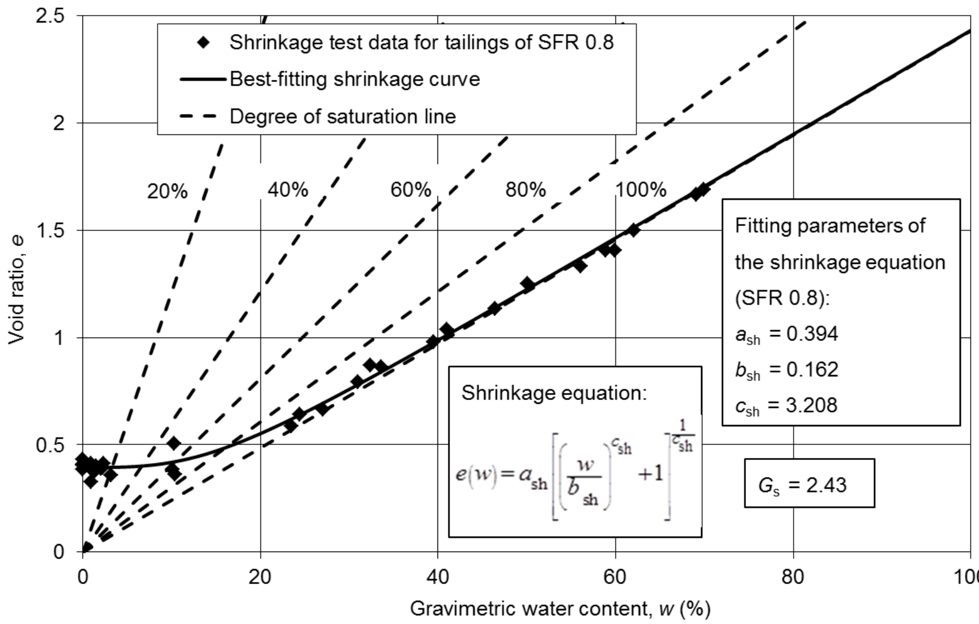

Figure 4-3. Shrinkage curve for thickened oil sands tailings

The experimental data is used to test the proposed theory for the estimation of the permeability function. The oil sands tailings results presented are for thickened tailings with a sand-to-fine ratio (SFR) of 0.8 (Fredlund et al., 2011). The oil sands thickened tailings had a liquid limit of 35% and a plastic limit of 15%. The shrinkage curve and the soil-water characteristic curves were measured. The shrinkage curve results are presented in Figure 4-3. The best-fitting parameters of the shrinkage curve for the oil sands tailings are, a_{sh} = 0.394, b_{sh} = 0.162, and c_{sh} = 3.208. The average specific gravity was 2.43. The gravimetric water content, w, plotted versus soil suction for oil sands tailings is shown in Figure 4-4. The oil sands w-SWCC data are best-fit using both of the Fredlund-Xing (1994) unimodal equation (Eq. [41]) and the simplified bimodal w-SWCC equation (Eq. [44]) for the purpose of comparison. The best-fit parameters of the Fredlund-Xing (1994) equation are a_f = 1.250 kPa, n_f = 0.982, m_f = 0.612, and ψ_r = 107.4 kPa. The best-fit parameters of the simplified bimodal equation are a_{f1} = 0.306 kPa, a_{f2} = 10355 kPa, n_{f1} = 1.181, n_{f2} = 0.946, m_{f1} = 0.794, m_{f2} = 35.773 and ψ_{rb} = 1.875 kPa, p = 0.767. The initial gravimetric water content was 73.8%. The measured w-SWCC data for the thickened oil sands tailings display a bimodal feature as shown in Figure 4-4. Thus, the best-fitting curve obtained by the simplified bimodal equation (Eq. [44]) represents the measured data points more closely than the best-fitting curve obtained by the unimodal Fredlund-Xing (1994) equation as shown in Figure 4-4. The w-SWCC is used in conjunction with the shrinkage curve to calculate S-SWCC and θ_i-SWCC. The quality of the fitting of the w-SWCC can influence the closeness of the fitting of the subsequent other forms of SWCCs (i.e., θ_i-SWCC and S-SWCC).

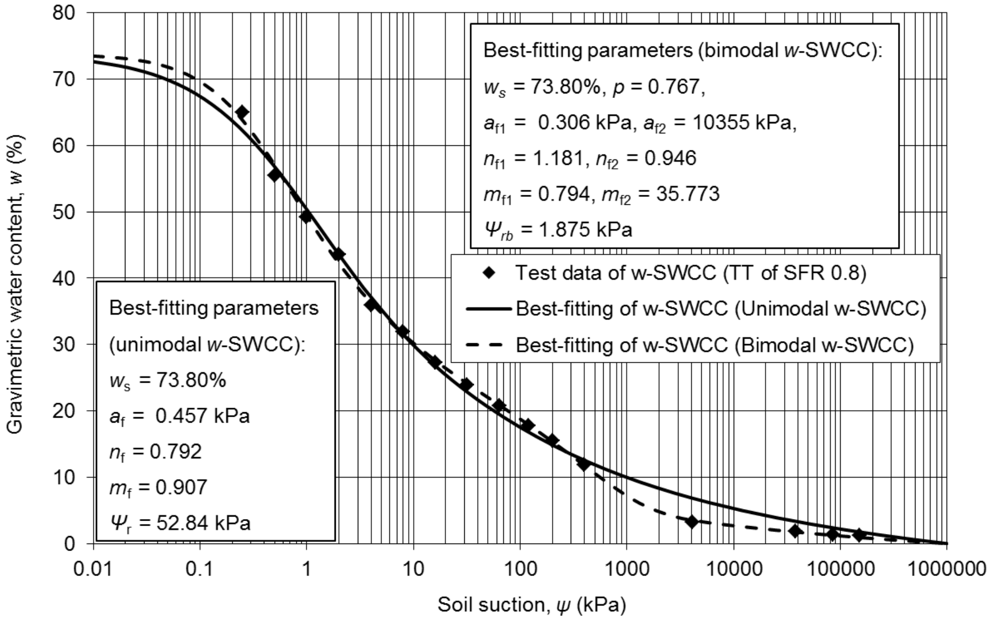

Figure 4-4. Gravimetric water content versus soil suction for thickened oil sands tailings.

The relationship between the saturated coefficient of permeability and void ratio was also measured in the laboratory and the experimental data were best-fitted using Eq. [50]. Figure 4-5 shows the measured results and the best-fitting curve. Equation [50] produces a reasonable fitting curve for the saturated permeability versus void ratio relationship for thickened oil sands tailings with the fitting parameters A = 1.263×10^{-9} and B = 3.042.

The shrinkage curve (Figure 4-3), the *w*-SWCC (Figure 4-4) and the curve of saturated permeability versus void ratio (Figure 4-5), form the basis for the subsequent calculation for the permeability function for thickened oil sands tailings.

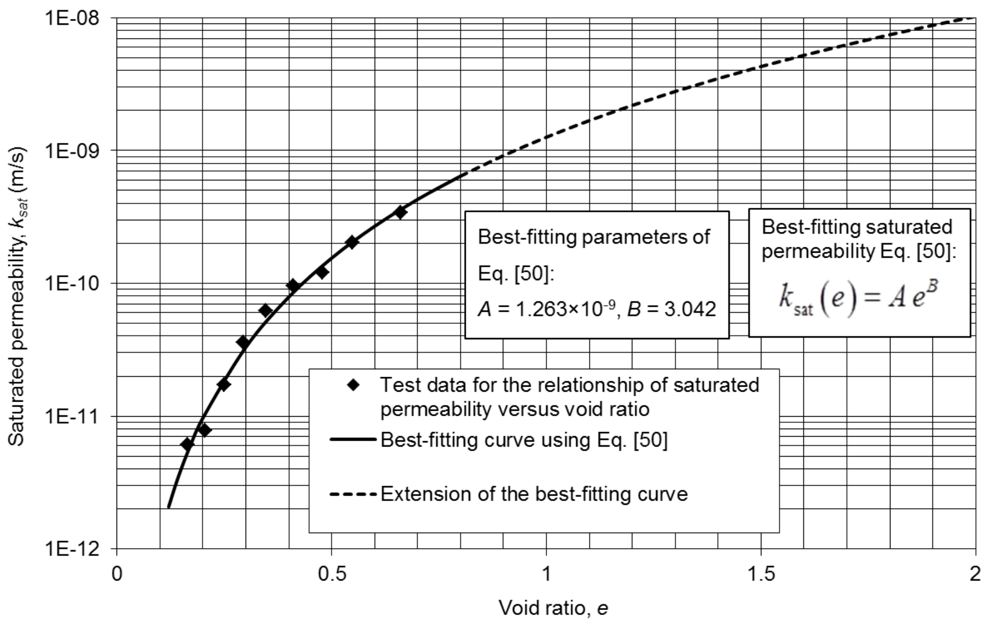

Figure 4-5. Measured data of saturated permeability versus void ratio and its best-fitting curves for thickened oil sands tailings

4.10 Interpretation of the experimental data

The gravimetric water content SWCC, (w-SWCC) is combined with the shrinkage curve to obtain the S-SWCC and θ_i-SWCC (i.e., Eq. [46] and Eq. [47]). Figure 4-6 shows a relationship of the void ratio versus soil suction, which is calculated from the w-SWCC and the shrinkage curve. The resulting plot of degree of saturation versus soil suction is shown in Figure 4-7. The plot of θ_i-SWCC is shown in Figure 4-8. The dash fitting curves on Figures 4-6 to 4-8 are calculated on the basis of the fitting curve for the w-SWCC obtained using the simplified bimodal Eq. [44]. The solid fitting curves on Figures 4-6 to 4-8 are obtained using w-SWCC best-fitted by the unimodal Eq. [41]. The dash lines are closer fits to the data than the solid lines for the relationship between void ratio and soil suction, S-

SWCC and θ_i-SWCC. Plots of Figures 4-6 to 4-8 illustrate the superior fit that can be obtained as a consequence of a better fit of the w-SWCC.

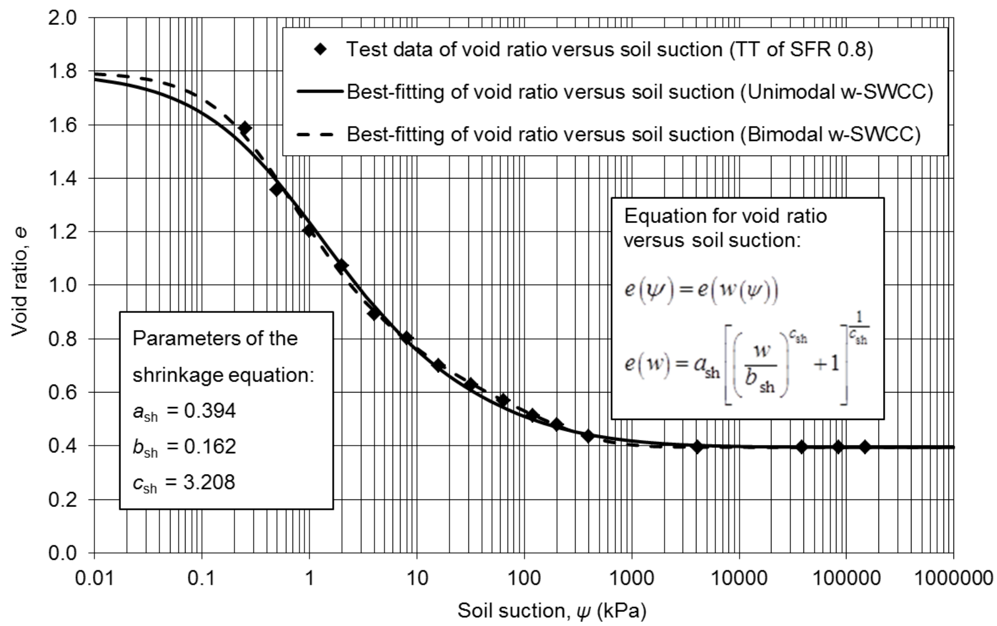

Figure 4-6. Void ratio versus soil suction for thickened oil sands tailings.

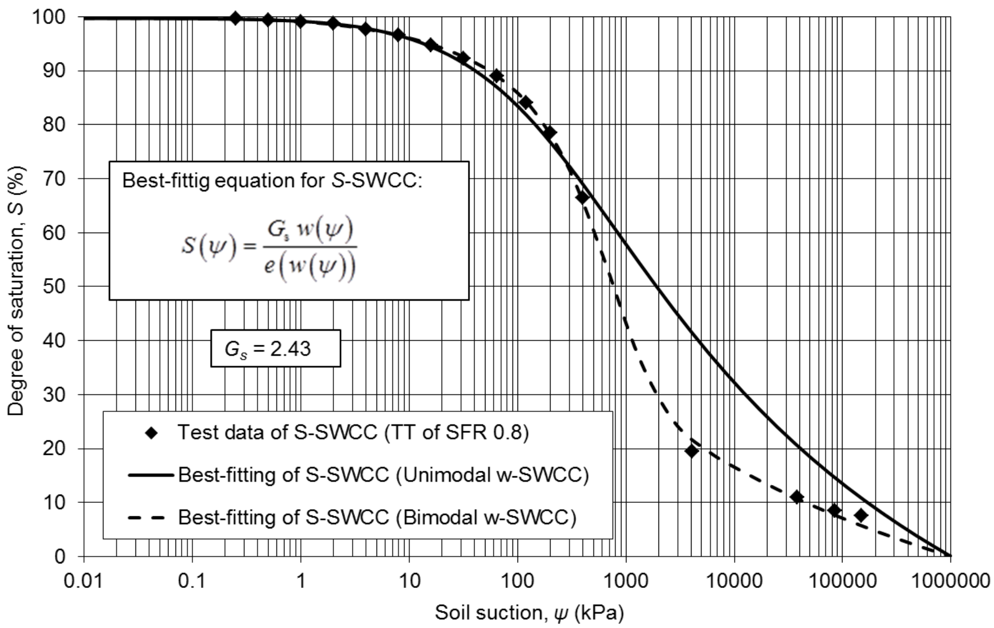

Figure 4-7. Degree of saturation versus soil suction for thickened oil sands tailings.

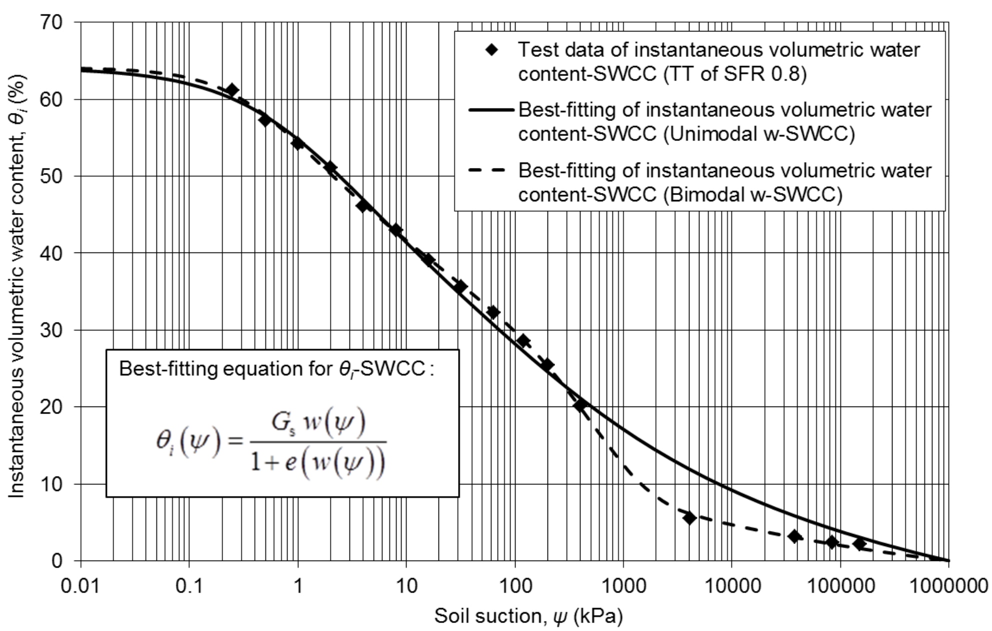

Figure 4-8. Instantaneous volumetric water content versus soil suction for thickened oil sands tailings.

The best-fit curves for the SWCCs obtained using the simplified bimodal equation for the *w*-SWCC are used to illustrate the importance of applying the correct form of SWCC in the estimation of the correct air-entry value and the relative permeability function. Table 1 lists the breaking points on various SWCCs. For soils that undergo large volume changes such as thickened oil sands tailings, the breaking points on different SWCCs appear at different soil suctions (Table 4-1). The breaking point on the *w*-SWCC is at a soil suction of 0.113 kPa. The breaking point on the *S*-SWCC is at a soil suction of 111 kPa. The breaking point on the θ_i-SWCC is at a soil suction of 0.183 kPa. The air-entry value, AEV, of the soil must be estimated from the *S*-SWCC. The degree of saturation versus soil suction plot (Figure 4-7) indicates that the AEV is 111 kPa.

Table 4-1. Breaking point on different SWCCs

Type of SWCC	*w*-SWCC	*S*-SWCC	θ_i-SWCC
Suction at the first breaking point	0.113 kPa	111 kPa	0.183 kPa

The relative permeability function is an important component constituting the permeability function for a soil that undergoes volume change as soil suction changes. Different permeability functions are obtained when using different forms of SWCC for estimation. Figure 4-9 shows three curves of the relative permeability function obtained respectively from *w*-SWCC, θ_i-SWCC, and *S*-SWCC. These three curves are obtained using Eqs. [53] to

[55]. Soil suction at the breaking point on each SWCC was used as the lower limit of integration for the integral in the denominator of each estimation equation. The correct estimation of the relative permeability is the one obtained from the *S*-SWCC. Figure 4-9 shows that the results obtained from the *w*-SWCC under-estimated the relative permeability by 6.38 orders of magnitude, while the results obtained from the θ_i-SWCC under-estimated the relative permeability by 5.07 orders of magnitude. The differences shown in Figure 4-9 are substantial.

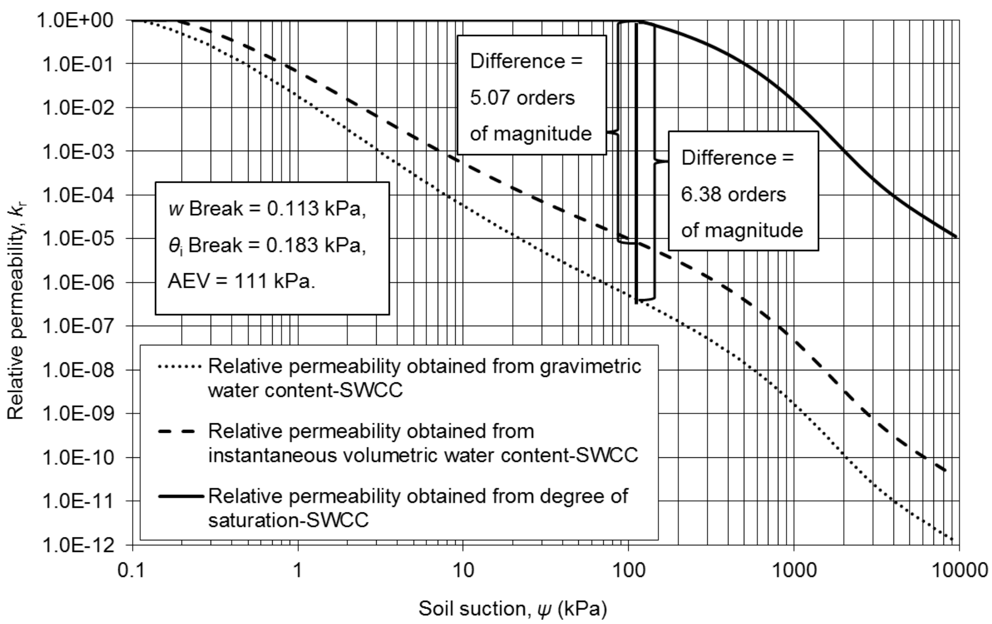

Figure 4-9. Relative permeability versus soil suction for thickened oil sands tailings.

Figure 4-10 illustrate the importance of the AEV when estimating the relative permeability function. The results show that the relative permeability versus soil suction obtained from *S*-SWCC differs when different values are used for the lower limit of integration. The $k_r^s(\psi)$ function (Eq. [53]) specifies that the AEV should be used as the lower limit of integration for the integral in the denominator of the equation. The most reasonable curve for the relative permeability function is the one obtained when using the AEV as the lower limit of integration.

Table 4-2 presents the difference that could result when using a smaller value as the lower limit of integration. When the value used as the lower limit of integration is 10 kPa, the results are underestimated by 0.898 orders of magnitude. When the value used as the lower limit of integration is 1 kPa, the resulting relative permeability would be underestimated by 1.828 orders of magnitude. When a value of 0.1 kPa is used as the lower limit of integration, the results are underestimated by 2.377 orders of magnitude. The difference in the resulting estimation for the relative permeability caused by using a lower limit of integration different than the AEV is significant (Zhang and Fredlund 2015).

Table 4-2. Difference in the estimated relative permeability in terms of orders of magnitude between using the AEV and using a different lower limit of integration.

Lower limit of integration	0.1 kPa	1 kPa	10 kPa
Difference in terms of orders of magnitude	2.377	1.828	0.898

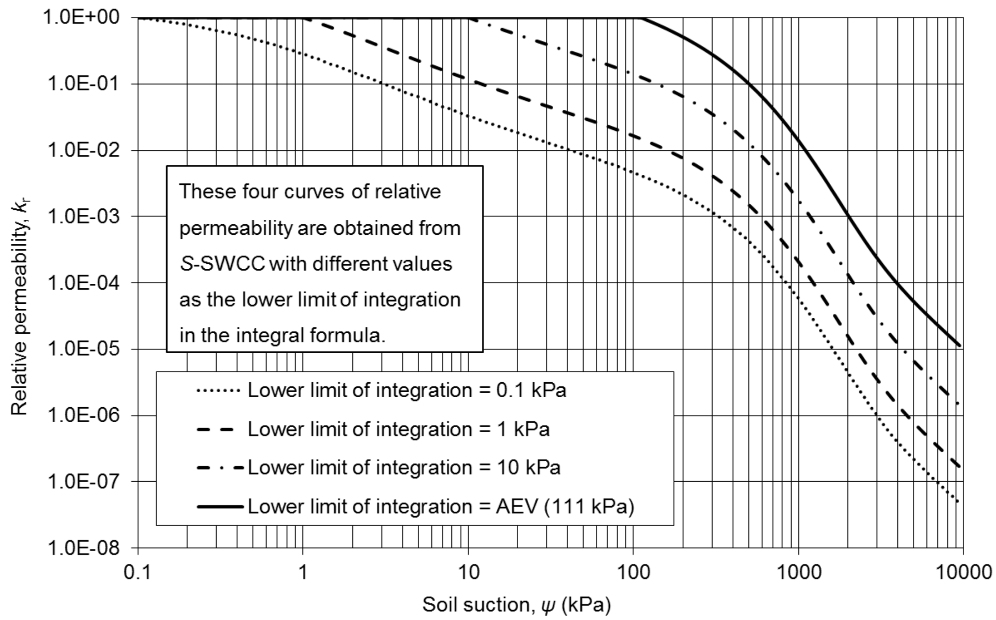

Figure 4-10. Relative permeability versus soil suction obtained from *S*-SWCC using different lower limits of integration for thickened oil sands tailings.

The quality of the best-fit for the *S*-SWCC also influences the correctness of the estimation results of the relative coefficient of permeability (Figure 4-11). Two curves of the relative coefficient of permeability in Figure 4-11 are estimated respectively from the two best-fitting curves of the *S*-SWCCs shown in Figuire 4-7. The difference between two relative permeability curves at an AEV of 111 kPa is about 1.13 orders of magnitude. A superior fitting of the *S*-SWCC results in a more accurate estimation of the AEV and subsequently the relative permeability function. In the case of thickened oil sands tailings, the data are more closely fit when using the simplified bimodal *w*-SWCC equation and the corresponding subsequent forms of SWCCs. The AEV obtained from the *S*-SWCC best-fitted by the Eq. [61] is 33.2 kPa. The more accurate AEV is 111 kPa, the value obtained from the *S*-SWCC best-fitted by Eq. [46]. Eq. [46] is derived from the simplified bimodal *w*-SWCC equation, while Eq.

[61] is derived from the unimodal Fredlund and Xing (1994) *w*-SWCC equation.

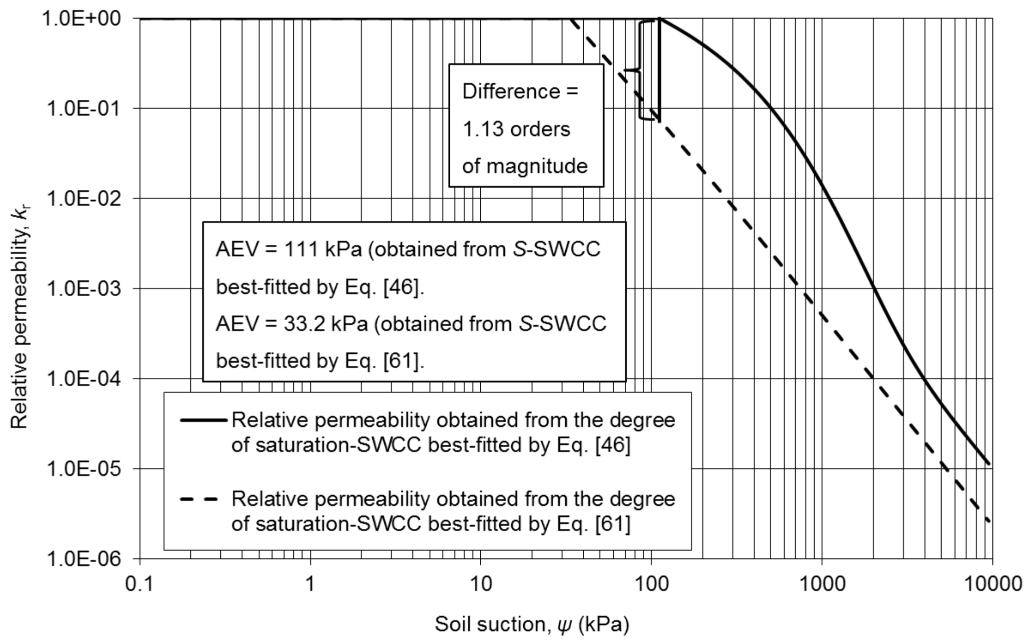

Figure 4-11. Relative permeability versus soil suction obtained from two best-fitting *S*-SWCCs for thickened oil sands tailings.

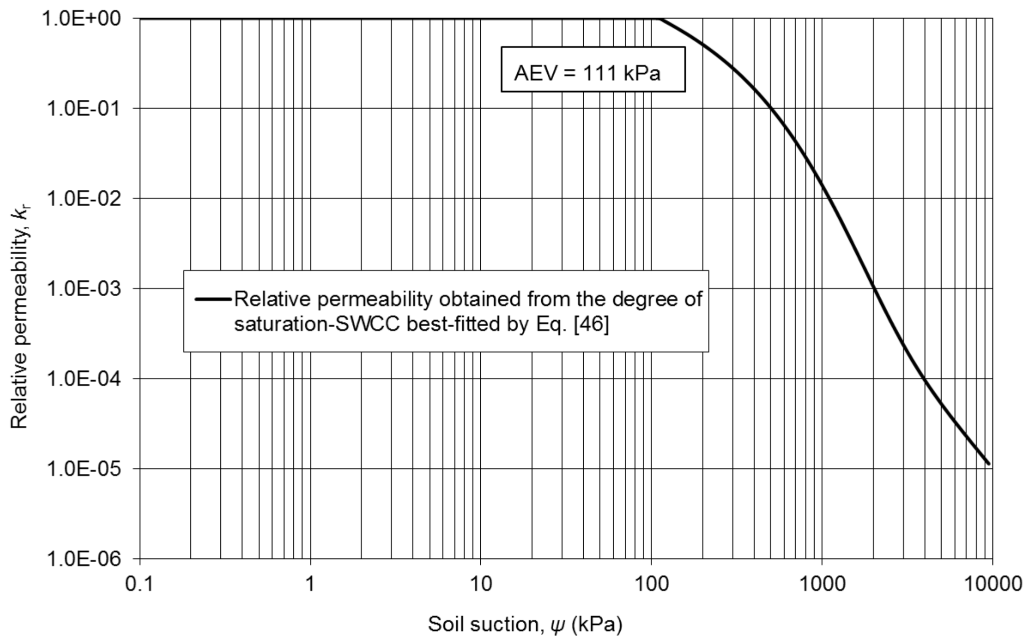

Figure 4-12. Relative permeability versus soil suction for thickened oil sands tailings.

Figure 4-12 shows the curve of the relative permeability versus soil suction obtained when using the superior fit of the *S*-SWCC and the AEV as the lower limit of integration. The curve shown in Figure 4-12 is used for the subsequent calculation of the permeability function with Eq. [48].

The saturated permeability is a function of void ratio as shown in Figure 4-5. Equation [50] is used to best-fit the measured data to obtain the mathematical relationship between the saturated permeability and the void ratio. The void ratio changes with soil suction during the drying process as shown in Figure 4-6. The relationship of the void ratio and soil suction can be represented by Eq. [45]. As a result, the saturated permeability can be related to soil suction. When the saturated permeability is related to soil suction, it is referred to the reference saturated permeability. The reference saturated permeability is the corresponding saturated permeability related to the void ratio at a particular soil suction as shown in Figure 4-13. The reference saturated permeability versus soil suction is mathematically represented by Eq. [51].

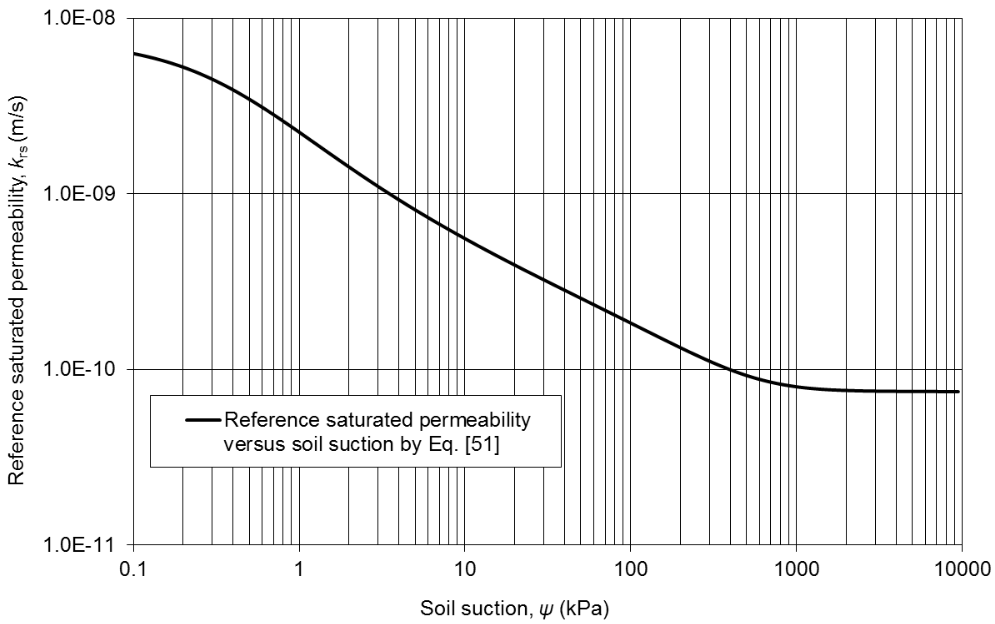

Figure 4-13. Reference saturated permeability versus soil suction for thickened oil sands tailings.

After obtaining the relative permeability function shown in Figure 4-12 and the reference saturated permeability function shown in Figure 4-13, the coefficient of permeability function can be obtained by multiplying the relative permeability function by the reference saturated permeability function in accordance with Eq. [48]. The relationship of the coefficient of permeability to soil suction for thickened oil sands tailings is shown in Figure 4-14.

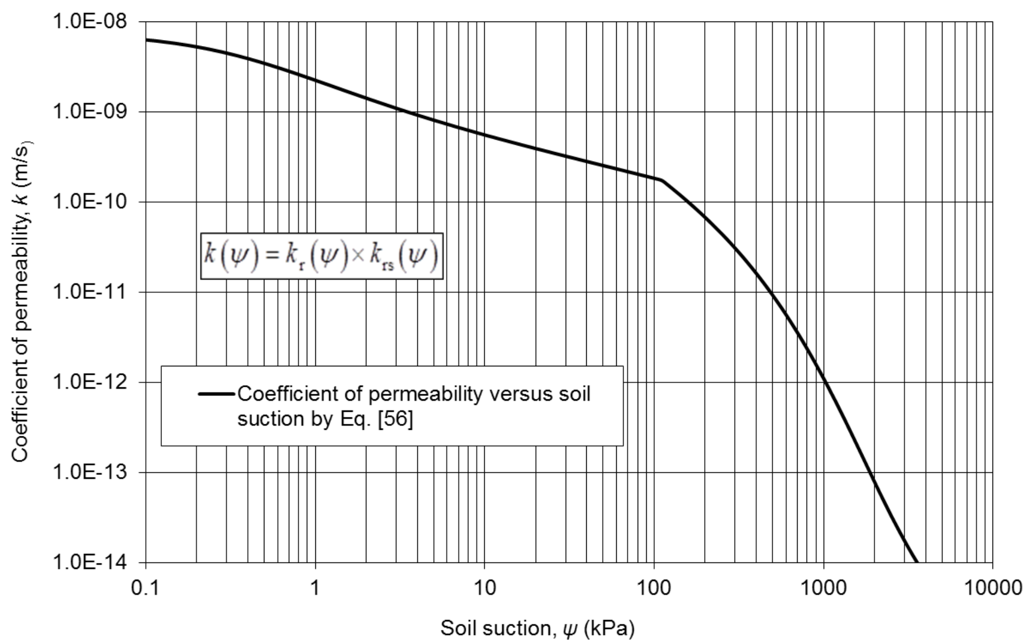

Figure 4-14. Coefficient of permeability versus soil suction for thickened oil sands tailings.

4.11 Conclusions

The void ratio and the degree of saturation are variables that influence the coefficient of permeability for a soil. Only the degree of saturation affects the coefficient of permeability when the soil does not change volume during a drying process. This paper presents a revised methodology for the estimation of the coefficient of permeability for a drying soil where both void ratio and degree of saturation change with soil suction. The proposed permeability function is the product of the reference saturated permeability function and the relative permeability function.

The effect of a change in void ratio on the coefficient of permeability function is presented as the reference saturated permeability function. The reference saturated permeability is the saturated permeability corresponding to a particular void ratio. The influence of a change in the degree of saturation is presented as a relative permeability function. The relative coefficient of permeability and the AEV should be estimated from the *S*-SWCC. The AEV should be used as the lower limit of integration in the integral of the denominator in the proposed permeability equation. Using other forms of the SWCC or other values as the lower limit of integration can lead to large estimation errors for the permeability function.

The quality of the fit of the *S*-SWCC affects the quality of the estimated permeability function. A superior fitting of the *S*-SWCC results in a more accurate estimation of the relative permeability function. The laboratory data for thickened oil sands tailings illustrate the detailed calculation procedure associated with the estimation of the coefficient of permeability function. The measured *w*-SWCC of thickened oil sands tailings exhibited a bimodal feature. A simplified bimodal *w*-SWCC equation was proposed and used to obtain a close fit for the *w*-SWCC. The shrinkage curve, the gravimetric water content versus soil suction and the saturated permeability versus void ratio are three basic experimental measurements required for the estimation of the coefficient of permeability function for soils that undergo volume change as soil suction is increased.

Acknowledgements

The authors want to acknowledge to contribution of TOTAL in support of the study that provided the laboratory test results that gave rise to the detailed analysis of the oil sands tailings material. The sponsorship of this study has led to improvements in the estimation of nonlinear soil property functions for large strain modeling of high volume change materials such as oil sands tailings.

References

Brooks, R.H., and Corey, A.T. 1964. Hydraulic properties of porous media. Hydrology Paper 3, Civil Engineering Department, Colorado State University, Fort Collins, CO.

Burdine, N. 1953. Relative permeability calculations from pore size distribution data. Journal of Petroleum Technology, 5 (03): 71–78.

Burger, C.A., and Shackelford, C.D. 2001a. Evaluating dual porosity of pelletized diatomaceous earth using bimodal soil–water characteristic curve functions. Can. Geotech. J., 38(1): 53–66.

Burger, C.A., and Shackelford, C.D. 2001b. Soil–water characteristic curves and dual porosity of sand-diatomaceous earth mixtures. J. Geotech. Geoenviron. *Eng.*, 127(9): 790–800.

Chapuis, R.P. 2012. Predicting the saturated hydraulic conductivity of soils: a review. Bulletin of Engineering Geology and the Environment, 71(3): 401-434.

Childs, E.C., and Collis-George, N. 1950. The permeability of porous materials. In Proceedings of the Royal Society of London A: Mathematical, Physical and Engineering Sciences. The Royal Society, 201(1066): 392-405.

Cornelis, W. M., Corluy, J., Medina, H., Hartmann, R., Van Meirvenne, M., and Ruiz, M. E. 2006. A simplified parametric model to describe the magnitude and geometry of soil shrinkage. European Journal of Soil Science, 57(2): 258-268.

Croney, D., and Coleman, J. D. 1954. Soil structure in relation to soil suction (pF). Journal of Soil Science, *5*(1): 75-84.

Fredlund, D.G., and Xing, A. 1994. Equations for the soil-water characteristic curve. Canadian geotechnical journal, 31(4): 521-532.

Fredlund, D.G., Xing, A. and Huang, S. 1994. Predicting the permeability function for unsaturated soils using the soil-water characteristic curve. Canadian Geotechnical Journal, 31(4): 533-546.

Fredlund, D.G., Stone, J., Stianson, J., and Sedgwick, A. 2011. Determination of water storage and permeability functions for oil sands tailings. Proceedings of the 15th International Conference on Tailings and Mine Waste, Vancouver, BC, Canada, November 6th to 9th, 2011.

Fredlund, D.G., Rahardjo, H., and Fredlund, M.D. 2012. Unsaturated soil mechanics in engineering practice. John Wiley & Sons, New York.

Fredlund, D.G., and Zhang, F-X. 2013. Combination of shrinkage curve and soil-water characteristic curves for soils that undergo volume change as soil suction is increased. Proceedings of the 18th International Conference on Soil Mechanics and Geotechnical Engineering, Paris, France.

Fredlund, M.D. 2000. The role of unsaturated soil property functions in the practice of unsaturated soil mechanics. Dissertation, University of Saskatchewan, Saskatoon, Saskatchewan.

Gardner, W. R. 1974. The permeability problem. Soil Science, 117(5): 243-249.

Haines, W. B. (1923) The volume-changes associated with variations of water content in soil. The Journal of agricultural science, 13(03): 296-310.

Huang, S., Barbour, S.L., and Fredlund, D.G. 1998. Development and verification of a coefficient of permeability function for a deformable unsaturated soil. Canadian Geotechnical Journal, 35(3): 411-425.

Kim, D. J., Vereecken, H., Feyen, J., Boels, D., and Bronswijk, J. J. B. 1992. On the characterization of properties of an unripe marine clay soil:

I. Shrinkage processes of an unripe marine clay soil in relation to physical ripening, Soil Science, 153(6): 471-481.

Leong, E.C., and Rahardjo, H. 1997. Permeability functions for unsaturated soils. Journal of Geotechnical and Geoenvironmental Engineering, 123(12): 1118-1126.

Marinho, F.A.M. 1994. Shrinkage behaviour of some plastic soils. Doctoral dissertation, University of London, UK.

Mbonimpa, M., Aubertin, M., Maqsoud, A., and Bussière, B. 2006. Predictive model for the water retention curve of deformable clayey soils. Journal of Geotechnical and Geoenvironmental Engineering, 132(9): 1121-1132.

Mualem, Y. 1976. A new model for predicting the hydraulic conductivity of unsaturated porous media. Water Resources Research, 12(3): 513-522.

Parent, S.E., Cabral, A., and Zornberg, J.G. 2007. Water retention curve and hydraulic conductivity function of highly compressible materials. Canadian Geotechnical Journal, 44(10): 1200-1214.

Rahimi, A., Rahardjo, H., and Leong, E.C. 2015. Effects of soil–water characteristic curve and relative permeability equations on estimation of unsaturated permeability function. Soils and Foundations, 55(6): 1400-1411.

Somogyi, F. 1980. Large-strain consolidation of fine-grained slurries. Proceedings of the Canadian Society for Civil Engineering 1980 Annual Conference, Winnipeg, Manitoba, Canada.

Sridharan, A., and Rao, G.V. 1971. Effective stress theory of shrinkage phenomena. Canadian Geotechnical Journal, 8(4): 503-513.

Taylor, D.W. 1948. Fundamentals of soil mechanics. J. Wiley & Sons; London: Chapman & Hall.

Tempany, H.A. 1917. The shrinkage of soils. The Journal of Agricultural Science, 8(03): 312-330.

Terzaghi, K. 1925. Principles of soil mechanics, IV -- Settlement and consolidation of clay. Engineering News-Record, 95(3): 874-878.

Tripathy, S., Tadza, M. Y. M., and Thomas, H. R. 2014. Soil-water characteristic curves of clays. Canadian Geotechnical Journal, 51(8): 869-883.

Van Genuchten, M.T. 1980. A closed-form equation for predicting the hydraulic conductivity of unsaturated soils. Soil science society of America journal, 44(5): 892-898.

Zhang, F-X, Fredlund, D. G., Wilson, G. W., and Sedgwick, A. 2014. Determination of the permeability function for drying oil sands tailings undergoing volume change and desaturation. Proceedings of the 4th International Oil Sands Tailings Conference, Banff, A.B.Dec 7th-10th, 2014.

Zhang, F-X, and Fredlund, D.G. 2015. Examination of the estimation of relative permeability for unsaturated soils. Canadian Geotechnical Journal, 52(12): 2077-2087.

Zhang, L., and Chen, Q. 2005. Predicting bimodal soil–water characteristic curves. Journal of Geotechnical and Geoenvironmental Engineering, 131(5): 666-670.

Appendix A: Procedure when estimating the permeability function of a high-volume-change soil with a unimodal *w*-SWCC using the revised methodology.

Step 1. Obtain fitting parameters for *w*-SWCC.

$$w(\psi)=\frac{w_{\mathrm{s}}\left(1-\ln\left(1+\psi/\psi_{\mathrm{r}}\right)\Big/\ln\left(1+10^{6}/\psi_{\mathrm{r}}\right)\right)}{\left(\ln\left(\exp(1)+\left(\psi/a_{\mathrm{f}}\right)^{n_{\mathrm{f}}}\right)\right)^{m_{\mathrm{f}}}} \qquad [57]$$

$$w(\psi)=w_{\mathrm{s}}\left(1-\frac{\ln\left(1+\dfrac{\psi}{\psi_{\mathrm{rb}}}\right)}{\ln\left(1+\dfrac{10^{6}}{\psi_{\mathrm{rb}}}\right)}\right)\left(\frac{p}{\left(\ln\left(\exp(1)+\left(\dfrac{\psi}{a_{\mathrm{f1}}}\right)^{n_{\mathrm{f1}}}\right)\right)^{m_{\mathrm{f1}}}}+\frac{1-p}{\left(\ln\left(\exp(1)+\left(\dfrac{\psi}{a_{\mathrm{f2}}}\right)^{n_{\mathrm{f2}}}\right)\right)^{m_{\mathrm{f2}}}}\right)$$

[58]

Eq. [57] is recommended for best-fitting unimodal experimental data; Eq. [58] is for bimodal measured data.

Step 2. Obtain fitting parameters for the shrinkage curve.

$$e(w)=a_{\mathrm{sh}}\left(\left(\frac{w}{b_{\mathrm{sh}}}\right)^{c_{\mathrm{sh}}}+1\right)^{\frac{1}{c_{\mathrm{sh}}}} \qquad [59]$$

Step 3. Calculate the void ratio versus soil suction relationship.

$$e(\psi)=a_{\mathrm{sh}}\left(\left(\frac{w_{\mathrm{s}}\left(1-\ln\left(1+\psi/\psi_{\mathrm{r}}\right)/\ln\left(1+10^{6}/\psi_{\mathrm{r}}\right)\right)}{b_{\mathrm{sh}}\left(\ln\left(\exp(1)+\left(\psi/a_{\mathrm{f}}\right)^{n_{\mathrm{f}}}\right)\right)^{m_{\mathrm{f}}}}\right)^{c_{\mathrm{sh}}}+1\right)^{\frac{1}{c_{\mathrm{sh}}}} \qquad [60]$$

Step 4. Calculate the *S*-SWCC.

$$S(\psi)=\frac{G_{\mathrm{s}}\,w_{\mathrm{s}}\left(1-\ln\left(1+\psi/\psi_{\mathrm{r}}\right)/\ln\left(1+10^{6}/\psi_{\mathrm{r}}\right)\right)}{a_{\mathrm{sh}}\left(\ln\left(\exp(1)+\left(\psi/a_{\mathrm{f}}\right)^{n_{\mathrm{f}}}\right)\right)^{m_{\mathrm{f}}}\left(\left(\frac{w_{\mathrm{s}}\left(1-\ln\left(1+\psi/\psi_{\mathrm{r}}\right)/\ln\left(1+10^{6}/\psi_{\mathrm{r}}\right)\right)}{b_{\mathrm{sh}}\left(\ln\left(\exp(1)+\left(\psi/a_{\mathrm{f}}\right)^{n_{\mathrm{f}}}\right)\right)^{m_{\mathrm{f}}}}\right)^{c_{\mathrm{sh}}}+1\right)^{\frac{1}{c_{\mathrm{sh}}}}}$$

[61]

Step 5. Calculate the θ_{i}-SWCC.

$$\theta_{\mathrm{i}}(\psi)=\frac{G_{\mathrm{s}}w_{\mathrm{s}}\left(1-\ln\left(1+\psi/\psi_{\mathrm{r}}\right)/\ln\left(1+10^{6}/\psi_{\mathrm{r}}\right)\right)}{\left(\ln\left(\exp(1)+\left(\psi/a_{\mathrm{f}}\right)^{n_{\mathrm{f}}}\right)\right)^{m_{\mathrm{f}}}\left(1+a_{\mathrm{sh}}\left(\left(\frac{w_{\mathrm{s}}\left(1-\ln\left(1+\psi/\psi_{\mathrm{r}}\right)/\ln\left(1+10^{6}/\psi_{\mathrm{r}}\right)\right)}{b_{\mathrm{sh}}\left(\ln\left(\exp(1)+\left(\psi/a_{\mathrm{f}}\right)^{n_{\mathrm{f}}}\right)\right)^{m_{\mathrm{f}}}}\right)^{c_{\mathrm{sh}}}+1\right)^{\frac{1}{c_{\mathrm{sh}}}}\right)}$$

[62]

Step 6. Calculate the relative coefficient of permeability function from *S*-SWCC data starting at AEV with Eq. [63]. Use Eq. [61] for the best-fitting of the *S*-SWCC.

$$k_{\mathrm{r}}^{S}(\psi)=\frac{\displaystyle\int_{\ln(\psi)}^{\mathrm{b}}\frac{S\left(e^{y}\right)-S(\psi)}{e^{y}}S'\left(e^{y}\right)dy}{\displaystyle\int_{\ln(\psi_{\mathrm{aev}})}^{b}\frac{S\left(e^{y}\right)-S\left(\psi_{\mathrm{aev}}\right)}{e^{y}}S'\left(e^{y}\right)dy} \qquad [63]$$

Step 7. Calculate the change in the reference saturated permeability function due to volume change.

$$k_{\mathrm{rs}}\left(\psi\right)=A\left(a_{\mathrm{sh}}\left(\left(\frac{w_{\mathrm{s}}\left(1-\ln\left(1+\psi/\psi_{\mathrm{r}}\right)/\ln\left(1+10^{6}/\psi_{\mathrm{r}}\right)\right)}{b_{\mathrm{sh}}\left(\ln\left(\exp\left(1\right)+\left(\psi/a_{\mathrm{f}}\right)^{n_{\mathrm{f}}}\right)\right)^{m_{\mathrm{f}}}}\right)^{c_{\mathrm{sh}}}+1\right)^{\frac{1}{c_{\mathrm{sh}}}}\right)^{B} \quad [64]$$

Step 8. Calculate the permeability function for a soil that changes volume as soil suction is increased considering both desaturation and volume change with Eq. [65] using Eq. [60] for $e(\psi)$ and Eq. [61] for $S(\psi)$.

$$k\left(\psi\right)=\frac{A\left(e\left(\psi\right)\right)^{B}\int\limits_{\ln\left(\psi\right)}^{\mathrm{b}}\frac{S\left(e^{y}\right)-S\left(\psi\right)}{e^{y}}S'\left(e^{y}\right)dy}{\int\limits_{\ln\left(\psi_{\mathrm{aev}}\right)}^{b}\frac{S\left(e^{y}\right)-S\left(\psi_{\mathrm{aev}}\right)}{e^{y}}S'\left(e^{y}\right)dy} \quad [65]$$

Chapter 5. Estimation of the water storage and coefficient of permeability functions for Devon silt and Bulyanhulu tailings

5.1 Introduction

Water storage and coefficient of permeability functions are two unsaturated soil property functions that are required in the numerical modeling of unsteady-state seepage problems. Inaccuracies in the estimation of the water storage and the coefficient of permeability function can lead to significant errors in numerical modeling results. Research has shown that changes in the void ratio and changes in the degree of saturation are factors that influence the water storage function and the coefficient of permeability function of a soil (Zhang et al. 2014). The effect of the void ratio changes has been previously considered in the estimation of the permeability function for a saturated soil that undergoes volume changes (Chapuis 2012; Taylor 1948). Lots of the existing estimation methodologies for the permeability function of an unsaturated soil have been based on an assumption that no volume change occurs as soil suction is changed. In other words, the change of the permeability of an unsaturated soil occurs as a result of changes in the degree of saturation. Reasonable permeability functions can be obtained with conventional unsaturated permeability estimation methodologies for unsaturated soils that do not undergo volume change. Oil sands tailings and Regina clay are two typical soils that undergo volume change as soil suction is increased during a drying process (Fredlund et al. 2011; Fredlund and Zhang 2013). Conventional unsaturated permeability estimation methodologies cannot adequately represent the permeability function for oil sands tailings or Regina clay subjected to drying. A revised methodology for the estimation of the permeability function for soils that undergo volume change as soil suction is changed is recommended and illustrated in Chapter 3 and Chapter 4 with Regina clay and oil sands tailings as examples respectively.

The revised methodology for the estimation of permeability function produces reasonable estimation results for Regina clay and oil sands tailings. Regina clay and oil sands tailings are two typical soils with relatively large volume change during a drying process. Soils with relatively small volume change during a drying process ought to be checked as well to verify the reasonability and applicability of the recommended revised methodology for the estimation of the permeability function for soils that undergo volume change as soil suction is increased.

This chapter is devoted to verify the proposed revised methodology with the experimental test results on Devon silt and Bulyanhulu Tailings. Both Devon silt and Bulyanhulu tailings are soils that undergo much less volume change during a drying process compared to Regina clay and oil sands tailings. The tests that have been conducted include grain size analysis, specific gravity tests, water content and Atterberg limit tests, the large strain consolidation with permeability test, shrinkage test and soil-water characteristic curve test. Testing results for SWCCs, the relationships of saturated permeability versus void ratio and shrinkage curves have been collected and are interpreted using the revised methodology for the estimation of the permeability function and the water storage function for verification.

5.2 Research Program

The materials used for the testing program are remolded Devon silt and remolded Bulyanhulu Tailings. Devon silt is an ideal natural soil that is often used as surrogate for fine tailings. Bulyanhulu tailings is non-plastic gold tailings obtained from the Bulyanhulu mine in Tanzania. The reason why Bulyanhulu tailing was chosen for the experimental testing program is that it is a typical fine grain gold tailings that represents other types of tailings.

Grain size analyses were conducted in order to characterize the gradation of the samples (e.g., Devon silt and Bulyanhulu tailings). These tests were conducted based on procedures in ASTM D422. Specific gravity tests were conducted to determine the density of the solids and for use in the consolidation, shrinkage curve and soil-water characteristic curve tests. Specific gravity tests were conducted based on procedures in ASTM D854.

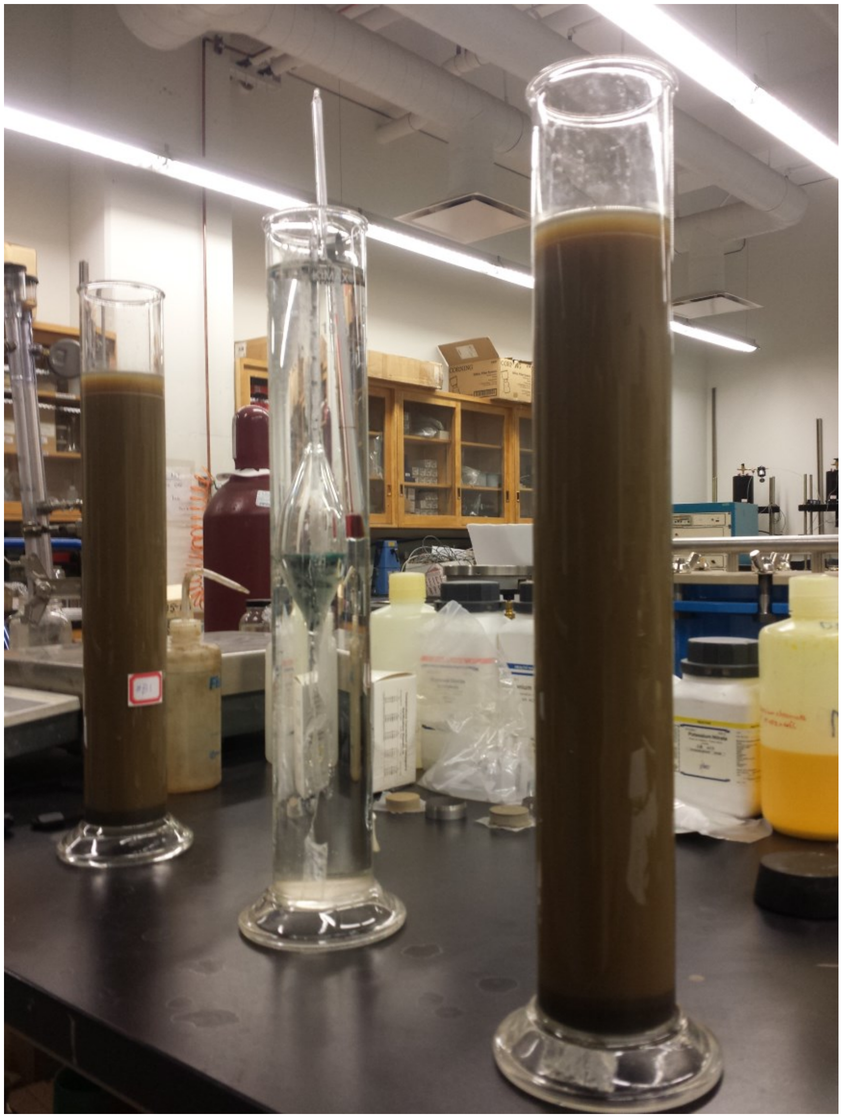

Figure 5-1. Hydrometer test on Bulyanhulu tailings.

Shrinkage curve tests were used to measure the relationship between void ratio change and water content change during a drying process. Samples were prepared at high initial water contents in a slurry state and loaded into shrinkage rings.

Figure 5-2. Slurry of Devon silt for the shrinkage test.

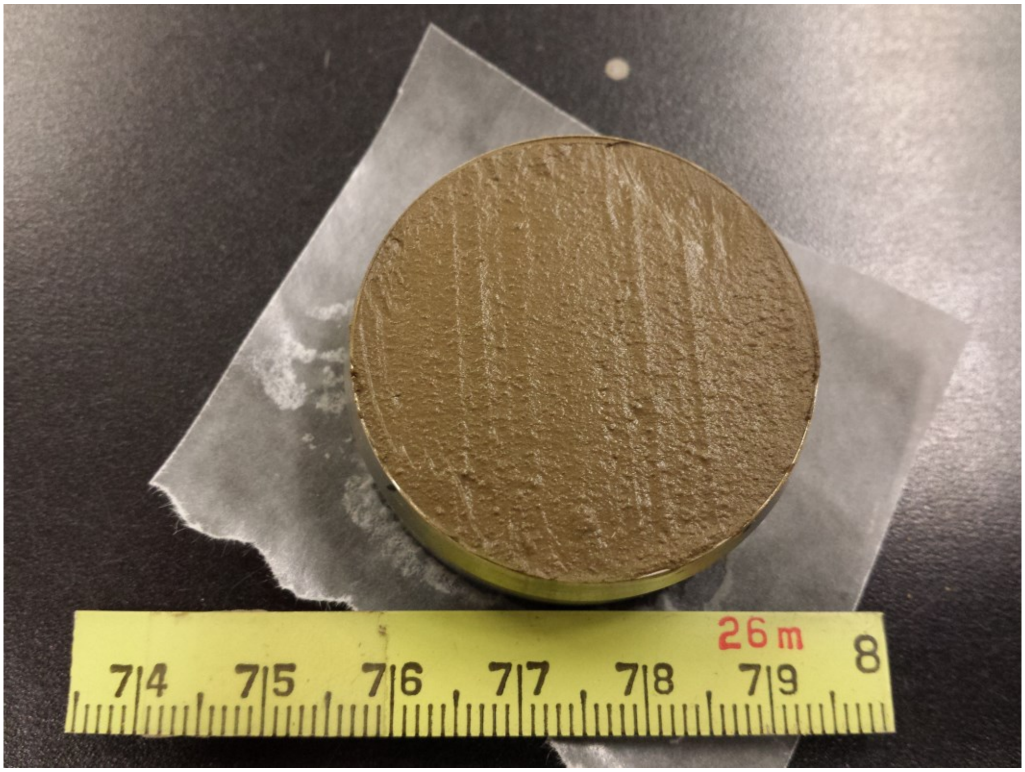

Figure 5-3. Shrinkage test on Devon silt.

Each shrinkage test specimen was exposed to the laboratory environment and water was allowed to evaporate over a period of time. The height and diameter of the material specimen decreased as water evaporated and the specimen shrank. The volume change and water content (i.e. mass of water) of the specimen was measured throughout the test. The shrinkage rings had a diameter of approximately 3.57 cm and were approximately 1.2 cm high. It is desirable to use relatively small rings to avoid the development of desiccation cracks across the surface or through the specimen. Cracks can interfere with height and diameter measurements making it difficult to determine the volume of the specimen. The results of the test indicate the relationship between volume change and water content change. The results are used to facilitate the interpretation of the results from the independently run soil-water characteristic curve (SWCC) test. The combined use of the shrinkage test and the conventional SWCC test is necessary when dealing with high volume change materials.

Soil-water characteristic curve, SWCC tests were conducted to determine the moisture retention characteristics of the Devon silt and the Bulyanhulu tailings. SWCCs were measured using single-specimen pressure plate devices developed at the University of Saskatchewan, Saskatoon, for applied suctions up to 500 kPa and using WP4-T (Water PotentiaMeter with internal temperature control) for the higher suction range.

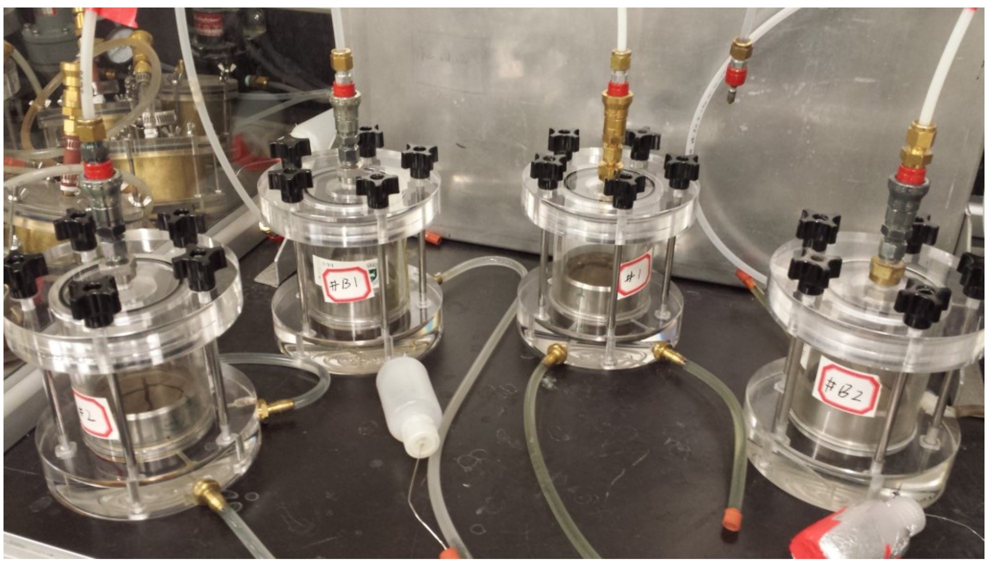

Figure 5-4. Measurement of SWCCs for both Devon silt and Bulyanhulu tailings at the low suction range using single-specimen pressure plate developed at the university of Saskatchewan, Saskatoon.

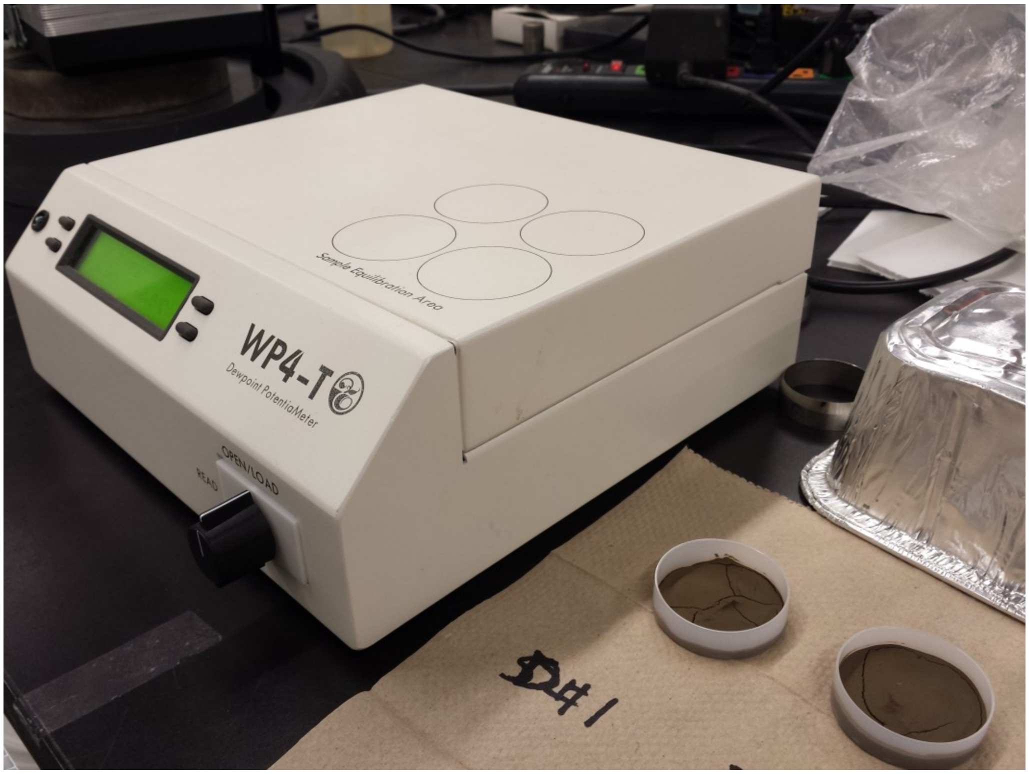

Figure 5-5. Measurement of SWCCs for both Devon silt and Bulyanhulu tailings at high suctions using WP4-T (Water PotentiaMeter).

Laboratory equipment for measuring the SWCC can broadly be divided into equipment that provides an applied matric suction and equipment that provides a controlled total suction. Matric suctions are applied to a soil specimen through use of a high-air-entry disk. The maximum value of most high-air-entry disks is 1500 kPa. The axis translation technique is used to develop a differential air and water pressure without producing cavitation in the water phase. The single-specimen pressure plate devices developed at the University of Saskatchewan, Saskatoon, can be applied with suctions up to 500 kPa. An air pressure can be applied to the specimen chamber through use of an air pressure regulator. Water drains against atmospheric pressure conditions and as a result a matric suction is applied to the soil specimen. The chilled-mirror Water PotentiaMeter, WP4, has been used to measure the total suction in the medium- to high-suction range through the measurement of water activity. WP4-T is the Water PotentiaMeter with internal temperature control to reduce temperature fluctuations in the ambient environment.

The relationship of saturated permeability to void ratio is one of those three necessary relationships that should be measured in the laboratory testing program for the estimation of the permeability function for soils that undergo volume change as soil suction is increased. The relationship of saturated permeability to void ratio is measured for both Devon silt and Bulyanhulu tailings. The textures of Devon silt and Bulyanhulu tailings are very different. Devon silt has more clay content than Bulyanhulu tailings does. In other words, Devon silt slurry is stickier than Bulyanhulu tailings slurry. As a result, two different ways were used to measure the relationship between saturated permeability and void ratio for Devon silt and Bulyanhulu tailings. One-dimensional consolidation test was used to indirectly measure the saturated permeability at various void ratios for Devon silt. Large strain consolidation with constant head hydraulic conductivity test at the end of each stage of consolidation was conducted to yield a curve defining the relationship between the saturated permeability and the void ratio for Bulyanhulu tailings.

Figure 5-6. One-dimensional consolidation test on Devon silt.

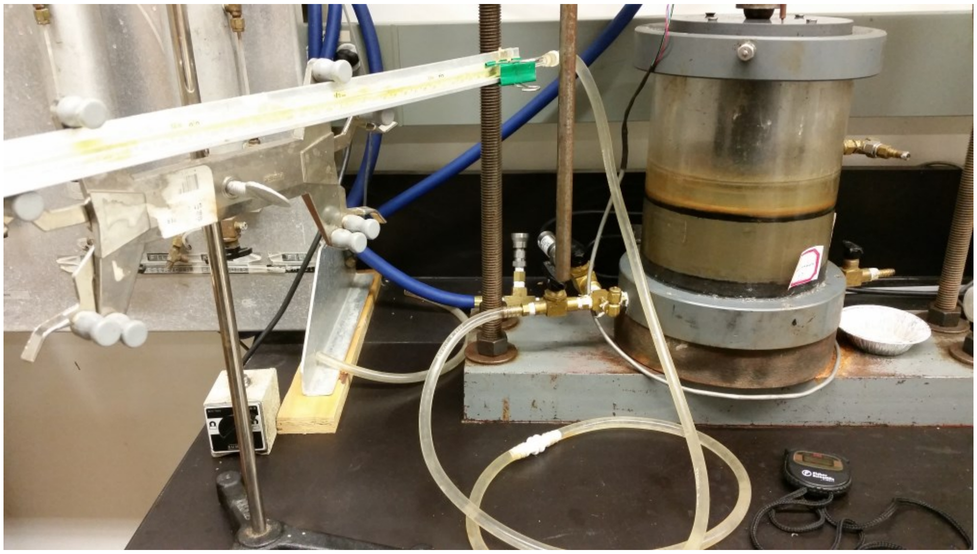

Figure 5-7. Large strain consolidation with constant head hydraulic conductivity test at the end of each stage of consolidation on Bulyanhulu tailings.

5.3 Presentation of Test Results

Basic soil properties for both Devon silt and Bulyanhulu tailings were determined. Devon silt had a liquid limit of 35.22% and a plastic limit of 20.46%. The average specific gravity for Devon silt was 2.664. The grain size distribution for Devon silt is shown in Figure 5-8. The shrinkage curve of Devon silt is presented in Figure 5-9. The best-fitting parameters of the shrinkage curve for Devon silt are a_{sh} = 0.432, b_{sh} = 0.162, and c_{sh} = 214.

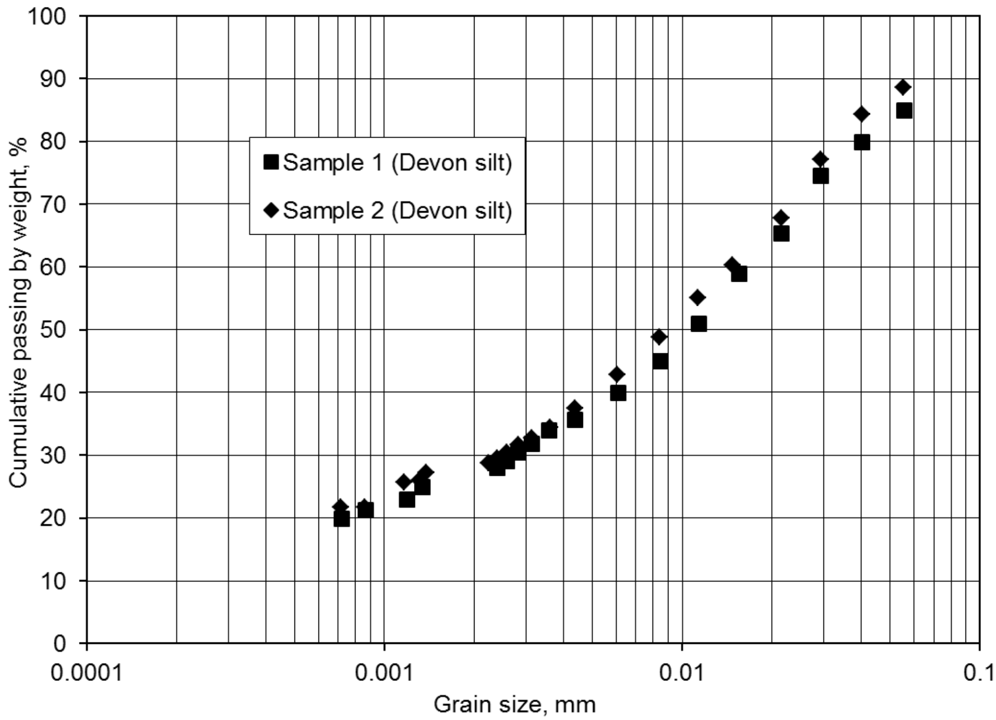

Figure 5-8. Grain size distribution for Devon silt.

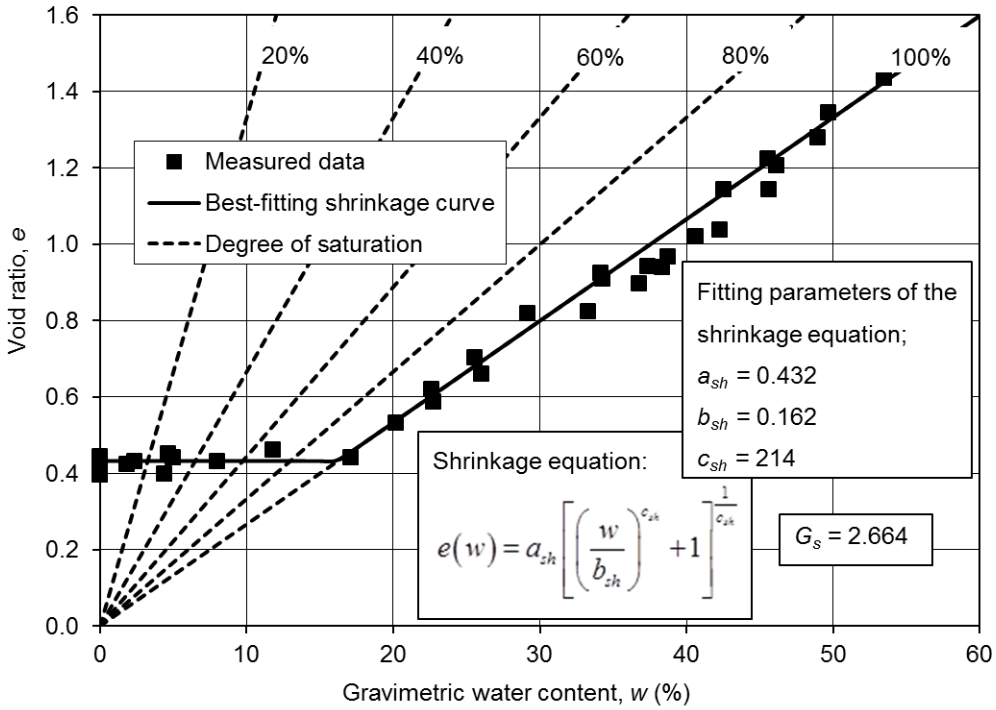

Figure 5-9. Shrinkage curve for Devon silt.

The gravimetric water content, w, plotted versus soil suction for Devon silt is shown in Figure 5-10. Two fitting equations were used to best-fit the experimental data of the gravimetric water content soil-water characteristic curve, w-SWCC. One is the sigmoidal Fredlund-Xing (1994) equation, Eq. [41]; and the other is a simplified bimodal equation, Eq. [44]. Both equations are used for the interpretation of the measured data in a comparative manner. The best-fit parameters of the Fredlund-Xing (1994) equation are a_f = 4.645 kPa, n_f = 0.852, m_f = 0.630, and ψ_r = 222.4 kPa. The best-fit parameters of the simplified bimodal equation are a_{f1} = 5639 kPa, a_{f2} = 3.281 kPa, n_{f1} = 0.883, n_{f2} = 1.538, m_{f1} = 16.430, m_{f2} = 0.489 and ψ_{rb} = 1137 kPa, p = 0.194. The initial gravimetric water content was 46.55%. The measured data of the w-SWCC for Devon silt displays a slight bimodal feature. The best-fitting curve obtained by the simplified bimodal equation (Eq.[44]) represents the measured data points more closely than the best-fitting curve obtained by the unimodal Fredlund-Xing (1994) equation, as shown in Figure 5-10. The *w*-SWCC is used in conjunction with the shrinkage curve to calculate other forms of SWCC and properly interpret the SWCC results to determine the correct AEV and estimate the relative permeability function.

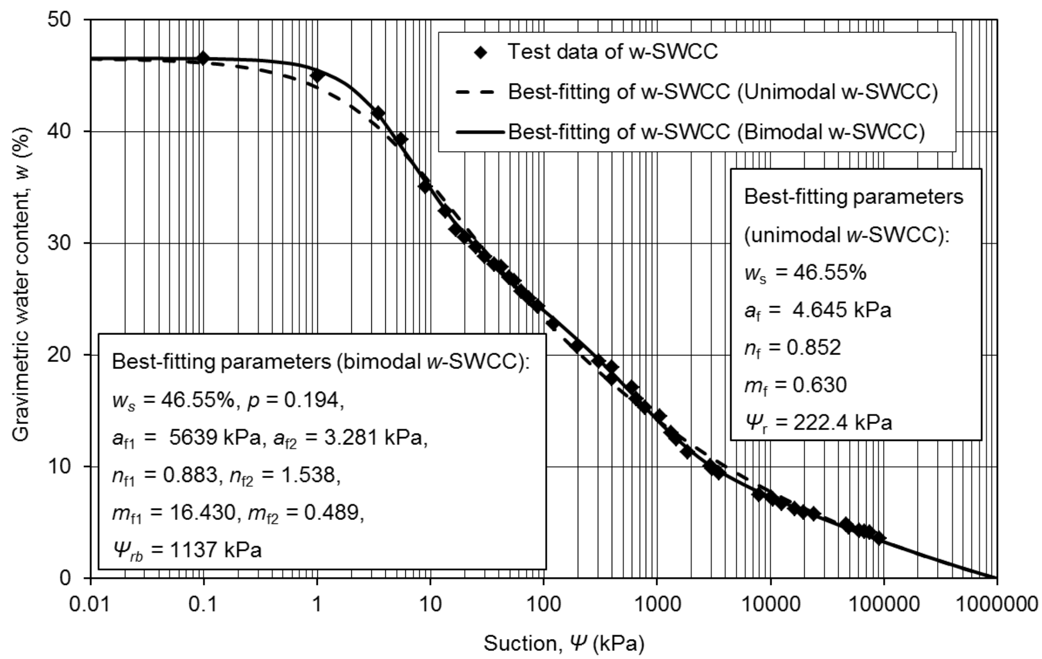

Figure 5-10. Gravimetric water content versus soil suction for Devon silt.

The relationship of saturated permeability versus void ratio was also measured in the laboratory test for Devon silt. The experimental data were best-fitted using Eq. [30] and Eq. [31]. Figure 5-11 shows the measured results and the best-fitting curves. Both equations produce reasonable fitting curves for the saturated coefficient of permeability versus void ratio relationship for Devon silt. The fitting parameters for Eq. [30] are C = 370 and x = 4.907, while the fitting parameters for Eq. [31] are A = 188 and B = 4.509.

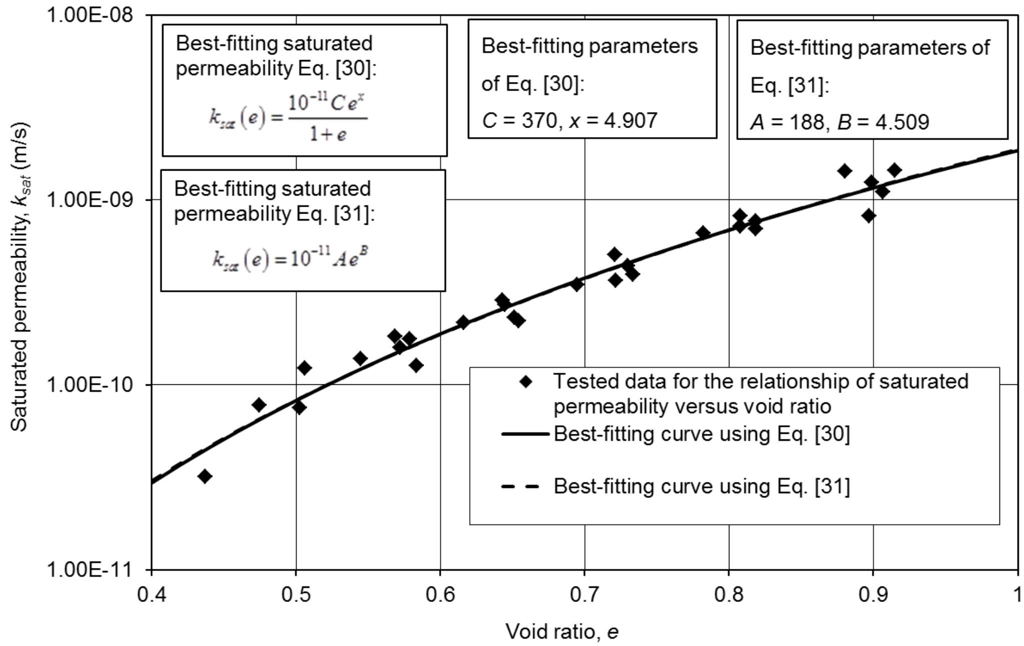

Figure 5-11. Saturated permeability versus void ratio best-fitted using Eq. [30] and Eq. [31] for Devon silt.

Bulyanhulu tailings was very sandy and didn't have a liquid limit or a plastic limit. The average specific gravity for Bulyanhulu tailings was 2.816. The grain size distribution for Bulyanhulu tailings is shown in Figure 5-12. The shrinkage curve of Bulyanhulu tailings is presented in Figure 5-13. The best-fitting parameters of the shrinkage curve for Bulyanhulu tailings are a_{sh} = 0.625, b_{sh} = 0.222, and c_{sh} = 23.19.

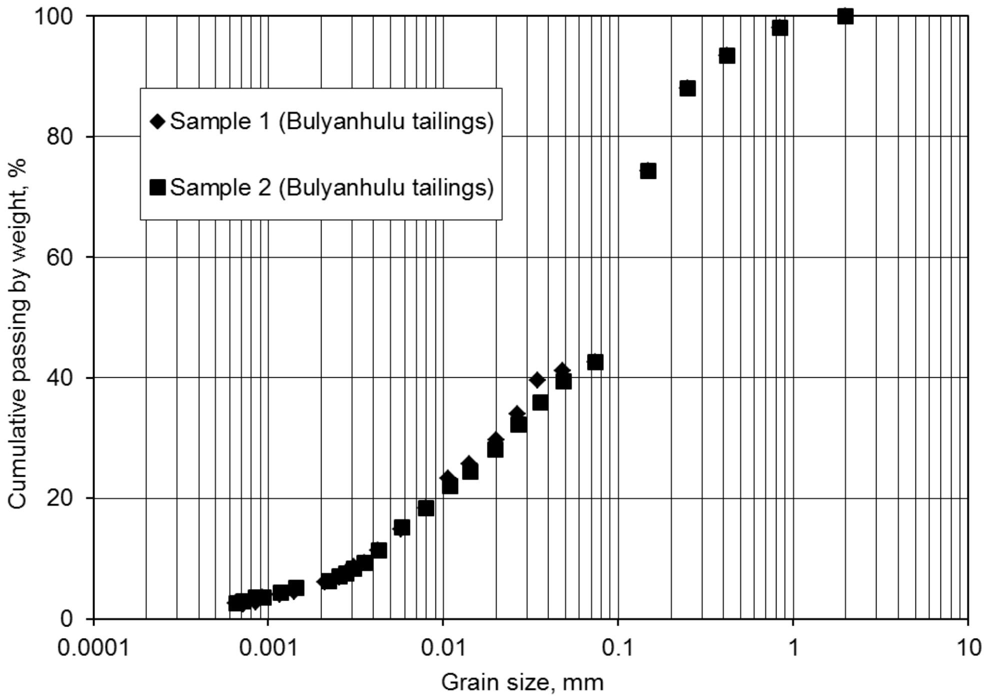

Figure 5-12. Grain size distribution for Bulyanhulu tailings.

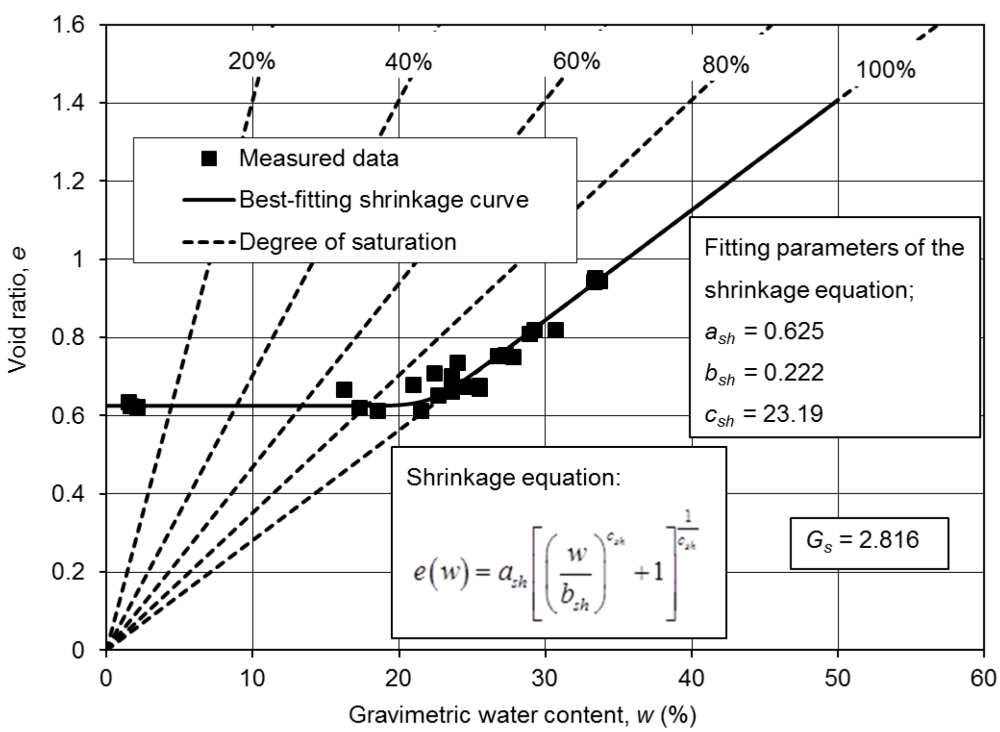

Figure 5-13. Shrinkage curve for Bulyanhulu tailings.

The gravimetric water content, w, plotted versus soil suction for Bulyanhulu tailings is shown in Figure 5-14. Two fitting equations were used to best-fit the experimental data of the gravimetric water content soil-water characteristic curve, w-SWCC. One is the sigmoidal Fredlund-Xing (1994) equation, Eq. [41]; and the other is a simplified bimodal equation, Eq. [44]. Both equations are used for the interpretation of the measured data in a comparative manner. The best-fit parameters of the Fredlund-Xing (1994) equation are a_f = 496.18 kPa, n_f = 0.418, m_f = 3.556, and ψ_r = 104.50 kPa. The best-fit parameters of the simplified bimodal equation are a_{f1} = 0.344 kPa, a_{f2} = 119.83 kPa, n_{f1} = 4.077, n_{f2} = 8.733, m_{f1} = 0.304, m_{f2} = 0.715 and ψ_{rb} = 39.79 kPa, p = 0.446. The initial gravimetric water content was 29.268%. The measured data of the w-SWCC for Bulyanhulu tailings displays a significant bimodal feature. The best-fitting curve obtained by the simplified bimodal equation (Eq. [44]) represents the measured data points more closely than the best-fitting curve obtained by the unimodal Fredlund-Xing (1994) equation, as shown in Figure 5-14. The w-SWCC is used in conjunction with the shrinkage curve to calculate other forms of SWCC and properly interpret the SWCC results to determine the correct AEV and estimate the relative permeability function.

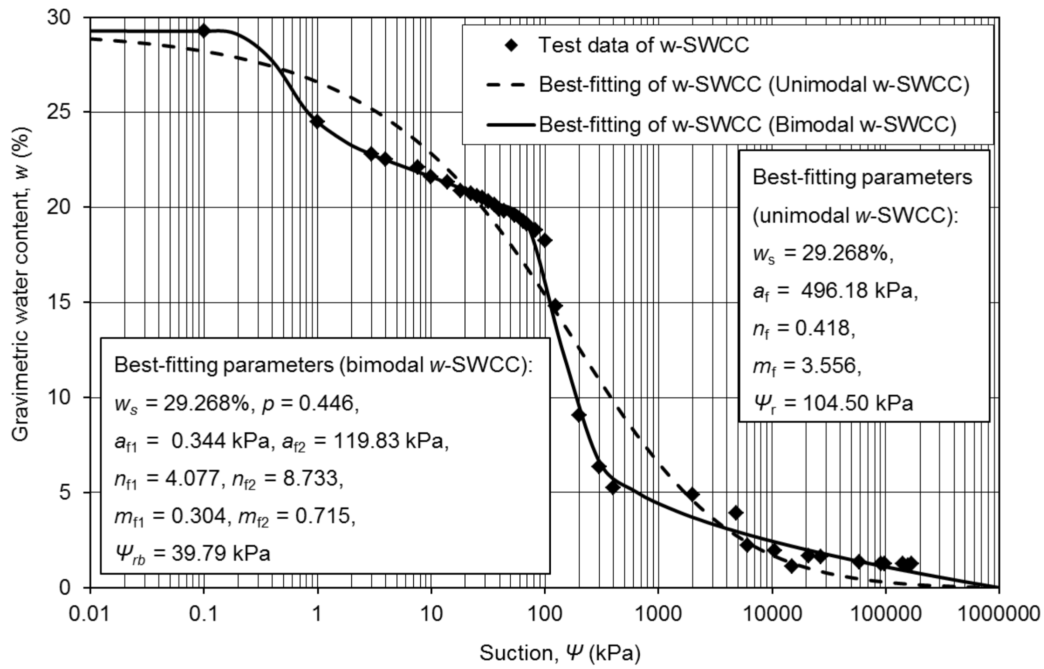

Figure 5-14. Gravimetric water content versus soil suction for Bulyanhulu tailings.

The relationship of saturated permeability versus void ratio was measured for Bulyanhulu tailings in the experimental testing program. The test data were best-fitted using Eq. [30] and Eq. [31]. Figure 5-16 shows the measured results and the best-fitting curves. Both equations produce reasonable fitting curves for the saturated coefficient of permeability versus void ratio relationship for Bulyanhulu tailings. The fitting parameters for Eq. [30] are $C = 2.44\times10^4$ and $x = 5.362$, while the fitting parameters for Eq. [31] are $A = 1.23\times10^4$ and $B = 4.952$.

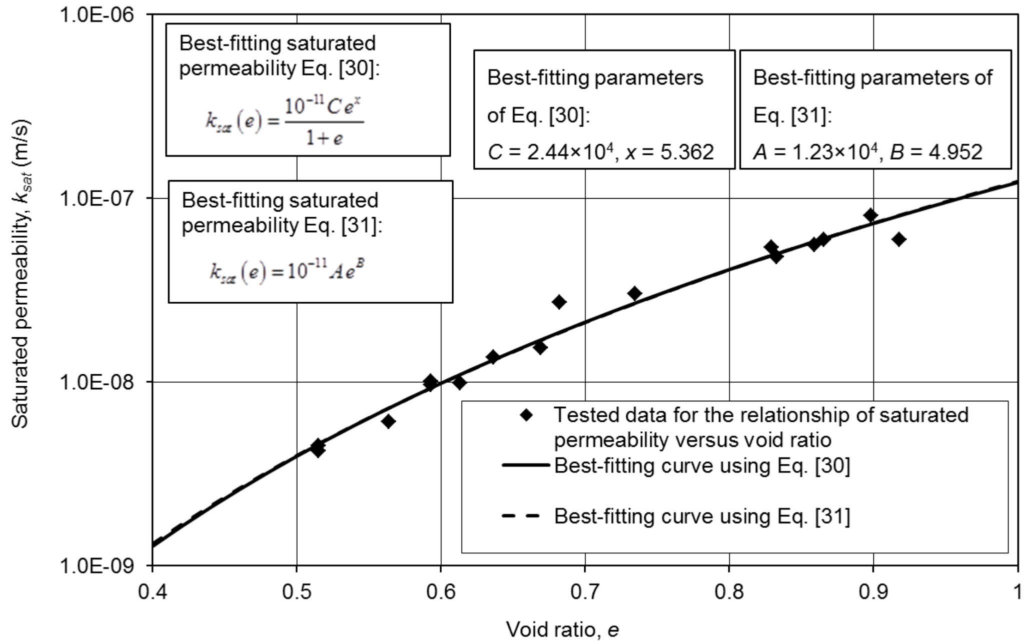

Figure 5-15. Saturated permeability versus void ratio best-fitted using Eq. [30] and Eq. [31] for Bulyanhulu tailings.

5.4 Interpretation of Test Data

Three curves obtained from the laboratory test, namely, the shrinkage curve, the gravimetric water content-SWCC (w-SWCC) and the curve of saturated permeability versus void ratio, are essentially necessary for the subsequent estimation of the permeability function for a soil that undergoes volume change as soil suction changes. The w-SWCC is combined with the shrinkage curve to obtain other forms of the SWCC (i.e., Eq. [26] to Eq. [28], Eq. [46] to Eq. [47]).

5.4.1 Devon silt tailings

The relationship of void ratio versus soil suction for Devon silt obtained by combining the *w*-SWCC and the shrinkage curve is shown in Figure 5-16. Figure 5-17 shows the resulting plot of degree of saturation, *S*, versus soil suction. The plot of instantaneous volumetric water content-SWCC, θ_i-SWCC is shown in Figure 5-18. The solid fitting curves on Figures 5-14 to 5-16 are calculated on the basis of the fitting curve of the *w*-SWCC obtained by the simplified bimodal Eq. [44]. The dash fitting curves on Figures 5-14 to 5-16 are obtained based on the fitting curve of the *w*-SWCC best-fitted by the unimodal Eq. [41]. The solid lines present better fitting than the dash lines for the relationship of void ratio versus soil suction, *S*-SWCC and θ_i-SWCC. Figures 5-14 to 5-16 illustrate that the better best-fitting of the subsequent SWCCs can be calculated when the better best-fitting of the *w*-SWCC is obtained.

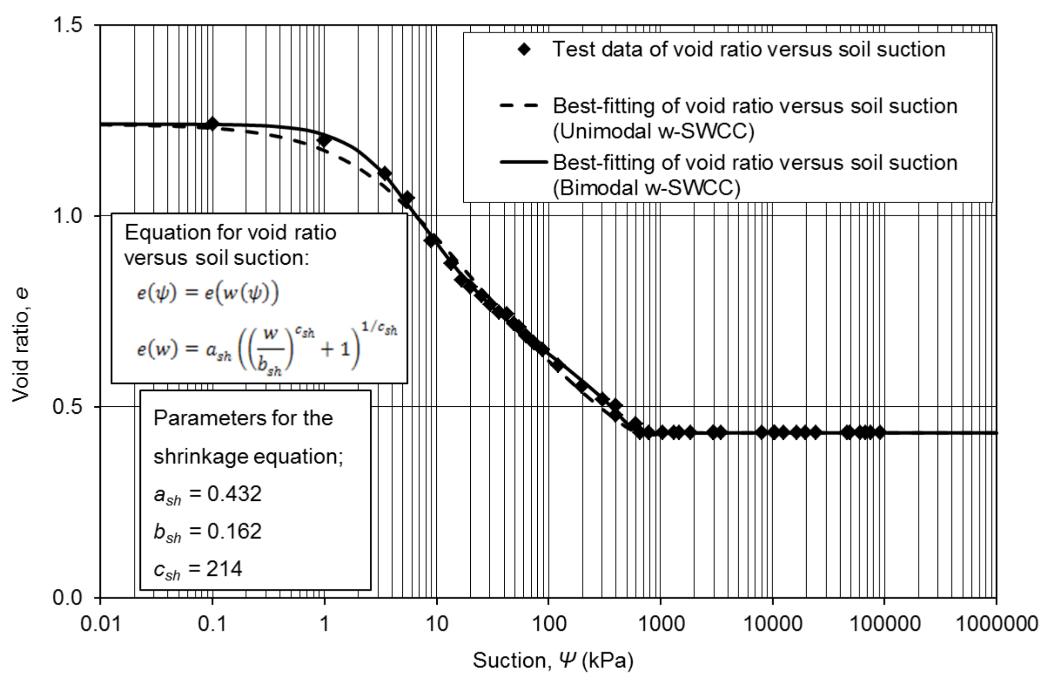

Figure 5-16. Void ratio versus soil suction for Devon silt.

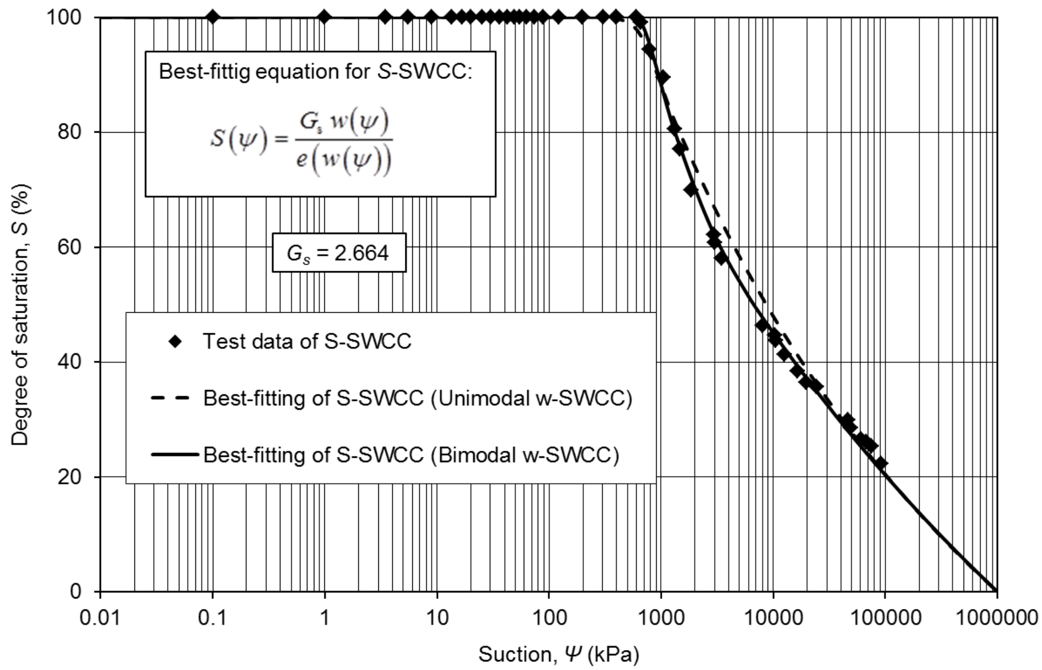

Figure 5-17. Degree of saturation versus soil suction for Devon silt.

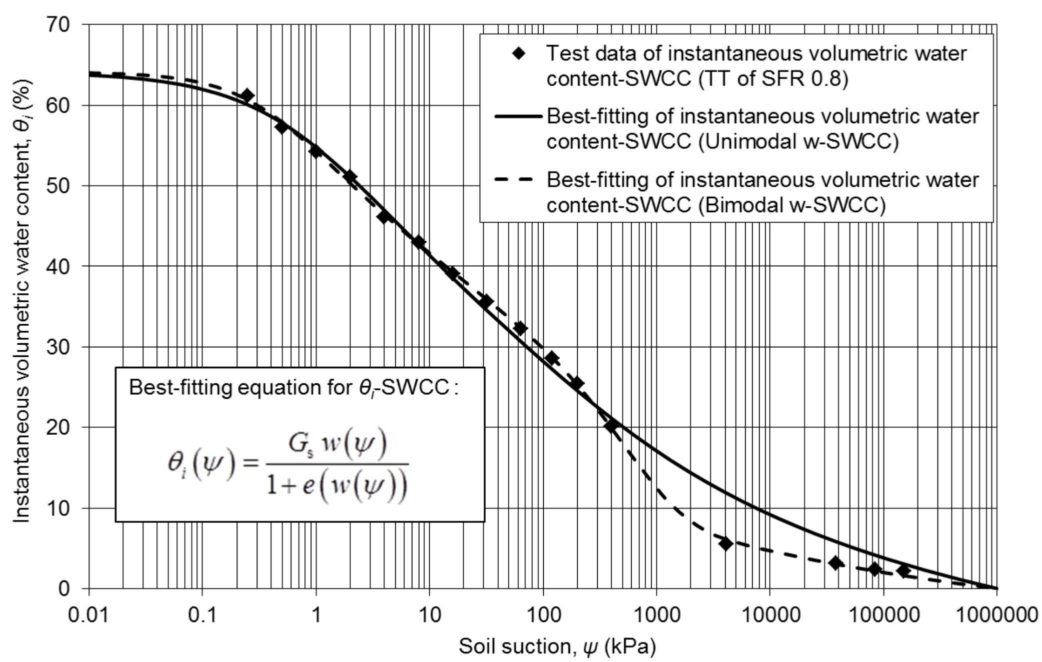

Figure 5-18. Instantaneous volumetric water content versus soil suction for Devon silt.

The best-fit curves for various forms of SWCC obtained with a simplified bimodal equation for the *w*-SWCC are used to illustrate the effect of choosing the SWCC on the estimation of the correct air-entry value and the relative coefficient of permeability function. Table 5-1 lists the breaking points on different SWCCs. The breaking points on different SWCCs appear on different soil suctions (Table 5-1) for Devon silt. The breaking point on the *w*-SWCC is at a soil suction of 1.89 kPa. The breaking point on the *S*-SWCC is at a soil suction of 593 kPa. The breaking point on the θ_i-SWCC is at a soil suction of 2.35 kPa. The air-entry value, AEV, of the soil must be estimated from the *S*-SWCC. The degree of saturation versus soil suction plot (Figure 5-17) indicates that the AEV is 593 kPa. The corresponding gravimetric water content and instantaneous volumetric water content at the point of AEV are 16.60% and 30.67% respectively.

Table 5-1. Breaking point on different SWCCs for Devon silt

Type of SWCC	*w*-SWCC	*S*-SWCC	θ_i-SWCC
Suction at the first breaking point	1.89 kPa	593 kPa	2.35 kPa

The relative permeability function is an important component constituting the permeability function for a soil that undergoes volume change as soil suction changes. Different permeability functions are obtained when using different forms of SWCC for the estimation (Table 3-2). Figure 5-19 shows three curves of the relative permeability function obtained respectively from w-SWCC, θi-SWCC, and S-SWCC. These three curves are obtained using $k_r^w(\psi)$, $k_r^S(\psi)$, $k_r^{\theta_i}(\psi)$ listed in Table 3-2. Soil suction at the breaking point on each SWCC was used as the lower limit of integration for the denominator of each estimation equation. The correct estimation of the relative permeability is the one obtained from the *S*-SWCC.

Misinterpretation of the SWCC can lead to erroneous results (e.g., using the wrong SWCC or the wrong starting point for integration). Figure 5-19 shows that the results obtained from the w-SWCC under-estimated the relative permeability by 5.27 orders of magnitude, while the results obtained from the θ_i-SWCC under-estimated the relative permeability by 4.26 orders of magnitude. The difference as shown in Figure 5-19 is substantial. It is important to use the *S*-SWCC for the estimation of the relative permeability function for soils that undergo volume change as soil suction changes.

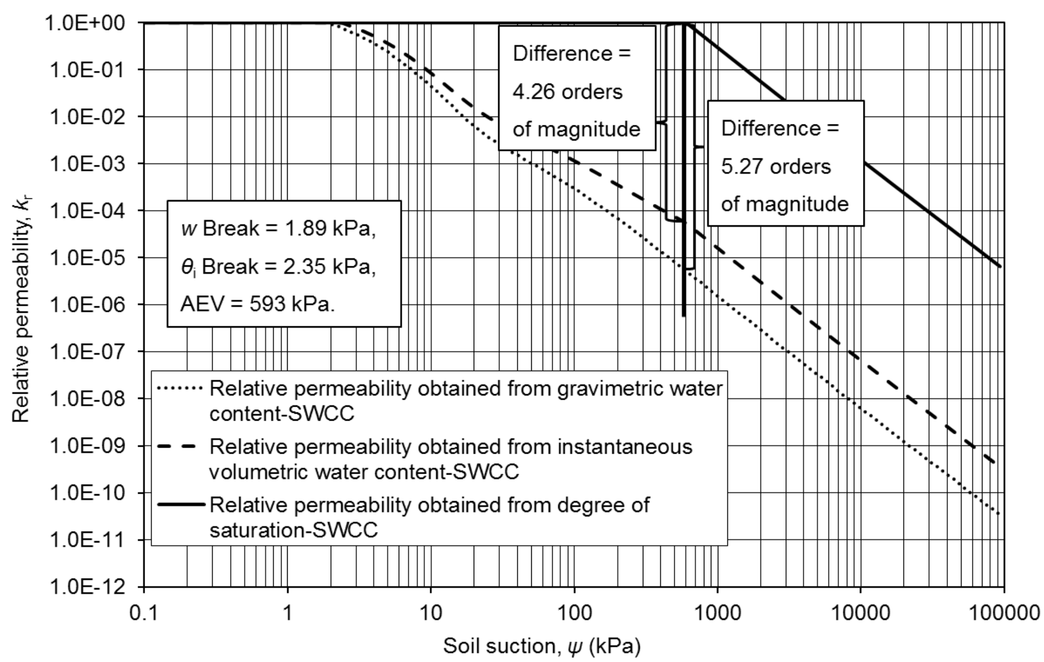

Figure 5-19. Relative permeability versus soil suction for Devon silt.

Figure 5-20 shows that the AEV has little influence when estimating the relative permeability function for Devon silt. The relative permeability versus soil suction obtained from *S*-SWCC doesn't vary much when different values are used for the lower limit of integration. The results obtained for Devon silt are different from what were obtained for Regina clay and Bulyanhulu tailings (Figure 3-10 and Figure 4-10). The *S*-SWCC for Devon silt has a sharper turn at the AEV compared to the *S*-SWCCs for Regina clay and Bulyanhulu tailings. The $k_{\mathrm{r}}^{s}\left(\psi\right)$ function listed in Table 3-2 specifies the AEV should be used as the lower limit of integration for the integral in the denominator of the equation. It is suggested that the most reasonable curve to use for the relative permeability function is the one obtained when using the AEV as the lower limit of integration, especially for a soil, the *S*-SWCCs of which has a round turn in the vicinity of the AEV. The difference in the resulting estimation for the relative permeability caused by using a lower limit of integration different than the AEV is negligible for Devon silt, while the difference for Regina clay and oil sands talings are significant. Zhang and Fredlund (2015) studied in detail the effect of the lower limit of integration on the calculation of the relative permeability function. The AEV should be used as the lower limit of integration when estimating the relative permeability function using the $k_{\mathrm{r}}^{s}\left(\psi\right)$ function.

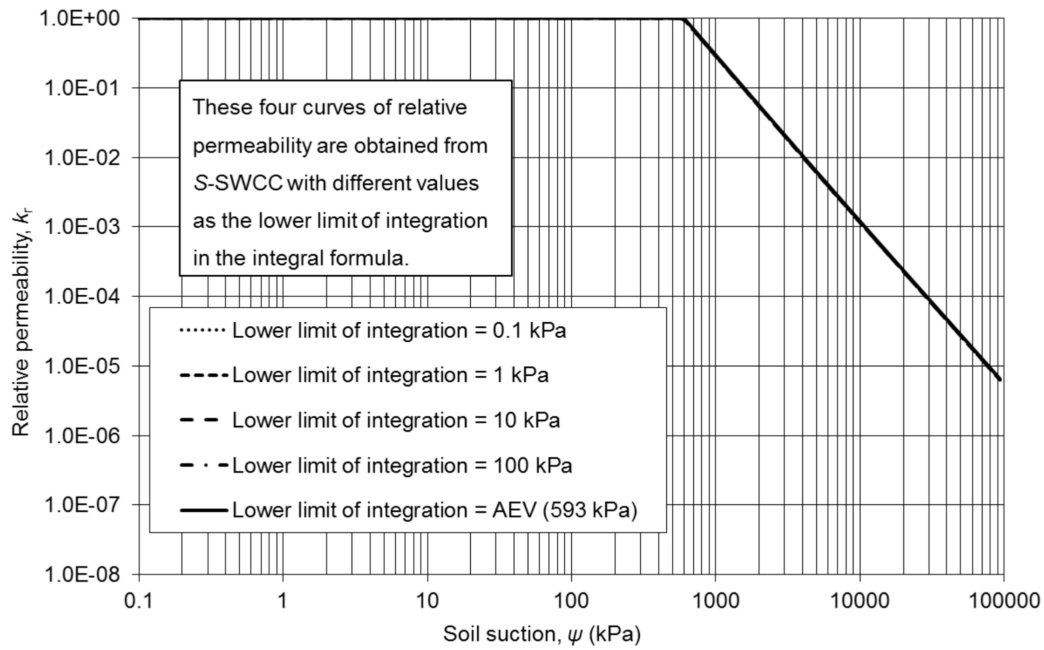

Figure 5-20. Relative permeability versus soil suction obtained from *S*-SWCC using different lower limits of integration for Devon silt.

Two curves of the relative coefficient of permeability function in Figure 5-21 are estimated respectively from the two best-fitting curves of the *S*-SWCC shown in Figure 5-17. The two best-fitting curves of the *S*-SWCC in Figure 5-17 are close to each other especially at the lower suction range. The resulting relative permeability functions estimated respectively from the two best-fitting curves of the *S*-SWCC don't have a significant difference from each other as shown in Figure 5-21. The negligible difference between the two curves of the relative permeability function at the AEV of 593 kPa is about 0.045 orders of magnitude. The quality of the best-fitting for the *S*-SWCC would influence the correctness of the estimation results of the relative coefficient of permeability function. The better the best-fitting of the *S*-SWCC, the more accurate the estimation results of the AEV and the relative permeability function will be. In the case of Devon silt, the difference between the two best-fitting curves of the

S-SWCC is insignificant. Therefore, the difference in the resulting estimations of the relative permeability function and the AEV is negligible. The AEV obtained from the *S*-SWCC best-fitted by Eq. [61] is 559 kPa. The More accurate AEV is 593 kPa, the value obtained from the *S*-SWCC best-fitted by Eq. [46]. The application of the simplified bimodal *w*-SWCC equation doesn't have a significant advantage over the use of the Fredlund-Xing (1994) *w*-SWCC equation in the case of Devon silt when calculating the relative coefficient of permeability function and the AEV.

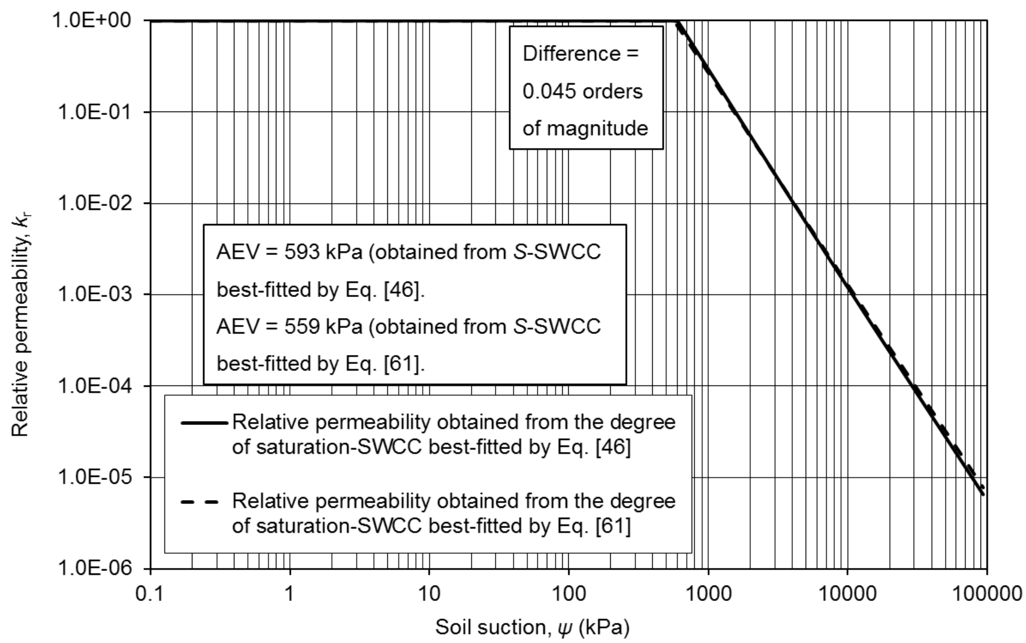

Figure 5-21. Relative permeability versus soil suction obtained from two best-fitting *S*-SWCCs for Devon silt.

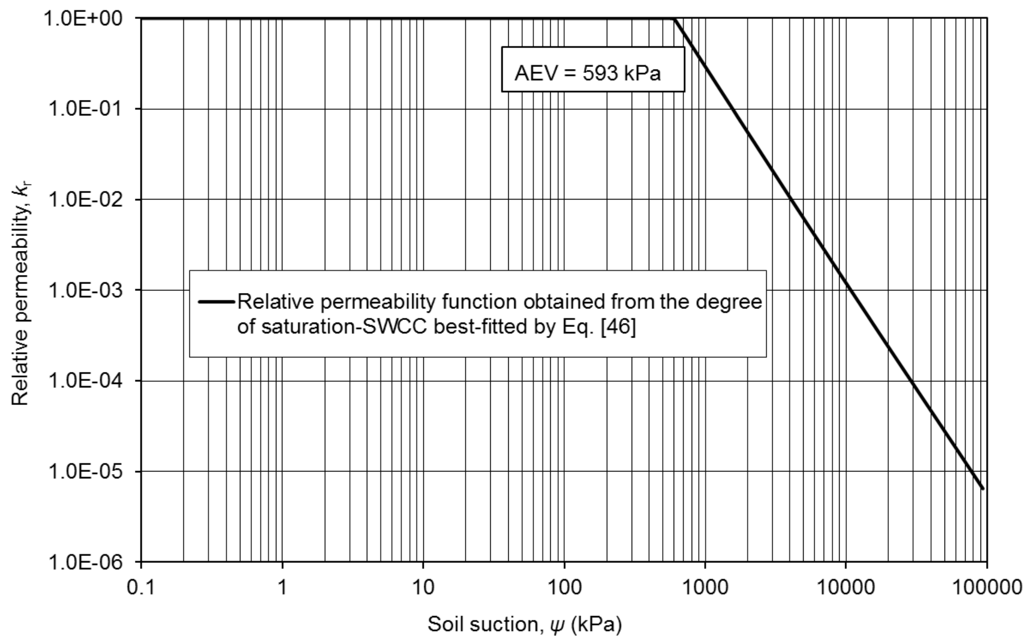

Figure 5-22. Relative permeability versus soil suction for Devon silt.

Figure 5-22 shows the curve of the relative permeability versus soil suction obtained from a better best-fitting of the *S*-SWCC with the AEV as the lower limit of integration. The curve shown in Figure 5-22 is used for the subsequent calculation of the permeability function with Eq. [48] for Devon silt.

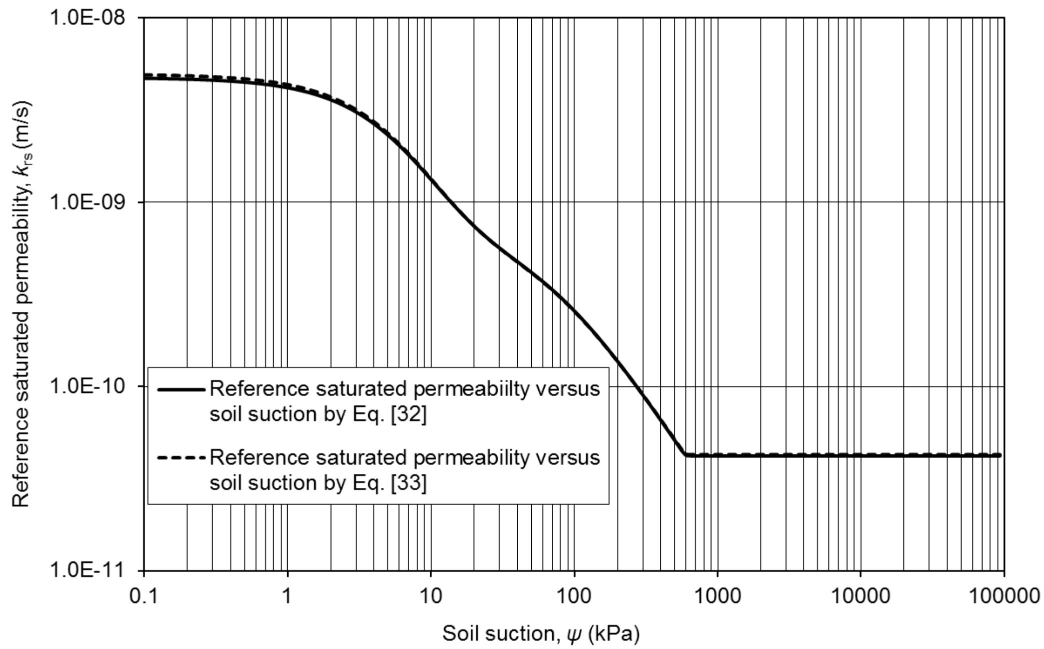

Figure 5-23. Reference saturated permeability versus soil suction for Devon silt.

The saturated permeability is a function of void ratio as shown in Figure 5-11. Both Eq. [30] and Eq. [31] are used to best-fit the measured data to obtain the mathematical description of the relationship of the saturated permeability versus the void ratio. The void ratio changes with the soil suction during the drying process as shown in Figure 5-16. The relationship of the void ratio versus the soil suction can be represented by Eq. [45]. As a result, the saturated permeability can be related to soil suction. When the saturated permeability is related to the soil suction, it is termed as the reference saturated permeability to make a distinction because both saturated and unsaturated conditions are involved in the entire drying process. The reference saturated permeability versus soil suction for Devon silt is shown in Figure 5-23. The curves in Figure 5-23 are obtained by using Eq. [32] and Eq. [33] in conjunction with Eq. [45].

After obtaining the relative permeability function shown in Figure 5-22 and the reference saturated permeability function shown in Figure 5-23, the coefficient of permeability function can be obtained by multiplying the relative permeability function with the reference saturated permeability function according to Eq. [48]. The relationship of the coefficient of permeability versus soil suction for Devon silt is shown in Figure 5-24.

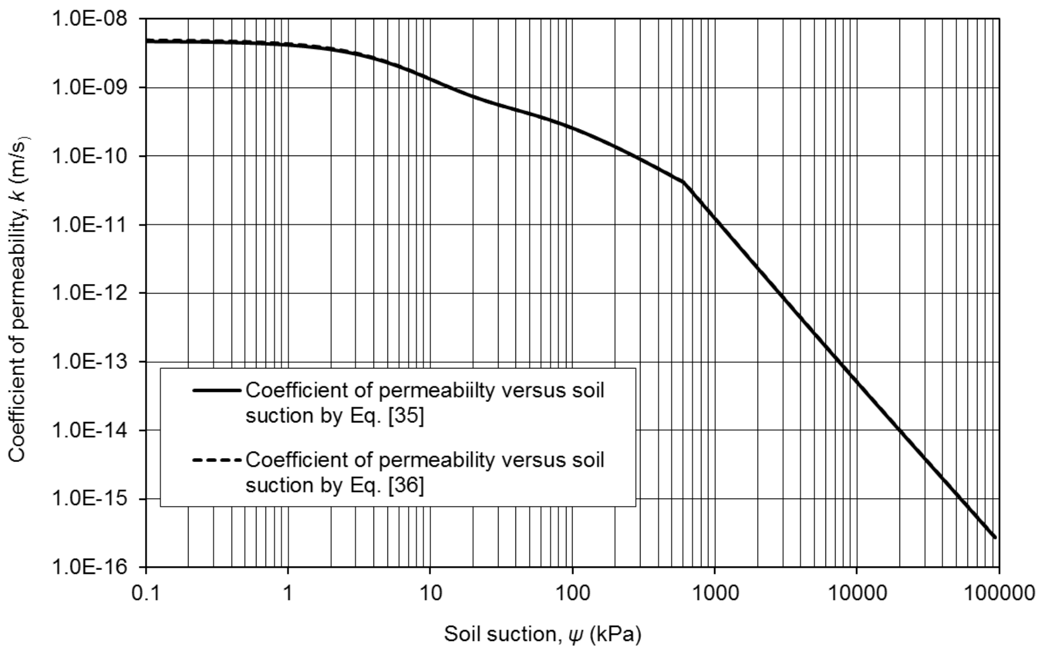

Figure 5-24. Coefficient of permeability versus soil suction for Devon silt.

5.4.2 Bulyanhulu tailings

The relationship of void ratio versus soil suction for Bulyanhulu tailings obtained by combining the *w*-SWCC and the shrinkage curve is sown Figure 5-25. Figure 5-26 shows the resulting plot of the *S*-SWCC. The plot of the θ_i-SWCC is shown in Figure 5-27. The solid fitting curves on Figures 5-23 to 5-25 are calculated on the basis of the fitting curve of the *w*-SWCC obtained by the simplified bimodal Eq. [44]. The dash fitting curves on Figures 5-23 to 5-25 are obtained based on the fitting curve of the *w*-SWCC best-fitted by the unimodal Eq. [41]. The solid lines present better fitting than the dash lines for Bulyanhulu tailings for the relationship of void ratio versus soil suction, *S*-SWCC and θ_l-SWCC. Figures 5-23 to 5-25 illustrate that the better best-fitting of the subsequent SWCCs can be calculated when the better best-fitting of the *w*-SWCC is obtained.

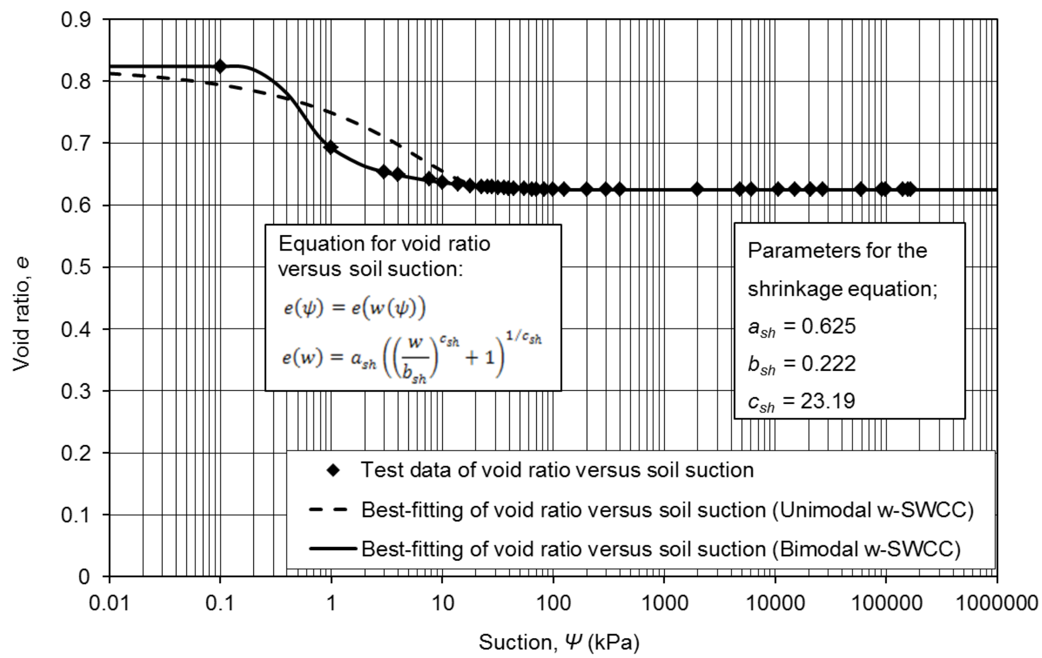

Figure 5-25. Void ratio versus soil suction for Bulyanhulu tailings.

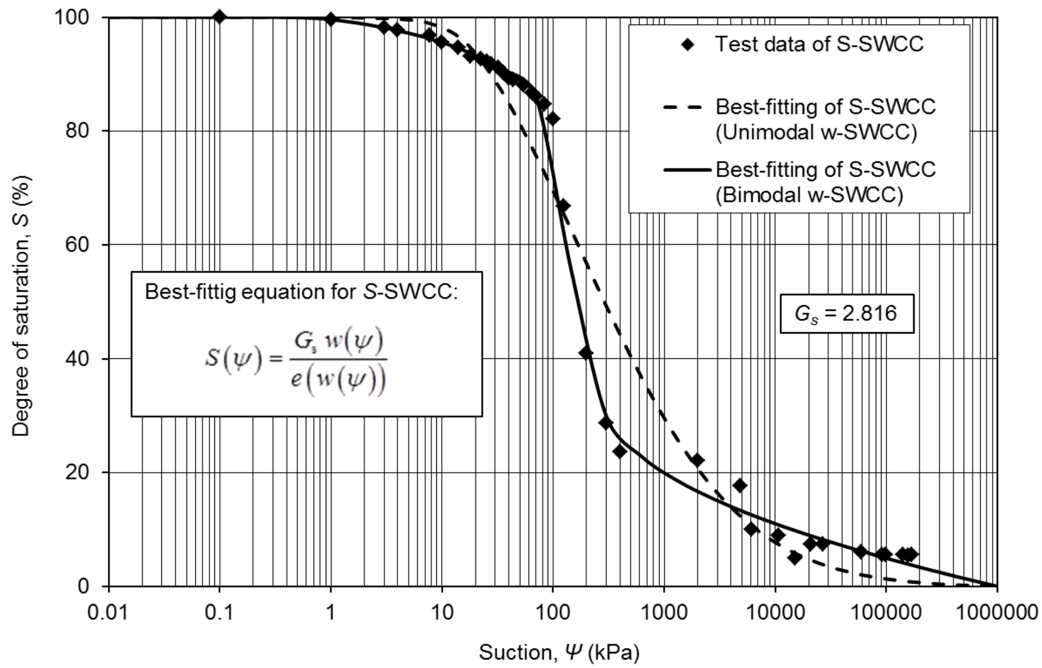

Figure 5-26. Degree of saturation versus soil suction for Bulyanhulu tailings.

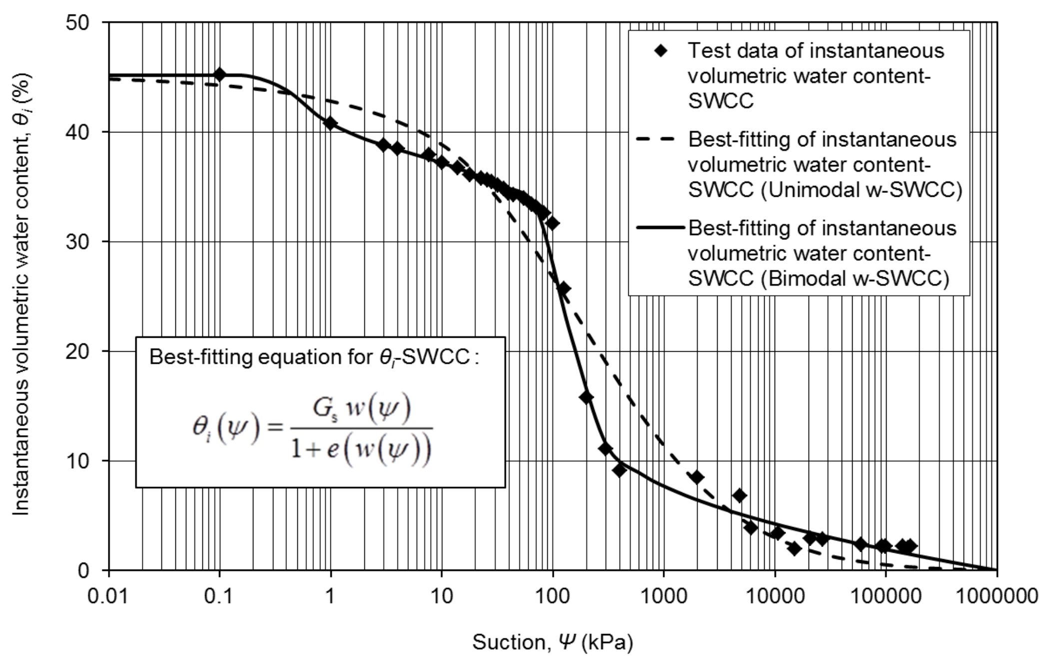

Figure 5-27. Instantaneous volumetric water content versus soil suction for Bulyanhulu tailings.

The best-fit curves for various forms of SWCC obtained with a simplified bimodal equation for the *w*-SWCC are used to illustrate the importance of applying the correct form of SWCC on the estimation of the correct air-entry value and the relative permeability function. Table 5-2 lists the breaking points on different SWCCs. The breaking points on different SWCCs appear on different soil suctions (Table 5-2) for Bulyanhulu tailings. The breaking point on the *w*-SWCC is at a soil suction of 0.276 kPa. The breaking point on the *S*-SWCC is at a soil suction of 86 kPa. The breaking point on the θ_i-SWCC is at a soil suction of 0.28 kPa. The air-entry value, AEV, of the soil must be estimated from the *S*-SWCC. The degree of saturation versus soil suction plot (Figure 5-26) indicates that the AEV is 86 kPa. The corresponding gravimetric water content and instantaneous volumetric water content at the point of AEV are 18.65% and 83.98% respectively.

Table 5-2. Breaking point on different SWCCs for Bulyanhulu tailings.

Type of SWCC	*w*-SWCC	*S*-SWCC	θ_i-SWCC
Suction at the first breaking point	0.276 kPa	86 kPa	0.28 kPa

The relative permeability function is an important component constituting the permeability function for a soil that undergoes volume change as soil suction changes. Different permeability functions are obtained when using different forms of SWCC for the estimation (Table 3-2). Figure 5-28 shows three curves of the relative permeability function obtained respectively from *w*-SWCC, θ_i-SWCC, and *S*-SWCC. These three curves are obtained using $k_r^w(\psi)$, $k_r^S(\psi)$, $k_r^{\theta_i}(\psi)$ listed in Table 3-2. Soil suction at the breaking point on each SWCC was used as the lower limit of integration for the denominator of each estimation equation. The correct estimation of the relative permeability is the one obtained from the *S*-SWCC. Misinterpretation of the SWCC can lead to erroneous results (e.g., using the wrong SWCC or the wrong starting point for integration). Figure 5-28 shows that the results obtained from the *w*-SWCC under-estimated the relative permeability by 4.03 orders of magnitude, while the results obtained from the θ_i-SWCC under-estimated the relative permeability by 3.49 orders of magnitude. The difference as shown in Figure 5-28 is substantial. It is important to use the *S*-SWCC for the estimation of the relative permeability function for soils that undergo volume change as soil suction changes.

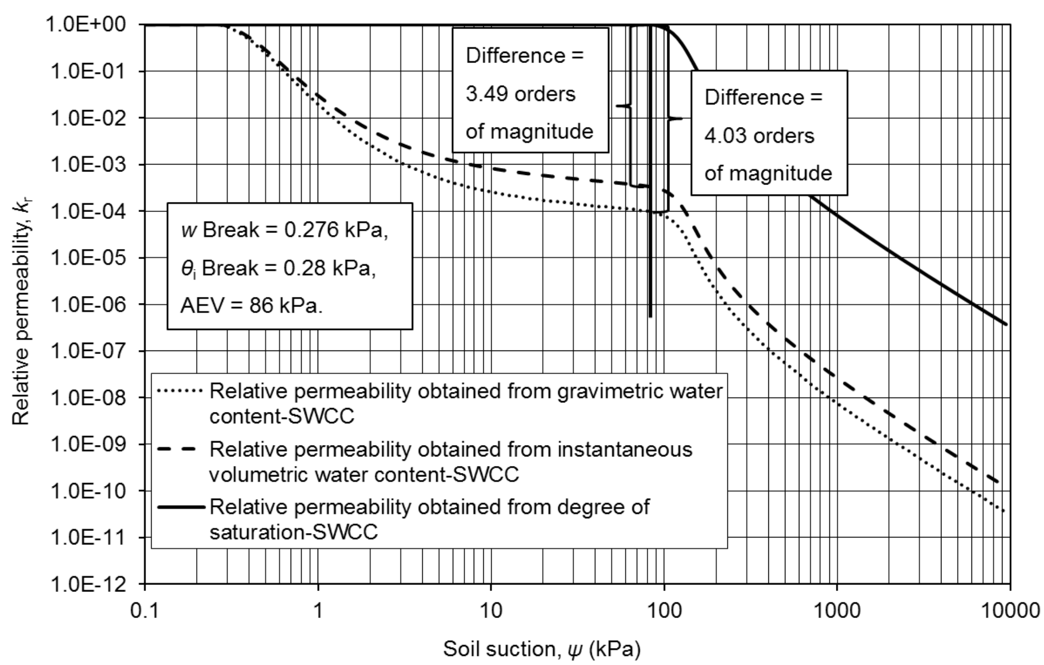

Figure 5-28. Relative permeability versus soil suction for Bulyanhulu tailings.

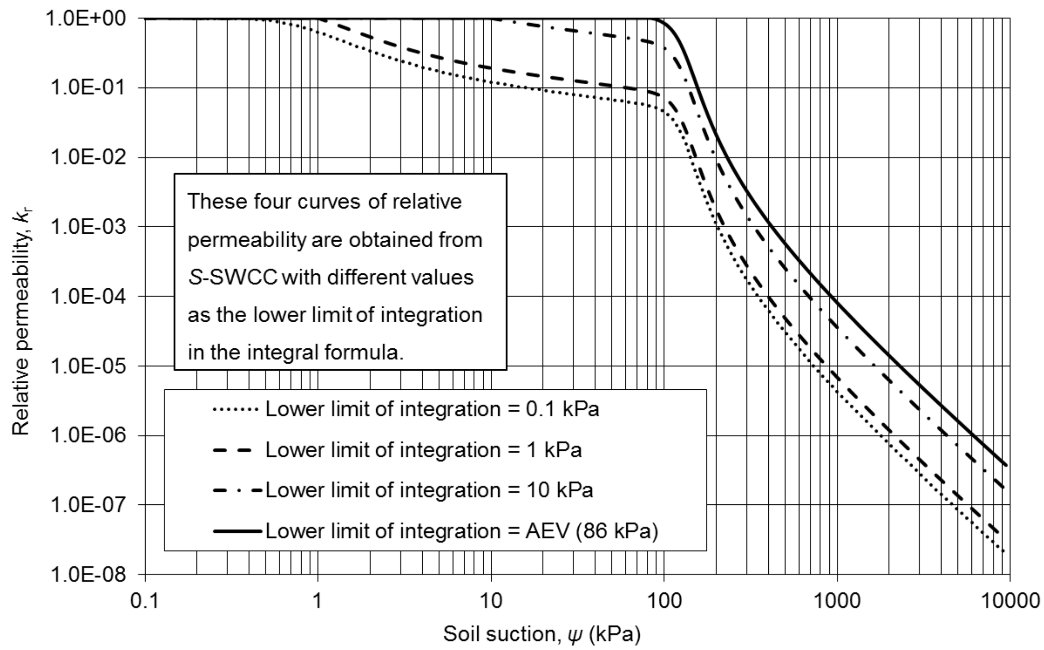

Figure 5-29. Relative permeability versus soil suction obtained from *S*-SWCC using different lower limits of integration for Bulyanhulu tailings.

Figure 5-29 shows that the AEV has a significant influence on the estimation of the relative permeability function for Bulyanhulu tailings. The curve of the relative permeability function versus soil suction varies when different values are used for the lower limit of integration. The $k_r^s(\psi)$ function listed in Table 3-2 specifies the AEV should be used as the lower limit of integration for the integral in the denominator of the equation. It is suggested that the most reasonable curve to use for the relative permeability function is the one obtained when using the AEV as the lower limit of integration.

Table 5-3. Difference in the estimated relative permeability between using the AEV and using a different lower limit of integration for Bulyanhulu tailings.

Lower limit of integration	0.1 kPa	1 kPa	10 kPa
Difference in terms of orders of magnitude	1.27	1.07	0.35

Table 5-3 presents the difference that could result when using a smaller value as the lower limit of integration. When the value used as the lower limit of integration is 10 kPa, the results are underestimated by 0.35 orders of magnitude. When the value used as the lower limit of integration is 1 kPa, the resulting relative permeability would be underestimated by 1.07 orders of magnitude. When a value of 0.1 kPa is used as the lower limit of integration, the results are underestimated by 1.27 orders of magnitude. The difference in the resulting estimation for the relative permeability caused by using a lower limit of integration different than the AEV is significant as presented in Figure 5-29. The AEV should be used as the lower limit of integration when estimating the relative permeability function using the $k_r^s(\psi)$ function.

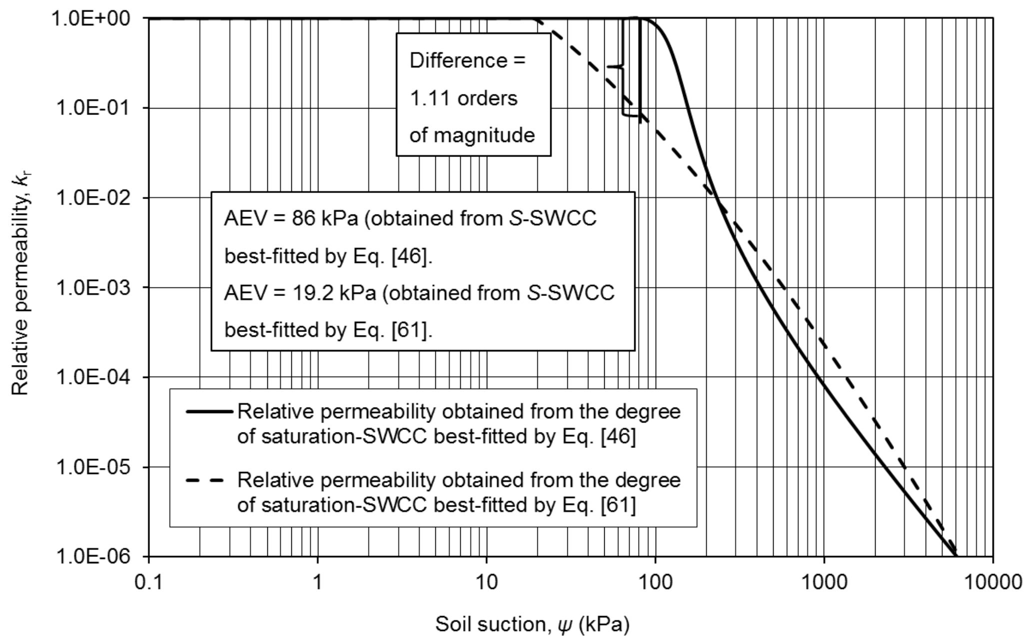

Figure 5-30. Relative permeability versus soil suction obtained from two best-fitting *S*-SWCCs for Bulyanhulu tailings.

The quality of the best-fitting for the *S*-SWCC would influence the correctness of the estimation results of the relative coefficient of permeability (Figure 5-30). Two curves of the relative coefficient of permeability in Figure 5-30 are estimated respectively from the two best-fitting curves of the *S*-SWCC shown in Figure 5-26. The difference between the two curves of the relative permeability at the AEV of 86 kpa is about 1.11 orders of magnitude. The better the best-fitting of the *S*-SWCC, the more accurate the estimation results of the AEV and the relative permeability function will be. In the case of Bulyanhulu tailings, the data are more closely fit when using the simplified bimodal *w*-SWCC equation and the corresponding subsequent forms of SWCCs. The AEV obtained from the *S*-SWCC best-fitted by the Eq. [61] is 19.2 kPa. The more accurate AEV is 86 kPa , the value obtained from the *S*-SWCC best-fitted by Eq. [46]. Eq. [46] is derived from the simplified bimodal *w*-SWCC equation, while Eq. [61] is derived from the unimodal Fredlund and Xing (1994) *w*-SWCC equation. Comparing Figure 5-26 and Figure 5-30, it can be concluded that the shape of the *S*-SWCC would influence the shape of the resulting curve of the relative permeability function.

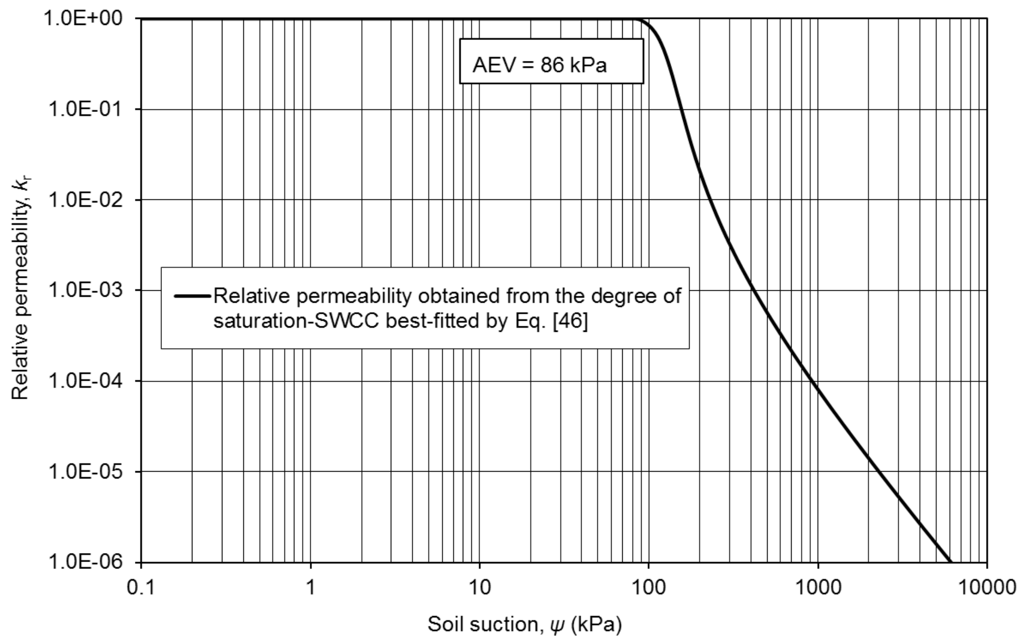

Figure 5-31. Relative permeability versus soil suction for Bulyanhulu tailings.

Figure 5-31 shows the curve of the relative permeability versus soil suction obtained from a better best-fitting of the *S*-SWCC with the AEV as the lower limit of integration. The curve shown in Figure 5-31 is used for the subsequent calculation of the permeability function with Eq. [48] for Bulyanhulu tailings.

The saturated permeability is a function of void ratio as shown in Figure 5-15. Eq. [30] and Eq. [31] are used to best-fit the measured data to obtain the mathematical description of the relationship of the saturated permeability versus void ratio. The void ratio changes with soil suction during the drying process as shown in Figure 5-25. The relationship of the void ratio versus soil suction can be represented by Eq. [45]. As a result, the saturated permeability can be related to soil suction. When the saturated permeability is related to the soil suction, it is termed as the reference saturated permeability function to make a distinction because both saturated and unsaturated conditions are involved in the entire drying process. The reference saturated permeability versus soil suction for Bulyanhulu tailings is shown in Figure 5-32. The curves in Figure 5-32 are obtained using Eq. [32] and Eq. [33] in conjunction with Eq. [45]. The two curves in Figure 5-32 are so close that they overlap each other.

After obtaining the relative permeability function shown in Figure 5-31 and the reference saturated permeability function shown in Figure 5-32, the coefficient of permeability function can be obtained by multiplying the relative permeability function with the reference saturated permeability function according to Eq. [48]. The relationship of the coefficient of permeability versus soil suction for Bulyanhulu tailings is shown in Figure 5-33.

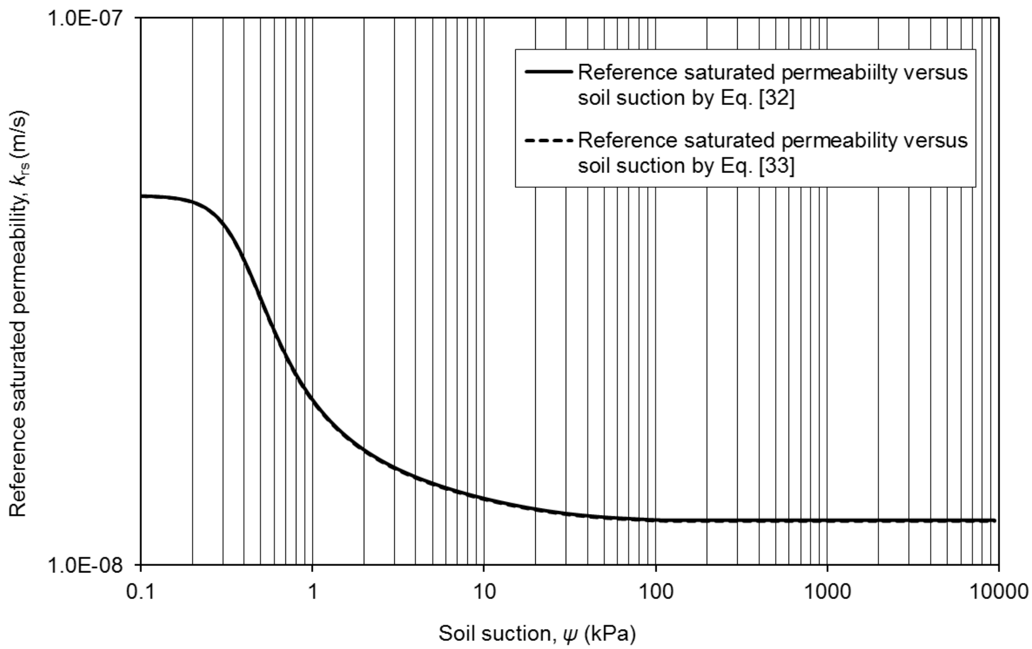

Figure 5-32. Reference saturated permeability versus soil suction for Bulyanhulu tailings.

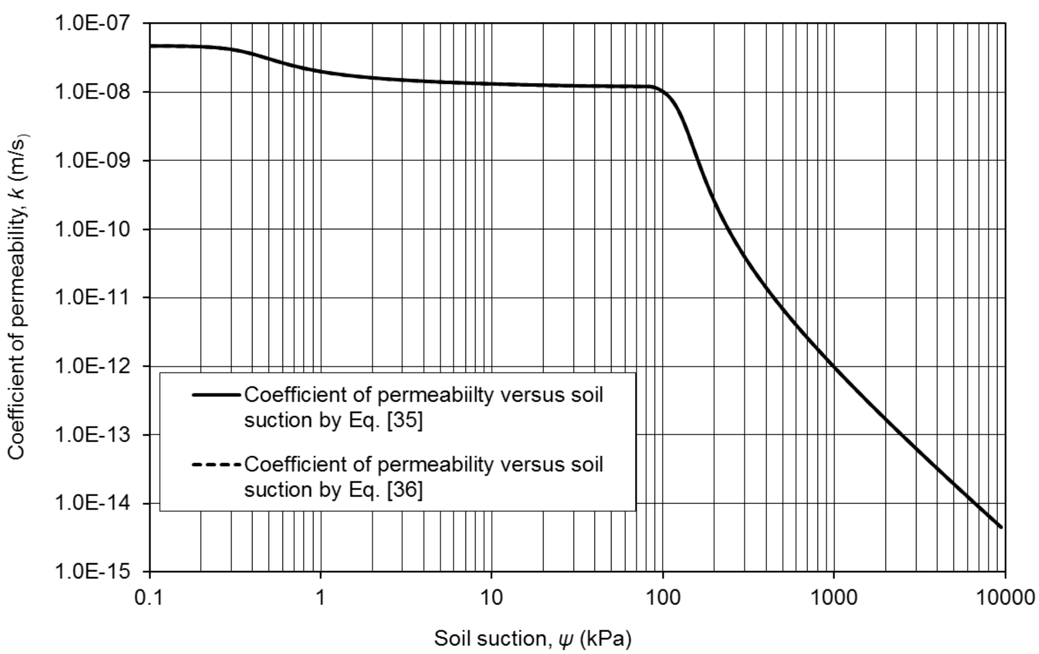

Figure 5-33. Coefficient of permeability versus soil suction for Bulyanhulu tailings.

5.5 Conclusions and Recommendations

Devon silt and Bulyanhulu tailings are two typical soils that undergo some volume change during a drying process but much less compared to Regina clay and oil sands tailings. Experimental tests were conducted on these two soils, including grain size analysis, specific gravity tests, water content and Atterberg limit tests, the large strain consolidation with permeability test, shrinkage test and soil-water characteristic curve test. Testing results for SWCCs, the relationships of saturated permeability versus void ratio and shrinkage curves have been presented and interpreted with the proposed revised methodology for the estimation of the permeability function. The testing results show how the void ratio and the degree of saturation influence the coefficient of permeability for a soil. The proposed permeability function is the product of the reference saturated permeability function and the relative permeability function. The effect of the change of the void ratio on the coefficient of permeability is accommodated in the reference saturated permeability function, while the influence of a change in the degree of saturation is considered in the relative permeability function.

The proper interpretation of SWCC is important when estimating the relative permeability function and the AEV. It should be noted that the *S*-SWCC should be used for the estimation of the relative permeability function with the AEV as the lower limit of integration. The test results on Devon silt don’t present a significant influence of the AEV on the estimation of the relative permeability function due to a sharp turn around the vicinity of the AEV on the *S*-SWCC for Devon silt. However, test results on Bulyanhulu tailings show the importance of the AEV used as the lower limit of integration in the integral of the denominator in the proposed permeability function.

The quality of the fit of the *S*-SWCC affects the quality of the estimation results. The better the fit of the *S*-SWCC, the more accurate the estimation results for the relative permeability function. Both the unimodal Fredlund and Xing (1994) equation and the simplified bimodal *w*-SWCC equation can be used for the development of the *S*-SWCC function. In the case of Devon silt, since the difference between the two best-fitting curves of the *S*-SWCC is negligible, the resulting relative permeability functions estimated respectively from the two best-fitting curves of the *S*-SWCC have an insignificant difference from each other. In the case of Bulyanhulu tailings, the measured *w*-SWCC exhibits a significant bimodal feature. As a result, the simplified bimodal *w*-SWCC equation can be used to obtain a better proper best-fit for the *w*-SWCC and subsequent other SWCCs. The resulting relative permeability functions estimated from the two best-fitting curves of the *S*-SWCC have an unnegligible difference.

Reference

Chapuis, R.P. 2012. Predicting the saturated hydraulic conductivity of soils: a review. Bulletin of Engineering Geology and the Environment, 71(3): 401-434.

Fredlund, D.G., and Xing, A. 1994. Equations for the soil-water characteristic curve. Canadian geotechnical journal, 31(4): 521-532.

Fredlund, D.G., Stone, J., Stianson, J., and Sedgwick, A. 2011. Determination of water storage and permeability functions for oil sands tailings. Proceedings of the 15th International Conference on Tailings and Mine Waste, Vancouver, BC, Canada, November 6th to 9th, 2011.

Fredlund, D.G., and Zhang, F-X. 2013. Combination of shrinkage curve and soil-water characteristic curves for soils that undergo volume change as soil suction is increased. Proceedings of the 18th International Conference on Soil Mechanics and Geotechnical Engineering, Paris, France.

Somogyi, F. 1980. Large-strain consolidation of fine-grained slurries. Proceedings of the Canadian Society for Civil Engineering 1980 Annual Conference, Winnipeg, Manitoba, Canada.

Taylor, D.W. 1948. Fundamentals of soil mechanics. J. Wiley & Sons; London: Chapman & Hall.

Zhang, F-X, Fredlund, D. G., Wilson, G. W., and Sedgwick, A. 2014. Determination of the permeability function for drying oil sands tailings undergoing volume change and desaturation. Proceedings of the 4th

International Oil Sands Tailings Conference, Banff, A.B.Dec 7th-10th, 2014.

Zhang, F-X, and Fredlund, D.G. 2015. Examination of the estimation of relative permeability for unsaturated soils. Canadian Geotechnical Journal, 52(12): 2077-2087.

Zhang, L., and Chen, Q. 2005. Predicting bimodal soil–water characteristic curves. Journal of Geotechnical and Geoenvironmental Engineering, 131(5): 666-670.

ASTM D422–63 (2007) Standard test method for particle-size analysis of soils. ASTM International, West Conshohocken. doi,*10*, 1520.

ASTM D854-14 Standard Test Methods for Specific Gravity of Soil Solids by Water Pycnometer, ASTM International, West Conshohocken, PA, 2014, http://dx.doi.org/10.1520/D0854-14

Chapter 6. Summary of conclusions and recommendations

6.1 Summary of studies undertaken

Unsaturated soil properties are necessary in the numerical modeling of various geotechnical engineering problems. The correctness of the involved unsaturated soil property functions affects the accuracy of the numerical modeling results. This thesis is devoted to a detailed study on the hydraulic properties (mainly the coefficient of permeability function) for a soil that undergoes volume change as soil suction is changed. The study is limited to the drying process.

Numerous estimation techniques have been proposed in the literature to predict the coefficient of permeability function and water storage function. However, the conventional methodologies are developed on the basis that the soil doesn't undergo volume change as soil suction is changed. The assumption of no volume change may be suitable for sands or coarse-grained materials, but it is not acceptable for some fine-grained silts and clays. The study in this thesis made a revision to the conventional estimation methodologies and developed a revised method for the estimation of the coefficient of permeability function and water storage function for soils that undergo volume change as soil suction is changed. Both degree of saturation and void ratio are taken into account for the development of the revised method. The Fredlund et al. (1994) permeability function is the function revised in this study to develop a permeability function suitable for volume change materials.

The original relative permeability theory published by Fredlund et al. (1994) specified the air-entry (AEV), ψ_{aev}, as the lower limit of integration. However, implementations in engineering practice appear to have used other values between zero and ψ_{aev} as the starting point of integration when calculating the relative coefficient of permeability. The study assessed whether the choice for the lower limit of integration influences the calculation of the Fredlund, Xing and Huang permeability function. The effect of the lower limit of integration is examined in terms of the effect of each of the SWCC fitting parameters (i.e., a_f, n_f, m_f, ψ_r) on the resulting error. The definition of the "permeability error" is described. An empirical procedure for the determination of the AEV is also presented.

Typical soils of volume change during a drying process (e.g., Regina clay and oil sands tailings) were used to illustrate and explain the estimation procedure of using the proposed method to estimate the coefficient of permeability function and the water storage function. Devon silt and Bulyanhulu tailings are two types of soils that undergo some volume change but not as much as what Regina clay and oil sands tailings would experience. Devon silt and Bulyanhulu tailings were used in the experimental program. Tests were carried out to obtain the shrinkage curves, *w*-SWCCs and the relationships of saturated coefficient of permeability versus void ratio and other basic soil physical properties such as grain size distributions, Atterberg limits and specific gravities. The revised estimation methods were applied to interpret the test results to predict the hydraulic property functions for Devon silt and Bulyanhulu tailings as a means of verification.

6.2 Conclusions based on the various research studies

There are four designations of water content, namely, gravimetric water content, w; volumetric water content, θ; instantaneous volumetric water content, θ_i ; degree of saturation, S. Accordingly, there are four types of soil water characteristic curve (e.g., gravimetric water content–soil water characteristic curve, w-SWCC; volumetric water content–soil water characteristic curve, θ-SWCC; instantaneous volumetric water content–soil water content characteristic curve, θ_i-SWCC; degree of saturation–soil water characteristic curve, S-SWCC). When soils do not change volume as soil suction is changed, these four SWCCs are essentially the same. However, three SWCCs, namely, w-SWCC, θ_i-SWCC and S-SWCC, are very different from each other when soils change volume as soil suction is changed. Though w-SWCC and θ-SWCC are basically the same for volume change soils, θ-SWCC has no meaningful value when there is volume change.

The choice of the appropriate SWCC is important in the estimation of the unsaturated soil property functions especially for soils that change volume. The S-SWCC should be used to determine the true AEV and estimate the relative coefficient of permeability function associated with the desaturation of the soil. The θ_i –SWCC should always be used for the estimation of the water storage function. Misuse of SWCC in the estimation of unsaturated soil property functions can cause erroneous results.

When the S-SWCC is used for the estimation of the relative coefficient of permeability, its correct interpretation is also crucial. The Fredlund, Xing and Huang (1994) permeability function is studied regarding the importance of the air-entry value, AEV as the lower limit of integration. Several conclusions drawn are: 1.) If a lower limit of integration used in the integral of Fredlund, Xing and Huang (1994) is smaller than the AEV, the computed results will underestimate the relative coefficient of permeability. The smaller the value used for the starting point of integration compared to the AEV, the greater will be the difference between the computed results and the relative permeability; 2.) The error caused by using a small value for the lower limit of integration is influenced by the fitting parameters of the Fredlund and Xing (1994) SWCC equation, namely a_f, n_f, m_f, and ψ_r. The analysis reveals that the influence of the n_f is much greater than the influence of the a_f, m_f, and ψ_r/a_f values; 3.) The difference caused by a particular lower limit of integration, defined in terms of a particular number of $\log_{10}$ cycles less than the AEV, decreases with an increase in the n_f value when the values of a_f, m_f, and ψ_r are fixed. This is particularly true when the n_f value is smaller than 2; 4.) The m_f value for the SWCC has limited influence on the difference in the estimation of the permeability function that may be caused by a low starting point of integration; 5.) The difference in the estimation of the relative coefficient of permeability caused by using a particular low starting point of integration usually does not change much with the change in the a_f value. However, the difference becomes more sensitive to the a_f value when it is combined with small n_f and m_f values; 6.) It is recommended that the AEV always be used as the lower limit of integration when estimating the relative permeability function with the Fredlund, Xing and Huang (1994) permeability function.

A revised theory for the estimation of the coefficient of permeability function was developed by modifying the Fredlund, Xing and Huang (1994) permeability function. Changes in the volume of a soil as soil suction is increased can significantly affect the interpretation of the SWCC and the estimation of the coefficient of permeability function. Both the degree of saturation and the void ratio need to be considered when estimating the coefficient of permeability function for soils that undergo volume change.

The proposed coefficient of permeability function in this study consists of two main components, namely, the reference saturated coefficient of permeability function and the relative coefficient of permeability function. The reference saturated coefficient of permeability function is controlled by the void ratio as soil suction changes and reflects the influence of volume change on the coefficient of permeability. The reference saturated coefficient of permeability at a particular soil suction is the corresponding saturated coefficient of permeability for the void ratio at the relevant soil suction. The reference saturated coefficient of permeability function is obtained through the combination of the saturated permeability function and the relationship of the void ratio versus soil suction. The relationship of the void ratio versus soil suction is obtained by combining the *w*-SWCC and the shrinkage curve. The influence of a change in the degree of saturation is considered in the relative permeability function. The change of the degree of saturation changes the tortuosity of the flow path, thus resulting in the changes of the relative permeability. Therefore, the relative coefficient of permeability function and the AEV should be estimated from the *S*-SWCC. The AEV should be used as the lower limit of integration of the integral in the denominator of the relevant relative permeability equation. Using other forms of the SWCC or other values as the lower limit of integration can lead to large estimation errors. The revised coefficient of permeability function is the result of the multiplication of the reference coefficient of permeability function by the relative coefficient of permeability function.

The quality of the fit of the *S*-SWCC affects the quality of the estimation results. The better the fit of the *S*-SWCC, the more accurate the estimation results for the relative permeability function. Both the Fredlund and Xing (1994) equation and the simplified bimodal equation can be used to best-fit the *w*-SWCC measured data. And the subsequent other types of SWCCs can be obtained on the basis of the basic volume-mass relationships. Fredlund and Xing (1994) is recommended to best-fit unimodal measured *w*-SWCC data, while the simplified bimodal equation is better suited for the *w*-SWCC of the bimodal features.

Four types of soils were studied in this thesis for illustration, explanation and confirmation of the proposed theory. These four types of soils are Regina clay, oil sands tailings, Devon silt and Bulyanhulu tailings. The experimental data of Regina clay were taken from Fredlund (1964). The laboratory test results for oil sands tailings were from previous TOTAL. Data for Devon silt and Bulyanhulu tailings were collected from the experimental program. Analysis of testing results on Regina clay, oil sands tailings, Devon silt and Bulyanhulu tailings demonstrated that different permeability functions were obtained when using different forms of SWCC for estimation. The appropriate one is estimated from the *S*-SWCC. Testing results also show that the AEV has a significant influence on the estimation of the relative permeability function for Regina clay, oil sands tailings, and Bulyanhulu tailings, though not on Devon silt due to the sharp turn around the vicinity of the AEV on the Devon silt's *S*-SWCC.

The *w*-SWCC data of Regina clay has a typical unimodal feature, which can be best-fitted by Fredlund and Xing (1994) equation very well. The *w*-SWCC data for oil sands tailings and Bulyanhulu tailings exhibit significant bimodal shapes. Simplified bimodal equation was used to obtain the better best-fit of the *w*-SWCC for oil sands tailings and Bulyanhulu tailings. The better best-fit of the *S*-SWCCs were obtained and the better estimation of the permeability function were calculated accordingly. The *w*-SWCC measured data for Devon silt shows a slight bimodal characteristic. The use of simplified bimodal equation doesn't have a significant advantage over the use of Fredlund and Xing (1994) equation when best-fitting the *w*-SWCC for the calculation of the other SWCCs and the estimation of the permeability function.

The shrinkage curve, the gravimetric water content versus soil suction (*w*-SWCC) and the saturated coefficient of permeability versus void ratio (the saturated permeability function) are three basic experimental measurements required for the estimation of the coefficient of permeability function for soils that undergo volume change as soil suction is changed.

6.3 Recommendations for future research

The research in this thesis is limited to the study of hydraulic and volume-mass properties related to the water phase, primarily emphasized on the coefficient of permeability function and the water storage function. Further studies can be done on the other unsaturated soil properties, such as shear strength properties, heat flow properties and fluid flow properties of the air phase for soils that change volume as soil suction is changed.

Hysteresis is a characteristic for unsaturated soil properties. The drying and wetting SWCCs are significantly different, and in many cases it becomes necessary to differentiate the soil properties associated with the drying curve from those associated with the wetting curve (Fredlund et al. 2012). This thesis studied the estimation of the permeability function and the water storage function for a soil that undergoes volume change as soil suction is increased during a dying process. Further study could be done on the estimation of the hydraulic property function for a soil changes volume during a wetting process.

Studies regarding the importance of the AEV in the estimation of the relative permeability function were carried out using the Fredlund, Xing and Huang (1994) permeability function. The revised permeability function for high volume change materials was developed by modifying Fredlund, Xing and Huang (1994) permeability function. Further studies on the importance of the AEV in the estimation of the permeability function for high volume change materials are recommended to be undertaken where other physical models are used along with other SWCCs.

References

Fredlund, D.G. 1964. Comparison of soil suction and one-dimensional consolidation characteristics of a highly plastic clay. Dissertation, University of Alberta.

Fredlund, D.G., and Xing, A. 1994. Equations for the soil-water characteristic curve. Canadian geotechnical journal, 31(4): 521-532.

Fredlund, D.G., Xing, A. and Huang, S. 1994. Predicting the permeability function for unsaturated soils using the soil-water characteristic curve. Canadian Geotechnical Journal, 31(4): 533-546.

Fredlund, D.G., Rahardjo, H., and Fredlund, M.D. 2012. Unsaturated soil mechanics in engineering practice. John Wiley & Sons, New York.

Bibliography

Assouline, S., D. Tessier, and A. Bruand (1998) A conceptual model of the soil water retention curve. Water Resources Research, 34(2): 223-231.

Assouline, S., D. Tessier, and A. Bruand (2000) Correction to "A conceptual model of the soil water retention curve" by S. Assouline, D. Tessier, and A. Braund. Water Resource Research, 36(12): 3769.

ASTM D422–63 (2007) Standard test method for particle-size analysis of soils. ASTM International, West Conshohocken. doi,*10*, 1520.

ASTM D854-14 Standard Test Methods for Specific Gravity of Soil Solids by Water Pycnometer, ASTM International, West Conshohocken, PA, 2014, http://dx.doi.org/10.1520/D0854-14

Bharat, T.V., and Sharma, J. 2012. Validity limits of Fredlund–Xing–Kunze model for the estimation of hydraulic properties of unsaturated soils. In Proceedings of the Canadian Geotechnical Conference, Winnipeg, Man., 30 September – 3 October. Paper No. 263.

Bronswijk, J. J. B. (1991) Relation between vertical soil movements and water-content changes in cracking clays. Soil Science Society of America Journal, 55(5): 1220-1226.

Brooks, R. H. and A. T. Corey (1964) Hydraulic properties of porous media. Hydrol. Pap. 3, Civ. Eng. Dep., Colo. State Univ., Fort Collins, Colorado.

Brutsaert, W. (1967) Some methods of calculating unsaturated permeability. Trans. ASAE, 10(3): 400-404.

Bumb, A. C., Murphy, C. L., and Everett, L. G. (1992) A comparison of three functional forms for representing soil moisture characteristics. Groundwater, 30(2): 177-185

Burdine, N. (1953) Relative permeability calculations from pore size distribution data. Journal of Petroleum Technology, 5 (03): 71–78.

Burger, C.A., and Shackelford, C.D. 2001a. Evaluating dual porosity of pelletized diatomaceous earth using bimodal soil–water characteristic curve functions. Can. Geotech. J., 38(1): 53–66.

Burger, C.A., and Shackelford, C.D. 2001b. Soil–water characteristic curves and dual porosity of sand-diatomaceous earth mixtures. J. Geotech. Geoenviron. *Eng.*, 127(9): 790–800.

Campbell, G. S. (1974) A simple method for determining unsaturated conductivity from moisture retention data. Soil science, 117(6): 311-314.

Chapuis, R. P. (2012) Predicting the saturated hydraulic conductivity of soils: a review. Bulletin of Engineering Geology and the Environment, 71(3): 401-434.

Childs, E. C., and Collis-George, N. (1950) The permeability of porous materials. In Proceedings of the Royal Society of London A: Mathematical, Physical and Engineering Sciences. The Royal Society, Vol. 201, No. 1066, pp. 392-405.

Cornelis, W. M., Corluy, J., Medina, H., Hartmann, R., Van Meirvenne, M., and Ruiz, M. E. 2006. A simplified parametric model to describe the magnitude and geometry of soil shrinkage. European Journal of Soil Science, 57(2): 258-268.

Croney, D., and Coleman, J. D. 1954. Soil structure in relation to soil suction (pF). Journal of Soil Science, *5*(1): 75-84.

Farrell, D. A., and W. E. Larson (1972) Modeling the pore structure of porous media, Water Resources Research, 8(3): 699-706.

Fredlund, D. G. (1964) Comparison of soil suction and one-dimensional consolidation characteristics of a highly plastic clay. Dissertation, University of Alberta.

Fredlund, D. G., and Rahardjo, H. (1993) Soil mechanics for unsaturated soils. John Wiley & Sons.

Fredlund, D. G., and Xing, A. (1994) Equations for the soil-water characteristic curve. Canadian geotechnical journal, 31(4): 521-532.

Fredlund, D. G., Xing, A. and Huang, S. (1994) Predicting the permeability function for unsaturated soils using the soil-water characteristic curve. Canadian Geotechnical Journal, 31(4): 533-546.

Fredlund, D.G., Stone, J., Stianson, J., and Sedgwick, A. 2011. Determination of water storage and permeability functions for oil sands tailings. In Proceedings of the Tailings and Mine Waste Conference, Vancouver, B.C.

Fredlund, D. G., Rahardjo, H., and Fredlund, M. D. (2012) Unsaturated soil mechanics in engineering practice. John Wiley & Sons, New York.

Fredlund, D. G., and Zhang, F. (2013) Combination of shrinkage curve and soil-water characteristic curves for soils that undergo volume change as soil suction is increased. Proceedings of the 18th International Conference on Soil Mechanics and Geotechnical Engineering, Paris 2013.

Fredlund, M. D. (2000) The role of unsaturated soil property functions in the practice of unsaturated soil mechanics. Dissertation, University of Saskatchewan.

Gardner, W. R. (1958) Some steady-state solutions of the unsaturated moisture flow equation with application to evaporation from a water table. Soil science, 85(4): 228-232.

Gardner, W. R. (1974) The permeability problem. Soil Science, 117(5): 243-249.

Groenevelt, P. H., and Grant, C. D. (2004) A new model for the soil-water retention curve that solves the problem of residual water contents. European Journal of Soil Science, 55(3): 479-485.

Haines, W. B. (1923) The volume-changes associated with variations of water content in soil. The Journal of agricultural science, 13(03): 296-310.

Huang, S., Barbour, S. L., and Fredlund, D. G. (1998) Development and verification of a coefficient of permeability function for a deformable unsaturated soil. Canadian Geotechnical Journal, 35(3): 411-425.

Keen, B. A. (1931) The physical properties of the soil. Longmans, Green.

Kim, D. J., Vereecken, H., Feyen, J., Boels, D., and Bronswijk, J. J. B. 1992. On the characterization of properties of an unripe marine clay soil: I. Shrinkage processes of an unripe marine clay soil in relation to physical ripening, Soil Science, 153(6): 471-481.

Kosugi, K. I. (1994) Three-parameter lognormal distribution model for soil water retention. Water Resources Research, 30(4): 891-901.

Laliberte, G. E. (1969) A mathematical function for describing capillary pressure-desaturation data. Hydrological Sciences Journal, 14(2): 131-149.

Leong, E. C., and Rahardjo, H. (1997) Permeability functions for unsaturated soils. Journal of Geotechnical and Geoenvironmental Engineering, 123(12): 1118-1126.

Marinho, F. A. M. (1994). Shrinkage behaviour of some plastic soils. Doctoral dissertation, University of London, UK.

Mbonimpa, M., Aubertin, M., Maqsoud, A., and Bussière, B. 2006. Predictive model for the water retention curve of deformable clayey soils. Journal of Geotechnical and Geoenvironmental Engineering, 132(9): 1121-1132.

McKee, C. R., Bumb, A. C. (1984) The importance of unsaturated flow parameters in designing a hazardous waste site. In Hazardous Waste and Environmental Emergencies, Hazardous Materials Control Research Institute National Conference, Houston, Texas, pp. 12-14.

McKee, C. R., and Bumb, A. C. (1987) Flow-testing coalbed methane production wells in the presence of water and gas. SPE formation Evaluation, 2(04): 599-608.

Mualem, Y. (1976) A new model for predicting the hydraulic conductivity of unsaturated porous media. Water Resources Research, 12(3): 513-522.

Mualem, Y., and Klute, A. 1986. Hydraulic conductivity of unsaturated soils: prediction and formulas. In Methods of soils analysis. Part 1. Physical and mineralogical methods. pp. 799–823.

Pachepsky, Y. A., Shcherbakov, R. A. and Korsunskaya, L. P. (1995) Scaling of soil water retention using a fractal model. Soil Science, 159(2): 99-104.

Parent, S. E., Cabral, A., and Zornberg, J. G. (2007). Water retention curve and hydraulic conductivity function of highly compressible materials. Canadian Geotechnical Journal, 44(10): 1200-1214

Pereira, J. H., and Fredlund, D. G. (2000) Volume change behavior of collapsible compacted gneiss soil. Journal of geotechnical and geo-environmental engineering, 126(10): 907-916.

Pham, H. Q., and Fredlund, D. G. (2008) Equations for the entire soil-water characteristic curve of a volume change soil. Canadian geotechnical journal,45(4): 443-453.

Rahimi, A., Rahardjo, H., and Leong, E.C. 2015. Effects of soil–water characteristic curve and relative permeability equations on estimation of unsaturated permeability function. Soils and Foundations, 55(6): 1400-1411.

Russo, D. (1988) Determining soil hydraulic properties by parameter estimation: On the selection of a model for the hydraulic properties, Water Resources Research, 24(3): 453-459.

Somogyi, F. (1980) Large-strain consolidation of fine-grained slurries. Proceedings of the Canadian Society for Civil Engineering 1980 Annual Conference, Winnipeg, Manitoba, Canada.

Sridharan, A., and Rao, G. V. (1971) Effective stress theory of shrinkage phenomena. Canadian Geotechnical Journal, 8(4): 503-513.

Stirk, G. B. (1954) Some aspects of soil shrinkage and the effect of cracking upon water entry into the soil. Crop and Pasture Science, 5(2): 279-296.

Taylor, D. W. (1948) Fundamentals of soil mechanics. J. Wiley & Sons; London: Chapman & Hall.

Tempany, H. A. (1917) The shrinkage of soils. The Journal of Agricultural Science, 8(03): 312-330.

Terzaghi, K. (1925) Principles of soil mechanics, IV -- Settlement and consolidation of clay. Engineering News-Record, 95(3): 874-878.

Tripathy, S., Tadza, M. Y. M., and Thomas, H. R. 2014. Soil-water characteristic curves of clays. Canadian Geotechnical Journal, 51(8): 869-883.

Van Genuchten, M. T. (1980) A closed-form equation for predicting the hydraulic conductivity of unsaturated soils. Soil science society of America journal, 44(5): 892-898.

Vanapalli, S.K., Sillers, W.S., and Fredlund, M.D. (1998) The meaning and relevance of residual state to unsaturated soils. Proceedings of the 51st Canadian Geotechnical Conference, Edmonton, AB, October 4-7, pp.1-8.

Williams, P.J. 1982. The surface of the Earth, an introduction to geotechnical science. Longman Inc., New York.

Zhang, F. (2010) Soil water retention and relative permeability for full range of saturation (No. PNNL-19800). Pacific Northwest National Laboratory (PNNL), Richard, WA (US).

Zhang, F., Fredlund, D. G., Wilson, G. W., and Sedgwick, A. (2014) Determination of the permeability function for drying oil sands tailings undergoing volume change and desaturation. Proceedings of the 4th International Oil Sands Tailings Conference, Banff, A.B. 2014.

Zhang, F. and Fredlund, D. G. (2015) Examination of the estimation of relative permeability for unsaturated soils. Canadian Geotechnical Journal, Published on the web 3 June 2015, 10. 1139/cgj-2015-0043.

Zhang, L., and Chen, Q. 2005. Predicting bimodal soil–water characteristic curves. Journal of Geotechnical and Geoenvironmental Engineering, 131(5): 666-670.

Appendixes

Appendix 1 Combination of shrinkage curve and soil-water characteristic curves for soils that undergo volume change as soil suction is increased

ABSTRACT: The soil-water characteristic curve, SWCC, is commonly used for the estimation of unsaturated soil property functions, USPF, in geotechnical engineering practice. The indiscriminate usage of the SWCC during the estimation of unsaturated soil property functions can lead to erroneous analytical results and poor engineering judgment. Essentially all the existed estimation procedures for unsaturated soil property functions, USPFs, are based on the assumption that the soil will not undergo volume change as soil suction is increased. Such an assumption places a limitation on the application of the current USPFs to high volume change soils, where volume changes cannot be neglected. The evaluation of the correct air-entry value has a significant effect on the estimation of subsequent USPFs. This paper describes how the SWCC laboratory results can be properly interpreted with the assistance of a shrinkage curve. Laboratory data sets are then used to illustrate how the test data should be interpreted for high volume change soils.

INTRODUCTION

The soil-water characteristic curve, SWCC, provides vital information for applying unsaturated soil mechanics in engineering practice. Much of the information regarding the use of SWCC originated in soil physics and agriculture-related disciplines. With time, information regarding the use of the SWCC has been embraced for geotechnical engineering applications (Fredlund, 2002; Fredlund and Rahardjo, 1993).

Some of the concepts and measurement procedures for determining the relationship between the amount of water in a soil and soil suction (i.e., SWCC) are now being re-evaluated to assess the acceptability of the estimation procedures for geotechnical engineering applications. Some differences between the goals to be achieved in agriculture-related disciplines and the goals of geotechnical engineering have been observed. Agriculture-related disciplines are mainly interested in water storage while geotechnical engineers are mainly interested in the use of the SWCC for the estimation of water permeability. Geotechnical engineers are now faced with the need to assess in greater detail various aspects of the application of the SWCC. One of the areas requiring further study for geotechnical engineering is highlighted in this paper; namely, the effect of volume change during soil suction increase, on the estimation of the permeability function. This paper illustrates how shrinkage curves can be used to more properly interpret the SWCCs, thus more reliably estimating the permeability function fora soil.

A common situation where large volume changes occur in the soil as soil suction is increased, involves the drying of initially wet or slurry materials. Sludge material and slurry material may be deposited at water contents above the liquid limit of the material. The material is deposited in ponds and allowed to dry in order to increase its shear strength. The geotechnical engineer may be called upon to undertake numerical modelling simulations of the drying process.

SIGMOIDAL EQUATIONS FOR SWCCS

There are several sigmoidal type equations that have been proposed to mathematically describe the relationship between water content and soil suction relationship (e.g., van Genuchten, 1980; Fredlund and Xing, 1994). The S-shaped sigmoidal equations have the appearance of being able to fit SWCC data regardless of the measure that is used to represent the amount of water in the soil (e.g., gravimetric water content, volumetric water content, or degree of saturation). The sigmoidal equations have a limitation in the extremely low suction range and the extremely high suction range. Although the shortcomings of the sigmoidal equations, their usage has never theless become prevalent in unsaturated soil mechanics.

The Fredlund and Xing, (FX), (1994) SWCC equation can be used to illustrate the usage of a sigmoidal equation for various designations of water content. The FX (1994) equation uses a correction factor that allows all SWCCs to go to zero water content as soil suction goes to 1,000,000 kPa. Laboratory measured SWCC data can be plotted as a relationship between gravimetric water content and soil suction. The Fredlund and Xing (1994) equation is first written in terms of gravimetric water content and can then be used to best-fit the SWCC.

$$w(\psi) = w_s\left(1 - \frac{\ln\left(1+\frac{\psi}{h_r}\right)}{\ln\left(1+\frac{10^6}{h_r}\right)}\right)\left(\frac{1}{\left(\ln\left(\exp(1)+\left(\frac{\psi}{a_f}\right)^{n_f}\right)\right)^{m_f}}\right) \quad \text{[A1]}$$

where: $w(\psi)$ = gravimetric water content at any specified suction, ψ; w_s = saturated gravimetric water content; h_r = residual soil suction; a_f , n_f , and m_f = the fitting parameters for the SWCC equation. Then, the gravimetric water content SWCC can be used in conjunction with a shrinkage curve to compute the degree of saturation versus soil suction SWCC and the volumetric water content versus soil suction SWCC, thus more accurately interpreting the parameters required for the estimation of unsaturated soil property functions.

The volumetric water content versus soil suction SWCC is required to obtain the water storage coefficient for the soil. The volumetric water content must be related to the instantaneous overall volume of the soil mass in order to obtain the correct value for numerical modelling purposes. Volume change of the overall soil specimen can be taken into consideration if a “shrinkage curve” is measured. The shrinkage curve is generally measured under conditions of zero net normal stress.

USE OF A SHRINKAGE CURVE

The shrinkage limit of a soil has been one of the classification properties in soil mechanics (ASTM D427). The shrinkage limit is defined as the water content corresponding to a saturated specimen at the void ratio achieved (minimum volume) upon drying to zero water content. The entire shrinkage curve, (i.e., the plot of total volume (or void ratio) versus gravimetric water content), from an initially saturated soil condition to completely oven-dry conditions is of value for the interpretation of SWCC data.

As saturated clay soil dries, a point is reached where the soil starts to desaturate. This point is called the air-entry value and is generally near the plastic limit of the soil. Upon further drying, another point is reached where the soil dries without significant further change in overall volume.

The corresponding gravimetric water content appears to be close to residual water content.

The shrinkage curve can be experimentally measured from initially high water content conditions to completely dry conditions. A digital micrometer can be used for the measurement of the volume at various stages of drying as shown in Figure A-1. Brass rings can be machined to contain the soil specimens (i.e., the rings have no bottom). The rings with the soil are placed onto wax paper and dried through evaporation. The dimensions of the soil specimens are appropriately selected such that cracking of the soil is unlikely to occur during the drying process. The initial dimensions selected for the shrinkage curve specimens used in this study were a diameter of 3.7 cm and a thickness of 1.2 cm.

The mass and volume of each soil specimen can be measured once or twice per day. Four to six measurements of the diameter and thickness of the specimen were made at differing locations on the specimens. It has been observed that as the specimen diameter begins to decrease, with the specimen pulling away from the brass ring and the rate of evaporation increases.

Figure A-1. Digital micrometer used for the measurement of the diameter and thickness of shrinkage specimens.

The "shrinkage curve" can be best-fit using the hyperbolic curve proposed by Fredlund et al., (1996, 2002). The equation has parameters with physical meaning and is of the following form:

$$e(w) = a_{sh}\left(\left(\frac{w}{b_{sh}}\right)^{c_{sh}} + 1\right)^{\frac{1}{c_{sh}}} \qquad \text{[A2]}$$

where: a_{sh} = the minimum void ratio (e_{min}), b_{sh} = slope of the line of tangency, (e.g., = e / w when drying from saturated conditions), c_{sh} = curvature of the shrinkage curve, w = gravimetric water content, G_s = specific gravity and S = degree of saturation.

Once the minimum void ratio of the soil is known, it is possible to estimate the remaining parameters required for the designation of the shrinkage curve. The minimum void ratio the soil can attain is defined by the variable, a_{sh}. The b_{sh} parameter provides the remaining shape of the shrinkage curve. The curvature of the shrinkage curve commences around the point of desaturation is controlled by the c_{sh} parameter.

OTHER DESIGNATIONS OF SWCC

Degree of saturation

The basic volume-mass relationship relates the degree of saturation, gravimetric water content and void ratio, shown as:

$$S = \frac{w\,G_s}{e} \qquad \text{[A3]}$$

As the shrinkage curve indicates, the void ratio is a function of gravimetric water content. Therefore, the degree of saturation can be further written as a function of gravimetric water content by substituting Eq. [A2] into Eq. [A3]. We have

$$S(w) = \frac{w\,G_s}{a_{sh}\left(\left(\frac{w}{b_{sh}}\right)^{c_{sh}} + 1\right)^{\frac{1}{c_{sh}}}} \qquad \text{[A4]}$$

The gravimetric water content is a function of soil suction as the gravimetric water content SWCC depicts. The degree of saturation can also be written as a function of soil suction with the fitting parameters for both the gravimetric water content SWCC and the shrinkage curve by substituting Eq. [A1] into Eq. [A4], as follows.

$$S(w)=\frac{w_s G_s C_r(\psi)}{a_{sh}\left(\ln\left(\exp(1)+\left(\frac{\psi}{a_f}\right)^{n_f}\right)\right)^{m_f}\left(\left(\frac{w_s C_r(\psi)}{b_{sh}\left(\ln\left(\exp(1)+\left(\frac{\psi}{a_f}\right)^{n_f}\right)\right)^{m_f}}\right)^{c_{sh}}+1\right)^{\frac{1}{c_{sh}}}} \quad \text{[A5]}$$

Volumetric water content (Instantaneous Volume)

It is the instantaneous volumetric water content versus soil suction SWCC that is required to obtain the correct water storage coefficient for the soil for numerical modelling purposes. The instantaneous volumetric water content can be computed as follows.

$$\theta=\frac{S\,e}{1+e} \quad \text{[A6]}$$

By combining Eqs. [A2)], [A3] and [A6], the volumetric water content can be written in terms of gravimetric water content with fitting parameters for corresponding shrinkage curve, which is indeed a function of soil suction.

$$\theta(\psi)=\frac{w(\psi)G_s}{1+a_{sh}\left(\left(\frac{w(\psi)}{b_{sh}}\right)^{c_{sh}}+1\right)^{\frac{1}{c_{sh}}}} \quad \text{[A7]}$$

Volumetric water content (Initial Volume)

It is possible to write the volumetric water content referenced to the initial volume of the soil; however, it should be noted that this designation has little or no value in unsaturated soil mechanics. Only under conditions of no volume change during suction change does the equation become equal to the instantaneous volumetric water content SWCC.

$$\theta(\psi) = \frac{w(\psi) G_s}{1 + e_0} \qquad \text{[A8]}$$

RESULTS ON REGINA CLAY

The effect of volume change on the interpretation of SWCCs was studied for Regina clay. The laboratory test results are presented and show the significant effect of overall volume change on the interpretation of the SWCC.

Regina clay had a liquid limit of 75%, a plastic limit of 25% and contained 50% clay size particles. The material was prepared as slurry and then subjected to various consolidation pressures under one-dimensional loading. After the applied load was removed, the soil specimens were subjected to various applied matric suction values. High suction values were applied through equalization in a constant relative humidity environment.

The experimental results demonstrated that the break in curvature, as soil suction increases, determined from the degree of saturation SWCC remained a constant value for a soil pre-consolidated under different pressures. Such a constant break determined from the degree of saturation SWCC can be defined as the correct air-entry value, AEV, for a soil. The AEV for Regina clay remained constant around 2500 kPa. An empirical construction procedure involving the intersection of two straight lines on a semi-log plot was used to determine a single number associated with the break in curvature (Vanapalli et al, 1999).

The breaks on the SWCCs of the other water content designations for a soil change as the pre-consolidation pressure changes. The “w Break” on the gravimetric water content SWCCs were then compared to the air-entry value for the soil. The ratio of AEV to w Break was used as a measure of the effect of volume change on the interpretation of the correct air-entry value for the soil.

Shrinkage curves and soil-water characteristic curves were measured on Regina clay. Slurry Regina clay was prepared at a gravimetric water content slightly above its liquid limit. The shrinkage curve results are presented in Figure A-2. The void ratio of Regina clay decreases as water evaporates from the soil surface. The clay begins to desaturate near its plastic limit. The best-fit parameters for the shrinkage curve are a_{sh} = 0.48, b_{sh} = 0.17, and c_{sh} = 3.30. The specific gravity of the soil was 2.73.

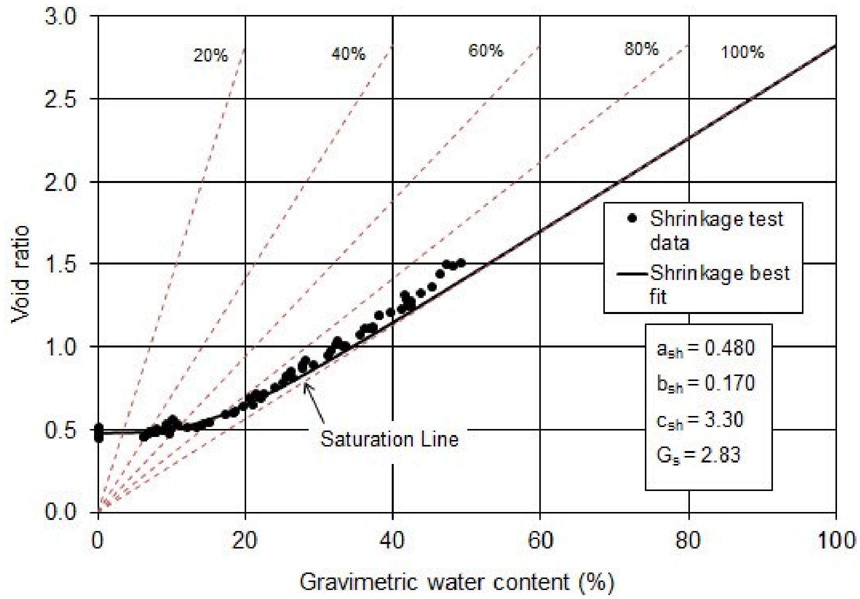

Figure A-2. Shrinkage curve for several samples of Regina clay.

Figure A-3 shows the gravimetric water content, w, plotted versus soil suction for Regina clay was preloaded at 196 kPa. Its initial water content was 53.5%. The high water content specimen showed that a gradual break or change in curvature around 50 kPa. The curvature is not distinct and does not represent the true air-entry value of the material. The gravimetric water content SWCC was best-fit with the Fredlund and Xing (1994) equation and yielded the following parameters; that is, a_f = 140 kPa, n_f = 0.87, and m_f = 0.72. Residual suction was estimated to be around 200,000 kPa. It is necessary to use the shrinkage curve to calculate other volume-mass soil properties and properly interpret the SWCC results for the true AEV.

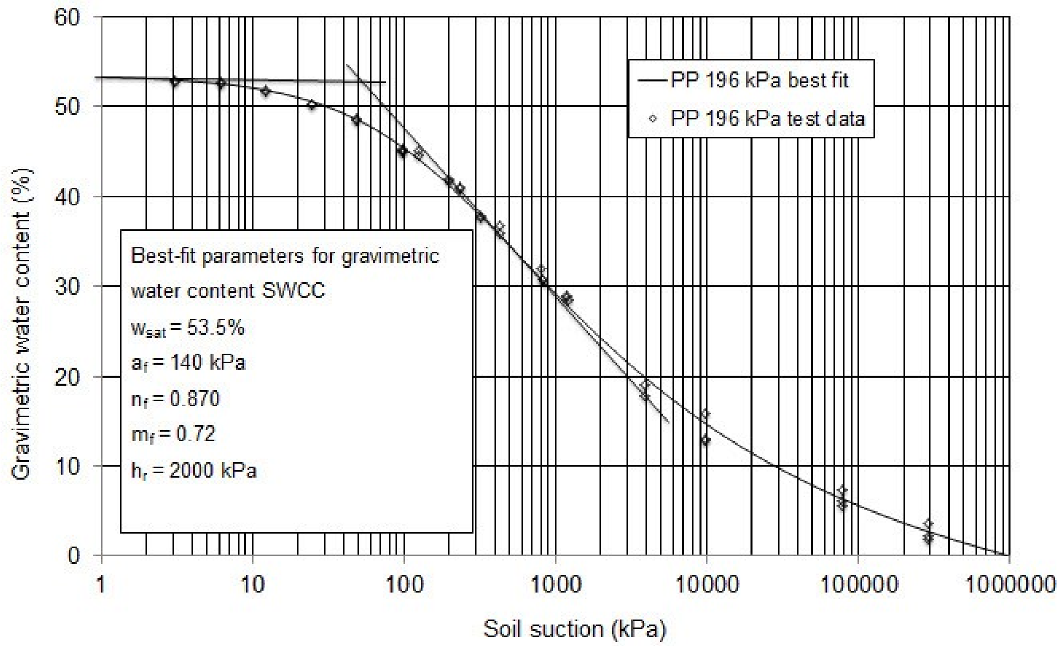

Figure A-3. Gravimetric water content versus soil suction for Regina clay preconsolidated to 196 kPa.

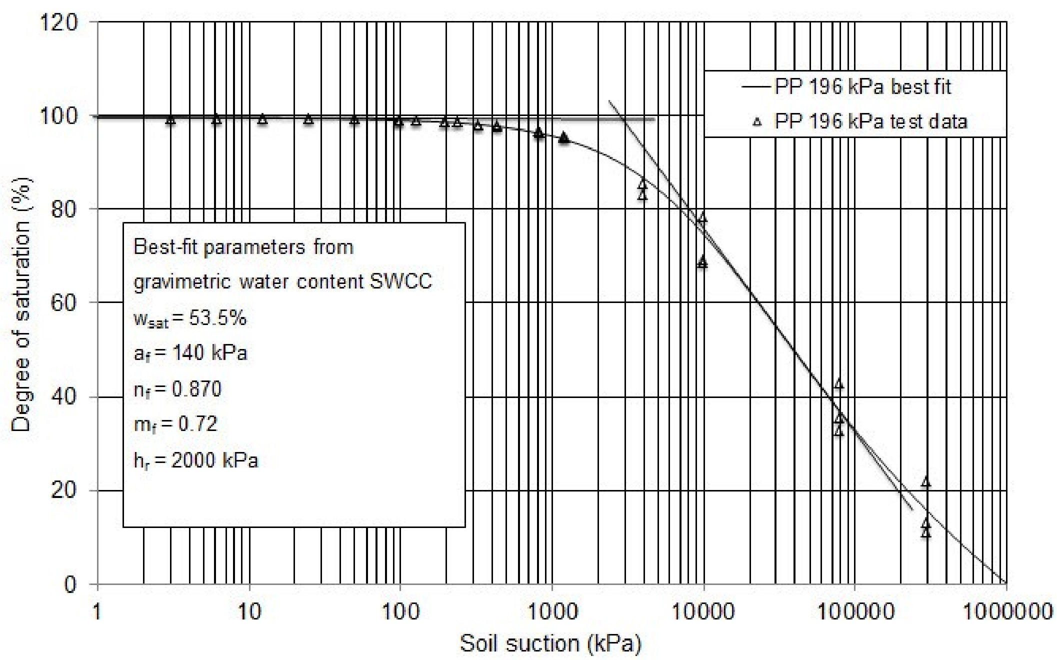

Figure A-4. Degree of saturation versus soil suction for Regina clay preconsolidated to 196 kPa.

The best-fit shrinkage curve equation can be combined with the Fredlund and Xing (1994) equation to obtain the SWCCs of other water content designations. The resulting plot of degree of saturation, *S*, versus soil suction is shown in Figure A-4. The results show that there is a distinct air-entry value for Regina clay that is about 2,500 kPa. The true air-entry value was also found to be the same for all Regina clay samples preconsolidated at differing pressure values. It is more correct to use the degree of saturation SWCCs for the estimation of the AEV of the soil and subsequently the calculation of the unsaturated hydraulic conductivity function. The degree of saturation also indicates that residual condition can be more clearly identified as being at a suction of about 200,000 kPa and a residual degree of saturation of about 20 percent.

Several other SWCC tests were performed on the Regina clay; each test starting with soil that had been preconsolidated from slurry to differing applied pressures. Figure A-5 shows the gravimetric water content versus soil suction plot for a soil preconsolidated to 6.125 kPa. The Fredlund and Xing (1994) fitting parameters are a_f = 18.0 kPa, n_f = 0.88, m_f = 0.76 and h_r = 800 kPa. The degree of saturation SWCC is the same as shown in Figure A-4.

Figure A-6 shows the gravimetric water content versus soil suction plot for a soil preconsolidated to 49.0 kPa. The Fredlund and Xing (1994) fitting parameters are a_f = 90.0 kPa, n_f = 1.10, m_f = 0.70 and h_r = 2000 kPa. Figure A-7 shows the gravimetric water content versus soil suction plot for Regina clay preconsolidated to the highest pressure of 392 kPa. The Fredlund and Xing (1994) fitting parameters are a_f = 120.0 kPa, n_f = 0.84, m_f = 0.70 and h_r = 2000 kPa.

The measured SWCCs for Regina clay show that the measurement of the gravimetric water content SWCC and the shrinkage curve for a soil are all that is required to obtain an approximation of the volume-mass versus soil suction relationships when the applied net normal stress is zero. The procedure that should be used for the interpretation of the laboratory data has also been described.

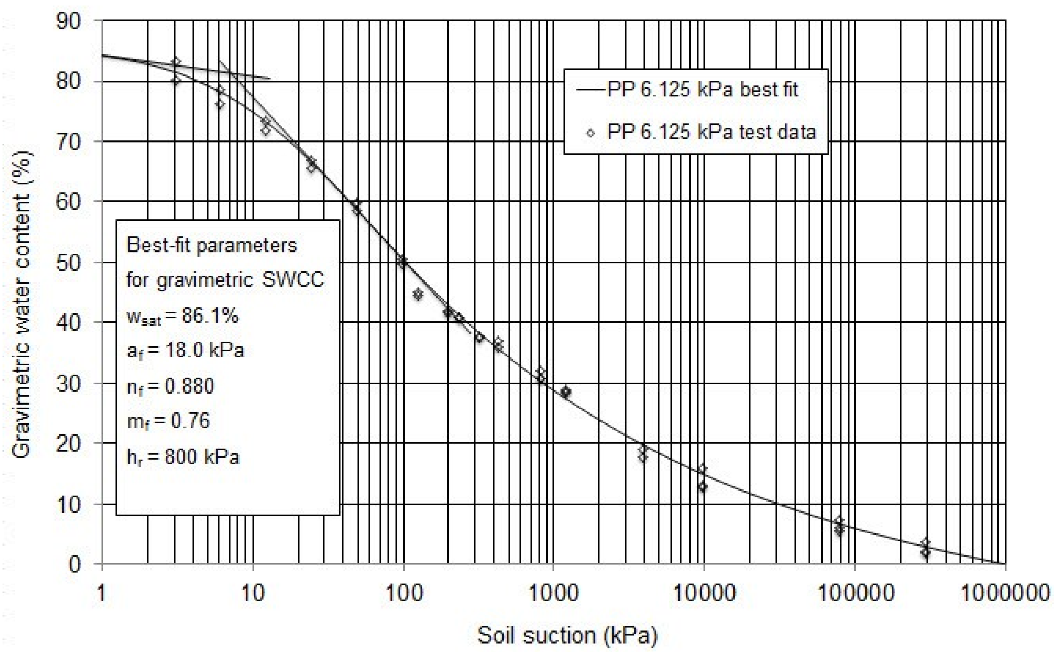

Figure A-5. Gravimetric water content versus soil suction for Regina clay preconsolidated to 6.125 kPa.

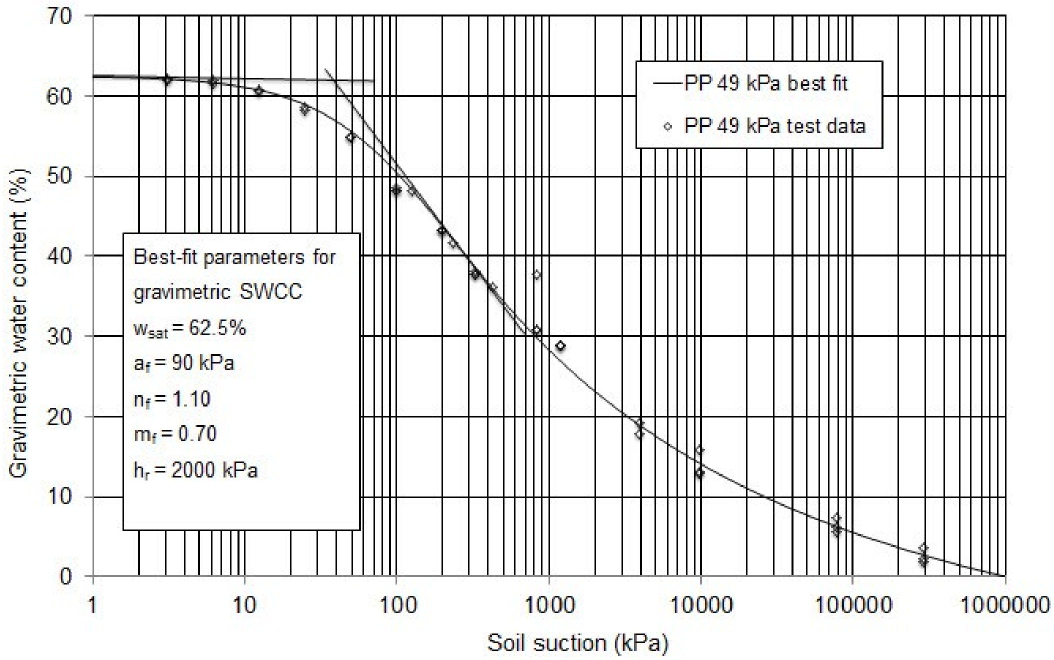

Figure A-6. Gravimetric water content versus soil suction for Regina clay preconsolidated to 49 kPa.

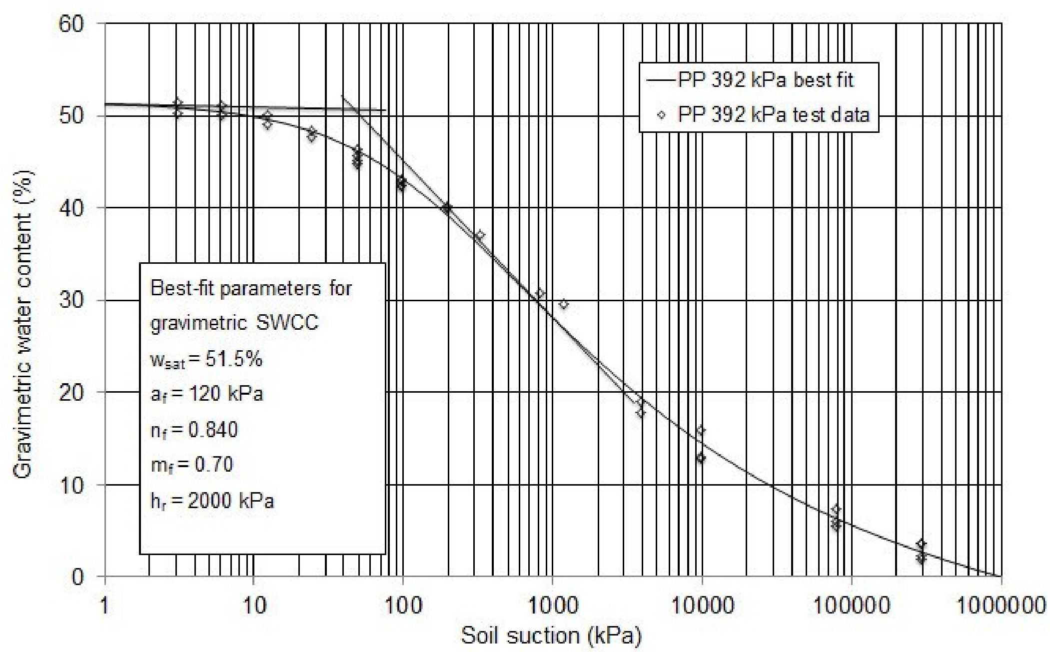

Figure A-7. Gravimetric water content versus soil suction for Regina clay preconsolidated to 392 kPa.

INTERPRETATION OF THE REGINA CLAY RESULTS

The difference between the break in the gravimetric water content SWCC and the true AEV for Regina clay is expressed as [AEV/(Break in curvature on *w*-SWCC)]. The volume change of the soil is once again expressed as the change in void ratio, Δe, divided by $(1 + e_0)$, where e_0 is the minimum void ratio the soil will achieve as the soil is oven-dried, and all void ratio values are determined from the shrinkage curve.

The horizontal axis of Figure A-8 shows that the Regina clay soil specimens changed in volume by 65% to 150% as soil suction was increased to residual suction conditions. At 70% volume change, the true AEV is 60 times larger than the break in curvature indicated by the gravimetric water content SWCC. Also at 120% volume change, the true AEV is 129 times larger than the break in curvature indicated by the gravimetric water content SWCC. The laboratory test results clearly indicate the significant influence that volume change as soil suction increases has on the interpretation of the data.

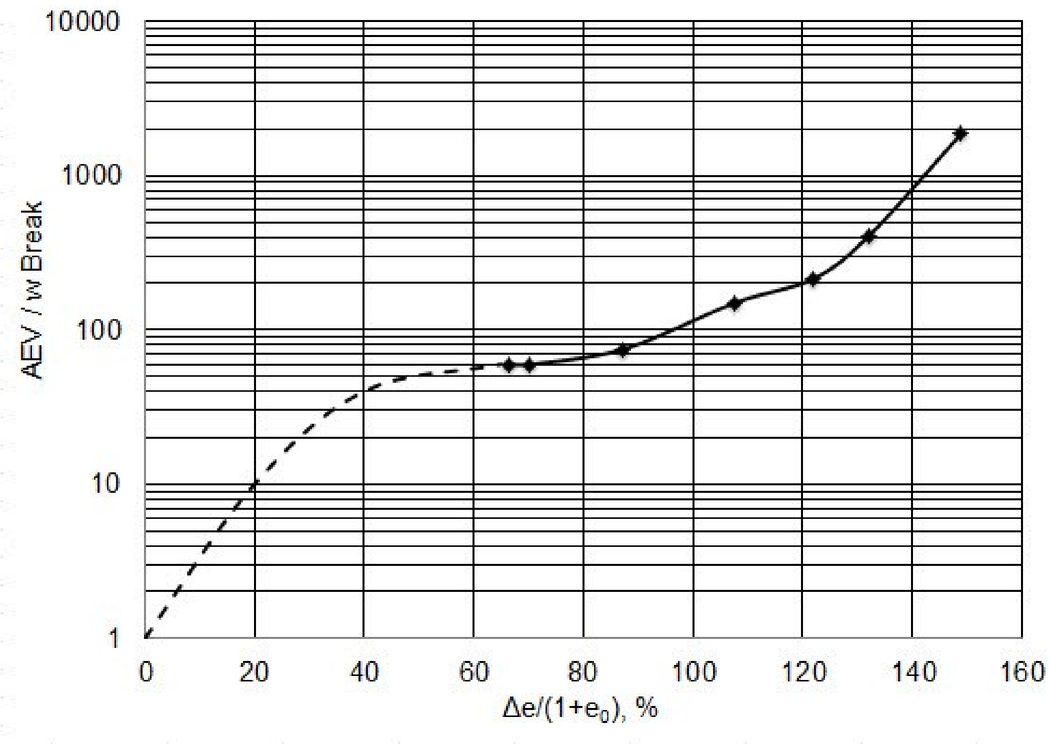

Figure A-8. Difference between the break in the gravimetric water content SWCC and the Air-Entry Value for Regina clay.

The laboratory SWCC test results on Regina clay illustrate the need to separate gravimetric water content SWCC into two components. Part of the change in water content is due to a change in volume while the soil remains saturated. The other part of the change in water content is associated with a change in degree of saturation.

The proposed estimation procedure based on the SWCC and the saturated hydraulic conductivity makes the assumption that the reduction in hydraulic conductivity with suction is due to desaturation of the soil (Fredlund et al. 1994). In other words, it is primarily the increase in tortuosity upon desaturation of the soil that causes the reduction in permeability. Therefore, it is the degree of saturation SWCC that should be used to estimate the reduction in hydraulic conductivity as suction is increased beyond the air entry value, AEV, of the soil.

Prior to reaching the AEV of the soil, volume change due to an increase in suction needs to be accommodated in an independent manner. In other words, a change in gravimetric water content due to a suction change prior to the AEV needs to be visualized as the result of a change in void ratio. Taylor (1948) suggested that the coefficient of permeability of a sand was proportional to $[e^3 /(1 + e)]$ where e is void ratio. While the proportionality was proposed and verified for sands, there has also been evidence that it might also be a reasonable approximation for silt and clay soils. Therefore, changes in the hydraulic conductivity (due to volume change), prior to the AEV of a soil, should be approximated in terms of a change in void ratio.

The estimation of the permeability function with respect to a change in suction can now be considered as having two components; one component due to a change in void ratio and the other component due to a change in the degree of saturation. Further research should be undertaken to verify that the unsaturated soil property functions can indeed be estimated for all types of material by using the interpretation procedure suggested in this paper.

CONCLUSIUONS AND RECOMMENDATIONS

Changes in the volume of the soil specimens as soil suction is increased can significantly affect the unsaturated soil properties. The effects of volume change are shown to be significant, resulting in erroneous calculations of the permeability function for a soil. Therefore, the way of the interpretation of the SWCC should be adjusted to get correct information from the SWCCs. This paper presents a procedure that can be used to independently consider the effects of volume change (where the soil remains saturated) from the desaturation of the soil specimen.

LIST OF REFERENCES

Fredlund, D. G., 1964. Comparison of soil suction and one-dimensional consolidation characteristics of a highly plastic clay. National Research Council of Canada, Division of Building Research, Technical Report No. 245, Ottawa, Ontario, Canada.

Fredlund, D. G. 2002. Use of soil-water characteristic curve in the implementation of unsaturated soil mechanics. UNSAT 2002, Proceedings of the Third International Conference on Unsaturated Soils, Recife, Brazil, March 10-13, pp. 887-904.

Fredlund, M. D., Wilson, G. W., and Fredlund, D. G. 2002. Representation and estimation of the shrinkage curve. UNSAT 2002, Proceedings of the Third International Conference on Unsaturated Soils, Recife, Brazil, March 10-13, pp. 145-149.

Fredlund, D. G., and Rahardjo, H. 1993. Soil Mechanics for UnsaturatedSoils. John Wiley and Sons, New York, N.Y.

Fredlund, D. G. and Xing, A. 1994. Equations for the soil-water characteristic curve. Canadian Geotechnical Journal, 31(3): 521-532.

Fredlund, D. G., Xing, A., and Huang, S. Y. 1994. Predicting the permeability function for unsaturated soils using the soil-water characteristic curve, Canadian Geotechnical Journal, Vol. 31, No. 4, pp. 533-546.

Taylor, D. W. 1948. Fundamentals of Soil Mechanics, John Wiley & Sons, New York, N.Y.

van Genuchten, M. T. 1980. A closed-form equation for predicting the hydraulic conductivity of unsaturated soils. Soil Science Society of America Journal, Vol. 44, pp. 892-898.

Appendix 2. Determination of the permeability function for drying oil sands tailings undergoing volume change and desaturation

ABSTRACT

The coefficient of permeability function is one of the soil properties required for numerical modeling of transient seepage problems. Inaccuracies in the estimation of the coefficient of permeability can lead to erroneous numerical modeling results and can significantly affect subsequent engineering decisions. Both the degree of saturation and void ratio are factors that influence the coefficient of permeability. Methodologies presently available estimating the coefficient of permeability for an unsaturated soil are based on an assumption that no volume change occurs when soil suction is changed. In other words, consideration is only given to the influence of changes in degree of saturation. Conventional estimation techniques produce reasonable results when estimating the coefficient of permeability for unsaturated soils with low compressibility such as sands or silts, but the analysis protocols require changes when predicting the coefficient of permeability for materials that undergo volume change as soil suction changes, (e.g., Oil Sands tailings slurry). This means that the void ratio changes need to be considered as well as changes in degree of saturation. This paper presents a revised estimation procedure that considers the controlling factors of both volume change and desaturation.

INTRODUCTION

The oil sands bitumen extraction process in northern Alberta produces large volumes of high water content tailings composed of sand, silt, clay, and a small amount of unrecovered bitumen. When discharged into the tailings pond, the extraction tailings segregate with the sand plus about one-half of the fines dropping out to form dykes and beaches. The remaining water, bitumen, and fines flow into the tailings pond as Thin Fine Tailings (TFT) at approximately 8% solids content (BGC Engineering Inc., 2010). The fines settle to 20% solids content in a few months and to 30%-35% solids content in a few years. Upon reaching a solids content of 30%, the fine tailings are referred to as Mature Fine Tailings (MFT). MFT remains in a slurry state for decades and may take many years for self-weight consolidation because of its low water release rate (FTFC, 1995).

Significant portions of the fines remain in suspension after deposition resulting in a tailings management challenge for the industry. Different processes and technologies have been suggested to improve the water release characteristics of tailings. A more advanced disposal methodology named Fines-Sand Mixture Tailings (FSMT) has been developed and applied to improve the dewatering behavior of MFT. Composite/consolidated tailings (CT), thickened tailings, non-segregating tailings, and MFT-sand-overburden mixtures are four different FSMT disposal opinions that have been considered for treating Oil Sands Tailings (Sobkowicz & Morgenstern, 2009; BGC Engineering Inc., 2010). Sorta (2013) investigated the fundamental geotechnical behavior of FSMT at various SFRs including the relationships between Atterberg limits and clay content. The preliminary design of the tailings disposal often involves the numerical modeling of the dewatering behavior of FSMT at various SFRs. The correct numerical modeling of the dewatering behavior requires an appropriate coefficient of permeability function and a proper water storage function.

Both the void ratio and the degree of saturation are factors that influence the coefficient of permeability. Historically, the study of the coefficient of permeability for a soil has been categorized into two groups, namely, saturated coefficient of permeability and unsaturated coefficient of permeability. Saturated coefficient of permeability for most soils is a constant and thus measured experimentally. For a saturated soil that changes volume, the saturated coefficient of permeability becomes a function of the changing void ratio (Taylor, 1948; Chapuis, 2012). In unsaturated soil mechanics, the methods present in the existing literature for estimating the coefficient of permeability for an unsaturated soil is based on an assumption that no volume change occurs as soil suction is changed, considering only the influence of the degree of saturation. Van Genuchten-Burdine equation (1980), van Genuchten-Mualem equation (1980) and Fredlund, Xing and Huang (1994) permeability function are three well-known unsaturated coefficient of permeability functions. These conventional methods produce reasonable estimations for the coefficient of permeability functions for either unsaturated soils with no volume changes or saturated soils with volume changes. FSMT has been found to be a typical soil that undergoes volume change as soil suction is increased during a drying process. In other words, neither a conventional unsaturated coefficient of permeability function nor a saturated coefficient of permeability function can mathematically describe the coefficient of permeability function of FSMT that undergoes a drying process featured by both desaturation and volume change. Both the void ratio and the degree of saturation must be considered when estimating the coefficient of permeability function for a drying FSMT.

This paper presents a revised methodology for the estimation of the coefficient of permeability function for soils that undergo volume change as soil suction is changed (e.g., Oil Sands tailings). Both the void ratio and the degree of saturation are taken into account as two influencing factors. Experimental data for Total tested thickened tailings are used to illustrate and explain the new estimation method.

CONCEPTUAL THEORY

Oil Sands tailings are a typical material that undergoes volume change as soil suction changes during a drying process. The drying process of such materials is complicated by the fact that both volume change and desaturation can occur during an increase in suction. The entire drying process can conceptually be divided into three stages. The first stage is within a suction range from zero suction up to the air-entry value (AEV) of the material. The AEV of the material (i.e., bubbling pressure) is the matric suction where air starts to enter the largest pores in the soil (Fredlund and Xing, 1994). The soil undergoes volume change with no desaturation during the first stage. During stage 1, the void ratio is the only factor controlling the coefficient of permeability of the material. In other words, the coefficient of permeability for a soil at the first stage is really the saturated coefficient of permeability changing with soil suction because of the changing void ratio that occurs with changing soil suction. The soil remains saturated as soil suction increases from zero to its AEV. Once the AEV is reached and exceeded, desaturation commences featuring the beginning of the second stage. The second stage of the drying process starts at the AEV and ends at a point where no further volume change occurs as desaturation continues with increasing soil suction. During the second stage, both volume change and desaturation impact the coefficient of permeability of the material.

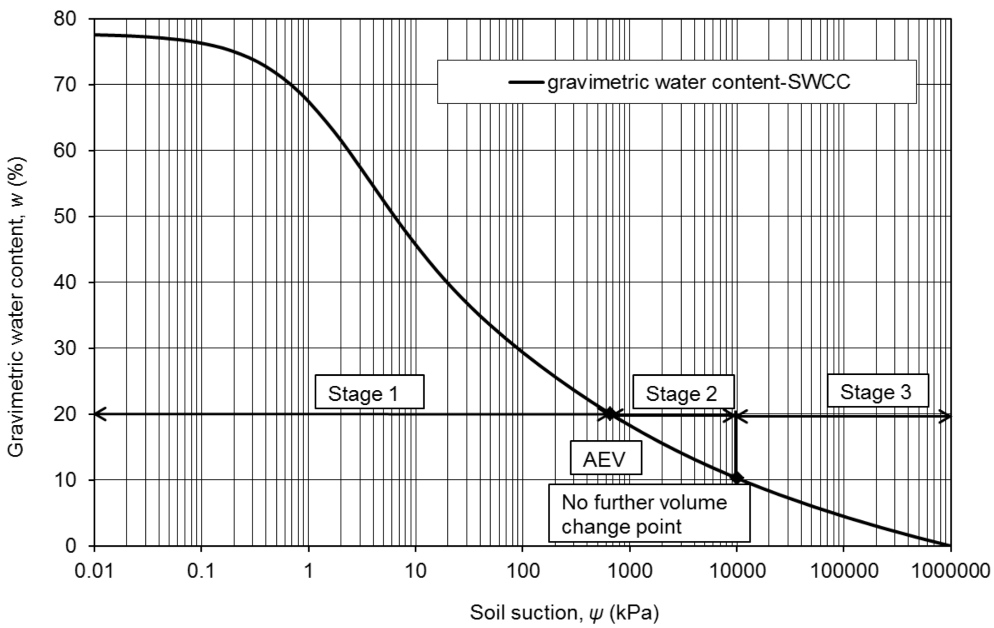

Figure A-9. Conceptual plot showing three stages distinguished on the *w*-SWCC of a typical high volume change material.

At the end of the second stage, the third stage starts from the no-further-volume-change point and lasts until the zero water content point is approached. The coefficient of permeability for the soil at this stage is influenced by the degree of saturation.

The total suction corresponding to zero water content appears to be essentially the same for all types of materials. All materials become completely dry at a suction of approximately 106 kPa (Fredlund and Xing, 1994). Figure A-9 is a conceptual plot showing the three stages distinguished for the *w*-SWCC (i.e., gravimetric water content SWCC) of a typical high volume change soil. The true air-entry value (AEV) should be determined from *S*-SWCC (i.e., degree of saturation SWCC).

ESTIMATION OF COEFFICIENT OF PERMEABILITY FUNCTION

Degree of saturation and void ratio are two controlling factors that influence the coefficient of permeability for a particular soil. Both degree of saturation and void ratio need to be considered in the estimation of the coefficient of permeability function over the entire suction range for a material that undergoes volume change during a drying process.

The coefficient of permeability at a particular soil suction during a drying process is the product of the relative coefficient of permeability and the saturated coefficient of permeability of the soil at the same state when it is undergoing single-phase water flow. A material at the same state means that it has the same skeleton with the same porous structure and void ratio without considering the degree of saturation.

$$k(\psi) = k_r(\psi) \times k_{ps}(\psi) \qquad \text{[A9]}$$

where,

$k(\psi)$ = coefficient of permeability at a particular suction ψ,

$k_r(\psi)$ = relative coefficient of permeability at the suction of ψ,

$k_{ps}(\psi)$ = potential saturated coefficient of permeability at a suction of ψ.

The potential saturated coefficient of permeability, $k_{ps}(\psi)$ does not mean that the material remains saturated at the suction of ψ with a saturated coefficient of permeability of $k_{ps}(\psi)$. $k_{ps}(\psi)$ indicates the saturated coefficient of permeability of a saturated material which has the same solid porous skeleton as the material at a suction of ψ during a drying process.

The relative coefficient of permeability must range between zero and one. In Phase 1, when soil suction ψ is less than the air-entry value (AEV), the soil remains saturated. The relative coefficient of permeability $k_r(\psi)$ for a saturated soil is 1.0. The coefficient of permeability $k(\psi)$ is the saturated coefficient of permeability equal to the relating potential saturated coefficient of permeability $k_{ps}(\psi)$ when the soil suction ψ is less than the AEV. In Phase 2 and Phase 3, when soil suction ψ exceeds the AEV, desaturation starts and the relative coefficient of permeability decreases from one down toward zero as the soil continues drying out. The coefficient of permeability $k(\psi)$ for a soil in the unsaturated state is smaller than the potential saturated coefficient of permeability $k_{ps}(\psi)$ due to the influence of desaturation.

Degree of saturation and void ratio are two main factors that control the coefficient of permeability of a particular material. Eq. [A9] reveals that degree of saturation influences the relative coefficient of permeability $k_r(\psi)$ while void ratio affects the potential saturated coefficient of permeability $k_{ps}(\psi)$. Changes in the degree of saturation change the tortuosity of the flow path within the porous media. The tortuosity controls the relative coefficient of permeability. In other words, the degree of saturation exerts an influence upon the relative coefficient of permeability by impacting the tortuosity of the flow path within the porous media. Theoretically, the saturated coefficient of permeability of a soil depends on pore sizes and the pore distribution or arrangement within the soil (Chapuis, 2012). A change in void ratio changes pore sizes, thus influencing the saturated coefficient of permeability of the soil. Degree of saturation and void ratio together govern the coefficient of permeability for a material that undergoes volume change as soil suction changes during a drying process, $k(\psi)$.

A number of research studies have been undertaken on changes in the saturated coefficient of permeability as a function of void ratio for saturated soils that undergo volume change (Chapuis, 2012). Eq. [A10] (Taylor, 1948) is found to be able to mathematically describe the relationship between the experimentally measured saturated coefficient of permeability, k_{sat} and void ratio, e. This equation can be utilized in conjunction with a relative coefficient of permeability function to generate a coefficient of permeability function for a material that undergoes volume change as soil suction is changed during a drying process.

$$k_{sat}\left(e\right)=\frac{10^{-11}C\,e^{x}}{1+e} \qquad \text{[A10]}$$

where:

k_{sat} = saturated coefficient of permeability,

e = void ratio,

C, x = fitting parameters.

Void ratio is related to soil suction during a drying process where the material undergoes volume change as soil suction is increased (Fredlund et al., 2011). The relationship of void ratio to soil suction can be mathematically described by combining the shrinkage equation (Fredlund et al, 2002) and the mathematical equation for the gravimetric water content, w-SWCC (Fredlund and Xing, 1994). The potential saturated coefficient of permeability, $k_{ps}(\psi)$ can be mathematically described based on Eq. [A10] used in conjunction with the relationship of void ratio versus soil suction. The shrinkage curve equation (Fredlund et al, 2002) is shown as Eq. [A11].

$$e\left(w\right)=a_{sh}\left(\left(\frac{w}{b_{sh}}\right)^{c_{sh}}+1\right)^{\frac{1}{c_{sh}}} \qquad \text{[A11]}$$

where:

a_{sh} = the minimum void ratio, e_{min},

a_{sh}/b_{sh} = slope of the line of tangency,

c_{sh} = curvature of the shrinkage curve,

w = gravimetric water content.

And the equation for the gravimetric water content, w-SWCC (Fredlund and Xing, 1994) can be written as shown in Eq. [A12].

$$w(\psi)=\frac{w_s\left(1-\ln\left(1+\psi/\psi_r\right)/\ln\left(1+10^6/\psi_r\right)\right)}{\left(\ln\left(\exp(1)+\left(\psi/a_f\right)^{n_f}\right)\right)^{m_f}} \qquad \text{[A12]}$$

where:

ψ = soil suction;

a_f, n_f, m_f, and ψ_r = mathematical fitting parameters;

w_s = initial saturated gravimetric water content;

$w(\psi)$ = gravimetric water content at a designed soil suction of ψ;

The relative coefficient of permeability function $k_r(\psi)$ forms another important component composing the coefficient of permeability function $k(\psi)$ for a soil that undergoes volume change as soil suction changes. The relative coefficient of permeability of a material is a function of soil suction reflecting the influence of degree of saturation on the coefficient of permeability. Considerable research has been undertaken on the estimation of the relative coefficient of permeability in unsaturated soil mechanics. The relative coefficient of permeability is primarily determined by the pore-size distribution of the soil and its prediction is generally based on the soil-water characteristic curve. The Fredlund et al., (1994) permeability function is one of those commonly used unsaturated permeability functions. The Fredlund et al. (1994) permeability function takes the following form:

$$k_{\mathrm{r}}(\psi)=\frac{\int_{\ln(\psi)}^{\mathrm{b}}\frac{\theta(e^{y})-\theta(\psi)}{e^{y}}\theta'(e^{y})dy}{\int_{\ln(\psi_{\mathrm{aev}})}^{b}\frac{\theta(e^{y})-\theta(\psi_{\mathrm{aev}})}{e^{y}}\theta'(e^{y})dy} \qquad \text{[A13]}$$

where:

b = ln(1000000),

y = a dummy variable of integration representing the logarithm of soil suction.

The soil-water characteristic curve, SWCC, presents the relationship between the amount of water in a soil and various applied soil suctions. There are four designations of water content commonly used to define the amount of water in a soil, namely, gravimetric water content, *w*, volumetric water content, θ (where the volume of water is referenced to the original total volume of the soil specimen), instantaneous volumetric water content, θ_i (where the volume of water is referenced to the instantaneous total volume of the soil specimen), and degree of saturation, *S*. With each designation of the water content, there is one form of the SWCC. As a result, there are four different forms of SWCC, namely, gravimetric water content-SWCC (*w*-SWCC), volumetric water content-SWCC (θ-SWCC), instantaneous volumetric water content-SWCC (θ_i-SWCC), and degree of saturation-SWCC (*S*-SWCC).

For soils that do not undergo volume change as soil suction changes, all four SWCCs provide the same information to the geotechnical engineer when estimating other unsaturated soil property functions. However, for a soil that undergoes volume change as soil suction changes in a drying process, *w*-SWCC, θ_i-SWCC and *S*-SWCC are different from one another. It should be noted that *S*-SWCC must be used for the estimation of the relative coefficient of permeability function with Eq. [A13], while θ_l-SWCC should be used for the estimation of the water storage function in all cases.

PRESENTATION OF THE EXPERIMENTAL DATA

The thickened tailings, tested by Total E&P Canada (Total) are typical materials that undergo volume change as soil suction changes in a drying process. Box #11 and Box #2 (Fredlund et al., 2011) are two thickened tailings with different SFRs (sand fine ratios). Box #11 has a SFR of 0.8, and Box #2 has a SFR of 0.1. The experimental data of Box #11 and Box #2 are presented and interpreted using the proposed theory for the estimation of the coefficient of permeability function.

The thickened tailings in Box #11 had a liquid limit of 35% and a plastic limit of 15%. Box #2 had a liquid limit of 55% and a plastic limit of 22%. Shrinkage curves and soil-water characteristic curves were measured. The shrinkage curve of the thickened tailings with SFR 0.8 (Box #11) is presented in Figure A-10. The best-fitting parameters of the shrinkage curve for the thickened tailings with SFR 0.8 are a_{sh} = 0.394, b_{sh} = 0.162, and c_{sh} = 3.208. The average specific gravity of the tailings with SFR 0.8 was 2.43. The shrinkage curve of the thickened tailings with SFR 0.1 (Box #2) is presented in Figure A-11. The best-fitting parameters of the shrinkage curve for the thickened tailings SFR 0.1 are a_{sh} = 0.440, b_{sh} = 0.185, and c_{sh} = 7.277. The average specific gravity of the thickened tailings with SFR 0.1 was 2.38.

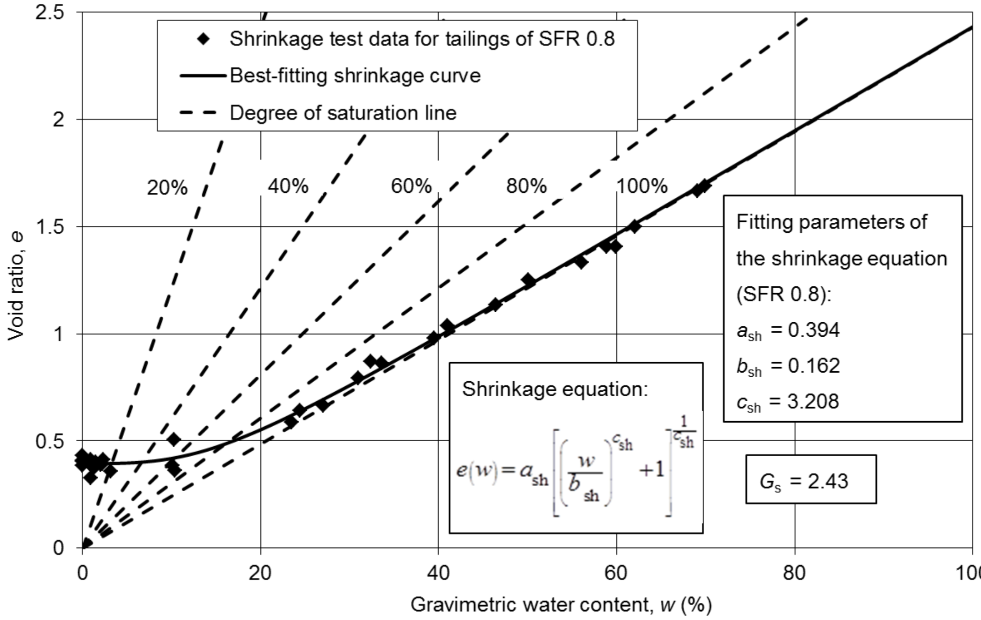

Figure A-10. Shrinkage curve for Total tested thickened tailings of SFR 0.8 (Box #11).

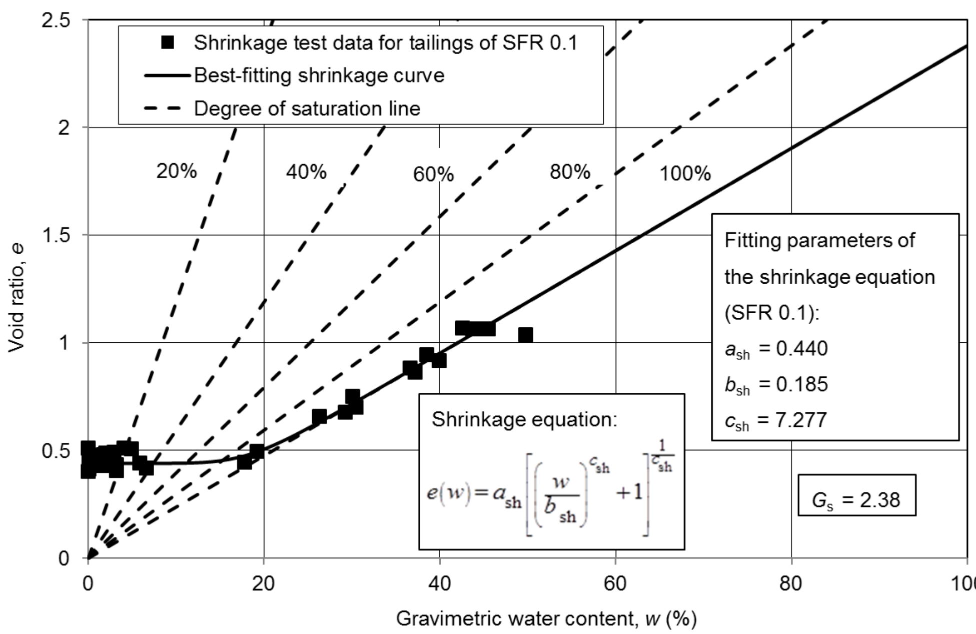

Figure A-11. Shrinkage curve for Total tested thickened tailings SFR 0.1 (Box #2).

Figure A-12 shows the gravimetric water content, *w*, plotted versus soil suction for Total tested thickened tailings Box #11 and Box #2. The experimental data for the gravimetric water content soil-water characteristic curve, *w*-SWCC was best-fitted with Fredlund and Xing (1994) equation, Eq. [A12]. The best-fitting parameters for Box #11 are a_f = 0.457 kPa, n_f = 0.792, m_f = 0.907 and ψ_r = 52.84 kPa. The initial gravimetric water content for Box #11 was 73.8%. The best-fitting parameters for Box #2 are a_f = 1.250 kPa, n_f = 0.982, m_f = 0.612 and ψ_r = 107.4 kPa. The initial gravimetric water content for Box #2 was 77.70%. *w*-SWCC is used in conjunction with the shrinkage curve to calculate other forms of SWCC and properly interpret the SWCC results to determine the true AEV and estimate the relative coefficient of permeability function.

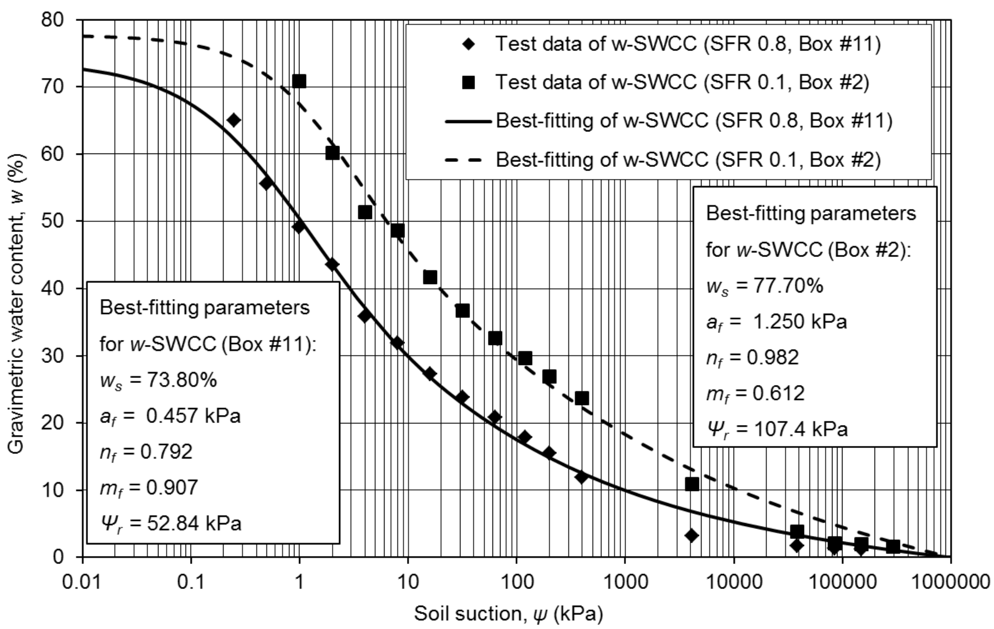

Figure A-12. Gravimetric water content versus soil suction

The experimental data for the relationship of saturated coefficient of permeability versus void ratio were also obtained for Total tested thickened tailings. The experimental data were best-fitted by Eq. [A10]. Figure A-13 shows the measured data and the best-fitting curves for Box #11 and Box #2. The fitting parameters for Box #11 are C = 226.47 and x = 3.277. And the fitting parameters for Box #2 are C = 8.073 and x = 3.042.

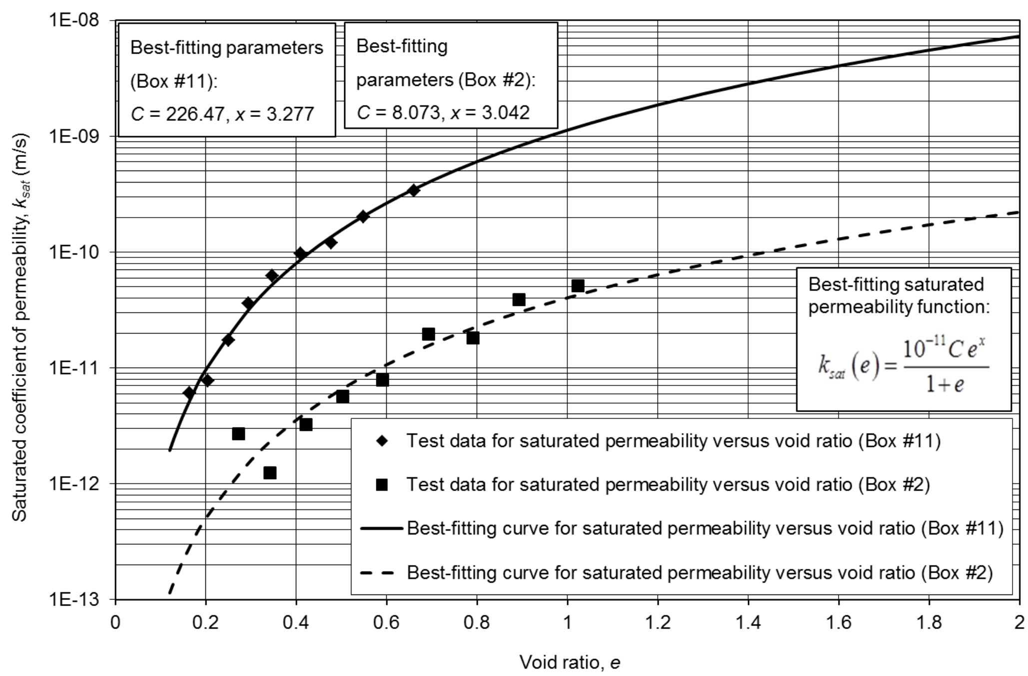

Figure A-13. Measured data and its best-fitting of saturated coefficient of permeability versus void ratio for Total tested thickened tailings (Box #11 and Box #2).

These three curves obtained from the laboratory test, namely the shrinkage curve, the *w*-SWCC and the curve of saturated coefficient of permeability versus void ratio form the basis to further estimate the appropriate coefficient of permeability function for a soil that undergoes high volume change as soil suction changes, such as thickened tailings tested by Total.

INTERPRETATION OF THE EXPERIMENTAL DATA

The gravimetric water content-SWCC, *w*-SWCC is combined with the shrinkage curve to obtain other forms of SWCC. The resulting plot of the *S*-SWCC is presented in Figure A-14. The true air-entry value (AEV) for a material that undergoes volume change as soil suction is changed is obtained from the *S*-SWCC of the soil. Using the graphical construction method suggested by Vanapalli et al., (1998), the true AEVs interpreted from the *S*-SWCCs in Figure A-14 are 33.2 kPa for Box #11 and 658 kPa for Box #2. The plot of θ_l-SWCC is shown in Figure A-15. The θ_l-SWCC is the correct form of SWCC that should be used for the estimation of the water storage function in the case where soil undergoes volume change as soil suction is increased in a drying process.

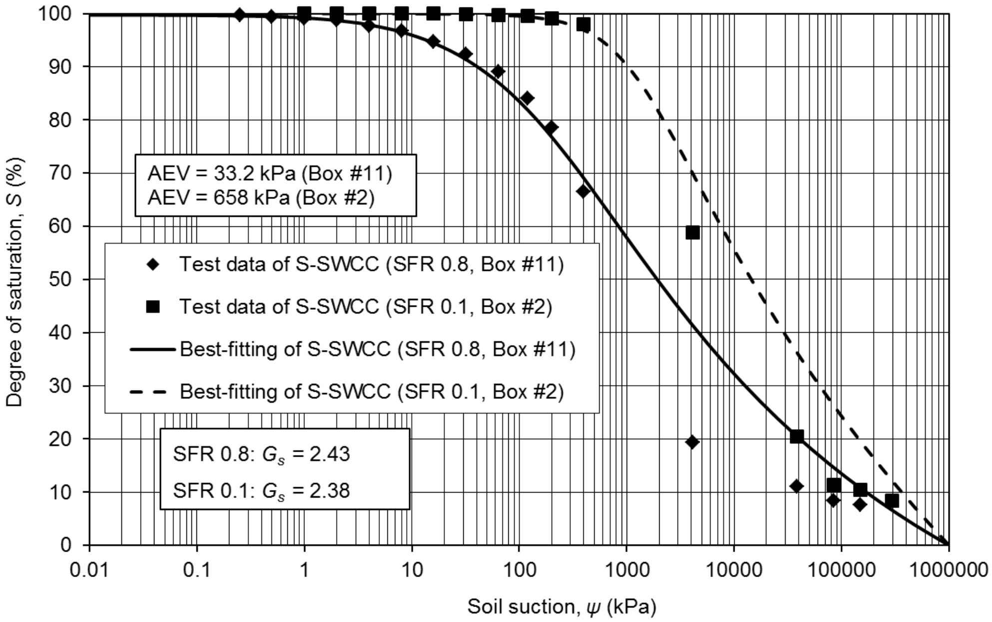

Figure A-14. Measured data and its best-fitting of the *S*-SWCC for Total tested thickened tailings (Box #11 and Box #2).

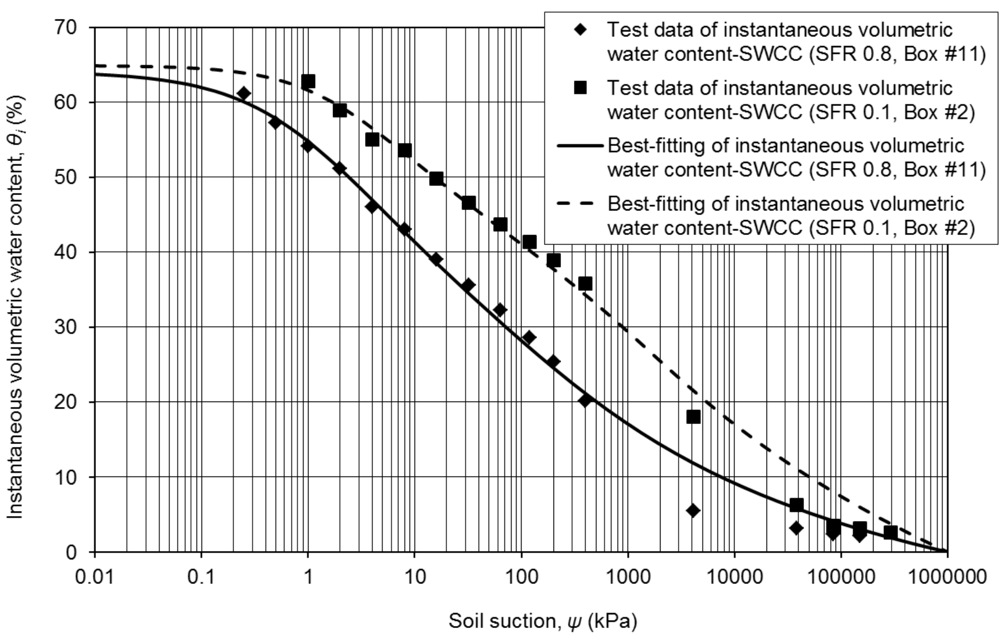

Figure A-15. Measured data and its best-fitting of the θ_i-SWCC for Total tested thickened tailings (Box #11 and Box #2).

The relationship between void ratio and soil suction is obtained by combining the *w*-SWCC and the shrinkage curve. The plot of void ratio versus soil suction is shown in Figure A-16. For Box #11, the void ratio decreases from 1.798 to 0.603 when the soil suction increases from 0 to its AEV of 33.2 kPa. The void ratio at the AEV of 33.2 kPa is 0.603 for Box #11. For Box #2, the void ratio decreases from 1.849 to 0.507 when the soil suction increases from 0 to its AEV of 658 kPa. The void ratio at the AEV of 658 kPa is 0.507 for Box #2. For both Box #11 and Box #2, the soil specimen experiences significant volume change before the soil suction reaches the AEV during its drying process. Comparing to the volume change at the early stage of the drying process before the AEV is approached, the volume change of the specimen is relatively small and insignificant after the soil suction exceeds the AEV.

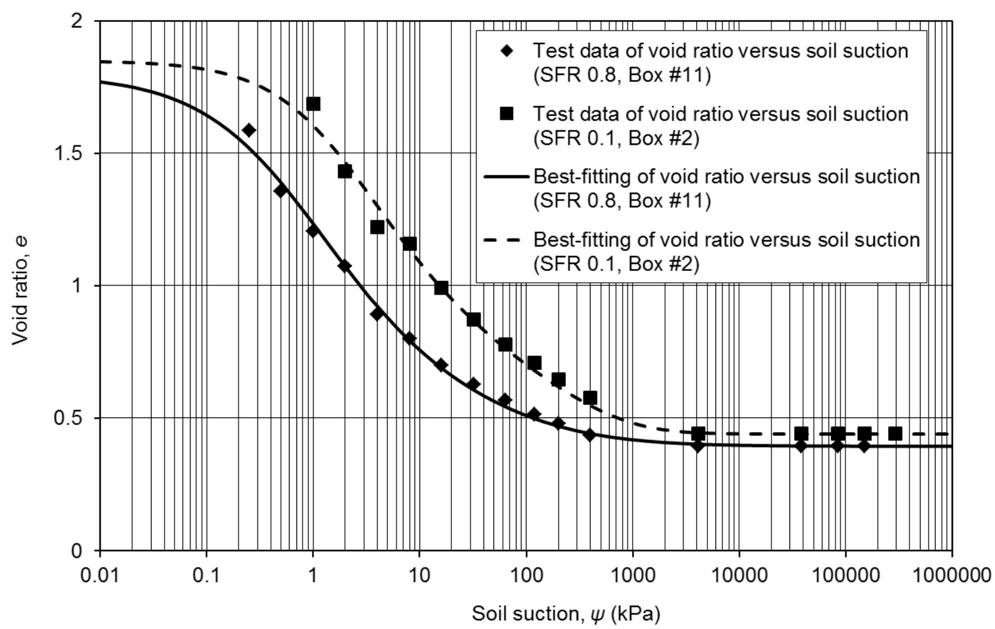

Figure A-16. Measured data and its fitting for the relationship of void ratio versus soil suction for Total tested thickened tailings (Box #11 and Box #2).

The saturated coefficient of permeability is related to void ratio, while void ratio changes with soil suction during the drying process of Total tested thickened tailings. As a result, saturated coefficient of permeability can be written in terms of soil suction. When the saturated coefficient of permeability is related to soil suction, it is referred to as potential saturated coefficient of permeability to make a distinction because there are both saturated and unsaturated conditions during the entire drying process. The curves of the potential saturated coefficient of permeability versus soil suction for both Box #11 and Box #2 are shown in Figure A-17.

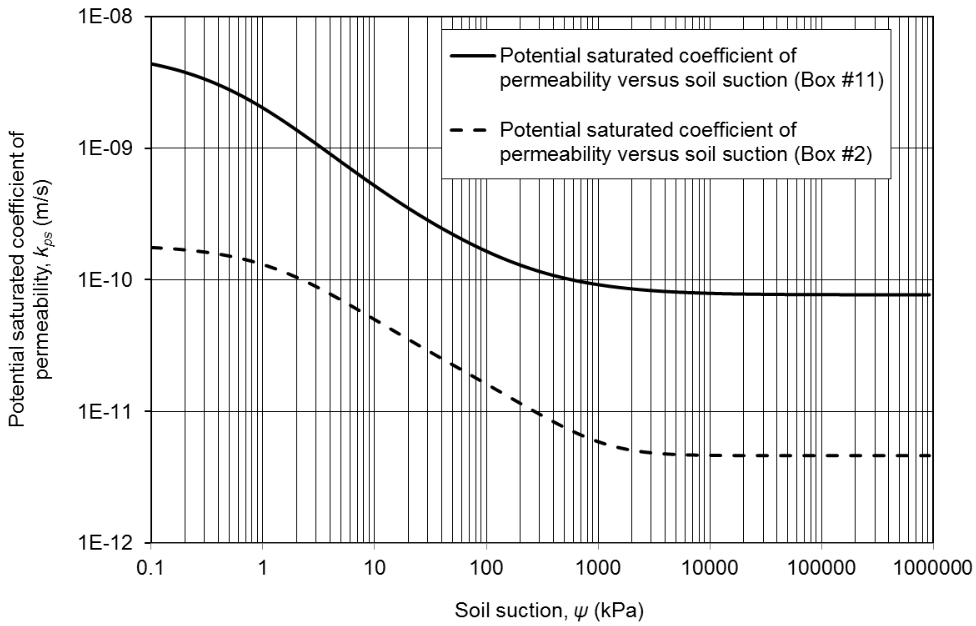

Figure A-17. Potential saturated coefficient of permeability versus soil suction for Total tested thickened tailings (Box #11 and Box #2).

The curves of the relative coefficient of permeability versus soil suction for Total tested thickened tailings Box #11 and Box #2 are presented in Figure A-18. Figure A-18 shows that the relative coefficient of permeability remains 1.0 until the soil suction approaches the AEV of the soil. When the AEV is surpassed, the desaturation starts and the relative coefficient of permeability reduces from 1.0 towards zero. The correct curve for the relative coefficient of permeability versus soil suction is obtained from *S*-SWCC with the AEV as the lower limit of integration for the integral in the denominator of Eq. [A13]. After having the relative coefficient of permeability function shown in Figure A-18 and the potential saturated coefficient of permeability function shown in Figure A-17, the coefficient of permeability function can be obtained by multiplying the relative coefficient of permeability function with the potential saturated coefficient of permeability function according to Eq. [A9]. The curves of the coefficient of permeability versus soil suction for Total tested thickened tailings for Box #11 and Box #2 are presented in Figure A-19.

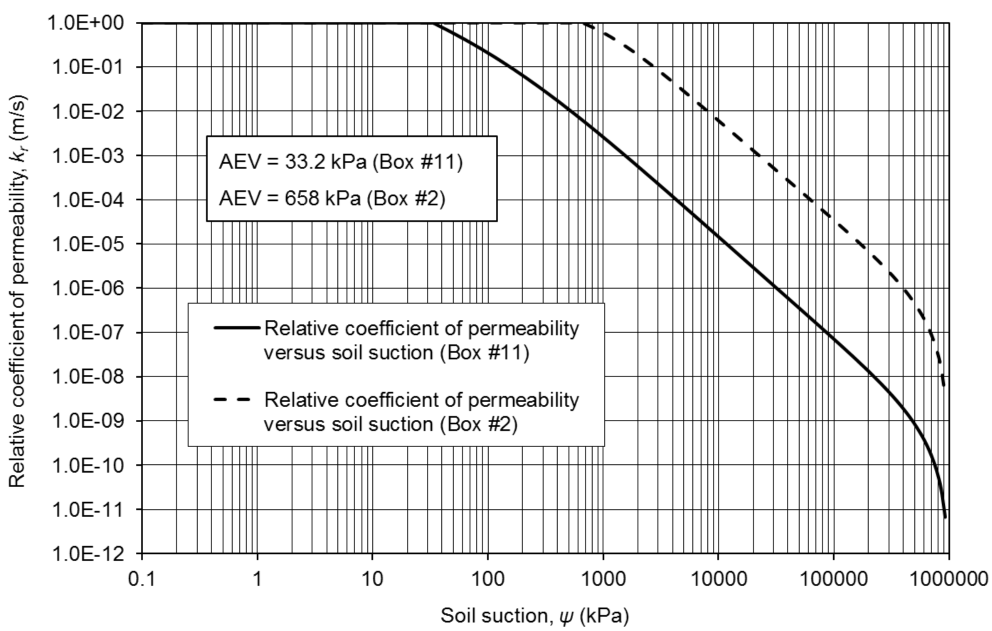

Figure A-18. Relative coefficient of permeability versus soil suction for Total tested thickened tailings (Box #11 and Box #2).

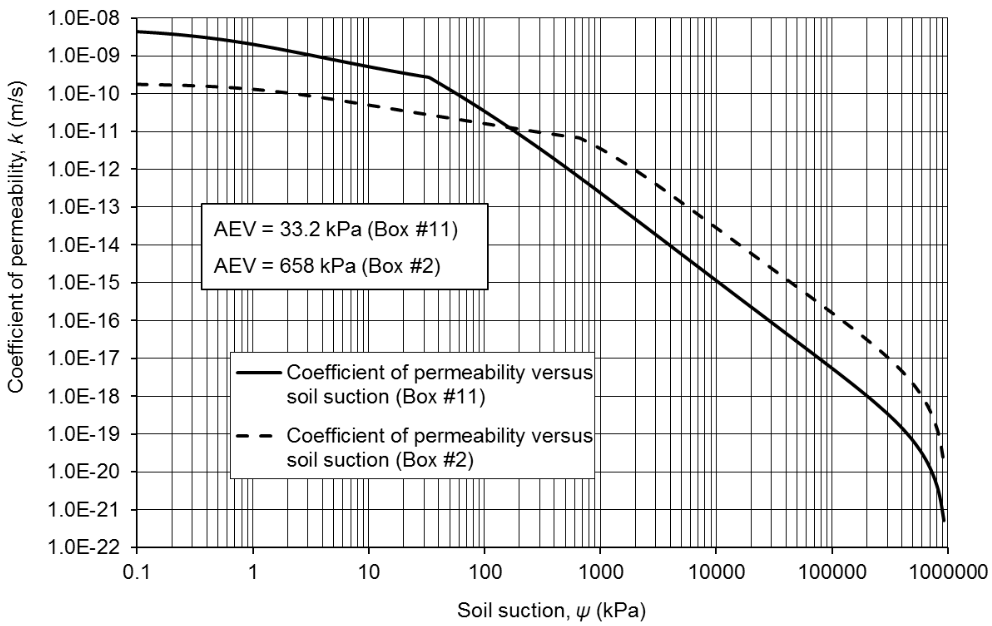

Figure A-19. Coefficient of permeability versus soil suction for Total tested thickened tailings (Box #11 and Box #2).

CONCLUSIONS AND SUMMARY

This paper presents a revised theory for the reasonable estimation of the coefficient of permeability function for materials that undergo volume change as soil suction changes based on the Fredlund et al., (1994) permeability function. Both volume change and desaturation are taken into account in the revised theory. The coefficient of permeability function proposed in this paper consists of two main components, namely, the potential saturated coefficient of permeability function and the relative coefficient of permeability function. The coefficient of permeability function is the result of the multiplication between the potential coefficient of permeability function and the relative coefficient of permeability function. The potential saturated coefficient of permeability function is controlled by the void ratio as soil suction changes and reflects the influence of volume change on the coefficient of permeability. The relative coefficient of permeability function must be estimated from *S*-SWCC using the AEV as the lower limit of integration. The influence of desaturation on the coefficient of permeability is reflected in the relative coefficient of permeability function. The experimental data for Total tested thickened tailings Box #11 and Box #2 are used to explain and illustrate the detailed procedure for the estimation of the coefficient of permeability function using the estimation method suggested in this paper.

REFERENCES

BGC Engineering Inc. (2010). Oil sands tailings technology review (OSRIN Report No. TR-1). Retrieved from http://hdl.handle.net/10402/era.17555

Chapuis, R. P. (2012). "Predicting the saturated hydraulic conductivity of soils: a review." Bull.Eng.Geol.Env.,71(3), 401-434.

Fine Tailings Fundamentals Consortium (FTFC). (1995). Vol. I, Clark hot water extraction fine tailings. In Advances in Oil Sands Tailings Research (pp. 5–8), Edmonton, AB: Alberta Department of Energy, Oil Sands and Research Division.

Fredlund, D. G., Stone, J., Stianson, J., and Sedgwick, A. (2011). "Determination of water storage and permeability functions for oil sands tailings." Tailings and Mine Waste 2011 .

Fredlund, D. G., and Xing, A. (1994). "Equations for the soil-water characteristic curve." Canadian Geotechnical Journal, 31(4), 521-532.

Fredlund, D., Xing, A., and Huang, S. (1994). "Predicting the permeability function for unsaturated soils using the soil-water characteristic curve." Canadian Geotechnical Journal, 31(4), 533-546.

Fredlund, M. D., Wilson, G. W., and Fredlund, D. G. (2002). "Representation and estimation of the shrinkage curve." Proc., 3rd Int. Conf. on Unsaturated Soils, UNSAT 2002, 145-149.

Sobkowicz, J. C., & Morgenstern, N. R. (2009). A geotechnical perspective on oil sands tailings. Proceedings of the Thirteenth International Conference on Tailings and Mine Waste, xvii–xl.

A. R. Sorta, D. C. Sego, and G.W. Wilson (2013). “Behavior of oil sands fines-sand mixture tailings.” CIM Journal, 4(4), 265-280.

Taylor, D. W. (1948). Fundamentals of soil mechanics.J. Wiley & Sons; London: Chapman & Hall.

Van Genuchten, M. T. (1980). "A closed-form equation for predicting the hydraulic conductivity of unsaturated soils."Soil Sci.Soc.Am.J.,44(5), 892-898.

Appendix 3. Role of air-entry value and choice of SWCC in the prediction of the unsaturated permeability

ABSTRACT

The permeability function is commonly estimated by integrating along the soil-water characteristic curve (SWCC) based on a particular integral formula. The Fredlund, Xing and Huang (1994) permeability function is a commonly used estimation technique. It has become common practice to start the integration procedure from a value near zero rather than the originally specified air-entry value (AEV). This paper undertakes a study on the effect of the lower limit of integration on the estimation of the permeability function. A mathematical algorithm is also proposed for the calculation of the AEV for integration purposes. The results reveal that the relative coefficient of permeability can be significantly under-estimated if the lower limit of integration is smaller than the AEV. The recommendation is that the AEV always be used as the lower limit of integration when using the Fredlund et al (1994) permeability estimation equation.

RÉSUMÉ

La fonction de perméabilité est fréquenment estimée en intégrant le long de la courbe caractéristique d'eau de sol (SWCC) basé sur une formule intégrante particulière. La fonction de perméabilité de Fredlund, Xing et Huang (1994) est une technique d'estimation fréquenment utilisée. C'est devenu une pratique courante de commencer la procédure d'intégration avec une valeur proche du zéro plutôt qu'avec la valeur d'entrée d'air (AEV) indiquée au départ. Cet article entreprend une étude sur l'effet de la limite plus basse d'intégration sur l'estimation de la fonction de

perméabilité. Un algorithme mathématique est aussi proposé pour le calcul de AEV pour les fins d'intégration. Les résultats révèlent que le coefficient relatif de perméabilité peut être sous-estimé de façon significative si la limite plus basse d'intégration est plus petite que AEV. La recommandation est que AEV soit toujours utilisé comme la limite plus basse d'intégration en utilisant l'équation d'estimation de perméabilité de Fredlund et al (1994).

INTRODUCTION

The unsaturated coefficient of permeability function is an important soil property function used in the numerical modeling of saturated-unsaturated soil systems. Direct measurement of the unsaturated permeability function is costly, technically-demanding, and time-consuming. Therefore, considerable research has been directed towards the estimation of the unsaturated coefficient of permeability function. There are four categories of models used for the estimation of unsaturated coefficient of permeability functions (Fredlund et al. 2012), namely, i.) empirical models, ii.) statistical models, iii.) correlation models and iv.) regression models. Empirical models and statistical models appear to be most extensively used in geotechnical engineering.

Empirical models make use of the similar character of the soil-water characteristic curve, (SWCC), and the permeability function in order to estimate the unsaturated coefficient of permeability function. The Brooks and Corey (1964) equation is one example of an empirical model. Statistical models make use of the fact that the permeability function and the soil-water characteristic curve are mainly controlled by the pore-size distribution of the soil. Consequently, the permeability function was developed based on the interpretation and application of the SWCC.

Childs and Collis-George (1950), Burdine (1953) and Mualem (1976) are three commonly used integral formulas of relative permeability based on different physical models.

The van Genuchten-Burdine (1980) equation, the van Genuchten-Mualem (1980) equation, and the Fredlund, Xing and Huang (1994) permeability function are three permeability functions for unsaturated soils commonly used in geotechnical engineering. These three unsaturated coefficient of permeability functions are developed by introducing various mathematical equations for the SWCC into different integral formulas based on different physical models. The unsaturated soil permeability function is obtained by combining the saturated coefficient of permeability and the relative coefficient of permeability. The Fredlund, Xing and Huang (1994) permeability function is an integral solution for the permeability equation, obtained by introducing the Fredlund and Xing (1994) SWCC equation into the Childs and Collis-George (1950) integral formula. The resulting permeability function has the advantage that the integral permeability function retains the independence of the SWCC fitting variables when estimating the permeability function. On the other hand, the van Genuchten permeability function has a closed form and is simpler to use in engineering practice.

The original relative permeability theory published by Fredlund et al. (1994) specified the air-entry value, ψ_{aev}, as the lower limit of integration. However, implementations in engineering practice appear to have used other values between zero and ψ_{aev} as the starting point of integration when calculating the relative coefficient of permeability. It doesn't appear that any study has been undertaken to assess whether the choice for the lower limit of integration influences the calculation of the Fredlund, Xing and Huang (1994) permeability function. In addition, the importance of using the degree of saturation SWCC (*S*-SWCC) for calculating the permeability function has not been clearly emphasized in the research literature.

This paper lays out an empirical procedure for the determination of the air-entry value and investigates the error caused by using various values for the lower limit of integration. The effect of the choice of SWCC on the estimation of the relative permeability function is also studied.

DETERMINATION OF THE AIR-ENTRY VALUE (AEV) FROM THE DEGREE OF SATURATION SWCC, (*S*-SWCC)

Different forms of soil-water characteristic curve (SWCCs)

The SWCC for a soil is defined as the relationship between the water content and soil suction (Williams 1982), and is commonly used as the basis for the estimation of unsaturated soil properties (e.g., the permeability function for an unsaturated soil). Different designations for the amount of water in the soil generate different forms of SWCC. The designations for these SWCCs can be referred to as the: gravimetric water content SWCC, volumetric water content SWCC, instantaneous volumetric water content SWCC, and degree of saturation SWCC. The volumetric water content is the water content with the volume of water referenced to the original total volume of the soil specimen. The instantaneous volumetric water content is the water content with the volume of water referenced to the instantaneous total volume of the soil specimen. Each form of the SWCC provides similar information to the geotechnical engineer if the soil does not undergo volume change as soil suction is increased (as shown in Figure A-20).

When soil undergoes volume change, as is the case for soft clays and slurry soils, the gravimetric water content SWCC, instantaneous volumetric water content SWCC and degree of saturation SWCC are distinctly different from one another (as shown in Figure A-21). Volumetric water content SWCC is not of significance when soil undergoes high volume change. Conventional permeability functions (e.g., Fredlund et al. (1994) equation; van Genuchten-Burdine (1980) equation; van Genuchten-Mualem (1980) equation) have been proposed based on the assumption that there is little or no volume change as the soil dries. The volumetric water content SWCC is no longer appropriate for the estimation of the relative permeability function when soil undergoes volume change. It is important to know that the relative coefficient of permeability function, as well as the air-entry value must be estimated from degree of saturation SWCC (Fredlund et al. 2011). This paper uses the degree of saturation SWCC to calculate the appropriate estimation of the relative permeability function.

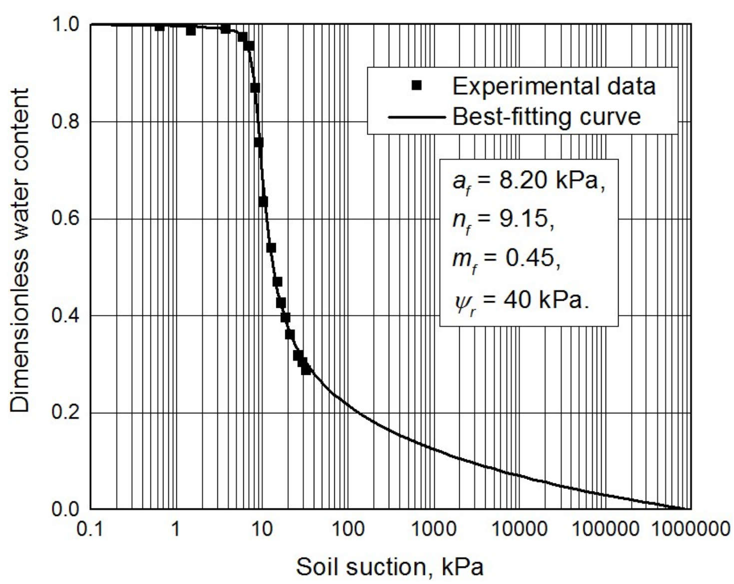

Figure A-20. SWCC experimental data for GE3 and its best-fitting curve. (Data from Brooks and Corey 1964)

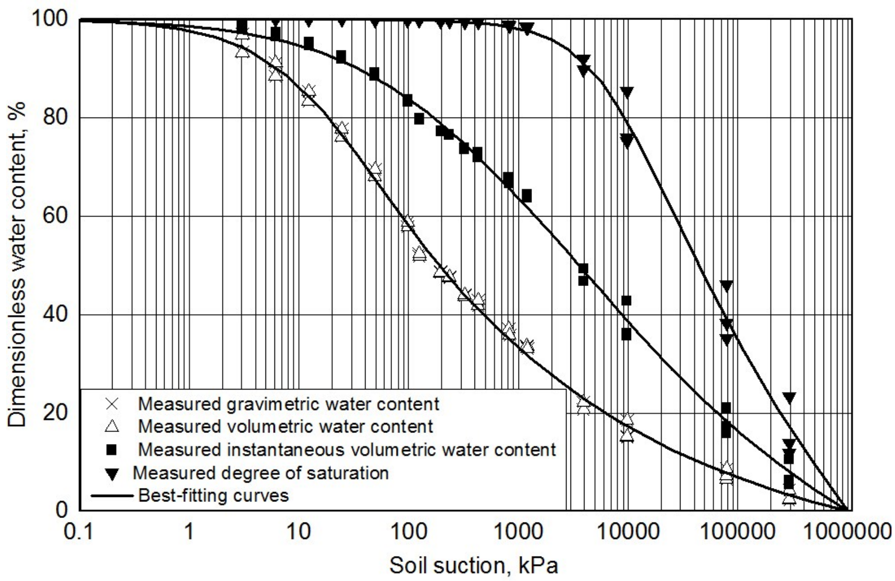

Figure A-21. SWCC experimental data for Regina clay and its best-fitting curves. (Data from Fredlund 1964)

Various forms of mathematical equations have been suggested to characterize the SWCC. The equation proposed by Fredlund and Xing (1994) has been shown to have sufficient flexibility to best-fit laboratory data reasonably well over the entire soil suction range from near zero to 106 kPa provided the material behaves in a mono-modal manner. The form of the Fredlund and Xing (1994) equation written in terms of degree of saturation, (i.e., *S*-SWCC) is shown in Eq. [A14].

$$S(\psi) = \frac{S_0\left(1 - \ln\left(1 + \psi/\psi_r\right)/\ln\left(1 + 10^6/\psi_r\right)\right)}{\left(\ln\left(\exp(1) + \left(\psi/a_f\right)^{n_f}\right)\right)^{m_f}} \qquad \text{[A14]}$$

where,

ψ = soil suction;

$S(\psi)$ = degree of saturation at a soil suction of ψ;

S_0 = initial degree of saturation at zero soil suction; and

a_f, n_f, m_f, ψ_r = four best-fitting parameters controlling the shape of the SWCC.

Mathematical algorithm for the empirical determination of the air-entry value (AEV)

The air-entry value, (AEV), of the soil is the suction at which air begins to enter the largest pores in the soil (Fredlund and Xing 1994). Vanapalli et al. (1998) proposed an empirical, graphical construction technique to estimate the air-entry value from the SWCC. The air-entry value must be determined from the degree of saturation SWCC (Fredlund et al. 2011).

A mathematical algorithm is proposed in this paper for the determination of the AEV based on the graphical construction method suggested by Vanapalli et al., (1998). The following steps are outlined with respect to the analysis for the AEV.

Step 1. Find the best-fitting curve for the degree of saturation SWCC using the Fredlund and Xing (1994) equation (Figure A-22).

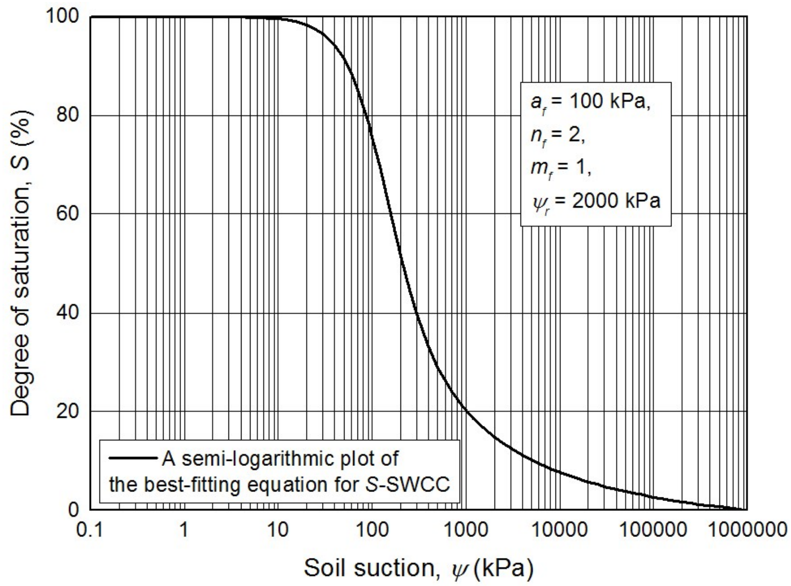

Figure A-22. *S*-SWCC for a hypothetical soil plotted using semi-logarithmic coordinate.

Step 2. Through use of a variable substitution technique, the Fredlund-Xing (1994) best-fitting equation can be transformed into a substitution equation (i.e., Eq. [A15]). The substitution equation describes the relationship between the degree of saturation and the logarithm of soil suction to base 10 (Figure A-23). The shape of the curve for the substitution equation plotted using arithmetic coordinates is the same as the shape of the curve for the best-fitting equation plotted using a semi-logarithmic coordinate system. The arithmetic plot of the substitution equation has the same inflection point as the semi-logarithmic plot of the best-fitting equation.

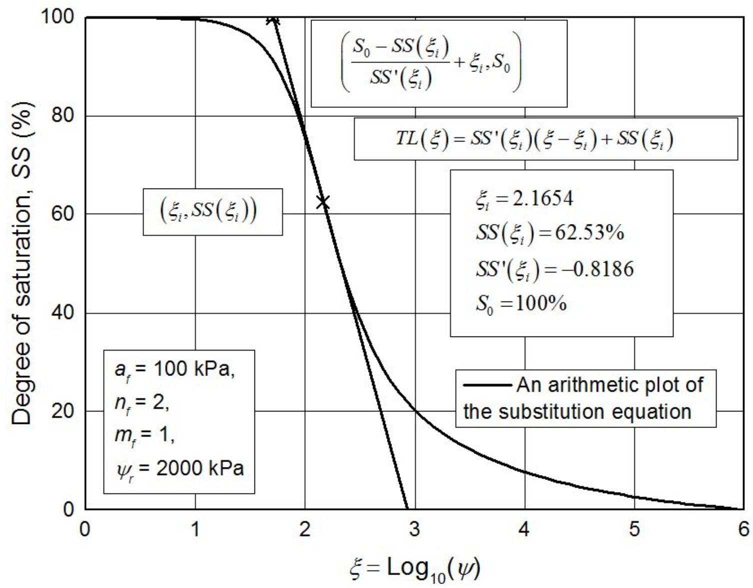

Figure A-23. The arithmetical plot of the substitution equation.

$$SS(\xi) = \frac{S_0\left(1 - \ln\left(1 + 10^{\xi}/\psi_r\right)/\ln\left(1 + 10^{6}/\psi_r\right)\right)}{\left(\ln\left(\exp(1) + \left(10^{\xi}/a_f\right)^{n_f}\right)\right)^{m_f}} \quad \text{[A15]}$$

where, $\xi = \mathrm{Log}_{10}(\psi)$; $SS(\xi)$ = the degree of saturation at a soil suction of ψ; ψ = soil suction.

Step 3. Determine the point of maximum slope (or the inflection point) on the arithmetic plot of the substitution equation. The point of maximum slope is also a point of zero curvature. Therefore, the second derivative of Eq. [A15] can be set equal to zero as shown in Eq. [A16].

$$\frac{\mathrm{d}^2 SS(\xi)}{\mathrm{d}\xi^2} = 0 \quad \text{[A16]}$$

Solving Eq. [A16] for the ξ value of zero curvature point and substituting the ξ value into Eq. [A15] yields the corresponding term, $SS(\xi)$. The determined point of zero curvature has coordinates (ξ_i, $SS(\xi_i)$) (Figure A-23).

Step 4. Draw a line tangent to the curve through the point of maximum slope (Figure A-23). The point of maximum slope is (ξ_i, $SS(\xi_i)$) and the maximum slope is $SS'(\xi_i)$. The equation for the tangent line is as shown in Eq. [A17].

$$TL(\xi) = SS'(\xi_i)(\xi - \xi_i) + SS(\xi_i) \quad \text{[A17]}$$

where, $TL(\xi)$ represents the function of the tangent line.

Step 5. Draw a horizontal line through the maximum degree of saturation. The intersection of the two lines indicates the air-entry value (Figure A-23). The horizontal line is given by Eq. [A18].

$$HL(\xi) = S_0 \quad \text{[A18]}$$

where, $HL(\xi)$ represents the function of the horizontal line.

The intersection point can be obtained mathematically by solving Eqs. [A18] and [A17]. The intersection point is, $\left(\dfrac{S_0 - SS(\xi_i)}{SS'(\xi_i)} + \xi_i, S_0 \right)$, on the arithmetic plot.

Step 6. Back-calculate the AEV through use of the relationship, ξ = $\mathrm{Log}_{10}(\psi)$. The air-entry value for the soil can be written as follows.

$$\psi_{AEV} = 10^{\frac{S_0 - SS(\xi_i)}{SS'(\xi_i)} + \xi_i} \qquad \text{[A19]}$$

ROLE OF AEV IN THE FREDLUND, XING AND HUANG (1994) PERMEABILITY FUNCTION

Fredlund, Xing and Huang (1994) suggested a mathematical function for the estimation of the relative coefficient of permeability based on a physical model proposed by Childs and Collis-George (1950) (see Eq. [A20]).

$$k_r^s(\psi) = \frac{\int_{\ln(\psi)}^{b} \frac{S(e^y) - S(\psi)}{e^y} S'(e^y)\,dy}{\int_{\ln(\psi_{aev})}^{b} \frac{S(e^y) - S(\psi_{aev})}{e^y} S'(e^y)\,dy} \qquad \text{[A20]}$$

where,

$k_r^s(\psi)$ = relative coefficient of permeability at soil suction of ψ. The superscript *s* means that the degree of saturation-SWCC is used for the estimation of the relative permeability in Eq. [A20];

b = upper limit of integration [i.e., ln(1000000)];

y = dummy variable of integration representing the logarithm of suction;

S = degree of saturation-SWCC equation;

S' = derivative of the degree of saturation-SWCC equation;

e^y = natural number raised to the dummy variable power.

The denominator of Eq. [A20] is an integral, the lower limit of the integration of which is the air-entry value, ψ_{aev}. Although the original theory (Fredlund et al. 1994) specified the air-entry value, ψ_{aev}, as the lower limit of integration, other values between a value close to zero and ψ_{aev} have been used as the starting point for integration while estimating the relative permeability function. The arbitrarily selected small value for the starting point of integration appears to have been used because no closed-form analytical procedure had been proposed for the calculation of the AEV. Details on how the integration using Fredlund et al. (1994) permeability is to be carried out can be found in the original paper.

If a suction value ψ_i between (near) zero and ψ_{aev} is used as the lower limit of integration, the permeability function of Eq. [A20] takes on the form shown in Eq. [A21].

$$k_{ri}^{s}(\psi)=\frac{\int_{\ln(\psi)}^{b}\frac{S(e^{y})-S(\psi)}{e^{y}}S'(e^{y})\,dy}{\int_{\ln(\psi_i)}^{b}\frac{S(e^{y})-S(\psi_i)}{e^{y}}S'(e^{y})\,dy} \quad \text{[A21]}$$

where, $k_{ri}^{s}(\psi)$ = relative coefficient of permeability at soil suction of ψ, when a suction value ψ_i is used as the lower limit of integration for the integral in the denominator of the Eq. [A21].

Childs and Collis-George (1950) proposed a statistical model for estimating the coefficient of permeability based on a random variation in pore sizes. There are three common assumptions for a methodology characterizing the statistical models: (a) The porous medium may be regarded as a set of interconnected pores randomly distributed in the sample. The pores are characterized by their length scale called “the pore radius”. (b) The Hagen-Poiseuille equation is assumed valid at the level of the single pore and thus used to estimate the hydraulic conductivity of the elementary pore unit. The total hydraulic conductivity has to be determined by integration over the contributions of the filled pores. (c) The soil-water characteristic curve is considered analogous to the pore radius distribution function. The capillary law is used to uniquely relate the pore radius to the capillary head (Mualem 1986). The air-entry value of the soil corresponds to the largest pore radius. This is the theoretical reason why the air-entry value has to be used as the lower limit of integration when estimating the relative permeability using Fredlund, Xing and Huang (1994) permeability function. The change of the lower limit of integration implies a change in the largest pore radius of the soil and thus the change in the pore radius distribution function.

The relative coefficient of permeability obtained using Eq. [A20] is theoretically correct and is used as the reference value. An error in the estimation of the relative permeability is introduced when using Eq. [A21] along with a variety of the lower limits of integration in the denominator. The slope on the soil-water characteristic curve, (SWCC), prior to the AEV (as defined by the degree of saturation-SWCC), contributes to the error in the computed permeability function.

Figure A-24 presents the relative coefficient of permeability for GE3 from Brooks and Corey (1964). The SWCC for GE3 is shown in Figure A-20. The best-fitting parameters of the Fredlund and Xing (1994) function for the *S*-SWCC of GE3 are a_f = 8.20 kPa, n_f = 9.15, m_f = 0.45, ψ_r = 40 kPa. GE3 has an AEV of 7 kPa. Figure A-25 presents the relative coefficient of permeability for Regina clay from Fredlund (1964). The SWCCs for Regina clay are shown in Figure A-21. It is the *S*-SWCC that is used for the estimation of the relative coefficient of permeability function. The best-fitting parameters of the Fredlund and Xing (1994) function for the *S*-SWCC of Regina clay are a_f = 7105 kPa, n_f = 1.348, m_f = 0.461, ψ_r = 47238 kPa. Regina clay has an AEV of 3500 kPa.

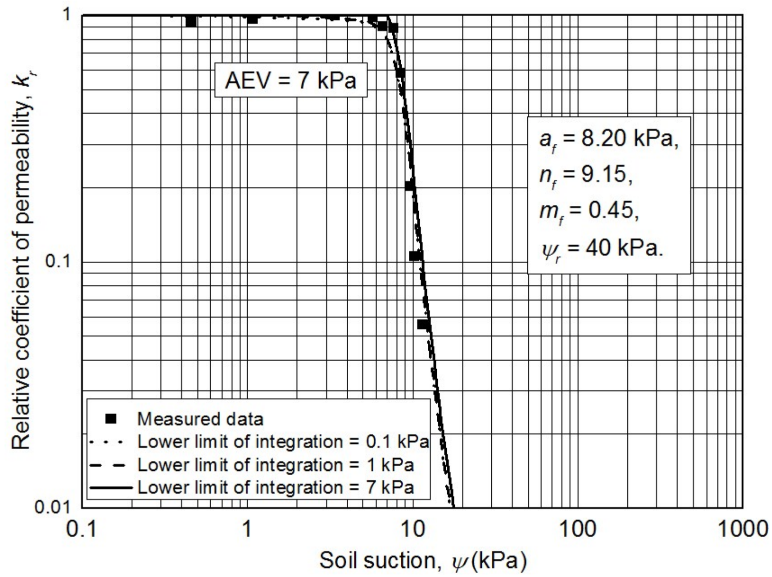

Figure A-24. Relative permeability for GE3 obtained using Eq. [A21] with different lower limits of integration. (Data from Brooks and Corey 1964)

Figure A-24 illustrates a situation where the effect of the starting point for integration is small. Starting integration at any point from 0.1 kPa to the AEV results in the computation of essentially the same relative permeability function. Figure A-25, on the other hand, shows how the starting point for integration can have a significant effect on the computed permeability function. The result computed by starting the integration from 0.1 kPa underestimates the permeability function by about one order of magnitude. The effect of the lower limit of integration on the calculation of the permeability function is studied in detail by the recently published paper of Zhang and Fredlund (2015).

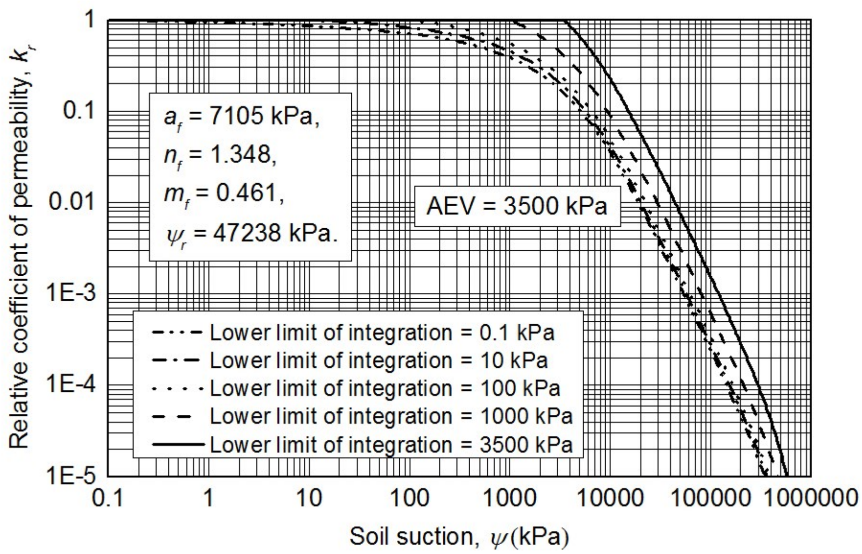

Figure A-25. Relative permeability for Regina clay obtained using Eq. [A21] with different lower limit of integration. (Data from Fredlund 1964)

THE CHOICE OF SWCC FOR THE ESTIMATION OF PERMEABILITY FUNCTION

The Fredlund, Xing and Huang (1994) permeability function was developed based on the interpretation of the SWCC. The choice of SWCC made could greatly affect the estimation results particularly when a soil's different forms of SWCC are distinct in shape and characteristics from each other. There are four forms of SWCCs, namely, gravimetric water content SWCC (*w*-SWCC), volumetric water content (θ-SWCC), instantaneous volumetric water content SWCC (θ_i-SWCC), and degree of saturation SWCC (*S*-SWCC). These four forms of SWCCs are essentially the same for no volume change soils (e.g., sands and silts) when plotted in terms of dimensionless water content versus soil suction as shown in Figure A-20. For soils that change volume when suction is increased, *w*-SWCC, θ_i-SWCC, and *S*-SWCC are distinctly different from each other. θ-

SWCC is of no significance for soils that change volume. Regina clay is a typical soil that undergoes volume change when soil suction is increased.

Different forms of SWCC for Regina clay are presented in Figure A-21. The best-fitting parameters of Fredlund and Xing (1994) SWCC function as well as the break point or AEV for each curve shown in Figure A-21 are listed in Table A-1. The results presented in Figure A-21 and Table A-1 reveal the significant difference among w-SWCC, θ_l-SWCC, and S-SWCC for Regina clay. θ-SWCC overlaps with S-SWCC, but θ-SWCC is of no significance in the case where there is volume change. θ-SWCC will be omitted in the following discussion. AEV is the soil suction that features the beginning of desaturation, thus it is reasonable that AEV should be obtained from S-SWCC. The break points on w-SWCC and θ_l-SWCC are 4.4 kPa, and 40 kPa respectively, both of which are significantly smaller than the AEV of 3500 kPa on S-SWCC. Wrong choice of SWCC could significantly underestimate the AEV for the large volume change Regina clay.

Table A-1. Break/AEV and best-fitting parameters for each form of SWCC for Regina clay (Data from Fredlund 1964)

	w-SWCC	θ-SWCC	θ_l-SWCC	S-SWCC
Initial water content, (%) (w_s/θ_0/S_0)	86.1	67.12	67.12	92.57
a_f (kPa)	17.2	17.2	88.34	7105
n_f	0.871	0.871	0.6023	1.348
m_f	0.770	0.770	0.589	0.461
ψ_r (kPa)	922	922	2600	47238
Break/AEV (kPa)	4.4	4.1	40	3500

The choice of SWCC also significantly influences the estimation results of the relative permeability function for soils that undergo volume change as soil suction is increased. Figure A-26 shows a typical example of Regina clay in which the relative permeability functions estimated from different forms of SWCC present distinct differences. Results obtained from *w*-SWCC and θ_i-SWCC greatly underestimate the relative permeability compared to the estimation results obtained from *S*-SWCC. Results obtained from *w*-SWCC underestimate the relative permeability by about 6 orders of magnitude. Results obtained from θ_i-SWCC underestimate the permeability by about 3 orders of magnitude. These significant differences among the estimated permeability function are mainly resulted from the significantly different break points on each form of SWCC used as the lower limit of integration when estimating the relative permeability function by the integral formula. It is appropriate to use the *S*-SWCC for the reasonable estimation of the relative permeability function, because the degree of saturation is the factor that affects the tortuosity of the flow path through the unsaturated soil thus influencing the relative permeability of the soil (Fredlund and Zhang 2013, Zhang and Fredlund 2014).

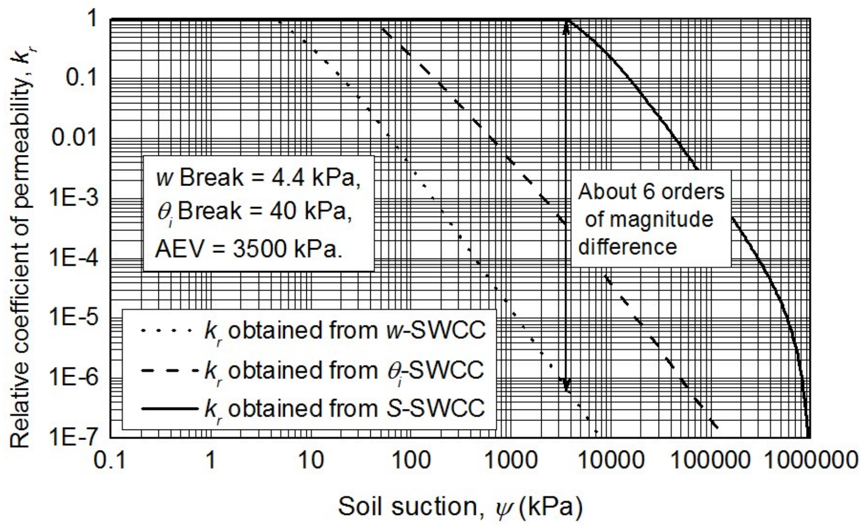

Figure A-26. Relative coefficient of permeability for Regina clay estimated from different forms of SWCC using each SWCC curve's break as the lower limit of integration.

CONCLUSIONS

A mathematical algorithm for the calculation of the AEV for the integration purposes is proposed in this paper. The effect of the lower limit of integration on the estimation of the permeability function is studied. The results show that if a lower limit of integration used in the integral of Fredlund et al. (1994) is smaller than the AEV, the computed results will underestimate the relative coefficient of permeability. The smaller the value used for the starting point of integration compared to the AEV, the greater will be the difference between the computed results and the relative permeability. This is particularly true for the high volume change Regina clay. It is recommended that the AEV always be used as the lower limit of integration when estimating the relative permeability function with the Fredlund et al. (1994) estimation method.

The study in this paper also reveals the importance of using *S*-SWCC in the determination of AEV and the estimation of the relative coefficient of permeability especially when soils undergo volume change as soil suction changes (e.g., Regina clay).

REFERENCES

Brooks, R. H., and Corey, A. T. 1964. "Hydraulic properties of porous media". *Colorado State University,* (March) Hydraulic Paper No. 3, 27 p.

Burdine, N. 1952. "Relative permeability calculations from pore size distribution data". Transactions of the AIME, Vol. 198, pp. 71-77.

Childs, E. C., and Collis-George, N. 1950. “The permeability of porous materials”. Proceedings of the Royal Society of London. Series A. Mathematical and Physical Sciences, 201(1066), pp. 392-405.

Fredund, D. G., and Zhang, F. 2013. “Combination of shrinkage curve and soil-water characteristic curves for soils that undergo volume change as soil suction is increased”. *Proceedings of the 18th International Conference on Soil Mechanics and Geotechnical Engineering, Paris 2013.*

Fredlund, D. G., and Xing, A. 1994. "Equations for the soil-water characteristic curve". *Canadian Geotechnical Journal,* 31(4), 521-532.

Fredlund, D. G., Xing, A., and Huang, S. 1994. "Predicting the permeability function for unsaturated soils using the soil-water characteristic curve". *Canadian Geotechnical Journal,* 31(4), 533-546.

Fredlund, D. G., Stone, J., Stianson, J., and Sedgwick, A. 2011. "Determination of water storage and permeability functions for oil sands tailings". *Proceedings of the Tailings and Mine Waste Conference, Vancouver, B.C..*

Fredlund, D. G., Rahardjo, H., and Fredlund, M. D. 2012. "*Unsaturated soil mechanics in engineering practice".* John Wiley & Sons, New York, N.Y., 926 p.

Mualem, Y., and Klute, A. (1986). "Hydraulic conductivity of unsaturated soils: prediction and formulas." Methods of Soils Analysis. Part 1. Physical and Mineralogical Methods, 799-823.

Mualem, Y. 1976. "A new model for predicting the hydraulic conductivity of unsaturated porous media". *Water Resources Research,* 12(3), 513-522.

Van Genuchten, M. T. 1980. "A closed-form equation for predicting the hydraulic conductivity of unsaturated soils." *Soil Science Society America Journal,* 44(5), 892-898.

Vanapalli, S.K., Sillers, W.S., and Fredlund, M.D. 1998. "The meaning and relevance of residual state to unsaturated soils", Proceedings of the Fifty-First Canadian Geotechnical Conference, Edmonton, AB, October 4-7, pp.1-8.

Williams, P.J. 1982. "The surface of the Earth, an introduction to geotechnical science". Longman Inc., New York.

Zhang, F. and Fredlund, D. G. 2015. “Examination of the estimation of relative permeability for unsaturated soils”. *Canadian Geotechnical Journal*.

Zhang, F., Fredlund, D. G., Wilson, G. W., and Sedgwick, A. 2014. “Determination of the permeability function for drying oil sands tailings undergoing volume change and desaturation”. Proceedings of the 4th International Oil Sands Tailings Conference, Banff, A.B. 2014.

Appendix 4. Hydraulic properties for soils that undergo volume change as soil suction is increased

ABSTRACT

The coefficient of permeability function and the water storage function are two hydraulic property functions required for numerical modeling of transient seepage problems. Methodologies presently available for the estimation of the unsaturated coefficient of permeability are based on an assumption that no volume change occurs as soil suction is changed. This assumption is generally valid when dealing with sands or silts. However, the estimation techniques need to be revised when predicting the hydraulic properties for soils that undergo significant volume change as soil suction changes, (e.g. slurry Regina clay). This paper is to investigate the hydraulic properties for soils that undergo volume change as soil suction is increased during a drying process. The revised methodology considers both the influence of void ratio change and degree of saturation change in an uncoupled manner. The influence of varying amounts of void ratio change is also discussed.

INTRODUCTION

Unsaturated soil mechanics plays an important role in geotechnical engineering practice involving unsaturated soils, such as foundation design for buildings constructed on unsaturated expansive soils, design of a highway built on unsaturated compacted soils. The success of the implementation of unsaturated soil mechanics into geotechnical engineering practice depends largely on the advancement of numerical computing techniques and the appropriate mathematical description of constitutive relationships. Advanced numerical computing techniques make it possible to solve the mathematical problems that are complex and highly nonlinear. Advanced numerical computing techniques require the input of appropriate mathematical constitutive relationships that characterizes the system being simulated. The unsaturated soils problems may involve volume-mass constitutive relationships, shear strength constitutive relationships and hydraulic conductivity constitutive relationships (Fredlund 2000).

Proper unsaturated soil property functions are required for numerical modeling of geotechnical engineering problems such as transient seepage problems and contaminant transport problems. Geotechnical engineering problems such as seepage from tailings and mine waste can be reduced to the solution of one or more partial differential equations. Each partial differential equation contains material properties that are either constants or mathematical functions. The material properties must be provided in order to obtain reasonable results. Most computer software for modeling unsaturated soils involves the solution of a partial differential equation (e.g. SVOffice 2009, GeoStudio 2012, etc.). The correctness of the numerical modeling results depends largely on the accuracy of the input of the material properties. This paper is dedicated to the study of hydraulic properties for the water phase.

The coefficient of permeability function and the water storage function are two hydraulic property functions required when modeling seepage through unsaturated soils. Considerable research has been directed towards the estimation of the coefficient of permeability function. The study of the coefficient of permeability for a soil can be categorized as the saturated coefficient of permeability and the unsaturated coefficient of permeability. Saturated coefficient of permeability for most soils is a constant that is measured experimentally. For a saturated soil that changes volume, the saturated coefficient of permeability becomes a function of the changing void ratio (Taylor 1948, Chapuis 2012). For unsaturated soils, there are four categories of models used for the estimation of unsaturated coefficient of permeability functions (Fredlund et al. 2012); namely, i.) empirical models, ii.) statistical models, iii.) correlation models and iv.) regression models. Empirical models and statistical models appear to be most extensively used in geotechnical engineering. The methods presently found in the research literature for estimating the unsaturated coefficient of permeability function are based on an assumption that no volume change occurs as soil suction is changed, considering only the influence of changes in the degree of saturation. Van Genuchten-Burdine equation (van Genuchten 1980), van Genuchten-Mualem equation (van Genuchten 1980) and Fredlund, Xing and Huang permeability function (Fredlund et al. 1994) are three well-known unsaturated permeability functions. These conventional methods produce reasonable estimations for the coefficient of permeability functions for unsaturated soils with no volume changes. Initially slurry Regina clay has been found to be a soil that undergoes significant volume change as soil suction is increased during a drying process. In other words, a conventional unsaturated coefficient of permeability function cannot mathematically describe the coefficient of permeability function of Regina clay that undergoes both desaturation and volume change during the drying process. Both the void ratio and the degree of saturation must be considered when estimating the coefficient of permeability function for a drying soil that undergoes volume change such as Regina clay.

This paper presents a methodology for the estimation of the coefficient of permeability function for soils that undergo volume change as soil suction is changed (e.g. slurry Regina clay). Both void ratio and the degree of saturation are taken into account as two influencing factors. Experimental data for Regina clay are used to illustrate and explain the new estimation method. The research study shows how volume change can influence the permeability function for a drying soil.

REVISED THEORY FOR THE COEFFICIENT OF PERMEABILITY FUNCTION

Degree of saturation and void ratio are two controlling volume-mass properties that influence the coefficient of permeability of a soil. The coefficient of permeability at a particular soil suction during a drying process, is the product of the relative coefficient of permeability and the saturated coefficient of permeability corresponding to the void ratio of the soil.

$$k(\psi) = k_r(\psi) \times k_{rs}(\psi) \qquad \text{[A22]}$$

where, $k(\psi)$ = coefficient of permeability at a particular suction of ψ; $k_r(\psi)$ = relative coefficient of permeability at a suction of ψ; $k_{rs}(\psi)$ = reference saturated coefficient of permeability at a soil suction of ψ.

Reference saturated coefficient of permeability is defined to be a function of soil suction. Reference saturated coefficient of permeability is the saturated coefficient of permeability corresponding to the void ratio of the soil at a particular soil suction. In other words, the material at a particular skeletal structure (or void ratio) has a particular saturated coefficient of permeability which is the reference saturated coefficient of permeability in Eq. [A22].

Shrinkage curve and soil-water characteristic curve (SWCC)

A shrinkage curve defines the relationship between the void ratio and the gravimetric water content. Fredlund et al. (2002) proposed a shrinkage curve equation that provides a mathematical description of the shrinkage curve. The shrinkage curve equation is shown as Eq. [A23].

$$e(w) = a_{sh}\left(\left(\frac{w}{b_{sh}}\right)^{c_{sh}} + 1\right)^{\frac{1}{c_{sh}}} \qquad \text{[A23]}$$

where: a_{sh} = the minimum void ratio, e_{min}; a_{sh}/b_{sh} = slope of the line of tangency; c_{sh} = curvature of the shrinkage curve; w = gravimetric water content.

The soil-water characteristic curve, SWCC, presents the relationship between the amount of water in a soil and various applied soil suctions. There are four designations of water content commonly used to define the amount of water in a soil, namely, gravimetric water content, w, volumetric water content, θ (where the volume of water is referenced to the original total volume of the soil specimen), instantaneous volumetric water content, θ_i (where the volume of water is referenced to the instantaneous total volume of the soil specimen), and degree of saturation, S. With each designation of the amount of water in the soil, there is a particular form of the SWCC. As a result, it can be said that there are four different forms of SWCC, namely, gravimetric water content-SWCC (w-SWCC), volumetric water content-SWCC (θ-SWCC), instantaneous volumetric water content-SWCC (θ_i-SWCC), and degree of saturation-SWCC (S-SWCC).

The equation for the gravimetric water content-SWCC, w-SWCC (Fredlund & Xing 1994) can be written as shown in Eq. [A24].

$$w(\psi) = \frac{w_s\left(1 - \ln\left(1 + \psi/\psi_r\right)/\ln\left(1 + 10^6/\psi_r\right)\right)}{\left(\ln\left(\exp(1) + \left(\psi/a_f\right)^{n_f}\right)\right)^{m_f}} \qquad \text{[A24]}$$

where: ψ = soil suction; a_f, n_f, m_f, and ψ_r = mathematical fitting parameters; w_s = initial saturated gravimetric water content; $w(\psi)$ = gravimetric water content at a designed soil suction of ψ.

Equations for other forms of SWCC (θ-SWCC, θ_l-SWCC, S-SWCC) can be obtained by combining of Eq. [A23] and Eq. [A24] based on basic volume-mass relationships.

For soils that do not undergo volume change as soil suction changes, all four SWCCs provide the same information to the geotechnical engineer when estimating other unsaturated soil property functions. However, for a soil that undergoes volume change as soil suction is increased in a drying process, w-SWCC, θ_l-SWCC and S-SWCC are different from one another. It should be noted that S-SWCC must be used for the estimation of the relative coefficient of permeability function, while θ_l-SWCC should be used for the estimation of the water storage function in all cases (Fredlund and Zhang 2013, Zhang and Fredlund 2014).

Consideration of the void ratio

Void ratio is one of the two main factors that govern the coefficient of permeability of a material that undergoes volume change as soil suction is increased. Void ratio affects reference saturated coefficient of permeability in Eq. [A22].

The saturated coefficient of permeability of a saturated soil depends on the pore sizes and the pore distribution or arrangement within the soil (Chapuis 2012). A change in the void ratio changes the pore sizes and the pore distribution, thus influencing the saturated coefficient of permeability of the soil. A number of research studies have been undertaken on the saturated coefficient of permeability as a function of void ratio for saturated soils that undergo volume change (Chapuis 2012). Eq. [A25] (Taylor 1948) has been found to mathematically describe the relationship between experimentally measured saturated coefficient of permeability, k_{sat} and void ratio, e.

$$k_{sat}(e) = \frac{10^{-11} C e^{x}}{1+e} \qquad \text{[A25]}$$

where: k_{sat}= saturated coefficient of permeability; e = void ratio; C, x = fitting parameters.

Void ratio is changing with soil suction during a drying process when the material undergoes volume change as soil suction is increased (Fredlund et al. 2011). This means the reference saturated coefficient of permeability is changing with soil suction as void ratio is changing. The relationship between the void ratio and the soil suction can be determined by combining the shrinkage equation (Fredlund et al. 2002), Eq. [A23] and the mathematical equation for the gravimetric water content-SWCC, *w*-SWCC (Fredlund & Xing 1994), Eq. [A24]. Then the reference saturated coefficient of permeability can be obtained by substituting the equation for the relationship of void ratio versus soil suction into the saturated coefficient of permeability function, Eq. [A25]. The change in the reference saturated coefficient of permeability is the result of a change in void ratio during the drying process as soil suction increases. The reference saturated coefficient of permeability reflects the influence of the void ratio on the coefficient of permeability for a soil that undergoes volume change as soil suction changes.

Consideration of the degree of saturation

Degree of saturation is another factor that influences the coefficient of permeability of a material. Degree of saturation influences the relative coefficient of permeability, $k_r(\psi)$ in Eq. [A22]. Changes in the degree of saturation change the tortuosity of the flow path within the porous media, thus affecting the relative coefficient of permeability.

The relative coefficient of permeability of a material is a function of soil suction reflecting the influence of the degree of saturation on the coefficient of permeability. Considerable research has been done on the estimation of the relative coefficient of permeability in unsaturated soil mechanics. The relative coefficient of permeability is primarily determined by the pore-size distribution (Brooks & Corey 1964), of a soil and its estimation is generally based on the soil-water characteristic curve. The Fredlund et al. (1994) permeability function is one of those commonly used unsaturated permeability functions. The relative permeability function (Fredlund et al. 1994)) takes the following form:

$$k_r(\psi) = \frac{\int_{\ln(\psi)}^{b} \frac{\theta(e^y) - \theta(\psi)}{e^y} \theta'(e^y)\, dy}{\int_{\ln(\psi_{aev})}^{b} \frac{\theta(e^y) - \theta(\psi_{aev})}{e^y} \theta'(e^y)\, dy} \qquad \text{[A26]}$$

where: b = ln(1000000); y = a dummy variable of integration representing the logarithm of soil suction.

It should be noted that *S*-SWCC must be used in Eq. [A26] for the estimation of the relative coefficient of permeability function with the air-entry value, AEV as the lower limit of integration. The effect of the lower limit of integration on the calculation of the permeability function is studied in detail by Zhang and Fredlund (2015).

The product of the reference saturated coefficient of permeability and the relative coefficient of permeability function generates the actual permeability function that considers both of the influence of void ratio change and degree of saturation change for a soil that undergoes volume change as soil suction is increased.

APPLICATION OF THE REVISED THEORY TO REGINA CLAY

Presentation of the experimental data

Initially slurry Regina clay is a material that undergoes large volume changes as soil suction is increased. Experimental data from Fredlund (1964) is presented and interpreted using the proposed theory for the estimation of the permeability function.

Regina clay had a liquid limit of 75%, a plastic limit of 25% and contained 50% clay size particles. The material is prepared at a water content slightly above the liquid limit and then subjected to various consolidation pressures under one-dimensional loading. After the applied load was removed, the soil specimens were subjected to a series of matric suction values. High suction values (in excess of 1500 kPa) were applied through equalization in a constant relative humidity environment.

Shrinkage curves and soil-water characteristic curves were measured on Regina clay. The shrinkage curve of Regina clay is shown in Figure A-27. The void ratio of Regina clay decreases with the gravimetric water content as water evaporates from the soil. The best-fitting parameters of the shrinkage curve are a_{sh} = 0.487, b_{sh} = 0.159, and c_{sh} = 4.422. The specific gravity of Regina clay is 2.835. Figure A-28 shows the gravimetric water content, w, plotted versus soil suction for Regina clay that was initially preloaded to 6.125 kPa. The gravimetric water content soil-water characteristic curve, w-SWCC was best-fitted with Fredlund and Xing (1994) equation, (i.e. Eq. [A24]. The best-fitting parameters are a_f = 17.2 kPa, n_f = 0.871, m_f = 0.770, and ψ_r = 922 kPa. The initial gravimetric water content was 86.10%. The w-SWCC was used in conjunction with the shrinkage curve to calculate other forms of the SWCC. The volume-mass properties versus soil suction were used to interpret the SWCC results. The "true" air-entry value, AEV was determined (Vanapalli et al. (1998)) and the relative permeability function was computed using the Fredlund et al. (1994) estimation theory.

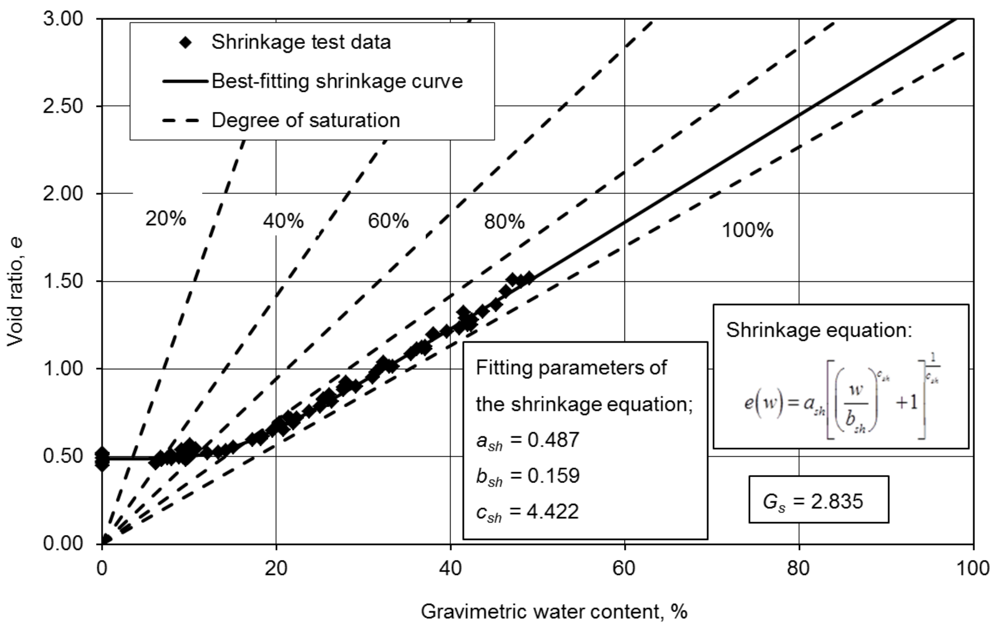

Figure A-27. Shrinkage curve of Regina clay.

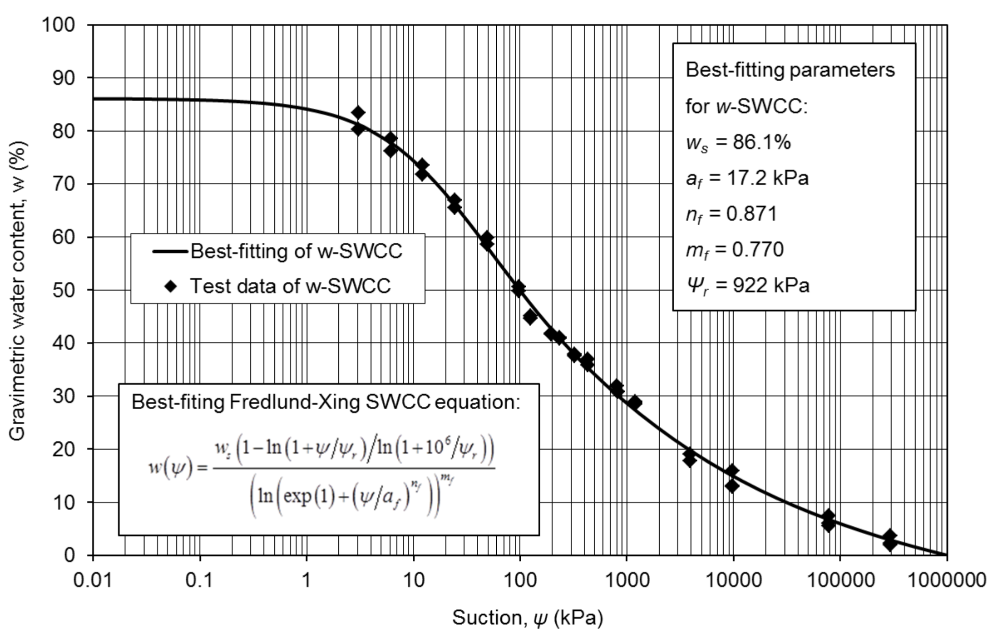

Figure A-28. Gravimetric water content versus soil suction.

The experimental data for the relationship of the saturated coefficient of permeability versus the void ratio were also obtained for Regina clay. The experimental data were best-fitted by Eq. [A25]. Figure A-29 shows the measured data and the best-fitting curve for the relationship of the saturated permeability versus the void ratio for Regina clay. The fitting parameters are C = 2.005 and x = 5.311.

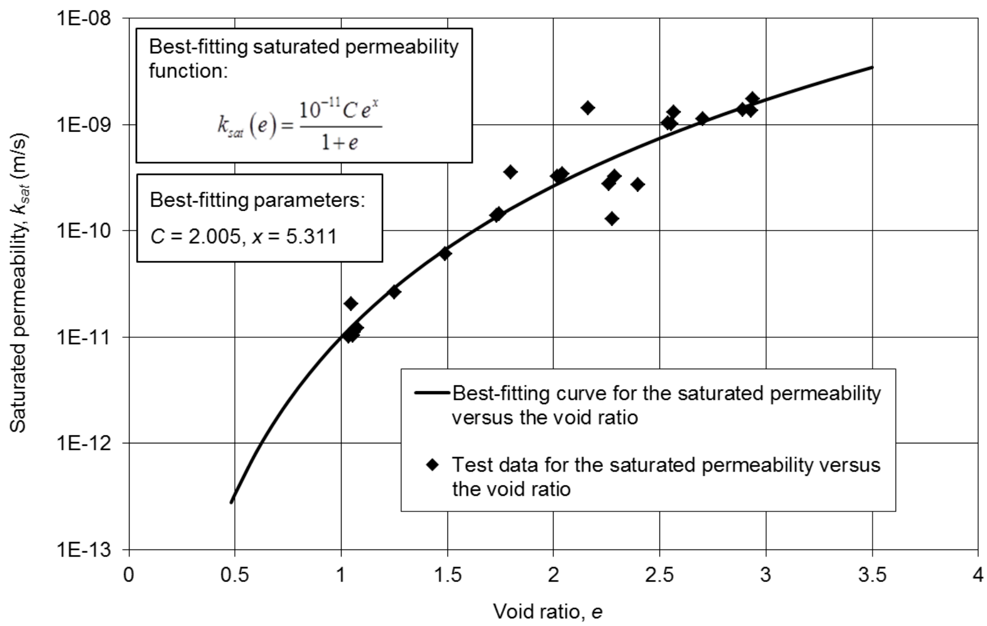

Figure A-29. Measured data and its best-fitting for the relationship of the saturated permeability versus void ratio for Regina clay.

The shrinkage curve, the w-SWCC and the curve of the saturated coefficient of permeability versus the void ratio were used to estimate the appropriate permeability function for Regina clay.

Interpretation of the experimental data

The gravimetric water content-SWCC, *w*-SWCC was combined with the shrinkage curve to obtain other forms of SWCC. The resulting plot of the degree of saturation-SWCC, *S*-SWCC is presented in Figure A-30. The "true" air-entry value (AEV) for a material that undergoes volume change as soil suction is changed is obtained from the *S*-SWCC of the soil. Using the graphical construction method suggested by Vanapalli et al. (1998), the "true" AEV was interpreted from the *S*-SWCC (see Figure A-30) as 4853 kPa. The plot of θ_l-SWCC is shown in Figure A-31. The θ_l-SWCC is the correct form of SWCC that should be used for the estimation of the water storage function. The θ_l-SWCC can be used for the water storage function in all cases, regardless of whether or not volume change takes place.

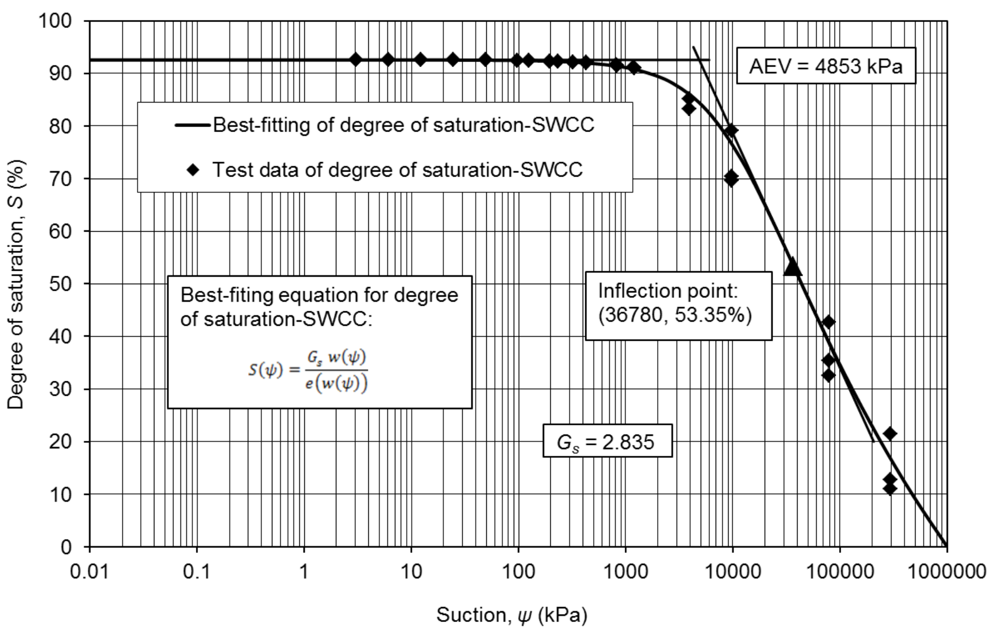

Figure A-30. Measured data and its best-fitting of the *S*-SWCC for Regina clay.

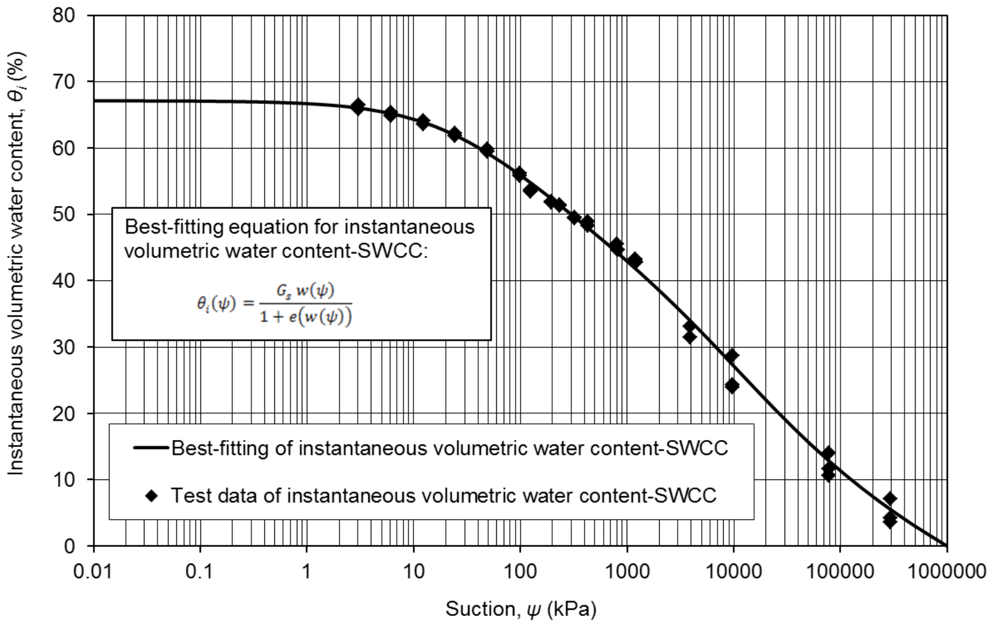

Figure A-31. Measured data and its best-fitting of the θ_i-SWCC for Regina clay.

The relationship between void ratio and soil suction is obtained by combining the *w*-SWCC and the shrinkage curve. The plot of void ratio versus soil suction is shown in Figure A-32. The void ratio decreases from 2.661 to 0.624 when the soil suction increases from 0 to its AEV of 4853 kPa. The void ratio at the AEV of 4853 kPa is 0.624 for Regina clay preloaded to 6.125 kPa. Regina clay experiences significant volume change before the soil suction reaches its AEV during its drying process. Comparing to the volume change experienced before the AEV, the volume change of the specimen is relatively small and insignificant after the soil suction exceeds the AEV.

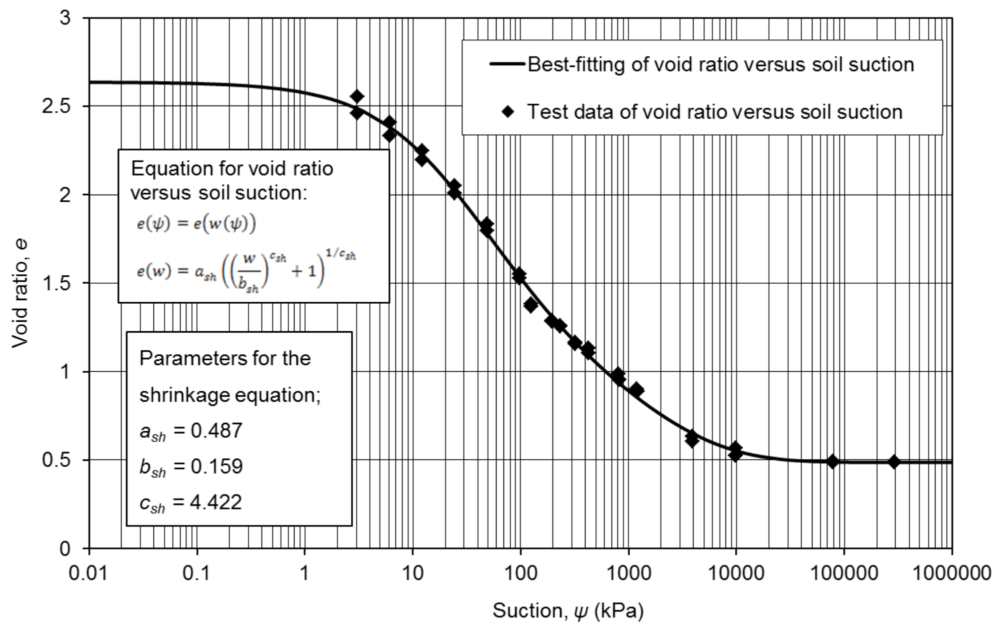

Figure A-32. Measured data and its fitting for the relationship of void ratio versus soil suction for Regina clay.

As void ratio changes with soil suction, the reference saturated coefficient of permeability changes with soil suction during the drying process of Regina clay. The reference saturated coefficient of permeability is a function of soil suction. It is the saturated coefficient of permeability corresponding to the void ratio at a particular soil suction during the drying process. The curve of the reference saturated coefficient of permeability versus soil suction for Regina clay is shown in Figure A-33.

The curve of the relative coefficient of permeability versus soil suction for Regina clay is presented in Figure A-34. Figure A-34 shows that the relative coefficient of permeability remains 1.0 until the soil suction approaches the AEV of the soil. When the AEV is surpassed, desaturation starts and the relative coefficient of permeability reduces from 1.0 towards zero. The correct curve for the relative coefficient of permeability versus soil suction is obtained from *S*-SWCC with AEV as the lower limit of integration for the integral in the denominator of Eq. [A26]. After having the relative coefficient of permeability function, $k_r(\psi)$ shown in Figure A-34 and the reference saturated coefficient of permeability function, $k_s(\psi)$ shown in Figure A-33, the coefficient of permeability function, $k(\psi)$ can be obtained by multiplying the relative coefficient of permeability function, $k_r(\psi)$ with the referenced saturated coefficient of permeability function, $k_s(\psi)$ according to Eq. [A22]. The coefficient of permeability versus soil suction for Regina clay is presented in Figure A-35.

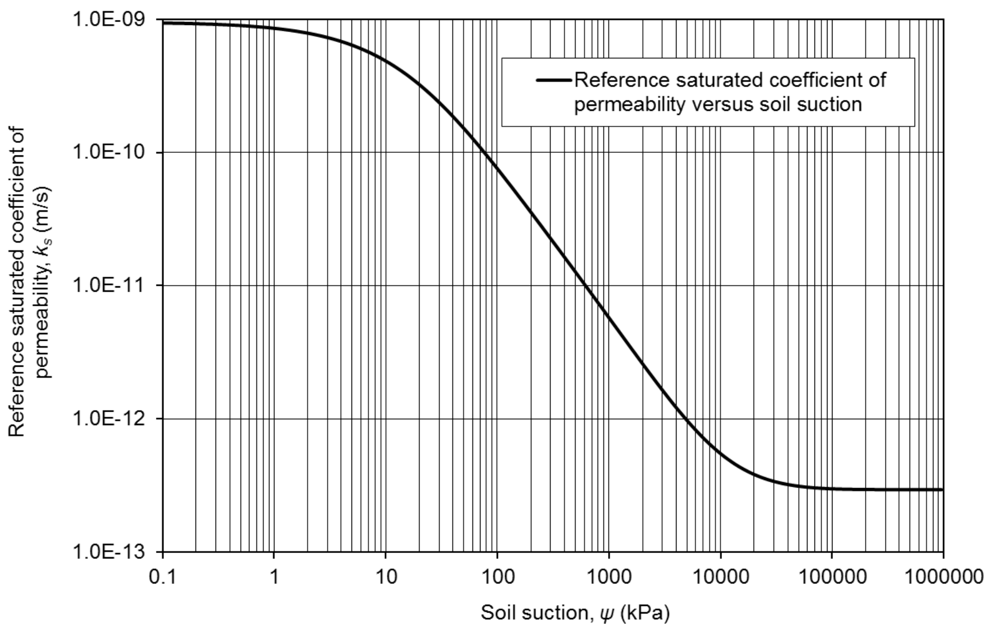

Figure A-33. Reference saturated coefficient of permeability versus soil suction for Regina clay.

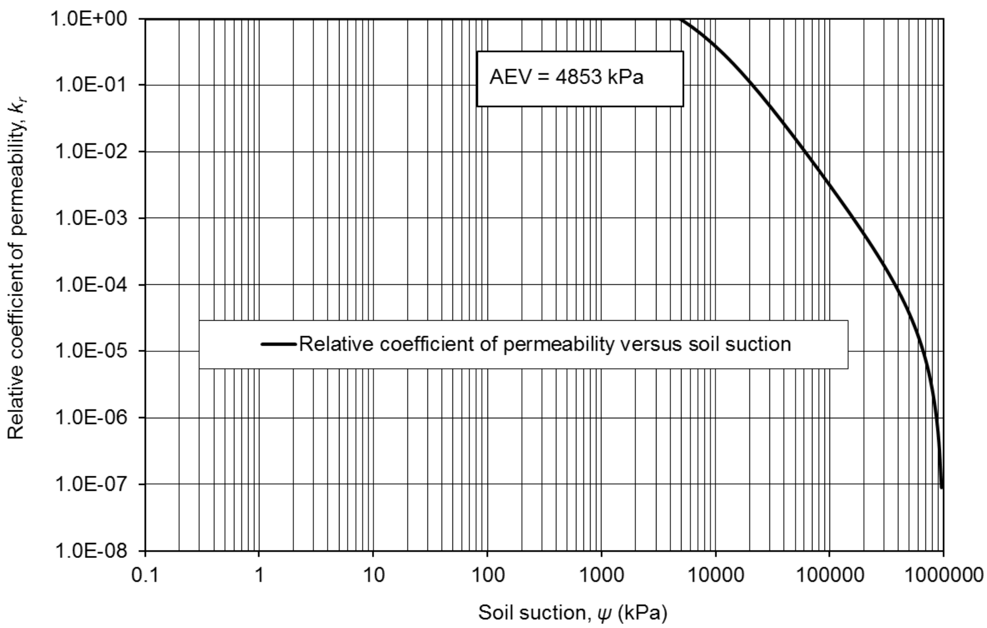

Figure A-34. Relative coefficient of permeability versus soil suction for Regina clay.

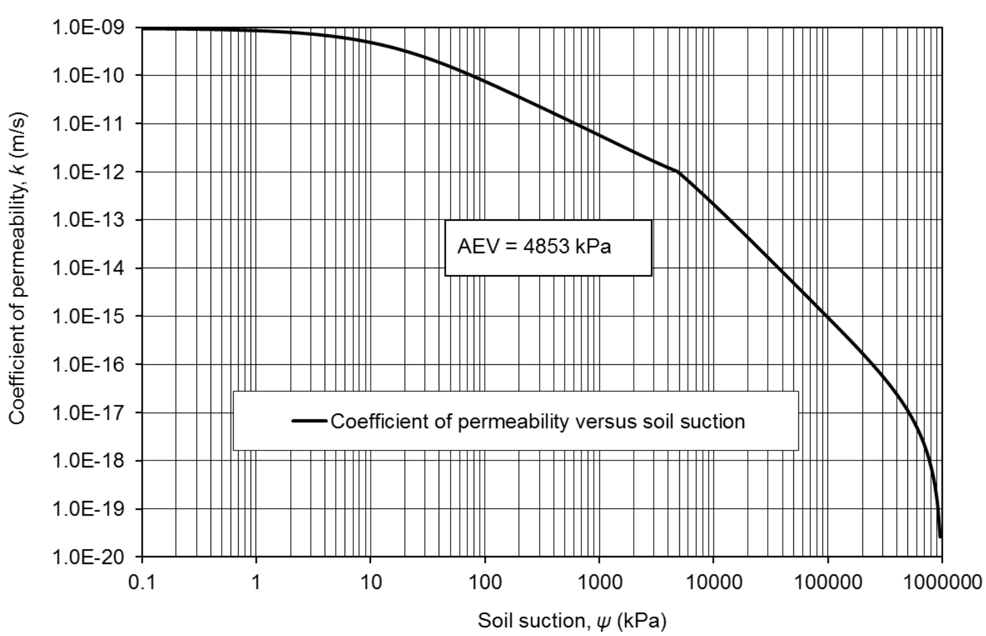

Figure A-35. Coefficient of permeability versus soil suction for Regina clay.

INFLUENCE OF THE VOLUME CHANGE

Three hypothesized soils are studied in a comparative manner to investigate the influence of the volume on the estimation of the coefficient of permeability for a soil, namely Soil #1, Soil #2, and Soil #3. Figure A-36 shows the different shrinkage curves for the three hypothesized soils. The fitting parameters for Soil #1 are a_{sh} = 0.981, b_{sh} = 0.37, and c_{sh} = 500. The fitting parameters for Soil #2 are a_{sh} = 0.7, b_{sh} = 0.264, and c_{sh} = 6. The fitting parameters for Soil #3 are a_{sh} = 0.48, b_{sh} = 0.181, and c_{sh} = 6. These three hypothesized soils share the same *w*-SWCC as shown in Figure A-37. The fitting parameters for Fredlund & Xing (1994) equation are a_f = 10 kPa, n_f = 2.0, m_f = 1.0, and ψ_r = 100 kPa. The initial gravimetric water content is 37.0%. However, these three hypothesized soils undergo different amounts of volume change as soil suction is increased during a drying process as Figure A-38 reveals. Soil #1 represents a soil that has no volume change as soil suction is increased. Soil #2 is a typical soil that experiences some volume change during the drying process. Soil #3 is the soil that would have the most volume change.

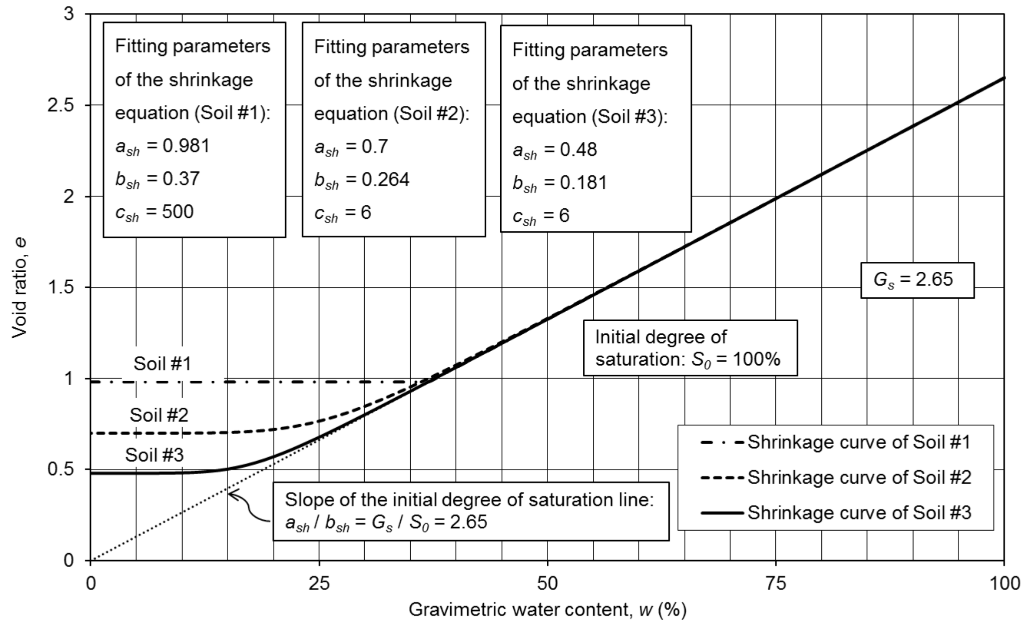

Figure A-36. Shrinkage curves for the three hypothesized soils.

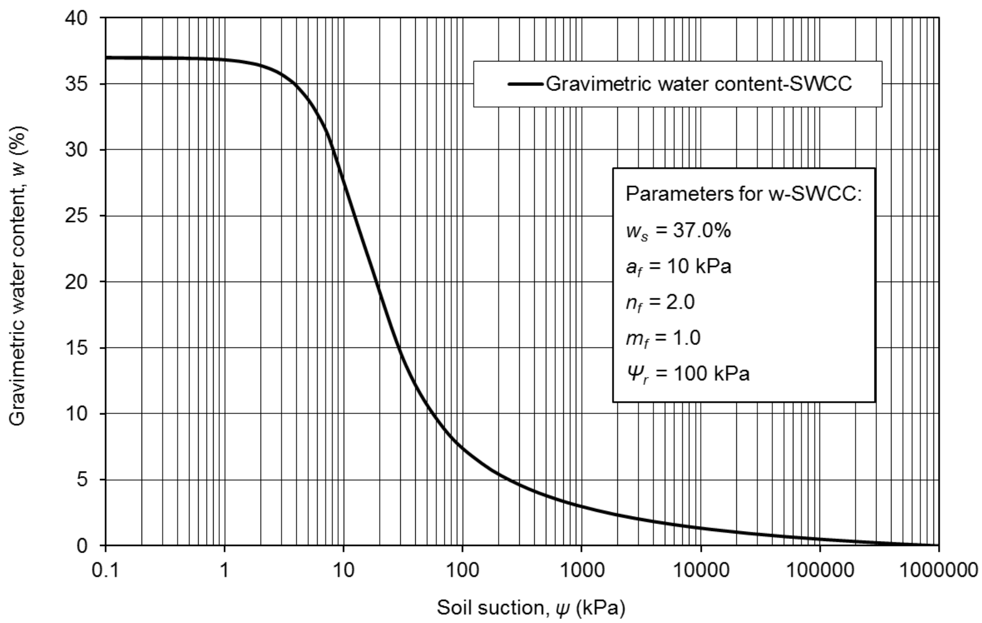

Figure A-37. w-SWCC for the three hypothesized soils.

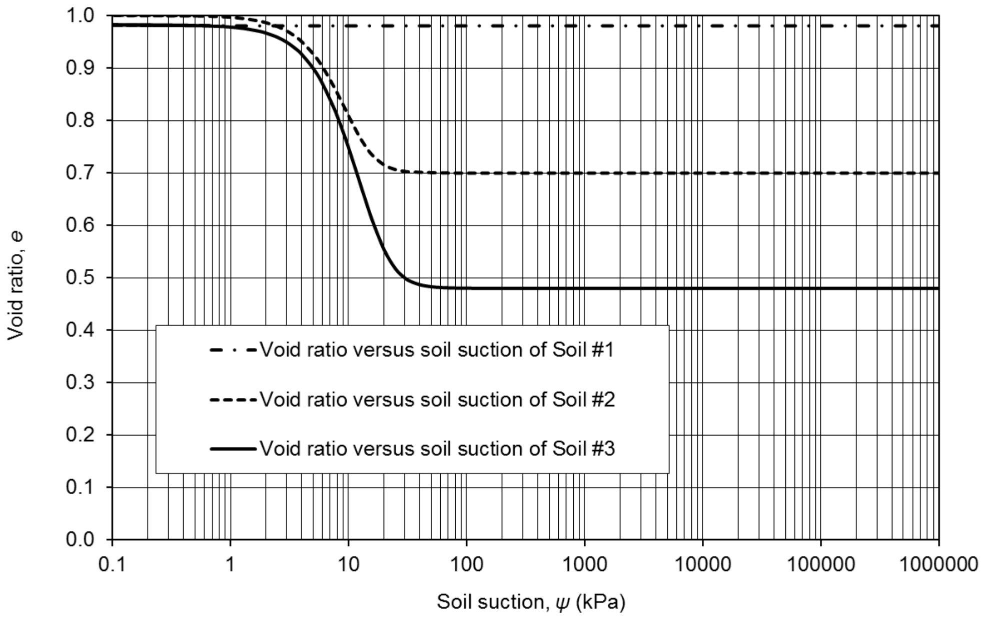

Figure A-38. The change of the void ratio with soil suction for the three hypothesized soils.

Figure A-39 shows the three different *S*-SWCCs for the three hypothesized soils that undergo different amounts of volume change. *S*-SWCC is the SWCC that should be used to determine the AEV, thus three AEVs obtained for the three soils are different. The AEV for Soil #1 is 5.10 kPa, for Soil #2 10.06 kPa, for Soil #3 17.11 kPa.

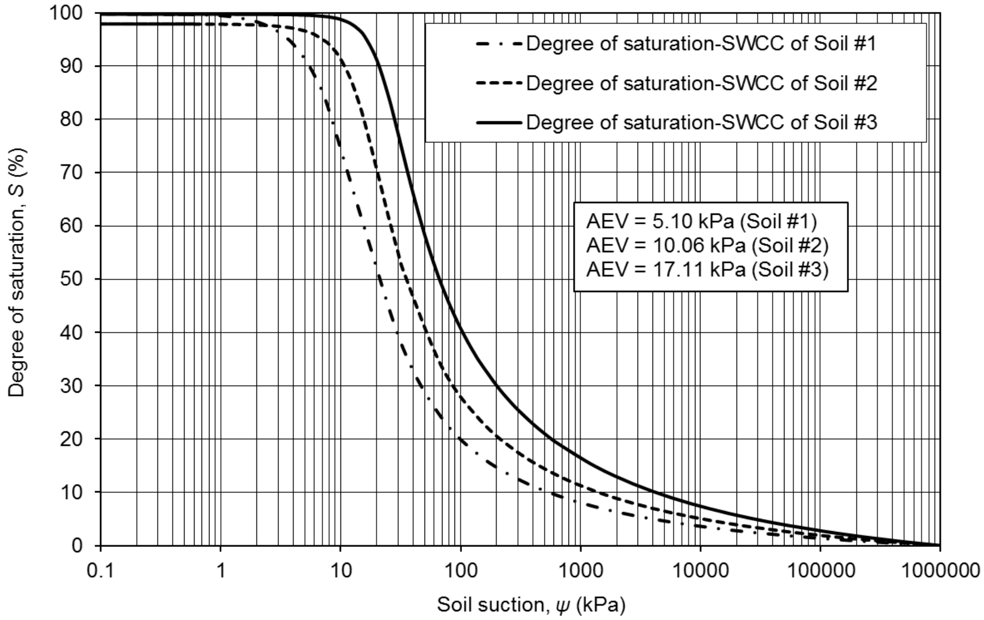

Figure A-39. *S*-SWCC for the three hypothesized soils.

S-SWCC is also the correct form of SWCC that should be used to estimate the relative coefficient of permeability function with Eq. [A26]. Figure A-40 presents the relative coefficient of permeability curves for the three hypothesized soils. The change of volume causes the change of the *S*-SWCC, thus changing the AEV and the relative coefficient of permeability function. The soil with more volume change has a higher relative coefficient of permeability at particular soil suction if *w*-SWCC is the same as Figure A-40 reveals.

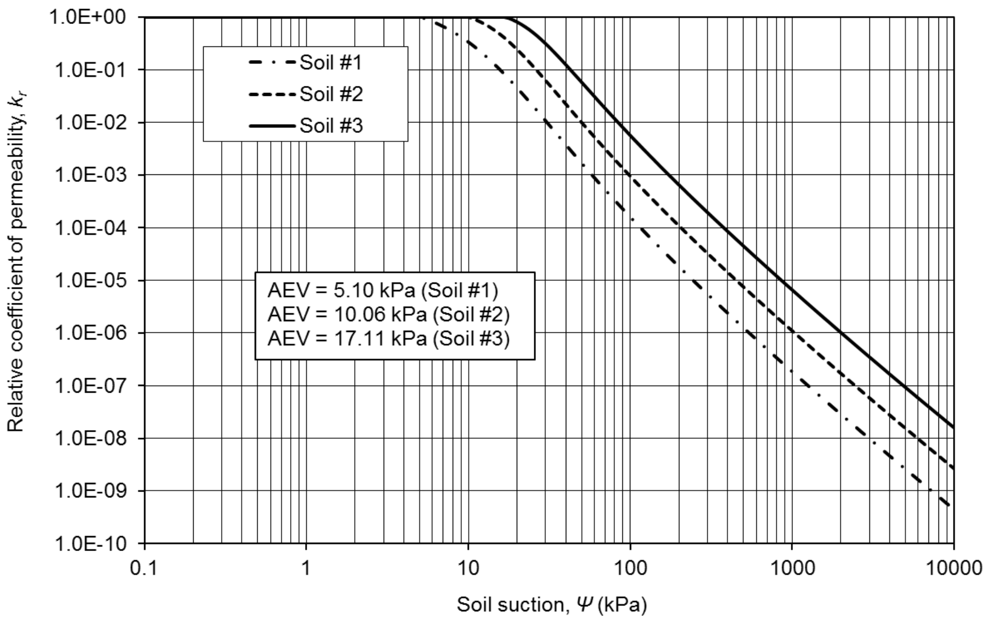

Figure A-40. The relative coefficient of permeability versus soil suction for the three hypothesized soils.

Assume that all these three hypothesized soils have a value of 3.0 for the *x* parameter in Eq. [A25] for the curve of saturated permeability versus void ratio. And assume the three hypothesized soils have the same saturated permeability at the void ratio of 0.981. Figure A-41 shows the dimensionless reference saturated coefficient of permeability curves for the three hypothesized soils. The dimensionless reference saturated coefficient of permeability curve shown in Figure A-41 is the reference saturated coefficient of permeability function referenced to the reference saturated coefficient of permeability at the void ratio of 0.981. The results in Figure A-41 show that the reference saturated coefficient of permeability of Soil #1 remains the same during the drying process since the Soil #1 doesn't change volume. The reference saturated coefficient of permeability of Soil #2 changes 0.5 orders of magnitude in value. Soil #3 has a change of 0.8 orders of magnitude in the reference saturated coefficient of permeability for it has the most volume change of these three soils. The decrease in the void ratio as soil suction is increased reduces the reference saturated coefficient of permeability.

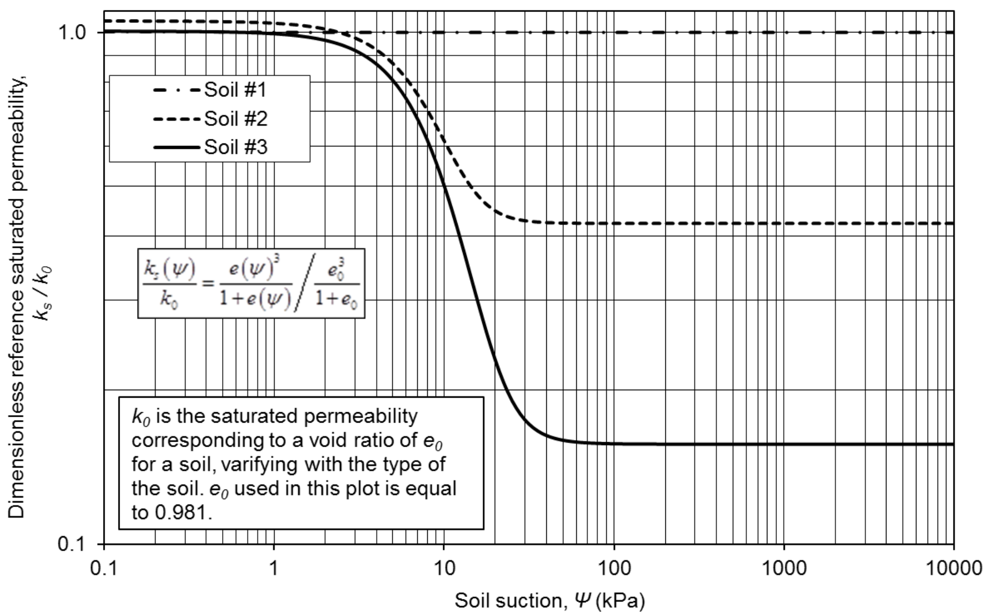

Figure A-41. The dimensionless reference saturated coefficient of permeability versus soil suction for the three hypothesized soils.

Figure A-42 shows the dimensionless coefficient of permeability versus soil suction for the three hypothesized soils. As analyzed above, the change in volume during a drying process reduces the reference saturated coefficient of permeability, but increases the relative coefficient of permeability. The combined impact shown in Figure A-42 is an increase in the coefficient of permeability due to the change of volume as soil suction is increased.

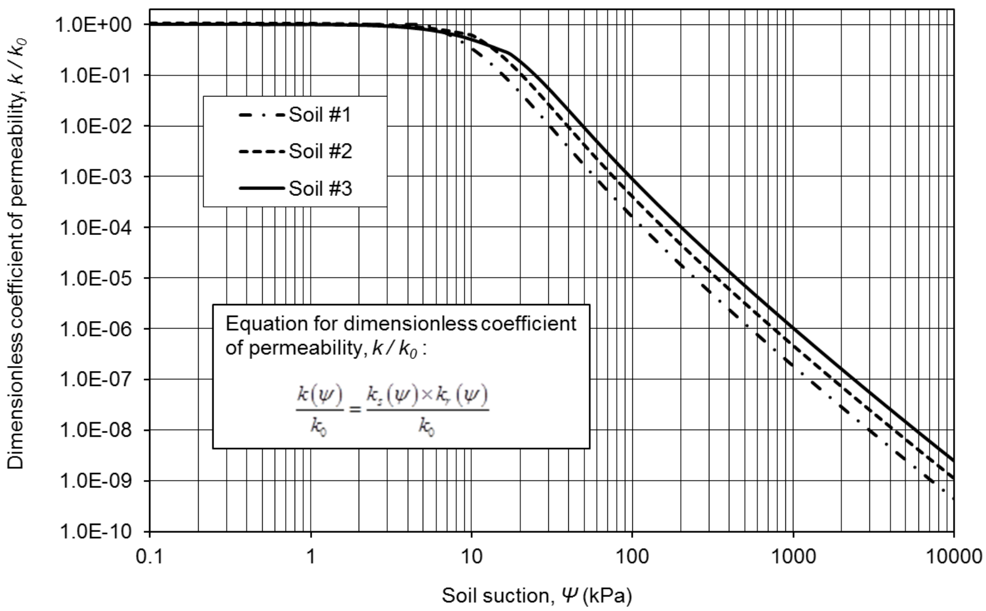

Figure A-42. The dimensionless coefficient of permeability versus soil suction for the three hypothesized soils.

CONCLUSIONS

The degree of saturation and the void ratio are two factors that govern the coefficient of permeability for a particular soil. Conventional methodologies for estimating unsaturated coefficient of permeability only take into account of the degree of saturation based on an assumption of no volume change during the drying process, while saturated soil mechanics limits to the cases of saturated soils investigating the relationship between the saturated permeability and the void ratio. This paper presents a revised theory considering both the degree of saturation and the void ratio for the estimation of the coefficient of permeability for soils that undergo volume change as soil suction is increased, such as Regina clay. The coefficient of permeability function proposed in this paper consists of two main components, namely, the reference saturated coefficient of permeability function and the relative coefficient of permeability function. The coefficient of permeability function is the result of the multiplication between the reference saturated coefficient of permeability function and the relative coefficient of permeability function. The reference saturated coefficient of permeability function is controlled by the void ratio as soil suction changes. The relative coefficient of permeability function is greatly influenced by the degree of saturation and must be determined from *S*-SWCC using the AEV as the lower limit of integration. The experimental data for Regina clay is used for the illustration of the proposed theory. A study concerning the influence of the volume change on the coefficient of permeability function reveals that the change of volume during a drying process causes changes in both *S*-SWCC and the curve of void ratio versus soil suction. The decrease in volume during the drying process reduces the reference saturated coefficient of permeability, but increases the relative coefficient of permeability. The combined impact is an increase in the coefficient of permeability due to the decrease of volume as soil suction is increased. Though the apparent influence is not significant in the case of this comparative study, it is important to realize the complicated mechanisms behind.

REFERENCES

Chapuis, R. P. 2012. Predicting the saturated hydraulic conductivity of soils: a review. *Bull.Eng.Geol.Env.*71(3): 401-434.

Brooks, R. H. & Corey, A. T. 1964. Hydraulic properties of porous media. *Hydrology Papers*. Colorado State University, (March).

Fredund, D. G., and Zhang, F. 2013. “Combination of shrinkage curve and soil-water characteristic curves for soils that undergo volume change as soil suction is increased”. *Proceedings of the 18th International*

Conference on Soil Mechanics and Geotechnical Engineering, Paris 2013.

Fredlund, D. G. 1964. *Comparison of soil suction and one-dimensional consolidation characteristics of a highly plastic clay*. The University of Alberta.

Fredlund, D. G. & Xing, A. 1994. Equations for the soil-water characteristic curve. *Canadian Geotechnical Journal* 31(4): 521-532.

Fredlund, D., Xing, A. & Huang, S. 1994. Predicting the permeability function for unsaturated soils using the soil-water characteristic curve. *Canadian Geotechnical Journal* 31(4): 533-546.

Fredlund, D. G., Stone, J., Stianson, J. & Sedgwick, A. 2011. Determination of water storage and permeability functions for oil sands tailings. *Tailings and Mine Waste 2011* . Vancouver, Canada.

Fredlund, D. G., Rahardjo, H., & Fredlund, M. D. 2012. *Unsaturated soil mechanics in engineering practice*. John Wiley & Sons.

Fredlund, M. D. 2000. *The role of unsaturated soil property functions in the practice of unsaturated soil mechanics*. The University of Saskatchewan.

Fredlund, M. D., Wilson, G. W. & Fredlund, D. G. 2002. Representation and estimation of the shrinkage curve. *Proc., 3rd Int. Conf. on Unsaturated Soils*. UNSAT 2002.

Taylor, D. W. 1948. *Fundamentals of soil mechanics*. J. Wiley & Sons; London: Chapman & Hall.

Van Genuchten, M. T. 1980. A closed-form equation for predicting the hydraulic conductivity of unsaturated soils. *Soil Sci.Soc.Am.J.*44(5): 892-898.

Vanapalli, S.K., Sillers, W.S. & Fredlund, M.D. 1998. The meaning and relevance of residual state to unsaturated soils. *Proceedings of the Fifty-First Canadian Geotechnical Conference*. Edmonton, AB.

Zhang, F. and Fredlund, D. G. 2015. “Examination of the estimation of relative permeability for unsaturated soils”. *Canadian Geotechnical Journal*.

Zhang, F., Fredlund, D. G., Wilson, G. W., and Sedgwick, A. 2014. “Determination of the permeability function for drying oil sands tailings undergoing volume change and desaturation”. *Proceedings of the 4th International Oil Sands Tailings Conference, Banff, A.B. 2014*.